Effects of modified bioactive pectins on colon cancer cells *in vitro*

Ellen G. Maxwell

Thesis submitted to the University of East Anglia in requirement for the degree of Doctor of Philosophy

School of Biological Sciences
University of East Anglia, Norwich, UK
And
Institute of Food Research, Norwich Research Park, Colney Lane, Norwich, UK

September 2014

Declaration

This thesis is submitted to the University of East Anglia for the Degree of Doctor of Philosophy and has not been previously submitted at this, or any other university for assessment or for any other degree. Except where stated, and reference or acknowledgement is given, this work is original and has been carried out by the author alone.

Abstract

Pectin is a complex structural polysaccharide present in the cell walls of terrestrial plants, fruit and vegetables. Modified pectin (MP), pectin treated with pH, heat or enzymes, has been shown to have anti-cancer activity in several cancer cell lines. The galactan chains of MP are postulated to be essential for bioactivity due to their ability to bind and inhibit the pro-metastatic protein galectin-3 (Gal3) on cancer cells. However, the structural requirements for bioactive MP, as well as interactions with Gal3 *in vitro*, have rarely been addressed. In this study several pectins from citrus, sugar beet and potato were screened for their biological effects on colon cancer cells, their structures characterised in detail to assess the structure-function relationship and the molecular mechanisms of action investigated. Alkali-treated sugar beet pectin (SSBA) reduced viability of HT29 cells via induction of apoptosis. The enzymatic removal of galactan side chains abolished activity indicating their importance for anti-proliferative action. Additionally, potato rhamnogalacturonan I (P-RGI) reduced viability of DLD1 cells and the homogalacturonan backbone, not the galactan side chains, was shown to be essential for bioactivity. siRNA-mediated knockdown of Gal3 expression in cells showed that bioactivities of SSBA and P-RGI are independent of Gal3, prompting an investigation into alternative mechanisms of action. Expression of the adhesion molecule ICAM1 was shown to be significantly reduced by P-RGI, suggesting a novel potential mode of action. Results presented in this thesis suggest that MPs of varying structures can exert anti-proliferative activity in colon cancer cells via Gal3-independent mechanisms and in a cell-specific manner. This study is also the first to report the anti-cancer activity of sugar beet pectin. The structural complexity of pectin makes it a potential multi-functional therapeutic agent, and results highlight the need for extensive structural characterisation of bioactive pectins as well as further exploration of Gal3-independent mechanisms of action.

Contents

List of Tables

List of Figures

Acknowledgements

I would like to give my sincerest thanks to my supervisors Dr Nigel J. Belshaw, Prof Vic J. Morris and Prof Keith W. Waldron for giving me the opportunity to pursue a PhD at the Institute of Food Research and for their invaluable advice and support at every stage of my PhD. Special thanks to Dr Belshaw, whose door was always open. I thank him for his time, patience and instructive comments.

I am deeply indebted to Dr Ian Colquhoun who kindly performed the NMR analysis of my pectins during this project, as well as his valued help in interpreting the data. Thanks to Claus Rolin from CPKelco for giving me the opportunity to visit the CPKelco facilities, and for the extraction of several pectins used in this study, as well as characterisation of the acetic acid and methyl-ester contents of those pectins. Also thanks to Dr Arland Hotchkiss from the United States Department of Agriculture Agricultural Research Service for carrying out the monosaccharide, molar mass and protein analysis.

I am also very grateful to Dr Kamal Ivory and Dr Roy Bongaerts for their guidance and help in planning and performing the flow cytometry experiments. Additional thanks goes to Dr Elizabeth Lund who initially recommended me to this research project and to Dr Wing Leung, Dr Giles Elliot, Dr Patrick Gunning, Mr Sam Collins and Dr Adam Elliston for their help and advice throughout my PhD.

Finally, many thanks to my CASE partner the International Pectin Producers Association (IPPA) and the BBSRC for funding my research.

Chapter 1
Introduction

1.1 Colorectal carcinogenesis

1.1.1 Epidemiology of colorectal carcinogenesis

Colorectal cancer (CRC) is a major cause of morbidity and mortality. It is the third most prevalent cancer worldwide and accounts for over 9% of all cancer incidences [1, 2]. Wide geographical differences in incidence rates and data from migrant studies indicate that diet and lifestyle play a major role, such as the high consumption of red meat [3, 4], fat and alcohol [5], smoking [6], lack of exercise and obesity [7] as well as the low consumption of fruit, vegetables and fibre [8].

1.1.2 The adenoma-carcinoma sequence

The multiplication of cells is carefully regulated by the body and loss of control can cause a cell to grow and divide in an unregulated fashion. Carcinogenesis is a complex multistep process whereby a normal cell undergoes a series of mutations (genetic, chromosomal or spontaneous) eventually transforming into a cancer cell [9]. It is widely accepted that CRC arises via the adenoma-carcinoma sequence of carcinogenesis (Figure 1). CRC originates from the epithelial cells lining the gastrointestinal (GI) tract. An accumulation of genetic and epigenetic mutations see the cells become hyper-proliferative, transforming into adenomatous polyps and benign tumours and ultimately producing a neoplastic phenotype [10, 11]. Mammalian cells have multiple safeguards to defend them against cancer gene mutations, and only when several genes are defective does an invasive cancer develop. Tumour suppressor genes contribute to this safeguarding process; however, when a tumour suppressor gene loses its normal function due to a mutation in both alleles or epigenetic changes such as promoter methylation, the first step of hyper-proliferation can occur. The tumour suppressor genes APC, TP53, SMAD4 and PTEN are major targets of these genetic changes [12-15]. Mutations in proto-oncogenes, genes that code for proteins that regulate cell growth and differentiation, also play a major part, over-expressing and increasing the genes already established role in promoting cell proliferation. KRAS and BRAF are two proto-oncogenes that have a significant role in the onset of CRC [12, 16-18].

1.1.3 Cell signalling

Cells depend on an elaborate intracellular communication network that co-ordinates growth, differentiation and metabolism, and the ability of cells to perceive and correctly respond to their microenvironment is essential for normal tissue homeostasis. Cells communicate by means of extracellular signalling molecules such as growth factors and cytokines which bind to specific target receptors to initiate a physiological response. Once a receptor protein is activated it undergoes a conformational change which subsequently promotes a series of protein-protein interactions that carries the signal to the cell interior. This process of converting extracellular signals into cellular responses is called signal transduction, or cell signalling. Cells employ several cell signalling pathways that cross-talk between each other to regulate activity, which results in numerous multifunctional proteins and transcription factors that can regulate many aspects of cell survival.

1.1.3.1 Cell cycle

Cells proceed through a sequence of phases called the cell cycle, regulation of which critical for the normal development of cells. The cell cycle is divided into four major phases. The first is the G1 phase where cells grow and synthesise proteins and mRNA ready for DNA duplication during the synthesis (S) phase. Following successful completion of DNA duplication the cell goes into a period of rapid cell growth and protein synthesis called the G2 phase during which the cell readies itself to enter the mitotic (M) phase which results in cell division into two daughter cells, each containing an identical copy of the parental cell's genetic material. Progress along the cycle is controlled at key checkpoints, which ensure that one phase has been successfully completed before proceeding to the next phase. The G1/S checkpoint guarantees the integrity of DNA before proceeding to DNA duplication, and the G2/M checkpoint verifies that DNA synthesis has been completed without mistakes before allowing mitotic division. If any problem is detected, the cell cycle is arrested until the problem is resolved, or cell death through apoptosis is induced when the damage cannot be repaired.

Progression through checkpoints is regulated by protein kinases called cyclins and cyclin-dependent kinases (CDKs) which form CDK-cyclin complexes [19]. Although CDKs are constitutively expressed in cells, cyclin expressions increase and decrease in phase with the cell cycle in response to various molecular signals such as growth factors. When a CDK is bound and activated by a cyclin it phosphorylates target proteins to coordinate progression into the next phase of the cell cycle. The first cyclin to be produced, cyclin D, complexes with CDK4/6, resulting in the production of the cyclin E-CDK2 complex which drives the cell from G1 to S phase. The cyclin B-CDK1 complex is necessary for the progression of the cells into and out of M phase of the cell cycle and cyclin A regulates multiple steps of the cell cycle, depending on its complex with either CDK1 or CDK2. Cdc25 is a family of phosphatases involved in activating CDKs and therefore control progression through various phases of the cell cycle [20]. Deregulation of these phosphatases has been implicated in CRC [21, 22]. Cyclins, particularly cyclin D, are frequently overexpressed in CRC, stimulated by an over expression of β-catenin and c-myc, resulting in cell proliferation [23-25].

Several tumour suppressor proteins keep the cell cycle in check by inhibiting these cyclin/CDK complexes including $p21^{CIP1/WAF1}$, $p27^{Kip1}$, $p15^{INK4B}$ and p16 that prevent progression through to S phase [26-29]. The tumour suppressor protein (TSP) p53 is at the centre of a complex network of extracellular signals (such as mitogen and anti-mitogen signals) and intracellular signals (such as revealing the presence of a viral infection). Activated by DNA damage signals, p53 can arrest cell cycle by activating $p21^{CIP1/WAF1}$ as well as activating DNA repair proteins. If damage cannot be repaired p53 can initiateapoptosis via activation of pro-apoptotic proteins Noxa and Puma (Figure 2g) [30, 31]. The p53 gene (TP53) is thought to be mutated in half of all CRCs [32], resulting in dysregulation of the cell cycle and uncontrollable cell growth.

1.1.3.2 Cell proliferation

The gene most commonly mutated in the adenoma-carcinoma sequence is in the tumour suppressor APC, which occurs early on in carcinogenesis [13].

However, this must be followed by further mutations in additional genes to progress to cancer. APC is a key member of the Wnt signalling pathway (Figure 2a), a critical pathway in CRC that regulates gene transcription. Wnt signalling begins when a Wnt protein binds to the Frizzled receptors. This causes an accumulation of β-catenin in the cytoplasm and its eventual translocation into the nucleus. Acting in conjunction with the transcription factor family TCF/LEF, β-catenin stimulates transcription of Wnt target genes including c-myc and cyclin D, integral to tumour formation because of their role in cell proliferation, apoptosis and cell-cycle progression [24, 33]. When the Wnt protein does not bind to the receptor, a destruction complex forms composed of APC, Axin and GSK3β, which phosphorylates β-catenin and degrades it [34-36]. When APC is mutated, truncations in the protein lack the Axin binding domains and subsequently the ability to join the destruction complex and target β-catenin for degradation [37]. The result is an accumulation of β-catenin in the nucleus, contributing to tumourigenesis.

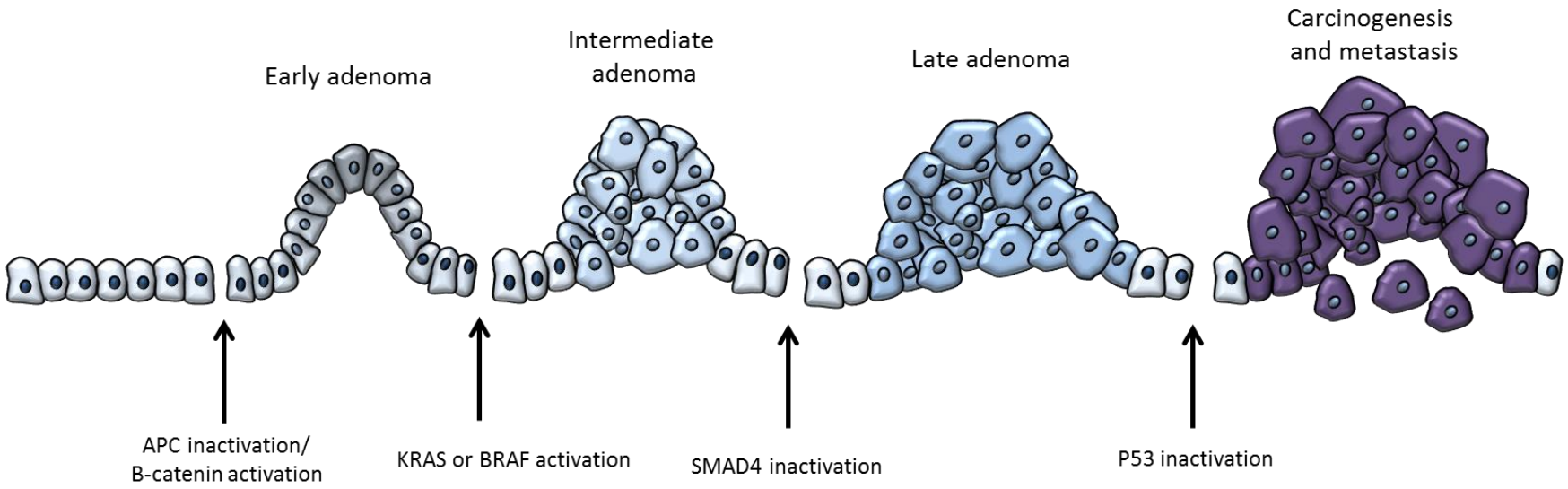

Figure 1 ***Representation of the adenoma-carcinoma sequence***

Another cell proliferation-associated protein is KRas of the Ras family of GTPases. Ras proteins regulate cell growth, differentiation and apoptosis. Other members include H- and N-Ras, which are regulated in a similar manner but differ slightly in sites and modes of action. Ras operates as a molecular on/off switch, alternating between GDP (inactive) and GTP (active) states. This rate of conversion is increased by accessory proteins such as SOS1 [38]. KRas is a crucial protein for the functioning of normal tissue signalling. 30% of tumours express oncogenic constitutively active Ras, with the most common mutations in the KRAS gene in pancreatic, colon and lung cancers [39]. Synthesised in the cytosol on free polysomes, KRas has a hypervariable region in the C-terminus that ends with a CAAX motif that directs it to the plasma membrane [40], where it is anchored via the C-terminal S-farnesylcysteine [41]. KRas can also be directed to the intracellular membranes of the endoplasmic reticulum [42]. Once activated it recruits and activates a multitude of effectors including Raf and PI3-Kinase and Ral-guanine exchange factors, essential players in cell proliferation, differentiation, survival and death (see Figure 2).

The MEK/ERK cascade (Figure 2c) is another pathway central to cell proliferation and survival. A key protein in the cascade, KRas, is typically activated by mitogens such as growth factors through receptor tyrosine kinases (RTKs). Adaptors like SHC or GRB2 link the receptor to a guanine nucleotide exchange factor such as SOS that transduces the signal to GTP-binding KRas. KRas activation triggers the protein kinase activity of Raf kinase which phosphorylates and activates MEK1/2 which in turn phosphorylates and activates mitogen-activated protein kinase (ERK1/2). Once activated, ERK1/2 can regulate targets in the cytosol and also translocate to the nucleus where it phosphorylates a variety of transcription factors that govern proliferation, differentiation and cell survival [43]. Two key components of this cascade, KRas and BRaf are often aberrantly expressed in CRC. The genes coding KRas (KRAS) and B-Raf (BRAF), are mutated in 30-40%, and 10% of all CRC's, respectively [6, 44], locking the proteins into a constitutively activated state in which they signal to downstream effectors such as those in the MEK/ERK pathway which drives the overexpression of oncogenes such as c-myc and c-fos which ultimately

drive cell growth and proliferation. KRas is also an effector of the PI3K/Akt pathway, explained further in this section [45].

NFκB is a protein complex that controls transcription of DNA and is therefore important to cell proliferation. There are five homologous subunits in the NFκB family: NFκB1, NFκB2, RelA, RelB and c-Rel. While in an inactivated state, NFκB (composed of subunits) is complexed with the inhibitory protein IκBα in the cytosol. A variety of extracellular signals, such as tumour necrosis factor alpha (TNFα), interleukin 1-beta (IL-1β) and reactive oxygen species (ROS) can activate the enzyme IκB kinase (IKK) (Figure 2b). IKK subsequently phosphorylates the IκBα protein, which results in its separation from NFκB, and consequent degradation. The activated NFκB is then translocated into the nucleus where it binds to specific sequences of DNA, ultimately resulting in a change of cell function [46]. NFκB can contribute to CRC progression by regulating the expression of genes that control cell proliferation, cell survival and angiogenesis such as c-myc, Ras, p53 and Cox-2 [47-49]. However, NFκB is better known for its role in the immune response and can induce cytokines IL-1 and TNF-alpha and endothelial-leukocyte adhesion molecules such as ICAM1 and VCAM1 [50-52].

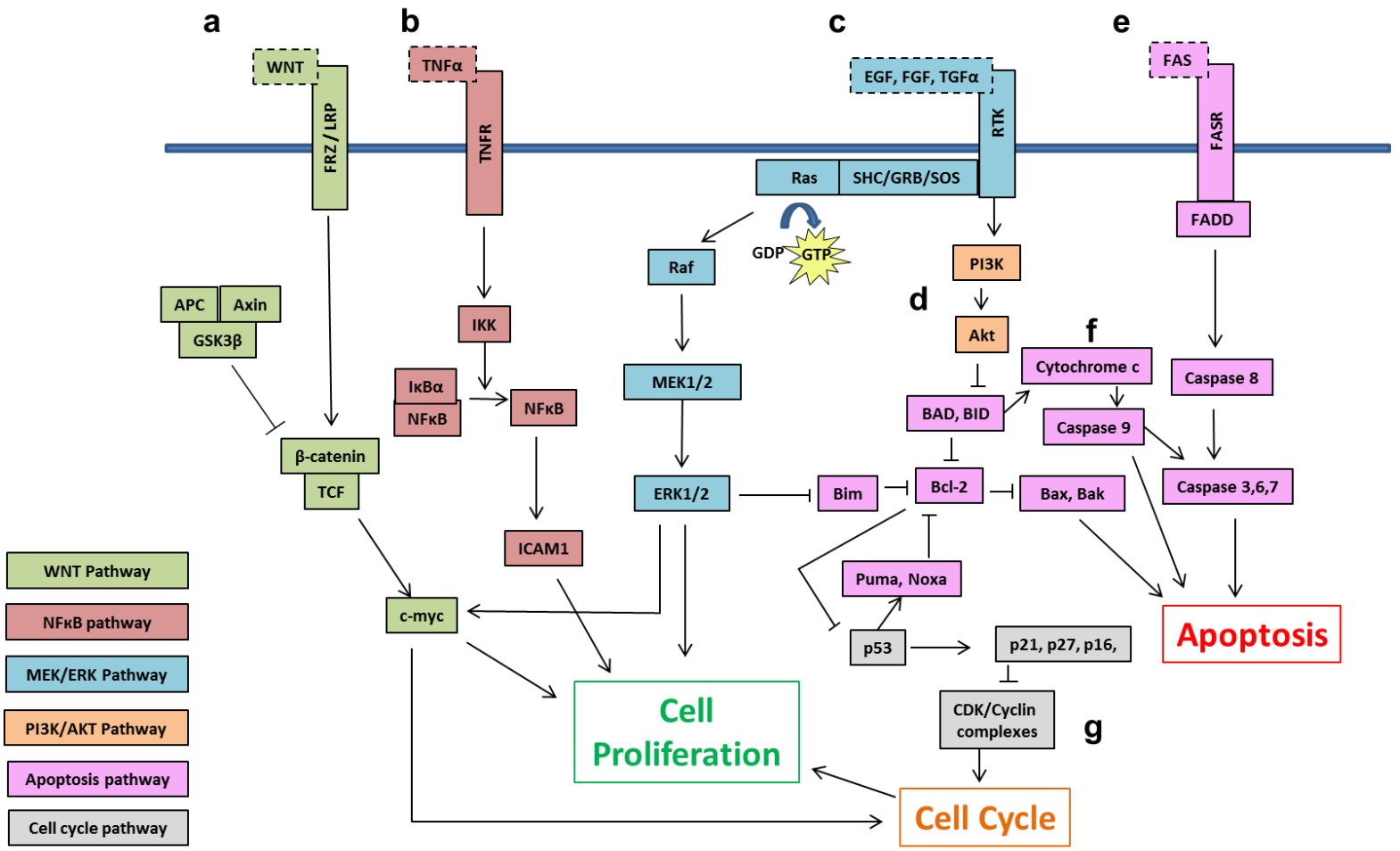

Figure 2 ***Example of intracellular cell signalling pathways in a colon cancer cell*** (a) Wnt signalling pathway (b) NFκB signalling pathway (c) MEK/ERK signalling pathway (d) PI3K/AKT signalling pathway (e) Extrinsic apoptosis pathway (f) Intrinsic apoptosis pathway (g) Cell cycle pathway. ---- Extracellular signalling molecule.

1.1.4 Apoptosis

Unchecked cell growth and multiplication can result in tumour growth. Apoptosis, a programmed mechanism of cell death, plays a very important role in cell population control. The first visible signs of apoptosis are condensation of the nucleus and DNA fragmentation, which are followed by shrinkage, blebbing, and the eventual consumption of the cell by phagocytic cells. There are two apoptosis signally pathways: the extrinsic, or death receptor pathway, and intrinsic or mitochondrial pathway [53]. The extrinsic pathway is mediated by members of the TNF-receptor family (e.g. Fas and TNFα), and once activated leads to the formation of the 'death inducing signalling complex' (DISC), composed of FADD and procaspase 8. This induces the activation of cysteine-aspartic proteases known as caspases, leading to the initiation of the caspase cascade which promotes cell death (Figure 2e). The intrinsic pathway (Figure 2f) is characterised by the depolarisation of the mitochondria and the release of cytochrome c which facilitates the formation of the apoptosome complex which initiates the activation of the caspase cascade through caspase 9. The initiation of the intrinsic pathway is regulated by members of the Bcl-2 family, which comprises pro-apoptotic (Bax, Bad, Bid, Bak, Bim, Puma, Noxa) and anti-apoptotic (Bcl-2 and Bcl-XL) proteins. Bcl-2 has been shown to suppress p53-dependent apoptosis [54] and loss of Bcl-2 expression has been shown to be a prognostic factor in CRC [55, 56].

The TSP, PTEN is essential in the regulation the PI3K/Akt pathway, a key pathway in the regulation of apoptosis as well as cell cycle progression and proliferation. 5-14% of CRCs have a PTEN mutation [57], resulting in the over-activation of this pathway. PI3-Kinase (PI3K) is an enzyme that activates PtdIns(3,4,5)P3 and PtdIns(3,4)P2 at the plasma membrane. These proteins recruit and bind the pleckstrin homology domain of Akt (also known as PKB), a serine/threonine protein kinase. Akt is important in regulating cell survival by binding and regulating downstream effectors such as the pro-apoptotic protein Bad and TNF-related apoptosis-

inducing ligand (TRAIL) [58, 59], as well as activation of β-catenin [60]. PTEN is an inhibitor of this pathway, blocking the recruitment of Akt to the membrane [61]. The transforming growth factor-β (TGFβ) pathway is another cascade involved in CRC apoptosis and cell proliferation. TGFβ superfamily ligands bind to receptors that recruit receptor-regulated SMADs which ultimately phosphorylate SMAD4, a transcription factor and TSP that can regulate apoptosis and cell cycle arrest [62]. SMAD4 mutations are found in approximately 10% of patients with sporadic CRCs, respectively [63, 64]. The SAPK/JNK pathway is also involved in cell survival. SAPK/JNK is activated by environmental stresses, inflammatory cytokines and growth factors. It translocates to the nucleus to regulate the transcription of genes such as p53 and c-jun involved in cell cycle progression and apoptosis [65-67]. Similar to the SAPK/JNK pathway, the p38 MAP kinase pathway is activated by cellular stresses. MKK3/4/6/7 activate p38 to mediate various genes involved in cell cycle progression and apoptosis [68].

1.1.5 Cell Adhesion

There is a close link between the survival of various normal and tumour cell types and adhesion to the extracellular matrix (ECM) [69]. The ECM provides structural support in tissues and is a network consisting of polysaccharides, fibrous proteins and adhesive proteins that are secreted by cells. Cell-cell and cell-ECM interactions are essential to provide signals for regulating cell growth and survival, particularly apoptosis. Integrins are a large family of transmembrane proteins that that promote adhesion of cells to the ECM or to the surface of other cells. When cells detach from the ECM, normal cell-ECM interactions are lost and this can result in anoikis, a form of programmed cell death. However, cancerous cells may be able to escape anoikis, allowing them to invade other organs. Focal adhesion kinase (FAK) is a protein kinase which is activated in response to integrin-mediated adhesion and controls a number of biological processes including cell spreading, proliferation, survival and motility [70, 71]. It has been shown that the adhesion of cells

to the ECM stimulates the interaction of PI3K with FAK, resulting in increased Akt expression and subsequent survival and growth [72]. FAK also enhances detachment and apoptosis in colon cancer cell lines [73]. CD44 is another important molecule whose role is to maintain organ and tissue structure via cell-cell and cell-matrix adhesion. CD44 gene transcription is in part activated by Wnt signalling pathway via β-catenin. Over expression of CD44 is a hallmark of CRC cells [74] and there is accumulating evidence that CD44 is involved in the initiation and progression of CRC [75-77].

As well as contact with the ECM, cell-cell interactions are fundamental for cell survival. Cell-cell contact is mediated by a variety of cell adhesion molecules including integrins, selectins and cadherins. Cadherins are a large family of transmembrane adhesion proteins that form adherens junctions to bind cells within tissues together, orchestrating crucial intracellular and extracellular signalling processes [78]. Down regulation of E-cadherin expression has been correlated with colorectal carcinoma tumour size, histopathology and differentiation [79] and has been shown to augment β-catenin nuclear localisation resulting in cell growth and survival [80]. As well as a Wnt transducer, β-catenin is also a vital component of adherens junctions where it links E-cadherin and α-catenin as well as binding actin and actin-associated proteins [81]. Additional cell adhesion proteins that mediate cell-cell contact are intercellular adhesion molecules (ICAMs) and vascular cell adhesion molecule-1 (VCAM1), predominantly known for their role in inflammation by mediating the adhesion of leukocytes and lymphocytes to the vascular endothelium. ICAM1 can be induced by cytokines IL-1 and TNFα and is expressed by the vascular endothelium, macrophages, and lymphocytes. However ICAM1 and VCAM1 are also expressed in colon cancer cells, mediating cell-cell adhesion [82-86]. It has been shown that over expression of VCAM1 and ICAM1 may stimulate tumour progression in CRC [87, 88].

1.1.6 Colon cancer cell lines as models to study colorectal cancer

Animal models and human studies have been used to demonstrate mechanisms that link the consumption of pectin to disease risk. However, *in vivo* models are not suitable for the initial screening of compounds or the investigation of molecular mechanisms, of which *in vitro* models are more suitable. In cancer biology, immortalised cell lines are often used because of their widespread availability and representation of the *in vivo* state. Five colon cancer cell lines were employed in this study. The DLD1 cell line was established from the colon of a male with colorectal carcinoma [89, 90]; HT29 cells were isolated from a primary colon adenocarcinoma in a 44 year old Caucasian female [91]; HCT116 were established from a primary tumour of the ascending colon of a 48 year old male [92]; Caco2 cells were derived from colorectal carcinoma [93]; the LoVo cell line was established from a colorectal adenocarcinoma of a 56 year old male [94]. Both HT29 and Caco2 cells are able to differentiate into cells acquiring enterocyte-like phenotypes. All five cell lines originate from colon carcinomas; however, the intricate cellular pathways in each cell line are different owing to mutations in different key genes. Table 1 shows the main mutations present in each of the five cell lines, although other mutations may exist. Although an effective tool to study molecular mechanisms, cell culture does have its limitations owing to the fact that cultured cells will not be fully representative of the tissue from which they are derived due to the absence of the cell microenvironment. However, providing that limitations are appreciated, cell culture is an immensely valuable tool in biomedical science.

Table 1 ***Colon cancer cell line mutations*****.** Adapted from [95].

Cell line	APC	KRAS	PIK3CA	P53	SMAD4	BRAF	PTEN
DLD	✓	✓	✓	✓	×	×	×
HCT116	✓	✓	✓	×	×	×	×
HT29	✓	×	✓	✓	✓	✓	×
Caco2	✓	×	×	✓	✓	×	×
LoVo	✓	✓	×	×	×	×	×

1.2 Colorectal cancer and diet

Diet is known to play a major role in CRC, particularly the high consumption of processed red meat [4, 96], and the low consumption of fruit, vegetables and fibre [8, 97, 98]. The European Prospective Investigation into Cancer and Nutrition (EPIC) study investigates the associations between fruit, vegetable and fibre consumption and cancer risk. It is an ongoing study, followed for almost 15 years, with more than half a million participants recruited across 10 European countries. 14 sites of cancer are investigated, including the colon where CRC risk is inversely correlated with total intake of fruit, vegetables and fibre [97].

Fibre has long been credited with protecting against the development of diseases such as cardiovascular disease [99], diabetes [100], as well as with reduced CRC risk [101]. In 1971, Burkitt observed the low incidence rate of CRC among rural Africans whose diet comprised a high content of fibre [102]. From this the hypothesis that dietary fibre reduces the risk of colorectal cancer was born. Until fairly recently, results of the epidemiological studies investigating the association between risk of CRC and intake of fibre have been inconsistent. However, recent studies support the connection [98, 103, 104]. Dietary fibre is found naturally in

fruits, vegetables and whole grains, but can also be obtained from plant raw material by physiological, enzymic or chemical means. It has been defined as carbohydrate polymers of ≥10 monomeric units occurring in the diet that are resistant to digestion and absorption in the small intestine, with complete or partial fermentation in the large intestine [105]. Dietary fibre encompasses a wide variety of plant matter including pectin, chitin, lignin, waxes, inulin, resistant starch, non-starch polysaccharides, β-glucans and oligosaccharides. Research into defining and measuring fibre as well as determining the health benefits of fibre consumption are ongoing. Fibre can be classed as soluble and insoluble. It is not clear which specific types of sources or which components of dietary fibre are associated with reduced risk of CRC. Several plausible mechanisms have been suggested to explain the association of fibre with CRC risk, including increased faecal bulk and reduced intestinal transit times [106], the dilution of faecal carcinogens [107], and the formation of short chain fatty acids from fermentation of colonic bacteria [108].

Pectin, largely a soluble fibre, has been shown to reduce cholesterol [109] and to have prebiotic properties [110-112], as well as anti-cancer effects that will be discussed later. Pectin is consumed in the diet predominantly as a component of fruit and vegetables. Values of pectin contents in fruit and vegetables can be highly variable depending on source, cultivar, genus, species and state of maturity [113]. The pectin contents of some fruits and vegetables are shown in Table 1. Contents are variable; however, an approximate mean of 0.6% can be used to estimate the daily intake of pectin as 1.8 g (assuming consumption of approximately 300 g fruits and vegetables per day). Pectin is also consumed as an additive in foodstuffs as it is used in the food industry as a gelling and thickening agent and stabiliser in food, for example in jams and yoghurt drinks. Pectin for commercial purposes is usually extracted from citrus peel due to its high pectin content (approximately 30-35%[114]).

Table 2 ***Published values of pectin contents of fruit and vegetables***. Taken from [113].

Food	Pectin content %	Reference
Apples	0.14-1.15	[115, 116]
Apricots	0.42-1.32	[115]
Bananas	0.44-1.02	[117]
Cherries	0.01-1.15	[115]
Grapes	0.12-0.8	[118, 119]
Grapefruit	0.24-0.65	[120, 121]
Oranges	0.25-0.76	[115]
Raspberries	0.1-0.88	[115]
Quince	1.4	[122]
Squash	0.67	[123]
Sweet potato	0.61-0.78	[123, 124]
Carrots	0.71-1.01	[125, 126]
Beans	0.27-0.63	[124]

1.3 Pectin

1.3.1 General pectin structure

Pectins are important structural components of cell walls of the soft, non-woody parts of fruit, vegetables and terrestrial plants. Within a living plant it is an important structural polysaccharide with functions in plant growth, morphology and development [127]. Fruit ripening involves pectin

breakdown induced by the enzymes pectinase and pectinerase leading to cell separation [128]. When extracted, the major commercial use for pectin is as a gelling or thickening agent and as a stabiliser in food, for example in jams and yoghurt drinks. The most important source of commercial pectin today is waste from the juice industry in the form of citrus peel, mainly from lemon and lime. Other commercial pectins are sourced from orange peel and apple pomace, and an emerging new source is from sugar beet from the sugar industry.

Pectins are conceivably the most complicated of the natural plant carbohydrates, both in terms of their chemical composition and their physical chemical structure. They contain a number of defined structural units [127]: homogalacturonans (HG), rhamnogalacturonan I (RGI), and substituted galacturonans such as rhamnogalacturonan II (RGII). Other substituted galacturonans (apiogalacturonans and xylogalacturonans) have been identified, but only in extracts from certain specific plant species. The familiar components of interest in discussing the bioactivity of pectin as an anti-cancer agent are HG and RGI.

The most predominant region of pectin is HG, composed principally of a homopolymer of (1→4)-linked α-D-galacturonic acid (GalA) partially methylated at C-6 [129] (Figure 3). The degree of methylation (DE) refers to the ratio between methylated and non-methylated GalA. Pectin with high DE is known as HM pectin and generally refers to pectin with 50% or more methyl ester groups on the HG backbone, and low DE pectin (LM pectin) with fewer than 50%. The methyl-ester content is particularly important in pectin research as it strongly determines the physical properties of pectin. The GalA residues at O-2 and O-3 may also be partially esterified with acetic acid in certain plant species such as sugar beet [130]. Again, the ratio between acetylated and non-acetylated GalA is referred to as the degree of acetylation (DAc) (Figure 3).

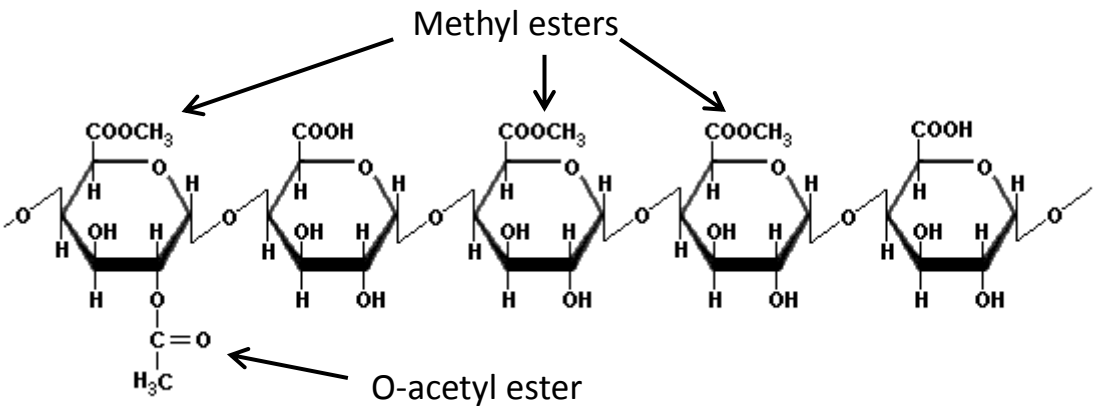

Figure 3 ***Primary structure of the polygalacturonic acid backbone of pectin***.

A second well-characterised component constitutes the 'hairy' regions of pectin or rhamnogalacturonan I (RGI) regions. RGI consists of a backbone composed of a repeating disaccharide of GalA and rhamnose (Rha) residues [-4)-α-D-GalA-(1,2)-α-L-Rha-(1-]n [131, 132]. They are highly branched structures with neutral sugar side chains of varying degrees of polymerisation attached to O-4 or O-3 position on the α-L-rhamnose residues [133, 134] (Figure 4). These side chains consist mainly of α-L-arabinose and/or β-D-galactose residues. The major types of sidechain present are: (i) Arabinan (Ara), comprising (1→5)-α-L-Ara units and often ramified with short (1→3)-α-L-Ara or single α-L-Ara non-reducing units at O-2, O-3 or O-5 positions (Figure 4b); (ii) Galactan (Gal) comprising linear, type I (1→4)-β-D-Gal (Figure 4a) or branched, type II (1→3,6)-β-D-Gal, depending on the plant source; (iii) Arabinogalactan I (AGI) consisting of a basal chain of (1→4)-β-D-Gal substituted at O-3 with short (1→2)/(1→3)-α-L-Ara or single α-L-Ara non-reducing units (Figure 4c); (iv) type II arabinogalactan (AGII) which has a backbone of (1→3)-β-D-Gal heavily substituted at position 6 by mono- and oligosaccharide Ara and Gal side chains. Recent studies on the bioactivity of pectin are beginning to emphasise the potential importance of these neutral sugar chain-containing regions. RGIs, as with whole pectins themselves are

highly variable depending on source and extraction. The RGI regions in Figure 4 are shown as containing all the identified types of sidechains, although it is not known whether there are different types of RGI regions containing just arabinans, galactans or arabinogalactans. Depending on the source the sidechains may contain minor amounts of other sugars such fucose, xylose, mannose, glucose [135], glucuronic acid and methyl esterified glucuronic acid and, in some cases, phenolics [136].

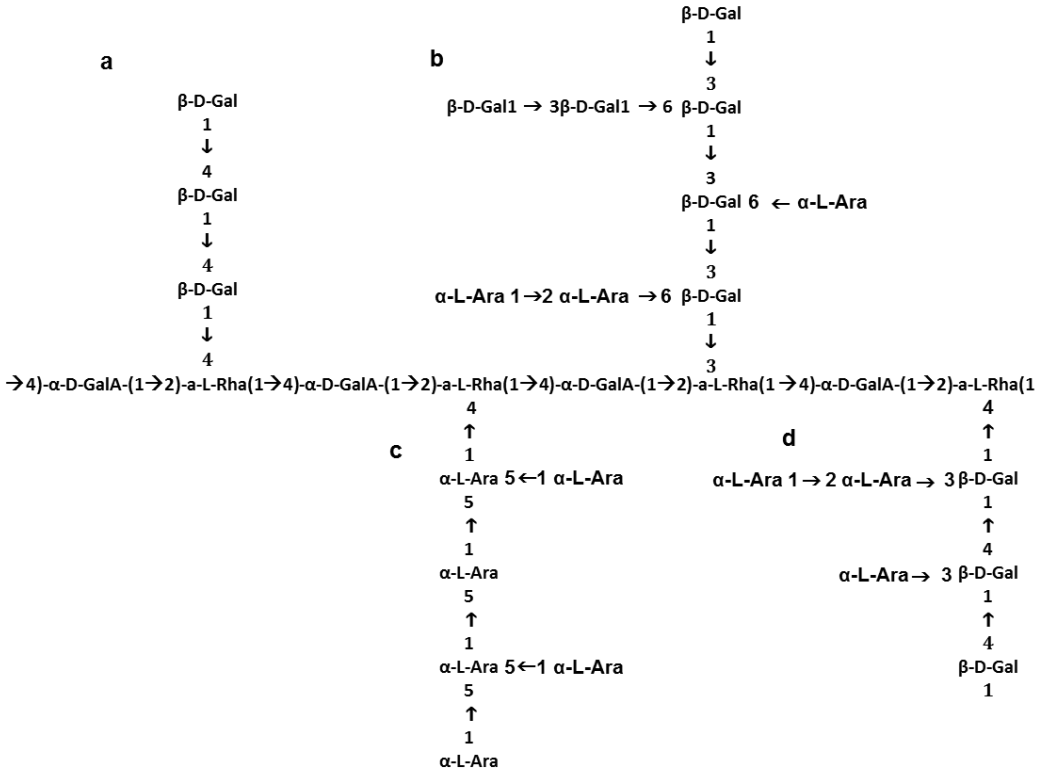

Figure 4 ***Schematic diagram of RGI.*** (a) Linear (1→4)-β-D-Galactan; (b) Arabinogalactan II; (c) branched (1→3,5)-β-L-Arabinan; (d) Arabinogalactan I

1.3.2 Pectin Models

The details of the exact molecular arrangement of the different pectic molecules relative to one another are still ill-defined. Pectins are usually considered to contain mainly HG and RGI with smaller amounts of RGII and are commonly represented as a contiguous structure with RGI and

RGII interspersed between smooth HG regions (Figure 5a). Enzymatic degradation of HG can enrich the RGI regions signifying that these regions are linked together; however RGI is not always dispersed within HG backbone, and can depend on the pectin source. Round and co-workers showed that RGI from tomato is found at the ends of HG or in aggregates [137]. Recent evidence additionally suggests an alternative structure in which HG may be present as side chains of RGI (Figure 5b). Direct observation of the molecular structure of pectin extracts by atomic force microscopy (AFM) reveals the presence of complex aggregated structures that release HG upon mild acid hydrolysis, as well as individual HG molecules, some branched with GalA sidechains [137]. HG was only degraded under conditionsthat break GalA-GalA linkages, and no detectable decrease in HG length was seen on removal of rhamnose by acid hydrolysis, which would be expected if the RGI region were interspersed with HG [137]. This suggests that the neutral sugars are located in the aggregates or at the ends of HG, favouring the alternative model [375].

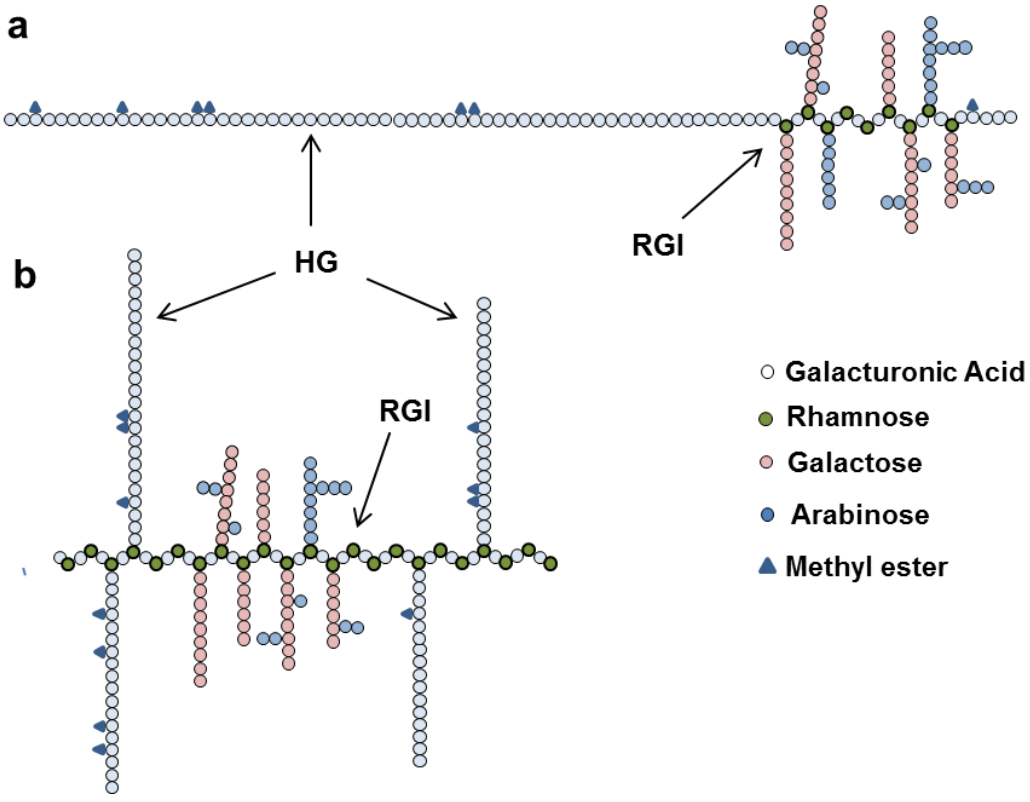

Figure 5 ***Schematic diagrams of two proposed structures of pectin.*** (a) The generally accepted contiguous model of pectin. (b) An alternative structure whereby HG are side chains of RGI.

1.4 Sources of Pectin

Industrial pectins have particular specifications, confirmed by the Food and Agriculture Organisation that includes no less than 65% GalA, as well as various other stipulations to fulfil the specification of E440 as a food additive. However, pectins from different sources can vary in polymer size distributions, molecular weight, DE, the nature and placing of the neutral sugars as well as the addition of acetyl and feruloyl groups. Pectin structure from the same sources also vary with respect to the differences between plantations, climates, hereditary traits of the trees and could even vary day to day owing to factors such as the ripeness of the fruit and the weather prior to harvest [138]. It is these diverse structures from different sources and extraction conditions and modifications that make it possible to tailor pectins for distinct functionalities.

1.4.1 Citrus peel

Traditionally, citrus peel and apple pomace, as waste products from juice production, are the main sources of industrial pectin. Citrus peel is the more widely used, desirable due to its high pectin yield of 30-35% [114] and superior gelling properties. Commercial citrus pectin has relatively long HG chains, with a MW of approximately 79-200 kDa, and a high DE of around 70% [139, 140]. It additionally has a low DAc, and comparatively low neutral sugar content which make it suitable as a gelling agent.

1.4.2 Sugar beet pulp

An emerging source of pectin is from sugar beet pulp. Each year it is estimated that about 4 million tons of sugar beet pulp is generated in the European community as a result of the extraction of sugar from sugar

beet. This pulp is used primarily as a low-value animal feed; however the increased production of this waste-stream, as well as the increased cost of energy to prepare animal feed has diminished demand for this product. However, sugar beet pectin comprises ~19% of the pulp [141], which, if its functional properties are characterised, could potentially add value to this waste-stream. Its relatively high pectin yield and the ready availability of the raw material have made it a source that has justified extensive study.

The chemical structure of sugar-beet pectin has been characterised by means of acid hydrolysis and enzymatic degradation [142, 143] [130, 144, 145] and AFM [146, 147]. It has a relatively high DAc [148], a low DE, higher neutral sugar and protein content than other commercial pectins [141, 145]. Furthermore, unlike pectins from many other sources, sugar beet pectin contains feruloyl groups attached to the O-2 position of (1→5)–α-L-arabinans and the O-6 position of (1→4)-β-D-galactans within the RGI regions [134, 142]. The foremost commercial distinction of sugar beet pectin is that it has poor gelling ability, which is thought to be the result of these chemical characteristics [149].

1.4.3 Potato pulp

Potato pulp is a waste material of the potato starch industry. It is estimated that one million tons of potato pulp are created annually, of which only a minimal amount is exploited as animal feed [150]. Like sugar beet pectin, potato pectin has poor gelling properties which have been associated with a relatively high neutral sugar content [150]. Potato pectin is especially rich in RGI, of which the neutral sugar side chains are predominantly linear galactans, arabinogalactan I, and to a lesser extent highly branched arabinans [151].

1.4.4 Additional sources

Other pectins under investigation that are thought to have attractive industrial properties are those extracted from sunflower head residues

[152], olive pomace [153], and peach [154]. As well as dietary sources, pectic polysaccharides are often extracted from plants usually associated with traditional medicine [155-159].

1.5 Pectin extraction and modification

1.5.1 Pectin Extraction

The physical properties of pectin are highly dependent on the conditions of extraction [148]. Pectins in an aqueous environment are not stable molecules, and under conditions of high temperature and a pH outside of the stable range of pH ~3-4, degradation reactions such as depolymerisation and de-esterification will occur. Therefore, conditions of extraction should be carefully controlled to attain the desired final properties of the pectin. Procedures for the extraction of industrial pectins are usually optimised to enhance not only the highest yield of pectin, but also a high content of HG and methyl esters, which generates the useful functional gelling properties of pectin. As well as the structures of pectin *in situ*, the extraction method will have a significant influence on the properties of pectins. Industrial methods generally involve extraction with hot acid. The peel or pulp is suspended in 70-90°C water with nitric acid to pH 1-3 for 3-12 hours. This is then filtered and the fluid that has been leached from the plant material is concentrated and mixed with alcohol to precipitate the pectin, after which it can be dried and milled [138].

For research purposes, pectin extraction in the laboratory tends to be under milder conditions and to have more complex steps [148]. Extraction may be optimised to preserve or isolate parts of the pectin depending on what is being researched. An alternative method of pectin extraction is microwave-assisted flash extraction. As hot acid extracted pectin undergoes a relatively long period of heating, it experiences thermal degradation, whereas microwave extracted pectin can take just 15 minutes of heating, therefore producing a higher yield and higher molecular weight pectin in a fraction of the time [160, 161].

1.5.2 Pectin modification

To create pectins for different functions, the pectin has to be modified. This is easily achieved as pectins are unstable and susceptible to changes in pH and temperature. Pectin has good stability in aqueous solution at around pH 3-4. At acidic conditions lower than pH 3 glycosidic bonds and methyl-ester linkages may undergo hydrolysis. The rate of hydrolysis increases with higher temperature and lower pH [162]. Hydrolysis of the sensitive neutral sugar side chains may lead to an increase in GalA content and decrease in neutral sugar content. Studies have shown that mild acid hydrolysis causes the progressive release of sugars accompanied by their rapid degradation in the order of Ara>Gal>Rha>>GalA. This cleavage of glycosidic linkages in the HG chain causes a decrease in viscosity, molecular weight and polymer length [137, 163].

Incubation at high pH can significantly alter pectin structure. At a high temperature, alkali treatment will cause depolymerisation of the HG backbone by β-elimination, which occurs for glycosidic bonds of GalA moieties that are methyl-esterified at C-6 [164]. The rate of this reaction is accelerated with increasing degrees of methylation, temperature and pH [165]. Furthermore, at a high pH rapid de-esterification occurs [164, 166]. This cleaving of methyl esters is the most common modification in the pectin industry as it creates LM pectin useful for making gels with low sugar content. Pectin is often used in the process of jam-making and the usual method involves boiling HM pectin with sugar and citric acid, which make the pectin less soluble in water and on cooling sets to form a gel network. However, products with reduced sugar content require LM pectins to set as a gel. After pectin extraction, pulp can be treated with alkali or acid at a low temperature to cleave methyl-esters while retaining the long HG chains. Once esters are cleaved, carbonyl acid groups remain, and these negative acid groups have a strong affinity for small counter ions, such as calcium. The removal of esters needs to be sufficient enough to create blocks of GalA which associate between chains via this calcium binding to enable a gel network to form in the

absence of sugar at room temperature. This interaction with calcium also makes LM pectins useful as a stabiliser in yogurt and milk-based drinks. Ammonia is also sometimes used to convert ester groups into amide groups to achieve amidated pectin, which behaves much in the same way as LM pectin.

Enzymes such as methylesterase can be used in the de-esterification process of pectins, and are known to give a more precise structural outcome [167]. However due to economic restraints they is rarely used in industry. In the laboratory enzymes are an extremely useful tool to characterise pectin subunits and study molecular structure [136, 168, 169], as well as create pectic fractions for the study of bioactivity [170, 171].

1.6 Pectin and cancer

1.6.1 Pectin and anti-cancer activity

Polysaccharides (glucans, glycans, galactomannans, pectins etc.) from plants and fungi have long been used by cultures around the world for their medicinal and dietary benefits, and recent studies have shown certain polysaccharides to have anti-cancer effects [172-174]. Pectins and pectic polysaccharides, such as RGI and arabinogalactan, are among these compounds. High intakes of dietary fibre have been associated with a lower incidence of certain cancers, and this has given rise to considerable research into the anti-cancerous effects of pectin and pectic polysaccharides. Okhami and colleagues discovered that rats with azoxymethane-induced colon tumours that are fed diets containing 20% apple pectin or 20% citrus pectin showed a decrease in the number of tumours, with apple pectin having the most significant impact. They believe this is due to pectin decreasing faecal bacteria enzymes, which are potentially key in the generation of carcinogens [175]. A corresponding study by Tazawa and co-workers reported that rats fed a diet supplemented by 20% apple pectin presented a significantly decreased number of colon tumours and tumour incidence [176]. Pectin

also has potential as a prebiotic, stimulating the growth and activity of advantageous bacteria in the colon [177, 178]. Short chain fatty acids (SCFA's) are produced when pectin is fermented in the gut and are thought to modulate various proteins associated with colon cancer progression [179, 180]. Avivi-Green and colleagues found that dimethylhydrazine-treated rats fed a pectin rich diet had decreased tumour number and volume, as well as cells with decreased Bcl-2 expression and a high apoptotic index. They assume that SCFA's may play a key role, although this is just speculation [181]. Reactive oxygen species (ROS) have also been implicated in the effect of dietary pectin on colonocyte modulation and apoptosis. ROS's have been implicated in the effect of dietary pectin on rat colonocyte apoptosis. Sanders and co-workers found that feeding rats a diet rich with fish oil and pectin enhances apoptosis, and this may be due to a modulation of the redox environment that promotes ROS-mediated apoptosis [182].

There is a large body of literature on the effects of pectin and pectic polysaccharides on immune system function. Citrus pectin [183] and apple pectin [184] can affect cytokine production by lymphocytes, and numerous pectic polysaccharides can stimulate NO secretion, increase lymphocyte proliferation, complement fixing activity, and macrophage phagocytosis [158, 185-187]. As the progression of cancer and the immune system are inextricably linked, these studies play an important role in understanding the benefits of pectin on cancer progression, as well as other conditions such as gastric ulcers [188], bacterial infection [189] and wound healing [190].

1.6.2 Modified pectins and anti-cancer activity

There is growing evidence linking modified forms of pectin with anti-cancer activity. These pectins are often referred to as 'modified pectin' (MP), an ambiguous term simply meaning pectin that has been modified using pH, heat or enzymes. The majority of studies into the anti-cancer effects of MP utilise pectin from citrus peel, presumably for the reason that this is the main source of commercial pectin. Studies using modified

citrus pectin (MCP) may have MCPs of different structures due to varying extraction and modification methods.

Studies have highlighted effects of MP that are considered distinct from the effects of unmodified pectin. A seminal study by Platt and Raz [191] indicated that citrus pectin modified with pH and heat (MCP) to purportedly become lower in molecular weight and richer in galactan side chains has anti-cancer activity while the unmodified citrus pectin (CP) does not. Mice were injected with melanoma cells, and the formation of tumour colonies in the lungs was measured. It was found that mice injected with CP suffered from several tumour colonies in the lungs, whereas mice injected with MCP saw a 90% decrease in tumour colonies. This study built on the original hypothesis of Uhlenbruck and co-workers [192] that β-galactose containing compounds could bind and block lectins. Since the study by Platt and Raz the principal explanation for the anti-cancer effects of MP is that galactan side chains on MP can bind to and inhibit Galectin-3 (Gal3), a multifaceted and pro-metastatic protein whose expression is upregulated in many cancers. Gal3 can preferentially bind to β-galactosides via its carbohydrate binding domain. The biology of Gal3 will be discussed later in section 1.7.

Numerous studies investigating the effects of MCP on cancer cell lines, rodents and human cancer patients have been published. In a similar vein to Platt's first study in mice, Pienta and colleagues investigated the effects of oral intake of MCP in rats injected with MAT-lylu prostate cancer cells. Again, MCP significantly reduced the number of tumour colonies in the lung, while CP did not. They also found that MCP inhibited the adhesion of MAT-lylu cells to endothelial cells *in vitro* [193]. Adhesion of cancer cells to the endothelium is a major step in the formation of tumours and the ability to metastasise. Another similar study looked at mice injected with colon cancer [194] and breast cancer cells, as well as the adhesion of breast cancer cells to endothelial cells [195]. All results were consistent with Pienta's study.

More recently, the majority of the studies relating to MP and cancer have been carried out with MCPs, specifically two patented MCPs; pH and temperature modified GCS-100 (La Jolla Pharmaceutical Co., CA, USA) and enzymatically modified Pectasol-C (Econugenics, CA, USA). Several studies confirm the anti-cancer effects of GCS-100. GCS-100 has been found to induce apoptosis, via activation of caspase-8 and -3, in multiple myeloma cells resistant to chemotherapeutic drugs melphalan, doxorubicin and bortezomib, possibly by overcoming the cytoprotective effects of Bcl-2 [196]. Extending this study, Streetly and co-workers confirmed an induction of myeloma cell apoptosis by GCS-100, this time via down-regulation of pro-survival proteins Bcl-XL and MCL-1, as well as up-regulation of p21, a regulator in cell cycle and cell growth progression [197]. In another study to demonstrate the effectiveness of GCS-100 in drug resistant cancer cells, GCS-100 was able to enhance cell sensitivity to cistplatin, a chemotherapy drug used to induce apoptosis [198]. GCS-100 has also proved to be successful in the treatment of patients with relapsed chronic lymphocytic leukaemia, with 4/24 patients showing >50% shrinkage of lymph node regions [199].

Pectasol-C is currently marketed in the US as a health supplement. Pectasol-C has a very low MW of 5-10 kDa and it has been postulated that this low MW allows it to be absorbed by the body, while larger MW pectin stays in the gut. Pectasol-C is known to chelate heavy metals in the bloodstream, which supports this claim [200]. Several studies have investigated the activity of Pectasol-C in numerous cancer cell lines, as well as in prostate cancer patients. Pectasol-C was found to inhibit proliferation [201], induce apoptosis and cell cycle arrest [202] in several prostate cancer cell lines, as well as inhibit breast and prostate cancer cell adhesion and migration when combined with two other Econugenic health supplements BreastDefend and ProstaCaid, respectively [203]. In a paclitaxel drug resistant ovarian cancer cell line, combination of this chemotherapy drug with Pectasol-C was found to overcome sensitisation and reduce cell viability [204]. Pectasol-C has also been found to have immunomodulatory properties including activation of NK cells, T-cytotoxic

and B cells against K562 leukemic cells [205] and reduce renal injury and fibrosis in rats with acute kidney injury [206]. Positive effects of Pectasol-C have also been shown in humans with prostate cancer. A phase II study reported that eight out of ten men, returning after an initial treatment with surgery or radiation for prostate cancer, showed increased prostate-specific antigen (PSA) doubling time after taking Pectasol-C every day for 12 months. Prostate-specific antigen (PSA) doubling time is a measure of the rate at which blood levels of PSA rise. PSA is a marker of prostate cancer progression or recurrence, and so longer PSA doubling time is associated with slower disease progression [207]. A later trial in patients with advanced solid prostate tumours demonstrated that 20.7% of patients studied had an overall clinical benefit from oral intake of Pectasol-C [208]. These results help to confirm an acceptable human safety profile of MCP.

Numerous studies have shown bioactivity from MPs from various other sources. Li and colleagues studied the effects of modified apple pectin on a mouse model of colitis-associated colon cancer and showed that it enhanced apoptosis, decreased inflammation and prevented tumour formation [209]. Pectic polysaccharides from various plants including swallow root and ginger, as well as CP and arabinogalactan from larchwood, induced breast cancer cell apoptosis [210]. RGI derived from okra reduced cell-cell contact and adhesion, increased apoptosis and decreased cell proliferation in a mouse melanoma cell line [211], and ginseng pectic polysaccharides were shown to reduce murine fibrosarcoma cell migration [212] and reduce colon cancer cell proliferation [213].

1.7 Galectins and Galectin-3

1.7.1 Galectins

Galectins are a family of soluble β-galactoside-binding lectins that have diverse biological functions both inside and outside cells and are implicated in cancer, immunity and inflammation. A lectin is a protein that

does not chemically modify its ligands but binds and forms multivalent non-covalent complexes with them. There are 15 mammalian galectins with distinct similarities. All have at least one carbohydrate recognition domain (CRD) of ~130 amino acids arranged in tight β-sheets, and have an affinity for β-galactose-containing carbohydrates and glycoconjugates. They are found in and on the surface of a variety of cell types, as well as the surrounding extracellular matrix. In the face of these common features, galectins have been split into three structural groups. Prototype galectins have just one CRD and are either monomers (galectin-5 and -10) or homodimers (galectin-1,- 2, -7, -11, -13, -14, -15). Tandem repeat galectins have two CRD's connected by a short linker peptide (galectin-4, -6, -8, -9, -12). Finally the chimera type, of which galectin-3 (Gal3) is the only member, contains one CRD and also a non-lectin domain [214, 215]. Evidence that galectins are found in many types of cells and have a wide cellular distribution, despite their lack of signalling peptides, points to a multifunctional set of proteins. Indeed, they have been implicated in controlling cell-cell and cell-matrix interactions, adhesion [216, 217], proliferation [218], apoptosis[219-221], and inflammation [222-225]. Evidence suggests that the structural arrangement of galectins determines the affinity and specificity of the CRD on interactions with multivalent carbohydrates [226]. Therefore different galectins can confer separate functions and mechanisms of action. Galectin-7 has been implicated in breast cancer metastasis, as well as inducing apoptosis and up-regulating MMP-9 expression in lymphoma cells [227, 228]. Conversely, galectin-4 has been named as a tumour suppressor, down-regulating Wnt signalling target genes [229]. Galectin-8 appears to have dual functionality of a pro- and anti-metastatic galectin, inhibiting cell adhesion, migration in colon cancer cells while increasing migration in endothelial cells [230, 231]. Similarly, Galectin-9 has been implicated as anti-metastatic in myeloma cells [232] and breast cancer mouse models [233, 234], while causing increased cell adherence and aggregation in squamous cell carcinomas [235, 236].

The most widely studied galectins are Gal3 and galectin-1 (Gal1). Gal1 has been pinpointed as a potential therapeutic target in cancer due to its pro-metastatic behaviour [237-239]. However, it has also been implicated in inducing apoptosis in breast, colon and prostate cells [240-242]. Conversely, Gal3 has been repeatedly implicated in tumourigenesis, with substantial evidence of inducing cell migration morphogenesis and adhesion [243-247], cell proliferation, and inhibiting apoptosis [248-256] in a wide variety of cancer cell lines.

1.7.2 Galectin-3

Gal3 (also known as CBP35, Mac2 and IgEBP) is a 30kDa chimeric protein unique to the galectin family. It is found in the nucleus, cytosol, plasma membrane and surface of various cell types including epithelial and endothelial cells, cells of the immune system and erythrocytes. It has three domains: a NH2-terminal domain containing a serine-6 phosphorylation site, a collagen like pro/gly rich domain, and a COOH terminal containing the CRD and the NWGR death motif emblematic of the Bcl-2 family (Figure 6) [257]. It exists as a monomer in solution [258]. As the NH2-terminal contains serine-6 and -12, it can be phosphorylated by casein kinase I (CKI) [259]. This is thought to occur in the nucleus, where Gal3 can then be translocated to the cytoplasm to carry out its cellular functions [252]. The amino terminal domain also regulates self-association into dimers or oligomers [260, 261], allowing for multivalent interactions of which its biological activities can depend on. To investigate the importance of the NH2-terminal, Gong and co-workers used site directed-mutagenesis to delete its 11 amino acids, resulting in loss of Gal3 nuclear localisation, abolition of secretion and diminished carbohydrate-mediated functions [257]. However, there is evidence the carboxyl-terminal domain may also have a role to play in oligomer formation [261, 262].

The Gal3 CRD is essential for binding with β-galactose containing carbohydrates and glycoconjugates. It is comprised of 5- and 6-stranded β-sheets forming a β-sandwich. An apolar patch in the face of the 5-

stranded β-sheet may provide a site for monomer-monomer interactions. Like other galectins, Gal3 CRD has an affinity for lactose and N-acetyllactosamine (LacNAc), but it has a distinct attraction for larger oligosaccharides found on many cell surface and extracellular matrix molecules [215]. Gal3's ubiquitous cellular localisation in the nucleus and cytoplasm, as well as the extracellular microenvironment, lends it great flexibility as a regulator of many biological systems. Its ability to bind multivalent molecules as well as modulate apoptosis and cell proliferation connects it with the pathogenesis of numerous diseases and conditions. Complicit in inflammation [225, 263, 264] and fibrosis [265-267], Gal3 has also been intensely studied with respect to carcinogenesis.

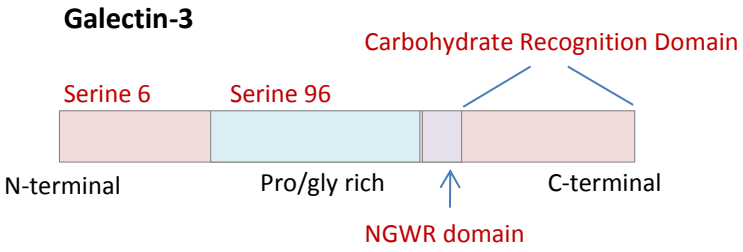

Figure 6 ***Galectin-3 Structure***

1.8 Galectin-3 and Cancer

1.8.1 Galectin-3 and cancer

There has been a great deal of conflicting data with respect to expression of Gal3 in carcinogenesis, depending on the type, the grade, and the localisation of Gal3. There is evidence that Gal3 is upregulated in cancers of the thyroid [268, 269], colon [270-272], liver [273], and downregulated in breast [274, 275] and prostate [237, 276] cancers. However, Gal3 has also been noted to be downregulated in CRC [277-279].

In malignant thyroid cells, there is significant evidence of high expression of Gal3 [268, 280], and there have been a number of published articles discussing the use of Gal3 expression as a diagnostic marker for thyroid carcinoma [281, 282]. A number of papers point to an overexpression of Gal3 in CRC [283, 284]. Analysing Gal3 expression in 153 tissue specimens of various stages of CRC, Schoeppner and colleagues found that there was a correlation between overexpression of Gal3 and the advancing stages of the disease, with survival greatest for patients with low grade Gal3 expression [270]. Further research confirms that by reducing Gal3 levels in mice, liver colonisation and spontaneous metastasis is clearly decreased [285]. Conversely, Lotz and co-workers concluded that progression from normal mucosa to carcinoma was associated with a significant fall in Gal3 protein and mRNA [277]. Decreased expression of Gal3 in breast cancer is associated with the invasive and metastatic phenotype, with reduced Gal3 correlating with increased histologic grade [274, 275]. Idikio and colleagues suggest this may be to do with decreased extracellular matrix binding and increased motility of invasive cells. However, an additional study found that if Gal3 is supressed in malignant breast cancer cells, this reduced tumour growth in nude mice indicating that Gal3 is necessary for the maintenance of the transformed tumorigenic phenotype [286].

There is also confirmation of decreased Gal3 in prostate cancer, and loss of Gal3 has been associated with cancer progression [237]. Pacis and colleagues found that Gal3 was expressed in 70% of benign or normal tissue compared to 10.5% of stage II and 53% of stage III tumours. The authors suggest that this alteration in Gal3 expression between tumour stages implies diverse roles for Gal3 in prostate cancer progression [276]. In fact, van den Brule and co-workers found that Gal3 translocating between the nucleus and cytoplasm in prostate carcinoma cells seemed to correlate with development of the disease. In normal lesions, Gal3 was found in the nucleus and cytoplasm, but in malignant lesions Gal3 was either non-existent or exclusively cytosolic [287]. This alteration of the cytoplasmic and nuclear expression pattern of Gal3 has been studied in

several papers. Gal3 can be predominantly cytoplasmic, predominantly nuclear, or dispersed between the two. Despite the differences in Gal3 expression in separate cancer types, the majority of research is agreed on the intracellular localisation. In normal or benign tissue Gal3 is either in the nucleus and cytoplasm, or mainly in the nucleus. In carcinogenic and metastatic tissues, Gal3 is always located in the cytoplasm and excluded from the nucleus [277, 287, 288]. This prompts a question mark as to whether Gal3 has anti-tumour activities in the nucleus.

1.8.2 Nuclear Galectin-3

Gal3 shuttles between the cytoplasm and the nucleus. The first 11 residues of the N-terminal and the last 28 residues of the C-terminal (within the CRD) are thought to be important for nuclear import [257, 289]. A study by Nakahara and colleagues found that Gal3 binds directly to importin-α, a protein that imports other proteins to the nucleus by binding a nuclear localisation signal (NLS), and is required for Gal3 nuclear localisation. The NLS equivalent in Gal3 is on the CRD and deletion of this sequence resulted in the complete loss of nuclear import [289]. Another critical factor in the export of Gal3 from the nuclear is its phosphorylation. Phosphorylated Gal3 is found in the nucleus and cytoplasm, whereas non-phosphorylated Gal3 is found exclusively in the nucleus. Takenaka and co-workers showed that in response to apoptotic insults, CKI phosphorylates Gal3 in the nucleus, so phosphorylated Gal3 can translocate to the cytoplasm to protect the cell from drug-induced apoptosis [252].

1.8.3 Intracellular Galectin-3

Gal3 is found intracellularly in the nucleus, cytoplasm, at the plasma membrane and at the mitochondria. Its main role inside the cell is thought to be in regulating apoptosis, proliferation and cell cycle progression, vital for the maintenance of tissue homeostasis and prevention of tumourigenesis. Its association with numerous ligands connected with cell survival illustrates Gal3's multifaceted behaviour.

Within its C-terminal, Gal3 encompasses a NWGR death motif emblematic of the Bcl-2 family (Figure 6, p.49). Members of the Bcl-2 family are vital to the intrinsic mitochondrial apoptotic pathway. Activated by events such as DNA damage, pro-apoptotic signals direct Bax, Bad and Bid to the mitochondria where they interact with anti-apoptotic Bcl-2 and Bcl-XL to establish whether or not apoptosis will be initiated. If the pro-apoptotic proteins prevail, cytochrome c is released from the outer membrane and interacts with the apoptosome, leading to the activation of effector caspases and apoptosis. For Bcl-2 to exert its anti-apoptotic actions, its BH1 domain is vital [290]. Within this domain is the highly conserved NGWR motif. As Gal3 is also anti-apoptotic, Yang and co-workers speculated whether Gal3 and Bcl-2 had common features. They indeed found that, unlike other galectins, Gal3 encompasses the NGWR motif [291]. They went on to demonstrate that Bcl-2 binds to Gal3 in a lactose-inhibitable manner. Bcl-2 is known to bind Bax via its BH1 domain, so it is possible that Gal3 regulates apoptosis via its interaction with Bcl-2. However, it should also be considered that Gal3 could mimic or replace Bcl-2. Akahani and colleagues mutated the NGWR motif of Gal3, and consequently found that it failed to inhibit apoptosis in breast carcinoma cells [292]. Gal3 also did not alter the expression levels of Bcl-2. Similar research by Yu and co-workers demonstrated that Gal3 is upregulated in the mitochondrial membranes following apoptotic stimuli. Here they revealed that Gal3 protects mitochondrial integrity and downregulates the caspase cascade following intrinsic apoptotic signals [251] Furthermore, they verified that synexin, a member of the annexin family of proteins that regulates intracellular vesicle fusion and membrane trafficking, is vital in translocating Gal3 to the mitochondrial membranes to carry out its anti-apoptotic functions. They note that while Bcl-2 exists on the mitochondrial outer membrane through its C-terminal anchor domains, Gal3 has no such domain, so the molecular actions are still unclear. They speculate that Gal3 could adhere to the mitochondria via Bcl-2, or directly interact with the mitochondrial permeability transition pore complex. Conversely, an additional study showed that Gal3 binds

and inhibits ATP synthase in the inner membrane of the mitochondria, and Gal3 suppression induces cell cycle progression in colon cancer cells [293]. In further research, Gal-3 null LNCaP prostate cancer cells were transfected with Gal3 and their reaction to pro-apoptotic treatments measured. To induce apoptosis, these agents induce DNA damage which increases Bad expression and increases its phosphorylation, leading to membrane depolarisation and cytochrome c release. In Gal3 transfected cells, induction of chemotherapeutic agents caused translocation of Gal3 from the nucleus to the cytoplasm where it reversed this pro-apoptotic effect by decreasing Bad phosphorylation and protecting mitochondrial integrity [255]

Another Gal3 associated ligand is KRas, a crucial protein in the regulation of cell growth, differentiation and apoptosis (Figure 7). KRas operates as a molecular on/off switch, alternating between GDP (inactive) and GTP (active) states. KRas has a region in the C-terminus that ends with a CAAX motif that directs it to the plasma membrane [40], where it is anchored via the C-terminal S-farnesylcysteine [41]. Once activated it recruits and activates a multitude of effectors including Raf and PI3K, essential players in cell proliferation, differentiation, survival and death. Gal3 is recruited by GTP bound KRas from the cytosol to the plasma membrane, where a hydrophobic pocket within the CRD of Gal3 is thought to accommodate the farnesyl group of KRas. KRas forms nanoclusters at the plasma membrane, which are essential for signal transduction. Once recruited to the plasma membrane, Gal3 becomes an integral nanocluster component, stabilising KRas in its active state and increasing signal output. Shalom-Feuerstein and colleagues found that when they mutated the Gal3 hydrophobic pocket, KRas nanocluster formation was reduced, along with cell proliferation and transformation [294].

Gal3 can also act on the PI3K/Akt pathway by upregulating Akt (Figure 7). Song and co-workers demonstrated that downregulation of Gal3 in colon cancer cells led to reduced phosphorylation of Akt, increased

GSK3β activity, and therefore phosphorylation of β-catenin and its degradation, leading to a reduction in cell proliferation [295]. Akt can also inhibit TRAIL sensitivity in bladder cells via inhibiting Bid cleavage, and therefore apoptosis, with Gal3 boosting this mechanism by activating Akt [296]. In keratinocytes, Gal3 was found to enhance Akt activity, while suppressing ERK activation [297].

Gal3 is additionally involved in the Wnt signalling pathway (Figure 7). Shi and colleagues showed that silencing Gal3 led to the inhibition of TCF/LEF-reporter activity, decreased cytosolic β-catenin and cyclin D1 expression in CRC cells [298]. Furthermore, Kobayashi and co-workers discovered that Gal3 upregulated β-catenin in pancreatic cancer cells. In addition, they found the mechanism to be Gal3 causing upregulation of phosphorylated Akt and GSK3β, and therefore β-catenin [299]. This theory is supported in a study of Gal3, β-catenin and cyclin D1 correlation in benign and malignant thyroid neoplasms [300]. Gal3 has also been shown to directly bind with β-catenin. Shimura and colleagues showed that the C-terminal of Gal3 (amino acid residues 63-250) binds the N-terminal of β-catenin, and co-localises with the β-catenin/TCF/LEF complex within the nucleus of CRC cells. This binding domain is within the CRD of Gal3 and is lactose inhibitable. They speculate whether Gal3 is involved in the nuclear retention of β-catenin, as the molecular mechanism that targets β-catenin to the nucleus is unclear [301]. In a corresponding study, Shimura and colleagues note that as well as phosphorylating β-catenin, GSK3β also phosphorylates Gal3 at serine 96 (Figure 7) [302]. As well as having an effect on cell proliferation via the Wnt pathway, Gal3 has also been shown to have an effect on cancer cell motility, morphology and malignant cell invasion. Kim and co-workers confirmed that Gal3 interacts directly with GSK3β. While investigating the effects of Gal3 on the actin bundling protein fascin-1, they found that mutating Gal3 at serine 96 decreased the level of fascin-1 expression, whilst also decreasing levels of phosphorylated GSK3β and nuclear β-catenin. They theorise that a Gal3, GSK3β, and β-catenin/TCF/LEF complex translocates to the nucleus, binds to the fascin-1 promoter,

increases fascin-1 expression, and therefore enhances cell migration [246].

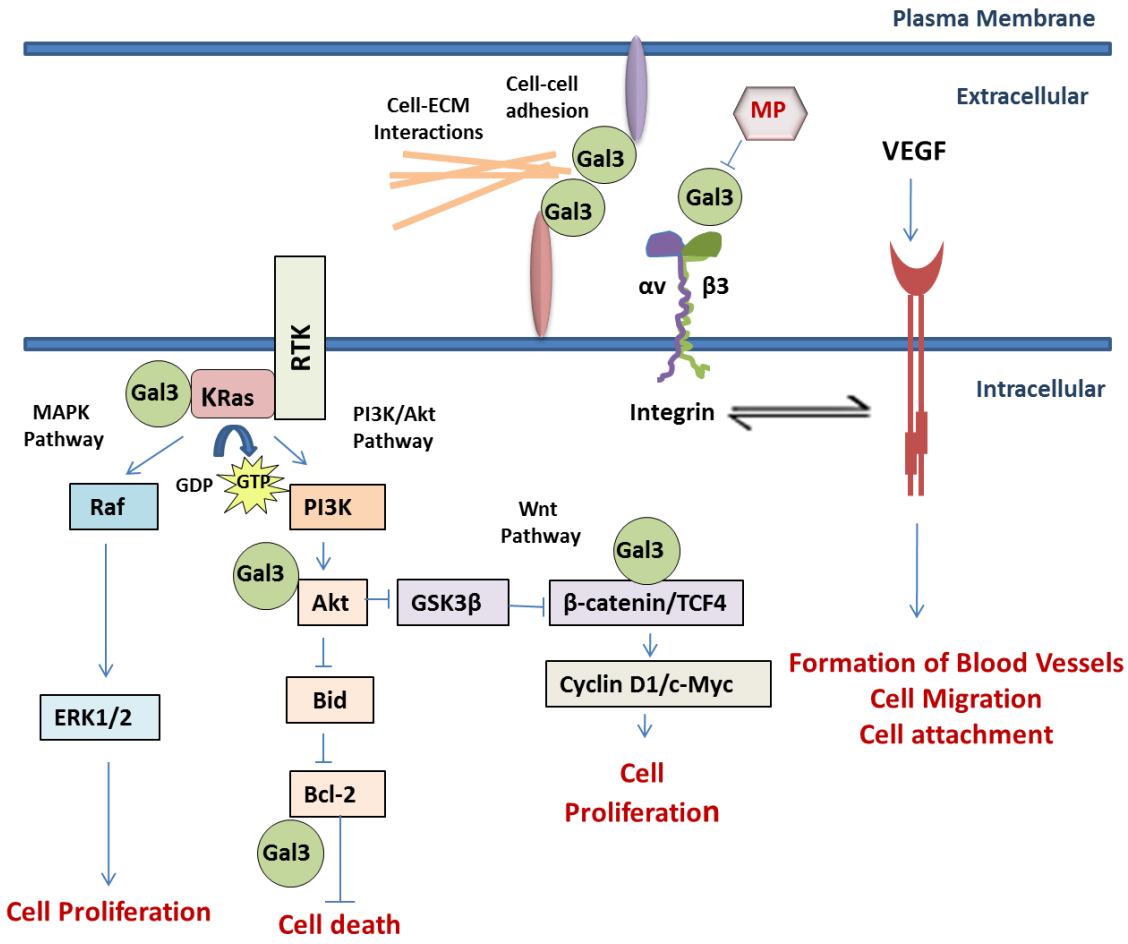

Figure 7 ***Cell signalling pathways associated with intra- and extracellular Galectin-3***

1.8.4 Extracellular Galectin-3

Galectins are well known to bind simple β-galactosides such as lactose, *N*-acetyllactosamine (LacNac) and poly-LacNac. Hydrogen bonding to O-4 and O-6 on galactose has been found to be important for stabilising lactose-based structures within the CRD [303], indicating the binding of terminal galactose residues within the CRD. Lactose is the simplest unit required for Gal3 binding [304], however the binding affinity is relatively weak and Gal3 has a stronger binding affinity for more complex oligosaccharides like polymers of β(1→3)-linked-LacNAc units found on many ECM and cell surface molecules [226]. The extracellular biological activities of Gal3 largely involve its interactions with β-galactoside-containing glycans on the surface of various cell types via the Gal3 CRD [305]. Extracellular Gal3 is thought to be involved in chemotaxis, chemoinvasion, aggregation and angiogenesis [243-247]. On the cell surface and in the microenvironment, Gal3 interacts with many ligands resulting in cell-ECM binding. These include laminin [306], collagen IV [307], fibronectin [308], and mucins. Colon cancer cells produce mucin glycoproteins on their surfaces and in the ECM, and production has been correlated with their metastatic ability [309]. The mucins contain polylactosamine chains which are a major ligand for endogenous Gal3.

Integrins are also major ligands for Gal3. Markowska and co-workers showed that Gal3 binds αvβ3 integrin N-glycans via its CRD. The ability to promote αvβ3 integrin clustering and subsequent activation of vascular endothelial growth factor (VEGF) and fibroblast growth factor (FGF) signalling drives angiogenesis. To confirm, the authors showed that when Gal3 was knocked down in cells this reduced VEGF and bFGF mediated angiogenesis [247]. Via another mode of action, Gal3 oligomer, α3β1 and NG2 proteoglycan (expressed by pericytes in newly formed blood vessels) form a complex on endothelial cell surfaces, activating α3β1 and inducing cell motility and morphogenesis [244]. Furthermore, a study by Nangia-Makker and colleagues showed that by injecting a mouse model with Gal3 expressing breast cancer cells and Gal3-null controls, tumour angiogenesis was significantly greater when Gal3 was present. They speculate that once

extracellular Gal3 binds to cell surface receptors, integrin αvβ3 increases, which causes endothelial cell migration and attachment. What is more, they found that if they neutralised Gal3 CRD, there was a reduction in tumour formation [243].

It is thought that for extracellular Gal3 to carry out its functions, the cleavage of secreted Gal3 is vital. Cleavage of galectins by matrix metalloproteinase's (MMPs) has been associated with progression of breast and prostate cancer in humans [310, 311]. The collagen α-like sequence of Gal3 contains a cleavage site for MMP-2 and -9 [312]. Nangia-Makker and colleagues showed that cleavage at this site is correlated with blood vessel density and progressive stages of breast cancer [313]. This cleavage is thought to allow the release of Gal3 into the tumour microenvironment, and subsequently induce chemotaxis, invasion and angiogenesis. In a pilot study, Balan and co-workers showed that a functional polymorphism in the Gal3 gene results in susceptibility to MMP2/9 cleavage. Using genotype analysis they also found that this polymorphism is related to racial disparity in breast cancer incidence in Asian and Caucasian women [292].

1.9 Modified pectin and Galectin-3

The pro-metastatic actions of extracellular Gal3 largely involve its interacting with oligosaccharides with terminal-linked galactose residues via the Gal3 CRD. Consequently, the hypothesis has arisen that it may be possible to inhibit metastasis of tumour cells by blocking lectins with galactose-containing polysaccharides. Given the structural and functional significance of the Gal3 CRD, numerous lactose-based compounds have been synthesised to bind specifically at this site [314-318]. However, due to non-specificity and potential side-effects, these synthetic inhibitors are potentially poor therapeutic clinical agents. Consequently, galactose-rich saccharides from food are thought to provide an attractive natural alternative.

A study by Evans and colleagues suggests that the protective effect of fruit and vegetable fibre in the diet could be related to their galactose content [319]. However, the majority of research into the galectin/galactose

hypothesis has been carried out mechanistically *in vitro* and *in vivo*. An early study by Beuth and colleagues showed that the metastasis of sarcoma cells to the liver in mice was inhibited by injection of arabinogalactan. The authors attributed this to the blocking of hepatic asialoglycoprotein receptor protein (liver lectin) by arabinogalactan, as it significantly delayed the elimination of asialoglycoprotein from the serum of mice. D-galactose delayed asialoglycoprotein elimination to a lesser extent to arabinogalactan and this was attributed to the rapid metabolism and elimination of D-galactose in the serum [320]. The direct binding of MPs to Gal3 was first demonstrated by Inohara and co-workers. Recombinant Gal3 added to plates coated with MCP or bovine albumin serum (BSA) as a control, stuck to MCP coated plates, but not BSA. This binding was completely blocked by lactose, which indicates a specific interaction between MCP and the Gal3 CRD [321]. Further investigations showed that MCP, but not CP, almost completely prevented the binding of Gal3 to endothelial cells [195]. A study utilising biophysical techniques including atomic force spectroscopy showed that specific binding to Gal3 CRD involves neutral sugar side chains containing terminal galactose at the non-reducing end of the polysaccharide chain. Studies on potato RGI and galactan showed that Gal3 specifically binds β(1→4)-linear galactans. NMR analysis of potato galactan showed the existence of linear side chains linked to the RGI backbone at an average length of 22 residues. The authors also reported that HG-domains derived from citrus pectin showed no specific interaction with Gal3 [322]. The disaccharide β-galactobiose was also shown to bind specifically to Gal3 [323].

MCP has also been shown to have an effect on Gal3 protein expression. In multiple myeloma cells, the anti-proliferative effect of chemotherapeutic agent dexamethasone was greatly enhanced by the MCP GCS-100, and was concomitant with a downregulation of Gal3 protein [196]. Conversely, melanoma cells incubated with okra RGI were shown to upregulate Gal3 protein located in the cell membrane. Okra RGI was shown to reduce melanoma cell proliferation and induce apoptosis and cell adhesion [211]. Similarly, modified apple pectin (MAP) increased levels of Gal3 in the

nucleus and cytoplasm of cells from a mouse model of colitis-associated CRC. As MAP enhanced apoptosis, decreased inflammation and prevented tumour formation in mice, as well as reduce levels of Gal3 in their serum, the authors speculate that the increase in intracellular Gal3 could be due to MAP preventing Gal3 binding to its targets, causing the cell to produce more Gal3 to compete with the actions of MAP [209]. Conversely, Liu and colleagues showed that despite MCP reducing liver metastasis in mice, serum Gal3 expression was shown to not be modulated by MCP, leading to speculation that extracellular Gal3 is blocked by MCP, while intracellular Gal3 remains unaffected [194].

As well as binding to Gal3, MCP has also been postulated to interact with and displace Gal3 from cells. In tumour bearing mice vaccinated with tumour antigen, injection with GCS-100 led to tumour rejection in 50% of the mice, whereas all control animals died. The effect was attributed to the ability of GCS-100 to displace Gal3 from the surface of tumour-infiltrating lymphocytes, facilitating surface mobility of T-cell receptors and their association with CD8, thus enhancing the cytotoxicity of the cells [324]. Additionally, Huang and colleagues showed that the concentration of Gal3 in culture medium after cultivation of liver and lung cancer cells was increased after incubation with enzyme-treated citrus pectin, as opposed to untreated or CP-treated cells. The authors speculate that the release of Gal3 from cancer cells could interrupt the binding of cancer-membrane bound Gal3 to normal cells, thus diverting adhesion, aggregation and subsequent metastasis.

A comprehensive study by Gao and colleagues has investigated the inhibitory effects of ginseng RGI on Gal3 [325]. The binding affinity of ginseng RGI for Gal3, determined by surface plasmon resonance, was significantly higher than that of MCP and potato galactan. Gal3 interactions were also verified by the binding of RGI to recombinant Gal3-coupled beads. Bound RGI was completely washed off by lactose, indicating a specific binding with the Gal3 CRD. However, the isolated backbone of RGI, devoid of galactan side chains, was also shown to bind tightly to Gal3, although this

was not lactose inhibitable indicating a non-specific interaction. The authors speculate that this could be an ionic interaction, although contemplate that it is possible that there may be secondary carbohydrate recognition sites within the Gal3 molecule. Additionally, ginseng RGI significantly inhibited the adhesion of HT29 cells to Gal3-coated plates, and inhibited the binding of Gal3 to T-cells. Furthermore, the authors employed a haemagglutination assay used in some investigations to measure the potential of Gal3 inhibitors. The assay was first employed by Sathisha and co-workers who showed that swallow root pectic polysaccharides significantly inhibited the agglutination of red blood cells. The agglutination is assumed to be Gal3-mediated as lactose also had inhibitory activity [210]. Ginseng RGI also significantly inhibited the agglutination of red blood cells, and the authors go on to demonstrate the importance of the galactan side chains of RGI in this activity. They attribute the inhibition of agglutination solely to the blocking of Gal3 by RGI [325].

Numerous studies investigating the effects of MP on cancer cells attribute anti-cancer effects to Gal3. Pectasol-C was shown to reduce cell viability, induce adhesion and apoptosis in ovarian cancer cells, with an enhanced effect when combined with the chemotherapy agent Paclitaxel. Conversely, exogenous recombinant Gal3 was shown to increase cell viability and inhibit adhesion and apoptosis. The authors claim Pectasol-C sensitises ovarian cancer cells to Paclitaxel via specific inhibition of Gal3 [204]. In another study, CP was shown to reduce proliferation in two colon cancer cell lines known to express Gal3, while CP had no effect in a Gal3 negative lymphoblast cell line, leading the researchers to believe that the anti-proliferative effect was possibly due at least in part to its capacity to inhibit Gal3 [326]. Induction of endothelial cell [327] colon [328], myeloma [197], and prostate cancer cell apoptosis [201], as well as fibroblast cell migration [212] has been attributed to the inhibition of Gal3 by Pectasol-C.

Despite numerous studies supporting the galectin-galactose hypothesis, it cannot be ruled out that MP may exert its bioactivity via Gal3-indepenent mechanisms. Two studies have showed that MCP significantly induced

apoptosis in the prostate cancer cell line LNCaP, which does not express Gal3 [201, 329], verifying that the mechanism must be Gal3-independent. A study into the relationship between guar galactomannan (HPGG) and Gal3 additionally showed that although HPGG bound strongly to recombinant Gal3, it bound weakly to endogenous Gal3 in a cell culture system, leading the authors to suggest that carbohydrate ligands on epithelial cell surfaces may impair HPGG binding [330]. Additionally, although MCP prevented Gal3-induced endothelial cell chemotaxis, MCP was also shown to prevent FGF-induced chemotaxis [195]. There are also a few studies that suggest distinct bioactive roles for pectin structures for oligomers of GalA. Pectic acid has been reported to induce apoptosis in rat pituitary tumour cells [331]. Liu and co-workers studied the effects of pentamers of GalA using a mouse model of colitis-associated CRC: the oligomers were found to be active against inflammation and carcinogenesis [332]. These studies demonstrate Gal3-independence as well as the bioactivity of non-Gal3-binding HG, which suggest possible multiple roles for pectin structures in bioactivity.

1.10 The structure-function relationship of modified pectin

Investigations into the bioactivity of pectins should be supplemented with an understanding of the structure of the biologically active pectin, although this can be complicated by the complex and often ill-defined nature of the starting material. A wide range of pectic polysaccharides, particularly from traditional medicinal plants, are known for possessing various immunomodulatory properties, and the relationship between structure and function of these polysaccharides is often addressed. Several studies have shown that the observed biological activities such as complement fixation [333-335] cytokine secretion [336, 337], increased phagocytosis [159], and lymphocyte proliferation [185], are due to neutral sugar-rich RGI regions. The immunomodulatory action of pectic polysaccharides is also thought to depend on the GalA content. GalA-rich pectins were shown to decrease accumulation of macrophages and inhibit leukocyte activity [159].

Despite the numerous studies investigating the structure-function relationship behind the immunomodulatory properties of pectic polysaccharides, no

mechanism of action has been identified. It has been suggested that the neutral sugar-rich RGI region of polysaccharides isolated from *Bupleurum falcatum* could cross-link with membrane B-cell receptors [338]. On the other hand, the anti-cancer activity of MP is habitually attributed to the inhibition of Gal3 by β-Galactan side chains on the RGI regions of MP. Consequently, the increased bioactivity of MCP to CP is often assumed to due be increased neutral sugar content. However, few studies have taken into account the structural aspects of MP to its ability to modulate cell activity or inhibit Gal3.

Evidence for the bioactivity of neutral sugars in MP is shown by studies into the anti-tumour effects of arabinogalactans, which have been shown inhibit the metastasis of sarcoma cells to the liver in mice [192, 320, 339] which the authors attribute to the binding of galactose to liver lectins. Sathisha and colleagues studied the effects of pectic polysaccharides from various plants including swallow root and ginger, as well as CP and larchwood arabinogalactan. In addition to inducing breast cancer cell apoptosis and reducing invasion, they found that swallow root pectin polysaccharides (SRPP) and CP inhibited the agglutination of red blood cells which they attributed to Gal3 inhibition. They suggest that this may be due to the presence of arabinose and galactose as major sugars in SRPP and CP, considering that ginger-derived pectic polysaccharide, which had no inhibitory activity, contained low levels of galactose. However, the authors suggest that the level of galactose alone may not be important as CP contained 19% galactose, compared with 25% galactose in Andrographis pectic polysaccharide, which had lower agglutination inhibitory activity. Arabinogalactan also had reduced activity, leading to the suggestion that the arrangement of galactose and arabinose as arabinogalactans may be important for activity, as well as galactose alone. Thus the steric accessibility of the galactose may be as important as the level of galactose present in the sample [210].

One research group has carried out extensive study into the structure and function of ginseng pectin. Ginseng pectin was broken down into neutral and acidic populations before fragmenting the latter into four parts using

sequential elution. Further purification resulted in four RGI-rich fractions and four HG-rich fractions. One HG-rich fraction was shown to reduce proliferation of HT29 colon cancer cells by 20% after 72 hours, while the RGI fractions had no effect [213]. HG-rich fractions also significantly inhibited L-929 murine fibrosarcoma cell migration, with the inhibitory effects increasing with GalA content, while RGI-rich fractions with low GalA content had no effect [212]. The authors suggest that the HG domain is an important functional element in the reduction of cell proliferation and the inhibition of cell migration. The latest study, by Gao and colleagues [325], has investigated the inhibitory effects of ginseng RGI, potato galactan, MCP and lactose on Gal3. An assay measuring the agglutination of red blood cells showed that the four samples greatly reduced agglutination in the order of ginseng RGI > MCP > potato galactan (P-Gal) ≥ Lactose, with ginseng RGI possessing the greatest inhibitory activity. As lactose was shown to inhibit agglutination, it was assumed agglutination was Gal3 mediated. Additional assays to measure the potential of Gal3 inhibition, including asialofetuin-induced breast cancer cell aggregation and recombinant Gal3 to HT29 colon cancer cell adhesion additionally showed the same sequence of Gal3 inhibitory activity. Subsequently, the importance of neutral sugar side chains on ginseng RGI activity was assessed. The enzymatic removal of 27% (1→4)-α-Ara side chains greatly increased the inhibitory activity of ginseng RGI, while the removal of 56% arabinan from AG chains was shown to decrease activity. The authors suggest that Ara could potentially regulate Gal3 binding depending on location. Two thirds of Rha residues in ginseng RGI were shown to comprise a side chain of between 1 to 4 Gal residues, with 20% of these side chains comprising 4 Gal residues. The complete removal of these long side chains greatly decreased inhibitory activity. However, activity was still relatively high and on a par with P-Gal and lactose. The importance of Gal chain length was consequently assessed using β(1→4)galacto-oligosaccharides. Agglutination inhibitory activity was shown to increase with Gal chain length, but only up to a tetramer, as chains between 5 and 65 residues did not provided additional activity. The Gal3 CRD is known to bind terminal galactose residues within the CRD and so the

authors suggest these results indicate that short chains of <4 Gal residues on ginseng RGI may still be significant in regulating the activity of Gal3. Furthermore, these β(1→4)galacto-oligosaccharides were shown to have significantly reduced inhibitory activity than ginseng RGI, indicating that the ginseng RGI backbone is as important to bioactivity as the Gal sidechains. Moreover, the ginseng RGI backbone, on complete removal of neutral sugar side chains, was shown to have a high binding affinity to Gal3. This binding was not lactose inhibitable indicating a non-specific interaction that could be an ionic interaction; however, the authors contemplate that it is possible that there may be secondary carbohydrate recognition sites within the Gal3 molecule. Additionally, a sample of HG-rich ginseng pectin was shown to have relatively high agglutination inhibitory activity.

Jackson and co-workers provided the first evidence that specific structural characteristics of pectin are responsible for inducing apoptosis in prostate cancer cells [329]. They investigated CP, Pectasol-C, a heat treated citrus pectin 'Fractionated Pectin Powder' (FPP, Thorne Research, Dover, ID, USA), as well as purified HG, sycamore RGI and red wine RGII. They wanted to investigate whether pectin prepared with different extraction protocols had similar biological effects. They found that out of all the samples, only FPP induced apoptosis in LNCaP prostate cancer cells. That HG, RGI and RGII had no effect implies that activity does not reside in the individual components. They also found no correlations between sugar ratios or molecular weight and bioactivity of these pectins. To assess the importance of methyl-esterification they treated FPP with alkali to remove ester linkages and found that this abolished the apoptotic effects. They also found that this alkali treatment also removed arabinan; however, they claim that specific removal of arabinan with endo-arabinase had no effect on apoptosis. They conclude that an ester-based cross-link in pectin is needed for the apoptotic activity of FPP. This study is additionally interesting as LNCaP cells do not express Gal3, demonstrating a Gal3-independent mechanism of action.

In conclusion, numerous different structures of MPs have been shown to modulate cell activity *in vitro* and *in vivo*; however, the structural elements of bioactive MP are rarely addressed. Exceptional studies have shown the significance of ester-based cross-links in HM pectin [329], β(1→4)-Gal side chains, the RGI backbone [325], as well as the HG backbone [212, 213]. Such a range of pectin structures suggests a structural polypotency whereby various structures of MP could potentially act by various mechanisms in order to modulate biological activity.

1.11 Modified Pectin Digestion and Absorption

Dietary pectin is typically assumed to be non-digestible, being resistant to hydrolysis during passage through the human GI tract and uptake into systemic circulation. Pectin has indeed been demonstrated to have significant advantages as a drug delivery system into the colon, as it has been found to not be broken down in the stomach or small intestine [340]. Despite the apparent inertness of pectin, it is known to have diverse roles in the GI tract including prebiotic activity [110, 177], modulation of intestinal nutrient uptake [341] and mucoadhesion [342]. LM and GalA-rich sugar beet pectin has been shown to adhere to porcine colon tissue via binding to mucins on the colon cell apical layer [343]. This has been corroborated in other studies, which showed that GalA-rich LM pectin can bind strongly to mucin [342, 344]. There is a surprising lack of information regarding the uptake and transport of pectin *in vivo*; however, there is recent intriguing evidence for the uptake of MP and pectic polysaccharides. Animal studies into the effects of oral consumption of MCP on tumours and metastasis suggest that MCP is effectively absorbed into the bloodstream and thereby able to act upon its sites of action. As confirmed in humans, MCP administered orally has been found to assist with the urinary excretion of toxic elements, with toxicity reduced in the bloodstream [200]. The authors attribute the uptake of MCP to low MW as compared with unmodified pectin which is thought to be too large to be absorbed and have an effect. However, Crinnion [345] has questioned the interpretation and structure of these trials.

Knaup and colleagues showed that amidated pectin and the monomer D-Galacturonic acid could have metabolic potential in the small intestine. Although stable in human saliva and simulated gastric juice, they found that in ileostomy fluid, representing the small intestine, 65-78% of the amidated pectin and 100% of the D-Galacturonic acid was degraded after 10 hours. Degradation produced SCFAs and methanol, but 15% of the pectin is unaccounted for [346]. Another study similarly found that 90% of ingested pectin was recovered in the terminal ileum, and suggest that 10% may have been degraded by bacteria at this site [347]. Bacterial degradation is entirely possible; however, it is feasible that some of the pectin could be absorbed in the small intestine. Support for the absorption of MP into the bloodstream comes from an early study by Sakurai and co-workers who showed that pectin RGI from *Bupleurum falcatum*, a Chinese medicinal plant, was detected in the bloodstream and liver of mice. Mice were fed purified polysaccharides from *B. falcatum* for one week and, using an antibody specific for *B. falcatum* RGI, detected it in the T-cell area of follicles in Peyer's patch staining, as well as in the liver. It is still not apparent whether the pectin was modified in the body by endogenous enzymes and other factors, but it could be concluded that at least some of the pectic polysaccharide was absorbed in the body after oral administration [348].

The theory that pectin fragments could be taken up by Peyer's Patches is intriguing, and a possible answer to the mechanism of systemic uptake of MP may be found in the studies on the uptake of β-glucans. β-Glucans, like pectin, are non-digestible carbohydrates that are fermented to some extent in the colon. Natural branched fungal β-(1-3,6)-linked glucans such as lentinan and schizophyllan are known for their immunomodulating effects [349], and although how β-glucans exert an effect in humans is still not completely understood, based mainly on animal studies, molecular mechanisms of uptake and the resultant anti-cancer effects have been suggested. β-glucans labelled with fluorescein have been used to track their uptake and processing following oral administration [350, 351]. It has been shown that soluble β-glucans such as lentinan and scleroglucan can be internalised by intestinal epithelial cells and gut-associated lymphoid tissue (GALT) cells [351],

facilitated by binding to receptors such as Dectin-1 and TLR-2. The internalised β-glucans were found to be engulfed by macrophages via the Dectin-1 receptor and then transported through the body to the spleen, lymph nodes and bone marrow. Whilst within the macrophage the β-glucans were broken down into smaller fractions which were released from the macrophages [350]. It remains to be determined whether there are analogous uptake and transport mechanisms involved in the bioactivity of MP.

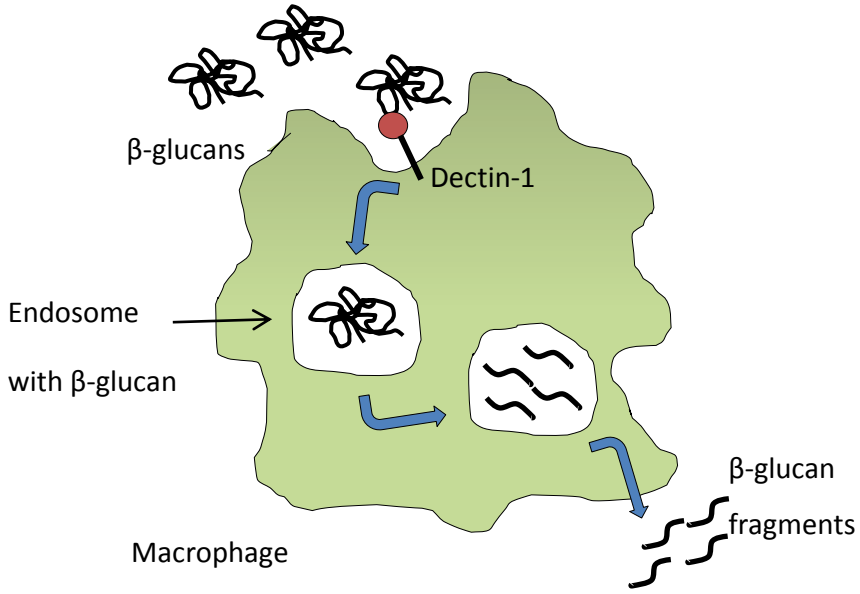

Figure 8 ***Uptake of β-glucans by macrophages***

As well as the uptake of pectin fragments via macrophages, another theory that fragments could directly traverse the small intestinal epithelium has been explored [352]. Utilising a Caco-2 cell monolayer representing the small intestine, transport of oligosaccharides across the cell barrier was monitored. On presenting FITC-labelled Pectasol-C to the monolayer, it was found that fragments of the pectin were transported; predominantly low DP RGI derived

neutral sugar fractions of linear galactan (DP 2-7) and arabinogalactan (DP 3-6). Epithelial cell junction tightness was inversely correlated with flux, confirming the paracellular pore as aroute for neutral oligosaccharide absorption. Intriguingly, acidic GalA oligomers of DP 2-26 were not able to traverse the barrier. However, an earlier study demonstrated modest transepithelial permeability of GalA polymers between 2-4 DP through Caco-2 monolayers [353].

Despite the long established acceptance that pectin is not broken down in the gut, evidence suggests that, although the bulk of pectin may not be absorbed, small MW fragments may be able to pass into the bloodstream and have systemic effects [200, 348]. The preparation of MP generates fragments that are potentially small enough to be absorbed, yet large enough to elicit bioactivity. It is not known whether these materials are further modified in the body. Knowledge of the uptake and transport within the body is important, both for understanding the fate of MP taken as drugs or dietary supplements, as well as the fate of native pectins on consumption of fruits and vegetables. Such studies would help answer the question as to whether health benefits of pectin can be obtained through the consumption of fruits and vegetables or processed foods or juices. Although the level of active components may be low compared to those used for treatment of cancer, lower levels might contribute to reduced risk factors for the onset and progression of cancers. Such studies would also help in proposing and testing the efficacy of claims for the bioactivity of medicinal plants and herbs.

Chapter 2
Materials and Methods

2.1 Cell culturing

2.1.1 Description of cell lines

All cell lines in this study are immortalised, adherent, epithelial colon cancer cell lines purchased from the American Type Culture Collection (Middlesex, UK). The DLD1 cell line was established from the colon of a male with

colorectal carcinoma; HT29 cells were isolated from a primary colon adenocarcinoma in a 44 year old Caucasian female; HCT116 were established from a primary tumour of the ascending colon of a 48 year old male; Caco2 cells were derived from colorectal carcinoma; the LoVo cell line was established from a colorectal adenocarcinoma of a 56 year old male (Ahmed 2013).

2.1.2 Passage and storage of cells

DLD1, HT29, HCT116, LoVo and Caco-2 cells were cultured in Dulbecco's Modified Eagle Medium: Nutrient Mixture F-12 (DMEM / F-12) (Invitrogen, Paisley, UK), supplemented with 10% heat inactivated foetal bovine serum (FBS) (Sigma, Poole, UK), and 2% Penicillin/streptomycin 1000U/ml (Invitrogen, Paisley, UK). Cells were maintained in a controlled atmosphere at 37°C with 5% CO2 in a HERAcell 150 CO2 incubator (Fisher Scientific, Loughborough, UK), and grown in TPP 75cm^2 or 25cm^2 filter screw cap tissue culture flasks (Helena Biosciences, Sunderland, UK). At 80% confluency they were passaged as follows. Medium was aspirated and cells washed with phosphate buffered saline (PBS) (Sigma, Poole, UK), then 1.2 ml Trypsin/EDTA (0.25% trypsin, 1 mM EDTA) (Invitrogen, Paisley, UK) was added and the flask incubated for 5-10 minutes at 37°C until cells were detached. 5 ml of medium was then added and the cells centrifuged at 200 g for 5 minutes. The pellet was re-suspended in 10mls medium and the cell number determined using a haemocytometer. Cells were disposed of after passage number 35. All filter pipette tips were sterile filter (Starlab, Milton Keynes, UK), and all equipment was sterilised and the cabinet carefully disinfected after each use with 70% ethanol and UV light twice a week.

2.1.3 Cell seeding concentrations

Table 3 shows the cell numbers required to be seeded per well depending on cell line (DLD1, HT29, HCT116, Caco-2 or LoVo), sample treatment time (24, 48, 72, 96 or 120 hours) and cell culture plate type (96- or 6-well plates).

Table 3 ***Cell seeding concentrations***

Cell line	96-well plate cells/well	6-well plate cells/well
24 hour treatment		
DLD1	15,000	150,000
HT29	15,000	150,000
48 hour treatment		
DLD1	4200	100,000
HT29	4200	100,000
HCT116	3500	85,000
72 hour treatment		
DLD1	2000	50,000
HT29	3000	75,000
HCT116	2000	50,000
Caco-2	6000	-
LoVo	2000	-
96 hour treatment		
DLD1	1000	30,000
HT29	2000	60,000
120 hour treatment		
DLD1	500	11,000
HT29	1500	30,000

2.2 Pectins and pectic polysaccharides

Commercial pectins were extracted and modified at CPKelco (section 3.3.1). Purified polysaccharide fractions potato galactan (Cat. P-GALPOT), β(1→4)-Galactobiose (Cat. O-GB1), larchwood arabinogalactan (Cat. P-ARGAL), Sugar beet arabinan (Cat. P-ARAB), citrus polygalacturonic acid (Cat. P-PGACT) and potato rhamnogalacturonan I (Cat. P-RHAM1, lot number 1201) were all purchased from Megazyme (Wicklow, Ireland). Pectasol-C modified citrus pectin was purchased from Econugenics (Santa Rosa, CA, USA).

2.3 Sample preparations for cell treatment

Pectins were dissolved by adding to filtered ultrapure water while vortexing at room temperature, to a concentration of 10 mg/ml. All pectins were placed under UV for 20 seconds using a Stratagene UV Stratolinker 1800 (Stratagene, Santa Clara, CA, USA), and all citrus pectins and pectic polysaccharides were filtered using a 0.2 µM syringe filter (Sartorius Stedim, Epsom, UK), before storage at -20°C. Pectin and cell culture medium solutions were made fresh for every experiment from stock solutions.

Farnesylsalicylic acid (Cambridge Bioscience, Cambridge, UK) was dissolved in DMSO (Sigma, Poole, UK) purged with argon gas for a stock solution of 50 µM. Staurosporine (Enzo Life Sciences, Exeter, UK) was dissolved in DMSO at a concentration of 0.01 µg/ml.

2.4 Cell viability assay

2.4.1 Sample preparation and WST-1 cell viability assay

Cells were seeded in Nunclon 96-well plates (Fisher Scientific, Loughborough, UK) at the densities specified in Table 3 (pg.72) in 100 µl medium and allowed to adhere overnight. Cells were then incubated with pectin samples or filtered ultrapure water at the concentration and times indicated at a final volume of 200 µl per well, using five biological replicates per sample concentration. Farnesylthiosalicylic acid (FTS, also known as Salirasib) (Cambridge Bioscience, Cambridge, UK), an anti-cancer drug known to reduce cell proliferation [354, 355] was used on every plate as a positive control at 150 µM. After incubation medium was removed and replaced with 100 µl fresh medium containing 10 µl WST-1 reagent (Roche Diagnostics, Burgess Hill, UK) used to create a formazan dye facilitated by the reaction between mitochondrial dehydrogenase released from viable cells and the tetrazolium salt of WST-1. To determine a suitable incubation time, absorption was initially measured at different time points after the addition of WST-1 (0.25, 0.5, 1, 2, 3, 4 and 5 hours), determining 3 hours as the optimal incubation time. The intensity of the coloured compound was then quantified using a Benchmark Plus microplate spectrophotometer with Microplate Manager 5.2.1 software (Bio-Rad Laboratories, Hercules, CA, USA), with absorbance measured at 450 nm, with the reference at 630 nm. Results were expressed as percentage of viable cells remaining after treatment relative to the untreated control. The statistical differences for the comparison of individual means were determined by the student's t-test. All analyses have been carried out using SPSS (IBM, Portsmouth, UK).

2.5 Cell imaging

Cells were grown in Nunclon 6-well plates (Fisher Scientific, Loughborough, UK) and exposed to pectins at the desired conditions. After the specified incubation times cells were imaged under a Leica M165C stereo microscope using Leica Application Suite V4.2 software (Leica microsystems, Wetzlar, Germany).

2.6 Apoptosis detection by flow cytometry

2.6.1 Sample preparation

2.6.1.1 Supernatants

Cells were grown in Nunclon 6-well plates and exposed to pectins at the desired conditions in Table 3 (pg.72). Staurosporine was used as a positive control at 0.1 ng/ml. After incubation, 200 µl supernatant from each well was removed, de-clumped with a CellTrics 50 µM filter (Partec, Milton Keynes, UK) and transferred to a Nunclon 96-well plate alongside corresponding 1 mg/ml pectin samples in medium, in triplicate, which were also filtered. Supernatant and pectin samples were then ready for analysis (section 2.4.2).

2.6.1.2 Cell samples

Adherent cells were washed with PBS, trypsinised for 20 minutes to detach all cells and after the addition of medium were put in 1.5 ml tubes, centrifuged at 200 g for 5 minutes and washed in 1 ml PBS. Cell staining was carried out using a FITC-Annexin V Apoptosis Detection Kit with PI (Biolegend, London, UK). Cells were twice centrifuged and washed with 1 ml 4°C cell staining buffer (Biolegend, London, UK), de-clumped with a CellTrics 50 µm filter and each sample re-suspended in 100µl Annexin V binding buffer, 2ul FITC-Annexin V and 4 µl PI. After gentle vortexing and a 15 minutes incubation in the dark, 100 µl Annexin V binding buffer was added and samples were transferred to a Nunclon 96-well plate along with the supernatants, pectins in medium at the concentrations specified, controls of unstained cells, and staining solution without cells. During apoptosis

phosphatidyl serine (PS) residues, which are normally located on the internal surface of the plasma membrane, are redistributed to the external surface. PS binds the protein Annexin V and so apoptosis can be observed by the incubation of cells with FITC labelled Annexin V [356]. PI is used for identification of dead cells with a loss of membrane integrity as it cannot penetrate an intact membrane.

2.6.2 Apoptosis data acquisition and analysis

Data acquisition and analysis were carried out using an EC800 Sony Eclipse flow cytometer with EC800 V1.3.6 software (Sony Biotechnology, Weybridge, UK) equipped with a 488 nm laser. Each sample was run at 20 µl/min for 4 minutes, capturing approximately 10,000 events. Fluorescence spill-over was appropriately compensated for. Figure 9A shows how the characteristic forward and side scatter profile of cells was used to construct gate (a) which distinguishes cells from debris. Both FITC and PI are excited by the 488nm laser, with FITC having an emission maximum of 520nm and PI of 617nm, allowing capture in separate PMTs (Figure 9).

2.6.2.1 Supernatants

Figure 9A was used to distinguish detached cells in the cell culture supernatant from debris and pectin. Any non-specific reactivity due to the presence of pectin in the culture medium was corrected for by subtracting the number of events acquired in culture medium containing pectin from those derived from the supernatant.

2.6.2.2 Cell samples

Gate (a) (Figure 9A) was used to examine PI and Annexin V reactivity of cells (Fig.9B). Next, through comparison with unstained control cells, a quadrant gate was constructed to distinguish the different patterns of PI and Annexin V reactivity. Within this quadrant live healthy cells have taken up neither PI nor Annexin V (b), early apoptotic cells have reacted with Annexin V alone (c), late apoptotic cells are Annexin V plus PI stained (d) and dead cells are stained with PI alone (e). The statistical differences for the

comparison of individual means were determined by the student's t-test using SPSS (IBM, Portsmouth, UK).

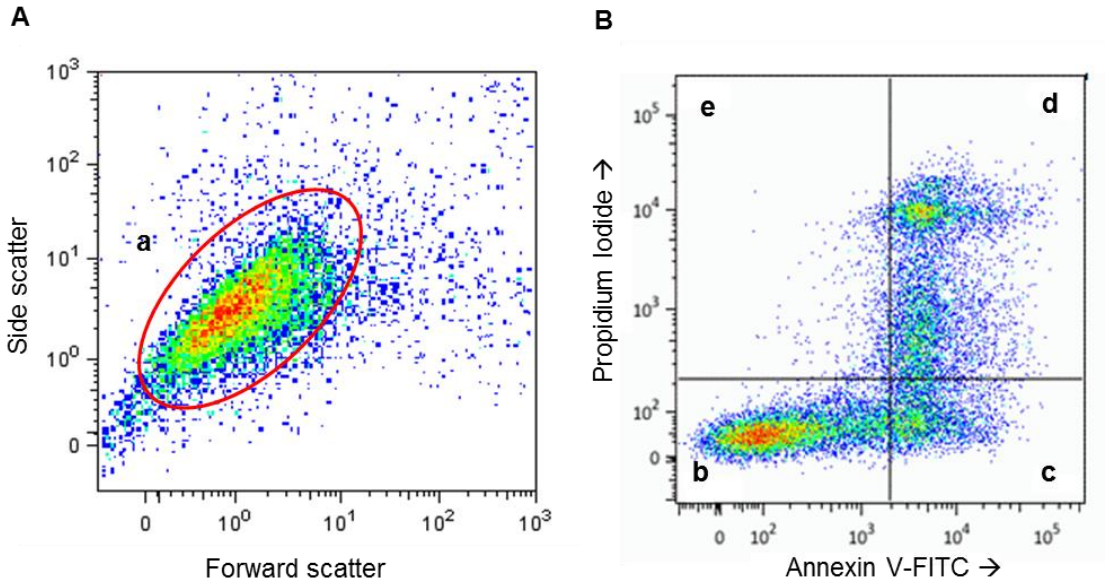

Figure 9 ***Flow cytometry method of analysis for apoptotic cells***. (A) Cells are gated by their characteristic light scatter profile to distinguish them from debris (a) live cells; (B) Cells within a quadrant gate show (b) live cells, (c) early apoptotic cells, (d) late apoptotic cells and (e) dead cells.

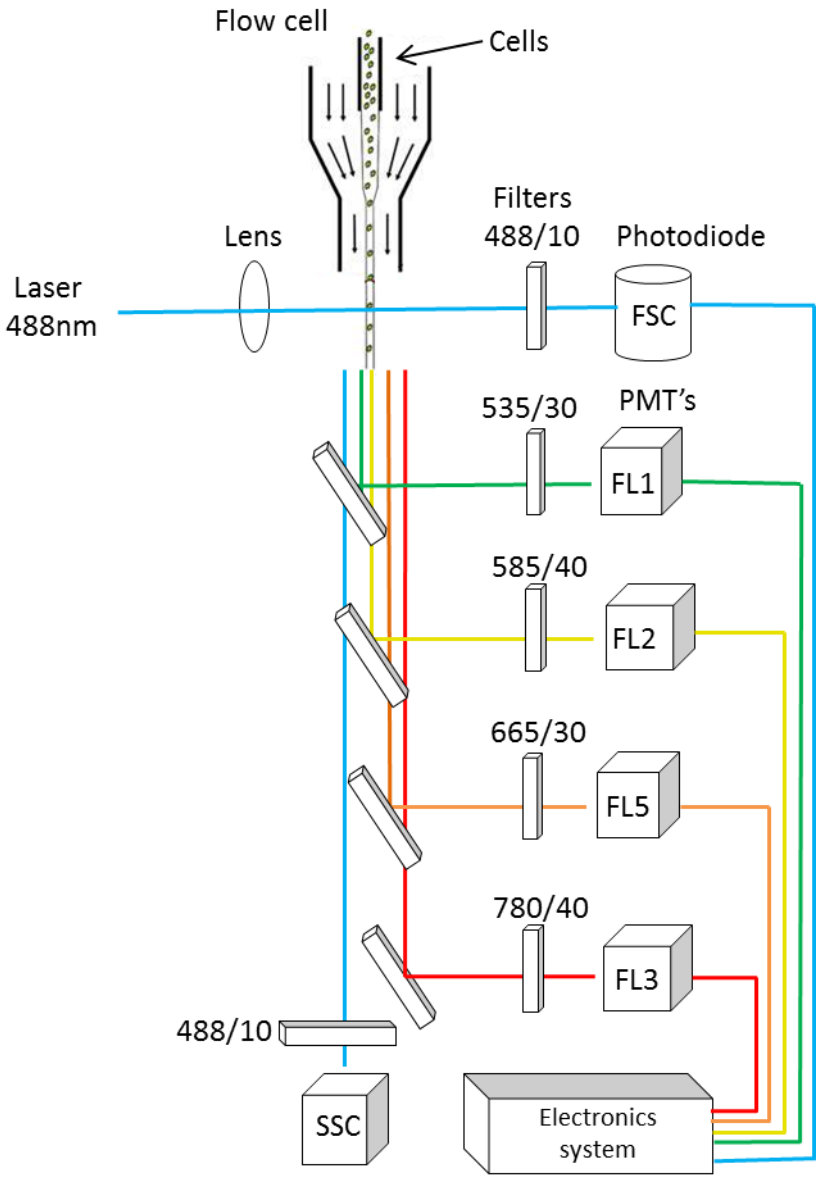

Figure 9 Simple layout of a flow cytometer. Particles are transported through a flow chamber into a laser beam. As the laser strikes the particle, some light is deflected off the surface. Forward scattered light (FSC), measuring cell size and surface area, is collected by a photodetector placed in line with the laser, while side scattered light (SSC), measuring cell shape and granularity, is collected by a photomultiplier tube (PMT) perpendicular to the laser beam. The laser beam additionally excites fluorophores, such as propidium iodide or FITC, attached to the particle which causes them to emit light at a longer wavelength than the laser. These signals are collected in the same direction as the SSC but pass through a series of filters to allow only certain wavelengths to reach the appropriate PMTs, which then generate electrical signals which are digitised and sent to the computer for analysis. Figure adapted from ('Flow cytometry, a basic intro' M. Ormerod)

2.7 Cell cycle detection by flow cytometry

2.7.1 Sample preparation

Cells were grown in Nunclon 6-wells plates and exposed to medium supplemented with or without pectins for the desired incubation times. FTS was used as a positive control. After incubation medium was removed and the cells washed with PBS and trypsinised (as described in section 2.6.1 above). After cell detachment and the addition of medium, cells were put in 1.5 ml tubes, centrifuged at 200 g for 5 minutes, washed in 1 ml PBS and centrifuged a second time. Cells were then re-suspended in 200 µl ice-cold PBS with 5 mM ethylenediaminetetraacetic acid (EDTA) and de-clumped slowly using a CellTrics 50 µM filter. Cells were then added drop wise to 1 ml 4°C 70% ethanol while vortexing, and incubated at 4°C for at least 2 hours. Before staining the cells were centrifuged at 200 g for 10 minutes, washed with 4°C PBS and centrifuged again before being re-suspended in a staining solution of 0.1% TritonX-100, 0.02 mg/ml PI and 0.2 mg/ml RNase A (Fisher Scientific, Loughborough, UK), made up to 200 µl with cold PBS. Samples were transferred to a Nunclon 96-well plate alongside controls of PBS only, staining solution only or unstained cells, and incubated at 37°C for 30 minutes ready for analysis. PI is used for the quantification of DNA content in the cells as it binds to DNA by intercalating between the DNA bases with no sequence specificity. PI also binds to double stranded RNA, which is removed by the RNase treatment.

2.7.2 Cell cycle data acquisition and analysis

Data acquisition was carried out with an EC800 Sony Eclipse flow cytometer (Sony Biotechnology, Weybridge, UK) equipped with a 488 nm laser. Each sample was run at 20 µl/min for 3 minutes, capturing approximately 10,000 events. Data acquisition and analysis were performed with EC800 V1.3.6 software. Figure 10 shows how cells were first gated to enable discrimation of single cells from doublets, multiplets and DNA fragments. To do this, a plot of pulse width versus pulse area was constructed (A). Doublets were identified by their higher area and width values than single cells which are

shown in oval gate (a). The PI uptake of cells within gate (a) was assessed in a histogram plot and markers were used to define phases of the cell cycle: sub-G1 (b); G0/G1 (c); S (d) and; G2/M (e). The statistical differences for the comparison of individual means were determined by the student's t-test using SPSS.

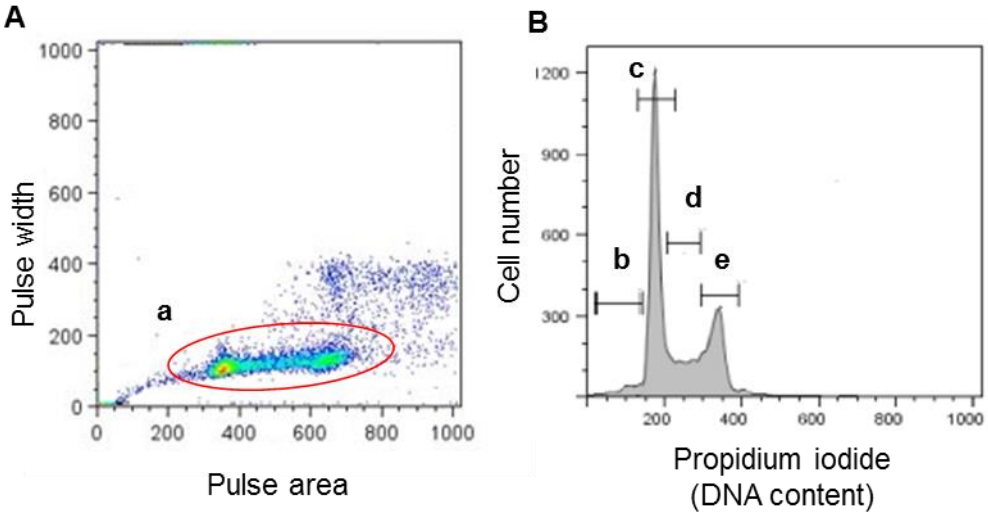

Figure 10 ***Flow cytometry method of cell cycle analysis***. (A) Single cells are gated (a); (B) Cells are gated into cells in (b) sub-G1; (c) G0/G1; (d) S and; (e) G2/M phases.

2.8 Cell counting

Nunclon 6-well plates were seeded at a concentration of 150,000 cells per well and 100,000 cells per well with HT29 and DLD1 cells, respectively, in 2ml cell culture medium. The initial cell concentration was chosen in order to have untreated cells at 80-90% confluency after 96 hours. After 24 hours, the culture medium was replaced with medium supplemented with or without 1 mg/ml pectin and incubated for the times specified. Each condition of treatment was carried out in duplicate over three independent experiments. After the desired incubation time 400 µl of trypsin-EDTA was added and

incubated at 37°C for 20 minutes to detach all cells. 1.6 ml of cell culture medium was added and cells were pipetted up and down carefully with a 1 ml pipette to de-clump, before being counted on a haemocytometer. Actual cell number was calculated by multiplying the mean number of cells counted by 10^4. Results were expressed as number of cells remaining after treatment relative to the untreated control. The statistical differences for the comparison of individual means were determined by the student's t-test. All analyses have been carried out using SPSS.

2.9 Analysis of gene expression

2.9.1 RNA isolation

RNA extraction was performed with the RNeasy Mini kit (Qiagen, Crawley, UK). Following exposure to pectins, cells were washed twice with PBS and then incubated with lysis buffer containing 1% (v/v) β-mercaptoethanol (Sigma, Poole, UK). Cells were scraped and lysate collected and transferred to 1.5 ml tubes on ice. An equal volume of 70% ethanol was added to each sample, and mixed before transferring into an RNeasy Mini spin column on a vacuum manifold. Under vacuum, samples were washed once with 700µl RWI buffer and twice with 500 µl RPE buffer. Columns were then transferred to a 2 ml tube and centrifuged at 13,000 g for 1 minute, before transferring again to a 1.5 ml tube. RNA was eluted by pipetting 30 µl of RNAse-free water directly onto the spin column membrane and centrifuging at 13,000 g for 1 minute.

2.9.2 DNase treatment

DNase treatment was carried out in order to degrade any DNA contamination in the RNA samples. This was carried out using DNase I kit (Sigma, Poole, UK). 1 µl 10x reaction buffer and 1 µl amplification grade DNase I was added to 8µl RNA extract, mixed and incubated for 15 minutes at room temperature. Duplicate tubes were prepared for reactions with and without reverse transcriptase to check amplification of contaminating DNA. 1 µl was then

added and heated to 70°C for 10 minutes to inactivate and denature DNase I and the RNA.

2.9.3 RNA quantification

A NanoDrop spectrophotometer (Labtech International, Uckfield, UK) was used to quantify RNA concentration by absorbance measurement at 260 nm. The 260/280 ratio was measured to assess the presence of contaminants, and samples with ratios ranging between 1.9 and 2.2 were accepted.

2.9.4 Reverse Transcription

cDNA was synthesised from total RNA. Amount of RNA (ng) was worked out for every plate according to the lowest concentration of the samples. RNA volume for 8 µl was between 250 and 470 ng for DLD1 cells and 740 to 760 ng for HT29 cells. Samples were made up to a total of 10ul with RNase free water. RNA samples were mixed, vortexed and centrifuged in a 96-well PCR plate (Fisher Scientific, Loughborough, UK) with 2 µl Quanta qScript cDNA Supermix (VWR International, Lutterworth, UK), which contains $MgCl_2$, dNTPs, recombinant RNase inhibitor protein, qScript reverse transcriptase, random primers and oligo (dT) primer. The plate was then incubated in a PCR thermal cycler (Applied Biosystem, Warrington, UK) using the following cycle: 5 minutes at 25°C followed by 30 minutes at 42°C and 5 minutes at 85°C. After the cycle was completed samples were diluted with EB buffer and EB buffer added to one well as a control. Samples were stored at -20°C for later use.

2.9.5 PCR Annealing Temperature Optimisation

Primers were designed using Universal Probe Library software (Roche Diagnostics, Burgess Hill, UK) and PCR was performed to determine optimal primer annealing temperatures (Tm). PCR reactions (10 µl) containing 5 µl Immomix (Bioline, London, UK), 1 µl BSA, 0.1 µl 50 mM $MgCl_2$, 2 pmol forward and reverse primer, 0.5 µl DLD1 cDNA and 0.5 µl HT29 cDNA made up to a volume of 7 µl with RNase free water. Reactions were incubated in a PCR thermal cycler (Applied Biosystems, Warrington, UK) and subject to the

following cycling conditions: 1 cycle of 95°C for 10 minutes, 35 cycles of 95°C 30 seconds, annealing temperature (58, 59, 60 and 61°C) for 30 seconds, followed by 72°C for 30 seconds. All reactions were then electrophoresed on a 3% agarose gel in Tris-acetate EDTA buffer (TAE buffer) supplemented with 0.01 µl/ml Ethidium Bromide (Fisher Scientific, Loughborough, UK). Samples were run for 50 minutes at 80 V and visualised by exposure to UV light to identify the annealing temperature that produced a single bright band.

2.9.6 Quantitative Real-Time PCR

RT-PCR was performed to measure the mRNA levels of target genes. The housekeeping gene 18S ribosomal RNA (18S) (Sigma, Poole, UK) was used as a reference gene for data normalisation. Primers were designed using Universal Probe Library software (Roche Diagnostics, Burgess Hill, UK). A probe labelled with 5' reporter dye, FAM (6-carboxyfluoroscein) and 3' quencher dye, TAMRA (6-carboxytetramethylrhodamine) (Sigma, Poole, UK) was used combined with primers based on 18S gene sequences. All other primers were combined with SYBR Green (Fisher Scientific, Loughborough, UK) to detect PCR product. 18S primer sequences are shown in Table 4.

Table 4 ***18S primer sequences for RT-PCR***

Gene		Sequence (5' - 3')
18S	F	GTATTAGCTCTAGAATTACCACAGTTATCC
	R	GGCTCATTAAATCAGTTATGGTTCCT
	Probe	[6FAM]TGGTCGCTCGCTCCTCTCCCAC[TAM]

mRNA quantification for all genes was performed in a 10µl reaction using a Mastermix of 5 µl Immomix (Bioline, London, UK), 1 µl BSA, 0.1µl 50mM $MgCl_2$, 2 pmol forward and reverse primer, 0.01 µl probe or 0.0625 µl SYBR Green, and 0.2 µl ROX, made up to a volume of 7 µl with RNase free water. A Corbett robot, set up with Robotics 4 software (Qiagen, Crawley, UK), and using Aeroguard T-Genesis pipette tips (Alpha Laboratories, Eastleigh, UK) was used to add 7 µl of the Mastermix to 3 µl cDNA in a Microamp optical 96-well reaction plate (Invitrogen, Paisley, UK). Microamp optical adhesive

film (Invitrogen, Paisley, UK) was used to seal the plate prior to analysis. Samples were run using the ABI 7500 Fast RT-PCR System (Applied Biosystems, Warrington, UK). Primers combined with probes were run using a 10 minute hot start at 95°C, followed by 40 cycles of denaturing at 95°C for 30 seconds and annealing/extension at 60°C for 60 seconds. Primers combined with SYBR Green were run using a 10 minute hot start at 95°C, followed by 40 cycles of denaturing at 95°C for 30 seconds and annealing/extension at the specified Tm for 30 seconds, and an extension of 72°C for 30 seconds.

Data were normalised against the reference gene 18S. The threshold cycle number (Ct) obtained was converted into fold of relative induction using the comparative $2^{-\Delta\Delta Ct}$ method [357]. The statistical differences for the comparison of individual means were determined by the student's t-test using SPSS software.

2.10 NMR spectroscopy

NMR analysis was carried out by Ian Colquhoun at the Institute of Food Research. NMR spectra were obtained on a Bruker Avance III spectrometer operating at 600 MHz for 1H and 151 MHz for 13C; the software was Topspin v3.2.The spectrometer was equipped with a TCI cryoprobe. Samples were prepared as solutions in D2O at concentrations between 10 and 40 mg/ml depending on solubility and viscosity. Spectra were usually recorded at 334°K or 338°K, although lower temperatures (320-330°K) were used in a few cases to avoid interference between the residual water signal and carbohydrate signals. 1H spectra were acquired using the water suppression sequence *noesygppr1d* (names of Bruker pulse programmes are italicised) with TD 65536 (time domain points); SW 20.49 ppm (spectral width); AQ 2.67 s (acquisition time); D1 3 seconds (relaxation delay); p1 ~7 µs (90° pulse length); NS 64 (number of scans). Free induction decays (FIDs) were Fourier transformed with an exponential window EM= 0.3 Hz and zero filling. ^{13}C spectra were acquired using the DEPT sequence, *deptsp135*, which gives positive CH and CH_3 signals with inverted CH_2 signals (quaternary carbons, e.g. –COOH are not observed). Key parameters

were TD= 65536, SW= 220.87 ppm, AQ= 0.98 s; D1= 2 s; P1= 12 µs (^{13}C 90^0 pulse); NS= 20000 to 80000, depending on sample concentration. FIDs were transformed with EM= 3.0 Hz and zero filling. Parameters used in the 2D NMR experiments are summarised Tables 5 and 6.

Table 5 *$^1H/^1H$ NMR correlation*

Experiment	Sequence	TD	SI	SW ppm	NS	Comments
COSY	*cosygpprqf*	2048x256	2048x1024	11.97x11.97	16	
TOCSY	*mlevphpr.2*	2048x512	2048x1024	11.97x11.97	24	MT= 0.1s
ROESY	*roesyphpr*	2048x512	2048x1024	11.97x11.97	24	MT=0.2s

Table 6 *$^1H/^{13}C$ NMR correlation*

Experiment	Sequence	TD $^1Hx^{13}C$	SI $^1Hx^{13}C$	SW ppm $^1Hx^{13}C$	NS	Comments
HSQC	*hsqcetgpprsisp2.2*	2048x256	2048x1024	11.97x165	72	
HSQC	*hsqcetgpprsisp2.2*	2048x256	2048x1024	11.97x70	72	High resoln. ^{13}C
HSQC-TOCSY	*hsqcdietgpsisp.2*	2048x256	2048x1024	11.97x165	192	MT= 0.15s
HSQC-TOCSY	*hsqcdietgpsisp.2*	2048x256	2048x1024	11.97x70	192	High resoln. ^{13}C
HMBC	*hmbcgplpndprqf*	2048x256	2048x1024	11.97x250	192	

TD is the number of time domain data points in each dimension (t_2xt_1); SI, the number of data points in each frequency dimension after 2D Fourier transformation (f_2xf_1); SW, the spectral width in ppm in each dimension; NS, the number of scans per t_1 increment; MT, the mixing time; in the high resolution versions of the $^1H/^{13}C$ experiments the chemical shifts of the sugar

ring ^{13}C signals are determined with greater accuracy, but the chemical shifts of e.g. acetate and rhamnose methyl groups fall outside the reduced ^{13}C SW.

Chapter 3
Analysis of the structure of commercial pectins and pectic polysaccharides

3.1 Introduction

Pectin is a family of heteropolysaccharides present in the cell walls of fruit, vegetables and land plants, with an extremely complex structure made up of several structural elements. However, a basic model of pectin comprises linear regions of HG interspersed with ramified RGI regions in which neutral sugars are present as side chains. HG is composed of linear stretches of α(1→4)-linked-GalA residues that are partially methylated at C-6 and acetyl-esterified at O-2 and/or O-3 [358]. The RGI region consists of repeating disaccharide units [→4)-α-D-GalA-(1→2)-α-L-Rha(1→]$_n$, highly branched with neutral sugar side chains attached to O-4 or O-3 position on the α-L-rhamnose. These side chains mainly consist of (1→4)-β-D-Galactans and (1→5)-α-L-Arabinans usually ramified with short (1→3)-α-L-Ara or single α-L-Ara residues. Depending on the source, pectin may also contain branched, type II (1→3,6)-β-D-Gal. AGI is also a common side chain with a basal chain of (1→4)-β-D-Galactan substituted with short (1→2)/(1→3)-α-L-Ara or single α-L-Ara non-reducing units, as well as AGII which has a backbone of (1→3)-β-D-Gal heavily substituted at position 6 by mono- and oligosaccharide Ara and Gal side chains. Other sugars including xylose, mannose, glucose and fucose can also be sometimes found covalently linked to the RGI backbone. Pectin additionally contains minor amounts of highly complex RGII regions that have a backbone similar to HG substituted with four side chains comprising ten different monosaccharides.

The predominant utilisation of pectin is in the food industry as a gelling agent and food stabiliser. Commercial pectin is produced mainly from citrus peel or apple pomace which is available as by-products from the juice industry. Additionally, a relatively small amount of pectin is produced from sugar beet pulp which is generated by the extraction of sugar from sugar beet. Pectins from different sources have individual structural characteristics which subsequently convey unique physicochemical properties which can be employed for particular commercial uses. Pectin from citrus peel is highly prized due to its substantial gelling properties, due to an abundance of long, highly methylated HG chains which form a gel network under acidic and high-sugar conditions. On the other hand, sugar beet pectin has inferior gelling properties which are understood to be due to their high acetyl content [149, 359]. Additionally, sugar beet pectin contains higher amounts of neutral sugars, particularly arabinan, which can be substituted with ferulic acid. Currently, the main use of sugar beet pectin is as an emulsion stabiliser, mainly due to the high protein content. Both citrus peel and sugar beet pulp, as industrial waste streams, are rich sources of pectin, with pectin making up 30% and 19% of dry weight, respectively [114, 360, 361].

Commercial extraction of citrus peel is optimised to extract a high yield of high MW and HM pectin in order to maximise gelling ability. Conditions of commercial extraction are generally to suspend the raw material in water at a high temperature (50-90°C) for 3-12 hours under acidic conditions (pH 1-3), usually brought about with nitric acid. The resulting solution is filtered, optionally concentrated and ion-exchanged, and then mixed with alcohol to precipitate the pectin [138]. The high temperature and low pH drive hydrolysis and subsequently depolymerisation of the pectic HG backbone. Acidic conditions also serve to reduce neutral sugar content, and acid hydrolysis is known to cause the release of sugar residues at different rates, in the order of Ara>Gal>Rha>>GalA [137, 358]. The higher the temperature and the lower the pH, the greater the rate of hydrolysis, neutral sugar breakdown and yield of pectin [163, 362].

Pectin can be further modified chemically or enzymatically. Incubation under alkaline conditions will reduce the DE of pectin [363], and is also known to reduce neutral sugar content, particularly arabinan [364]. β-elimination, and subsequent depolymerisation of the pectin backbone also occurs under these conditions unless the temperature is significantly lowered. Pectin structure can also be altered enzymatically. Polygalacturonase (PG), an enzyme that hydrolyses glycosidic bonds that link GalA residues of the pectin backbone, is sometimes employed to create low MW pectin, and methylesterase to remove methyl groups. However, due to high costs they are rarely used in industrial pectin production. Due to their specificity and selectivity in the degradation of pectins, enzymes are often employed alongside controlled chemical degradation in structural research to gain an understanding of pectin fine structure [143, 365, 366], as well as to create pectic oligosaccharides for experimental research into biological activity [170, 177, 325].

Nuclear magnetic resonance (NMR) spectroscopy is an analytical technique used in carbohydrate and polysaccharide chemistry to identify sugar constituents, their configurations and linkage positions. In addition it may be possible to determine the nature and location of any substituents. ^{1}H and ^{13}C NMR are the applications of NMR spectroscopy to hydrogen and carbon nuclei, respectively, these being the most important nuclei for carbohydrates. The ^{1}H spectrum is the foundation for most structure determinations particularly in conjunction with the powerful ^{1}H-^{1}H two-dimensional methods of COSY (correlation spectroscopy), TOCSY (total correlation spectroscopy) and NOESY/ ROESY (nuclear Overhauser effect spectroscopy and rotating frame Overhauser effect spectroscopy). The ^{13}C spectrum may be necessary for further characterisation of the molecule as the chemical shift range (~60-110 ppm for carbohydrates) is much greater than the corresponding ^{1}H range (~3-5.8 ppm) and the spectra are less overlapped. Additionally there is only one signal for each ^{13}C atom whereas ^{1}H signals are usually in multiplets. However, the NMR sensitivity of the ^{13}C nucleus is only $1.8x10^{-4}$ that of ^{1}H. Observation of ^{13}C signals with improved sensitivity is assisted by two-dimensional methods such as HSQC (heteronuclear single quantum

correlation for $^{1}H/^{13}C$ chemical shift correlation via one-bond hydrogen-carbon coupling, $^{1}J_{CH}$) and HMBC (heteronuclear multiple bond correlation for $^{1}H/^{13}C$ correlation via longer range H-C coupling, $^{n}J_{CH}$, where n = 2 or 3). Molecular structure can be ascertained from a combination of these homonuclear (^{1}H-^{1}H) and heteronuclear (^{1}H-^{13}C) 2D NMR methods to determine the connections between atoms within a molecule [367].

3. 2 Aims

This chapter will study the extraction and modification of ten pectins from citrus peel and sugar beet pulp, and study the structure of these and another seven pectic polysaccharides by way of anion exchange chromatography, size exclusion chromatography, mass spectrometry and NMR.

3.3 Materials and Methods

3.3.1 Pectin extraction and modification

Five sugar beet and five citrus pectin fractions were supplied by CPKelco. All extracts were filtered with Filtercel 450 (Advanced Minerals Corporation, CA, USA), precipitated in three parts 80% IPA, washed in 5L 60% IPA, adjusted to pH 4 with NaOH, then dried and milled. The procedure to extract and prepare the pectins is shown in Figure 11. The pectins were obtained by the following methods:

3.3.1.1 Raw materials

50 kg freshly dug sugar beet was chopped and washed in 30°C water under agitation for 30 minutes, drained, then washed once more for 30 minutes under agitation. Dried citrus peel was from lemons as a waste stream from the juice industry.

3.3.1.2 Commercial extraction of pectin

In a 50L extraction tank, 1000 g of dried citrus peel or 12.15 kg of washed sugar beet was mixed in a 50 L extraction tank with 70°C de-ionised water adjusted to pH 1.7 with nitric acid. Citrus peel and sugar beet pulp were then incubated for 3 and 4 hours under agitation, respectively. The liquid extracts were filtered and precipitated. The sugar beet extract was additionally vacuum evaporated at 60°C to concentrate to 5.4 times the original sugar content prior to precipitation, as measured by refractometry.

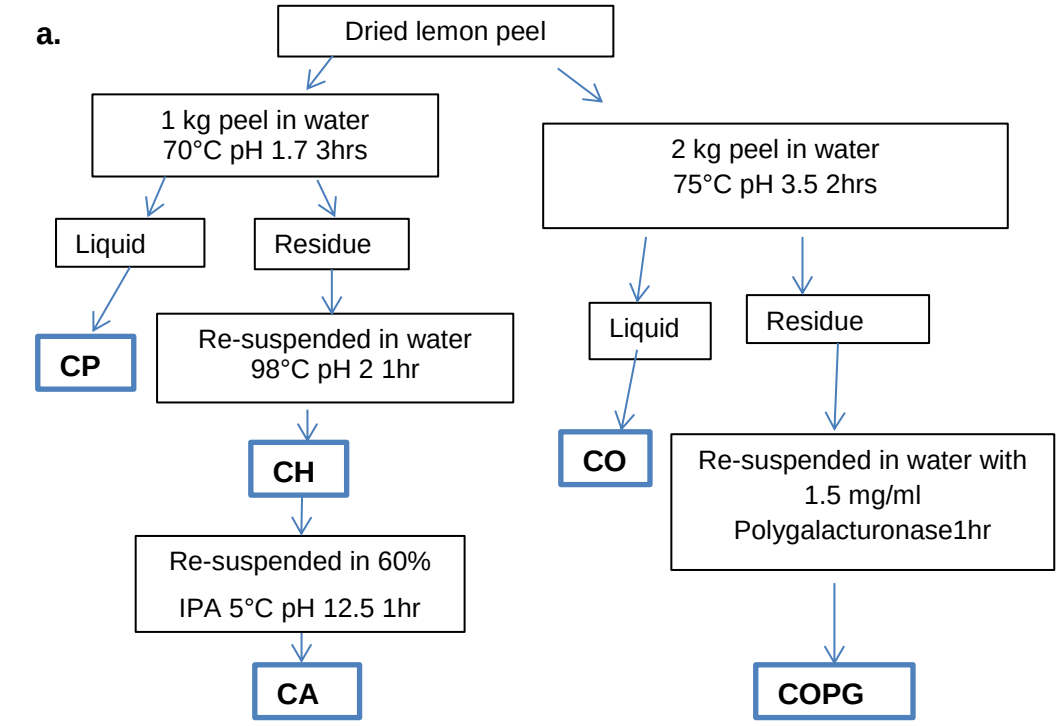

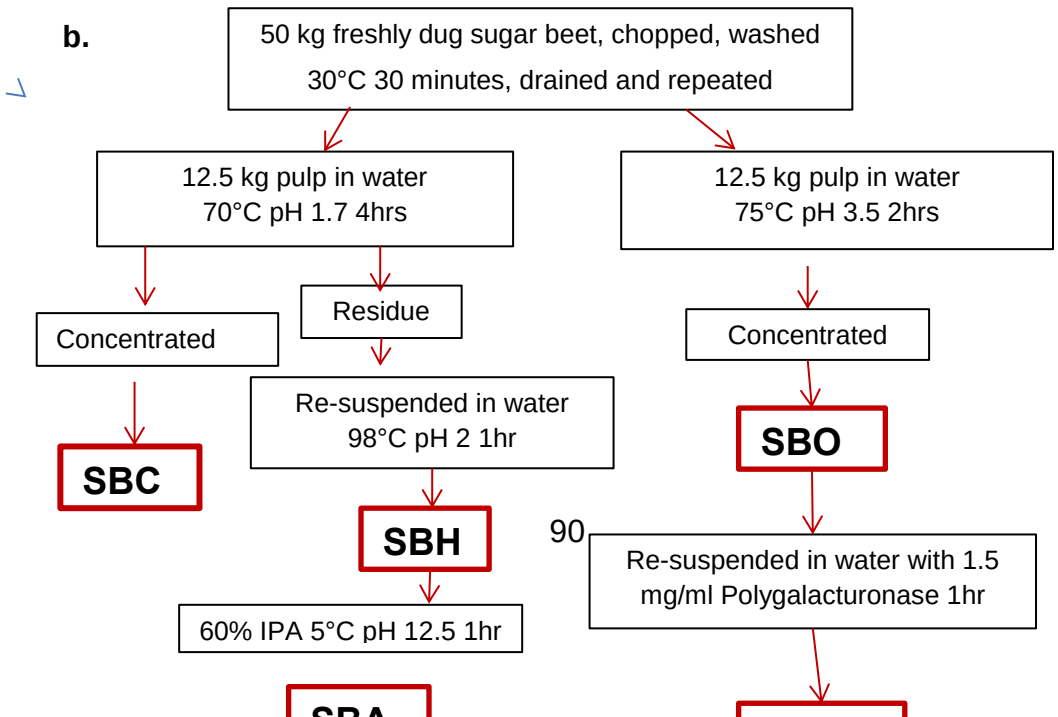

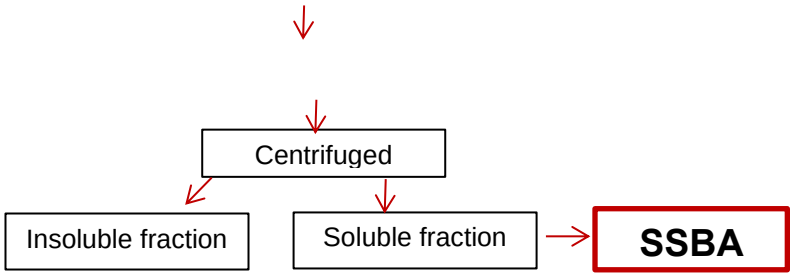

Figure 11 ***Procedure used to extract and prepare pectins*** (a) Citrus pectins; (b) Sugar beet pectins

3.3.1.3 Heat treatment of commercially-extracted pectin

The solid part from the commercially-extracted pectins (section 3.3.1.1) was mixed with de-ionised water at 98°C and adjusted to pH 2 with nitric acid for 1 hour.

3.3.1.4 Alkali-treatment of commercially-extracted pectin

Half the precipitate from the heat-treated pectin (section 3.3.1.2) was mixed in 5 L of 60% IPA at 5°C and adjusted to pH 12.5 with NaOH for 1 hour.

3.3.1.5 Oxalic acid extraction of pectin

In a 50 L extraction tank, 2000 g of dried citrus peel or 12.15 kg of washed sugar beet was mixed in a 50 L extraction tank with 70°C de-ionised water adjusted to pH 13.5 with oxalic acid/Na-oxalate buffer for 2 hours under agitation. Solids from the citrus peel extract then underwent re-extraction. Solids were mixed with 70°C de-ionised water adjusted to pH 3.5 for a further 2 hours. The liquid extracts were then filtered and precipitated. The sugar beet extract was additionally vacuum evaporated at 60°C to concentrate to 5.8 times the original sugar content prior to precipitation.

3.3.1.6 Polygalacturonase treatment of pectin

The solid parts from the oxalic-extracted pectins (section 3.3.1.4) were mixed in de-ionised water with 15 ml Rohament PL polygalacturonase (AB Enzymes, Darmstadt, Germany) in 100ml ion-exchanged water, pH 3.5 for 1

hour. The sugar beet extract was additionally vacuum evaporated at 60°C to concentrate to 5 times the original sugar content prior to precipitation.

3.3.2 Obtaining the soluble fraction of alkali-treated sugar beet pectin

Alkali-treated sugar beet pectin (SBA) was dissolved in water at 10 mg/ml and centrifuged at 3700 g for 1 hour. The supernatant (SSBA) was separated from the pellet and freeze dried.

3.3.3. Pectic polysaccharides

Purified polysaccharide fractions potato RGI (P-RGI and P-RGI-X), potato galactan (P-Gal), citrus polygalacturonic acid (C-PGA), galactobioase (GB), sugar beet arabinan (SB-Ara), and larchwood arabinogalactan (L-AG) were purchased from Megazyme and Pectasol-C modified citrus pectin was purchased from Econugenics (see section 2.2).

3.3.4 Structural analysis of pectins and pectic polysaccharides

3.3.4.1 Monosaccharide, molar mass and protein analysis

Monosaccharide, molar mass and protein analysis was carried out at the United States Department of Agriculture Agricultural Research Service (USDA-ARS), Philadelphia, USA. Monosaccharide analysis was carried out by high-performance anion-exchange chromatography with pulsed amperometric detection (HPAEC-PAD). Neutral and acidic monosaccharides were separated in a single run using a mobile phase that was 10 mM NaOH isocratic for 10 minutes, then a 0-60 mM CH_3COONa gradient in 100 mM NaOH by 13 minutes and 60-120 mM CH_3COONa in 100 mM NaOH by 30 minutes. The mobile phase returned to 10mM NaOH for 30 minutes prior to the next injection. Other conditions were reported previously [111]. Molar mass was determined by High Pressure Size Exclusion chromatography (HPSEC) using methods given by Qi and co-workers [368], and protein analysis methods are detailed by Fishman and colleagues [147]. The procedures as reproduced from these sources are detailed in Appendix B.

MW values quoted in the text and tables are weight average values (M_W) unless otherwise stated.

3.3.4.2 Acetate and methyl-ester analysis

Acetate and methyl-ester analysis was carried out at CPKelco, Koge, Denmark. 1g of each sample was washed with 10 ml acid alcohol (60% IPA + 35% water + 5% concentrated (37%) HCl) for 1 minute, centrifuged at 10,000rpm for 10 minutes, and repeated, discarding the supernatant each time. The samples were then washed in 30 ml 60% IPA for 1 minute, centrifuged at 10,000 rpm for 10 minutes, and repeated twice, discarding the supernatant each time. Each sample was mixed with 30 ml 100% IPA for 1 minute and centrifuged 10,000 rpm for 10 minutes, the supernatant discarded and the sample dried for 2.5 hours at 105°C. 0.2g of each dry sample was then wetted with 100% IPA and mixed with 50 ml CO2-free water for 15 minutes before titration with 0.1 M NaOH to pH 8.5. 10 ml 0.5 M NaOH was then added and left to stand for 15 minutes before the addition of 10 ml 0.5 M HCl and stirred until a constant pH is achieved, before titration with 0.1 M NaOH to pH 8.5. Acetic acid from saponification of acetate ester groups was determined with an enzyme kit (R-Biopharm, Darmstadt, Germany) following the instructions provided with the kit

3.3.4.7 NMR spectroscopy

NMR analysis was carried out by Ian Colquhoun at the Institute of Food Research. Samples were prepared as solutions in D_2O at concentrations between 10 and 40 mg/ml depending on solubility and viscosity. NMR was carried out as described in section 2.10. Data tables for pectins and pectic polysaccharide are supplied in Appendix B.

3.4 Results

3.4.1 Extraction, modification and chemical analyses of ten pectins from citrus peel and sugar beet pulp

Pectins were extracted from dried lemon peel and fresh sugar beet, either commercially or with a mild acid, and modified in a variety of ways to provide an array of pectins with varying sugar compositions, methyl-ester contents and MWs. Pectin from citrus and sugar beet was extracted commercially, with nitric acid at pH 1.7, 70°C to create pectin similar to that employed in food products (CP, SBC). As expected, CP yield was higher than SBC, while SBC has a considerably higher neutral sugar and lower GalA content (Table 7). The GalA:Rha ratios in Table 8 indicate the number of GalA residues to one Rha residue which gives an idea of the RGI backbone to HG content, and the Gal:Rha and Ara:Rha ratios the number of neutral sugar residues attached to the RGI backbone. These ratios indicate that SBC is almost 7-fold richer in RGI regions than CP, although the number of neutral sugar residues per Rha are similar. CP is richer in methyl-esters with a DE of 70% as opposed to 58% in SBC (Table 9). On the other hand, CP has a lower DAc (1.5% versus 20%), protein content (1.2% versus 8.5%). CP additionally has a lower MW (430 kDa versus 548 kDa) (Table 9), however this is unusual and could be explained by a potential greater presence of aggregated molecules in sugar beet pectin [369] or the cross-linking of ferulic acids [370, 371]. The polydispersity index (weight average molecular weight divided by the number average molecular weight, Mw/Mn) of both pectins is relatively high. Monodisperse polymers with equal chain lengths will have a polydispersity index of 1, and the larger the index, the broader the MW. CP has an index of 2.3, which suggests it consists of varying chain lengths; however, SBC has a higher index of 2.9 which indicates a broader spectrum of polymer sizes. SBC additionally contains higher amounts of xylose and glucose which could derive from an additional hemicellulose component extracted with the pectin, such as xyloglucan, or possibly sugars branched from RGII.

Further pectin samples, CH and SBH, were extracted from the solid part of the initial commercial extraction, at a higher temperature, 90°C, at pH 2.4, in order to depolymerise the backbone and create lower MW pectins. Contrary to these predictions, results indicate that MW was not significantly lowered in sugar beet pectin. However, the MW of citrus pectin was reduced considerably from 430 kDa to 144 kDa, indicating a smaller pectin size. These results additionally correspond with the vast increase in RGI to HG regions, implying a breakdown of the HG backbone. High heat extraction additionally decreased the arabinan content from 2.2% to 1% and 13.1% to 6.9% in citrus and sugar beet pectin, respectively. Sugar beet pectin structure did not appear to be effected in any other way, however, the DE of citrus pectin decreased from 70.2% to 63.1%, while protein content increased from 1.2% to 5.4%.

CH and SBH were further modified with alkali, pH 13 at 5°C, in order to yield pectins with low DE (CA and SBA). As predicted, alkali treatment significantly reduced DE from 63% to 45%, and 55% to 18% in citrus and sugar beet pectin, respectively. Sugar beet pectin appeared to be more vulnerable to alkali treatment with a 37% decrease in DE to 18% in citrus pectin. DAc of sugar beet pectin was also greatly reduced from 22% to 8.8%. Alkali treatment of pectin was carried out at a low temperature in order to inhibit β-elimination, and thus depolymerisation of the pectin backbone. On the contrary, alkali treatment significantly reduced sugar beet pectin MW from 535kDa to 362kDa, which coincides with a decrease in GalA and an increase in RGI to HG regions. However, it is possible that this reduction in MW could be due to the break-up of aggregates. Neutral sugar side chains remained unchanged by this treatment.

Table 7 ***Sugar analysis of pectins and Pec-C (%mol).*** Relative percent sugar composition analysis and uronic acid content of pectins isolated from citrus and sugar beet and Pec-C health supplement.

	GalA	Rha	Gal	Ara	Xyl	Glu	GlcA	Fuc
Citrus pectins								
CP	91	1.2	4.6	2.2	0.4	0.4	0.2	0.1
CH	89.7	2.3	5.8	1	0.4	0.8	0.1	0.1
CA	91.8	1.6	5	0.6	0.3	0.6	0.1	0
CO	83.2	1.4	3.8	10.3	0.5	0.5	0.3	0.1
COPG	82.2	1.9	4.3	9.2	1.1	0.8	0.3	0.2
Sugar beet pectins								
SBC	62	5.5	12.4	13.1	1.6	4.5	0.9	0.1
SBH	60.1	6.4	14.4	6.9	3.7	7.6	0.9	0.1
SBA	47.4	11.6	25.1	10.5	0.9	3.5	0.8	0.1
SSBA	52.5	11.4	18.5	7.8	3	4.1	2.6	0.2
SBO	43.6	3.2	9.4	31.4	3.9	8	0.5	0.2
SBOPG	36.9	3.9	11.1	36.5	3.3	2.4	0.7	0.1
Health supplement								
Pec-C	93.5	0.7	3	1.1	0.1	0.6	0.9	0.1

As well as commercial extraction, citrus peel and sugar beet pulp also underwent weak acid extraction with oxalic acid (pH 3.5) at 75°C in order to prevent degradation of the pectin and subsequently yield samples with high neutral sugar content (CO, SBO). Results revealed that MWs of the oxalic acid-extracted pectins were indeed considerably higher with an increase of 654kDa and 873kDa in CO and SBO, respectively, than their commercially extracted counterparts. These pectins were also revealed to have significantly higher arabinan contents, while galactan content was similar. Sugar analysis results showed SBO and CO to have arabinan contents of 31.4% and 10.3%, while the harsher, commercial extractions yielded pectins with 13.1% and 2.2% arabinan, respectively. Overall, yields of oxalic acid-extracted pectin were significantly lower than commercially extracted pectins.

Table 8 ***GalA, Gal and Ara to Rha ratios of pectins and Pec-C.*** Ratios of GalA (GalA:Rha), Gal (Gal:Rha), and Ara (Ara:Rha) to Rha, of ten pectins and Pectasol-C health supplement. Data are presented as number of GalA, or Gal and Ara residues to one Rha residue. Values taken from Table 7.

	GalA:Rha	**Gal:Rha**	**Ara:Rha**
Citrus pectins			
CP	73.9	3.7	1.8
CH	39.3	2.5	0.4
CA	58.9	3.2	0.4
CO	59	2.7	7.3
COPG	42.6	2.2	4.8
Sugar beet pectins			
SBC	11.4	2.3	2.4
SBH	9.3	2.2	1.1
SBA	4.1	2.2	0.9
SSBA	4.6	1.6	0.7
SBO	13.8	3	10
SBOPG	9.4	2.8	9.3
Health supplement			
Pec-C	133.6	4.3	1.6

Table 9 ***%DE, %DAc, %protein, MW, and polydispersity of pectins and Pec-C.*** %DE, %DAc, % protein, viscosity [η], molecular weight (MW) and polydispersity index (Mw/Mn) of pectins isolated from citrus and sugar beet and Pec-C health supplement. * no data available.

	%DE	%DAc	% protein	MW (kDa)	Mw/Mn
Citrus pectins					
CP	70.2	1.5	1.2	430	2.3
CH	63.1	2	5.4	144	3.1
CA	45.3	2.6	3.9	129	3.6
CO	76.5	1.1	1.5	798	2.5
COPG	67.5	2.1	2.4	653	2.9
Sugar beet pectins					
SBC	56.8	23.4	6.1	548	2.9
SBH	54.7	21.6	6.1	535	2.9
SBA	18	8.8	4.2	362	3.2
SBO	62.4	25.3	3.1	1381	2.5
SBOPG	62.4	32	2.8	594	2.1
Health supplement					
Pec-C	5	*	*	23	1.4

Further pectin samples, COPG and SBOPG, were extracted from the solid part of the initial oxalic acid-extraction by incubation with endo-polygalacturonase (PG), an enzyme that hydrolyses glycosidic bonds that link GalA residues of the pectin backbone, in order to create lower MW pectins without compromising the neutral sugar content. As expected, PG treatment depolymerised the HG backbone of both citrus and sugar beet pectin, considerably lowering the MWs by 145kDa and 787kDa in COPG and SBOPG. Accordingly, the GalA:Rha ratio was slightly lowered, indicating an increased concentration of highly branched regions of RGI. PG treatment also reduced DE in citrus pectin by 10%. Sugar compositions were unaffected.

The health supplement Pec-C has featured in a number studies into the anti-cancer effects of modified pectin [201, 205, 329] and so was employed in this study and its structure analysed. Results reveal that the content of Pec-C is largely GalA, with just 3% galactan and 1.1% arabinan. The sizeable GalA:Rha ratio and small branching ratio indicate that Pec-C is mainly HG backbone with few RGI regions with short galactan and arabinan side chains. Additionally, Pec-C is very small in size with a MW of 23kDa and an extremely low methyl-ester content of 5%.

It was noted in subsequent chapters that the sugar beet pectins were not completely soluble, and as SBA showed significant bioactivity, it was investigated if this played a role in reducing cell viability. The soluble and insoluble components of SBA were separated by centrifugation to yield the soluble fraction of SBA (SSBA). The monosaccharide composition of SSBA was assessed and shown to be very similar to that of the original SBA (Table 7), showing that the soluble part is representative of the whole SBA.

3.4.2 Chemical analyses of pectic polysaccharides

Pectic polysaccharides were employed in this study to ascertain which structural features of pectin have the optimum effect on colon cancer cells. Seven polysaccharides were selected to represent the two major regions of pectin, HG and RGI. Citrus polygalacturonic acid (C-PGA) represents the HG

backbone of pectin and potato RGI (P-RGI and P-RGI-X) the RGI regions. Potato galactan (P-Gal), sugar beet arabinan (SB-Ara) and larchwood arabinogalactan (L-AG) represent the neutral sugars that constitute RGI.

Table 10 shows the sugar composition of the six pectic polysaccharides as well as MW and polydispersity, as analysed for this study. Results showed the presence of Rha, Ara and Gal in varying proportions. Only traces of Xyl, Glu, Man and Fuc were present. Sugar compositions of some of the polysaccharides, particularly P-RGI-X, P-Gal and SB-Ara were shown to be different from those quoted by Megazyme (Table 11). According to the manufacturer, P-Gal is prepared by an alkali extraction of potato fibre followed by acid hydrolysis and enzymatic treatments to remove polysaccharides other than Gal. The sugar composition of P-Gal proved to be very different to that quoted by Megazyme. P-Gal consists of 63.5% Gal, rather than the quoted 88%, and considerably higher amounts of GalA and Rha than published. A ratio of 4.6 GalA residues to one Rha residue indicates a presence of RGI regions comparable with P-RGI, albeit with significantly more galactan residues. P-Gal has a MW of 390kDa, and a polydispersity index of 4, indicating that P-Gal consists of polymers with a wide range of molecular mass.

Table 10 ***Sugar analysis of pectic polysaccharides (%mol)*** Relative percent sugar composition analysis, uronic acid content, molecular weight (MW) and polydispersity index (Mw/Mn) of pectic polysaccharides.

	GalA	Rha	Gal	Ara	Xyl	Glu	Man	Fuc	MW	Mw/Mn
P-Gal	26	5.7	63.5	2.9	0.1	1.4	0	0.4	390	4
P-RGI	44.8	21.5	21.8	6.4	1.9	1.8	1.4	0.5	42	2.42
P-RGI-X	47.8	21.6	19.6	5.6	1.5	1.8	1.2	1	14.3	*
C-PGA	90.3	2	5.6	1	0.1	0.6	0.3	0.1	379	4.4
SB-Ara	19	7	15.8	57.7	0	0.2	0	0	206	1.5
L-AG	2.3	0	79.5	16.5	0.6	0.9	0	0.1	46	1.1

Table 11 ***Quoted sugar ratios of pectic polysaccharides (%mol)*** Quoted sugar ratios of pectic polysaccharides from Megazyme.

	GalA	Rha	Gal	Ara	Xyl	Glu	Man	Fuc
P-Gal	7	3	88	2	0	0	0	0
P-RGI	62	20	12	3	0	0	0	0
P-RGI-X	62	20	12	3	0	0	0	0
C-PGA	96	1	1	0.2	0	0	0	0
SB-Ara	7	2	3	88	0	0	0	0
L-AG	0	0	81	14	0	0	0	0

Table 12 ***GalA, Gal and Ara to Rha ratios of pectic polysaccharides.*** Ratios of GalA (GalA:Rha), Gal (Gal:Rha), and Ara (Ara:Rha) to one Rha residue. Values taken from Table 10.

	GalA:Rha	Gal:Rha	Ara:Rha
P-RGI	2.1	1	0.3
P-RGI-X	2.2	0.9	0.3
C-PGA	43.7	2.8	0.5
P-Gal	4.6	11.2	0.5
SB-Ara	2.7	2.3	8.2

Investigation into the sugar composition of P-RGI showed it was similar to that of the quoted sugar content. According to the producers, P-RGI is prepared by enzymatic hydrolysis of pectic galactan from potato, similar to P-Gal. Enzymes include endo-arabinanase, endo-galactanase, polygalacturonanase and a-L-arabinofuranosidase which hydrolyse the pectin backbone and cleave arabinan and galactan side chains. P-RGI consists of 44.8% GalA and 21.5% Rha. As the RGI backbone consists of repeating disaccharide units of GalA-Rha, results indicate that P-RGI is mainly composed of RGI, although regions of HG are still present. Neutral sugars of RGI are made up of 21.8% Gal and 6.4% Ara, with branching ratio of just one Gal and 0.2 Ara residues per Rha residue. This indicates P-RGI contains very short sugar side chains of mainly galactan. P-RGI has a relatively low MW at 42kDa. P-RGI-X is potato RGI from Megazyme with the same catalogue and lot number as P-RGI. P-RGI-X was shown to have a very similar monosaccharide composition to P-RGI, however it has a lower MW of 14.3 kDa (Table 10).

The producers of C-PGA assert that it is prepared from citrus pectin by enzymatic hydrolysis with polygalacturonase followed by de-methylation. C-PGA is intended to represent the HG backbone of pectin, and results show it is mainly composed of GalA. However C-PGA also contains 5.6% Gal and 1% Ara and has a ratio of 45 GalA residues to one Rha, which indicates that the structure is not pure HG, but also contains RGI regions with short sugar

side chains. MW is relatively high at 379kDa; however the polydispersity index is correspondingly high, signifying a wide range of polymer sizes within C-PGA.

SB-Ara is extracted from sugar beet pulp with calcium hydroxide solution at 90°C, according to the manufacturers. It is rich in arabinan, 57.7%, although the content is significantly less than the 88% quoted. SB-Ara also contains 15.8% Gal, 19% GalA and 7% Rha, indicating that arabinans exist as side chains of an average length of 10 residues on an RGI backbone. The polydispersity index of SB-Ara is relatively low, signifying a narrow size distribution with a molar mass of 206kDa MW. Results show that the sugar composition and MW of L-AG is almost identical of that quoted by the manufacturers. L-AG is composed of 79.5% Gal and 16.5% Ara, with a monodisperse MW of 46kDa. L-AG is extracted from larchwood, and differs from the other pectic polysaccharides as it does not contain an RGI backbone (and therefore has been excluded from Table 12). Published data confirms that larchwood arabinogalactan typically consists of a main chain of β(1→3)galactose units with 1-3DP side chains of β(1→6)galactan and α-L-arabinan [372]

3.4.3 NMR analysis of pectins and pectic polysaccharides

NMR spectroscopy was carried out to further characterise certain pectins and pectic polysaccharides that demonstrated bioactivity in colon cancer cells in the proceeding chapters. The partial ^{13}C NMR spectrum in Figure 12 shows that Gal chains in P-Gal are relatively long with major peaks characteristic of linear (1→4)-β-D-linked Gal chains [373] These chains are linked to Rha residues in the RGI backbone whose presence is shown by the appearance of two Rha Me signals in the ^{1}H spectrum, with intensity ratio 2:1, at 1.31 and 1.25 ppm (Figure 13B). Detailed analysis of the P-RGI spectrum (Appendix B, Table B1) had shown that the first of these two signals corresponded to Rha units substituted (at C4) by Gal, whilst the second signal arose from Rha units that were not Gal-substituted (Rha^{U}). Rha units either carry a long Gal Chain (Rha^{G}) or a single terminal Gal

(Rha^{GT}), and the intensities of the Rha Me signals show that (Rha^{G}+Rha^{GT}):Rha^{U} is 2:1. There was no signal for Ara. Estimation of the galactan chain length of P-Gal required quantification of minor signals. The Gal C2 signals were used since they allowed to distinguish between Gal units in the (1→4)-β-Gal chain (Rha^{G}, Figure 12B(h)), single terminal Gal residues linked to Rha (Rha^{GT}, Figure 12C(c)) and terminal Gal units that terminate the (1→4)-β-D-linked Gal chains (Gal^{T}, Figure 12C(i)). The intensities of the weak signals, c and i, were difficult to determine directly from the ^{13}C spectrum (Figure 12C) but better sensitivity and resolution was obtained by measuring intensities at the ^{13}C shifts indicated using cross-sections through the $^{1}H/^{13}C$ HSQC spectrum at the ^{1}H chemical shifts shown in Table 13. Peak c represents Rha^{GT} and is approximately equal to Gal^{T} (peak i), and the ratio of Rha^{G} (peak h) to Gal^{T} is 23:1, giving a mean chain length of 23 residues. Additionally the ratio of Rha^{US}: Rha^{G}: Rha^{GT} was 1:1:1. The ^{13}C NMR spectrum did not show signals for $GalA^{HG}$, presumably because of association between (1→4)-α-linked-GalA chains. The analytical data (Table 10) shows P-Gal is composed of 26% GalA and 6% Rha which leaves 20% $GalA^{HG}$ allowing for GalA in the RGI regions.

Table 13 ***$^{1}H/^{13}C$ HSQC NMR spectrum of P-Gal***. Peaks taken from Figure 12

Peak	^{1}H ppm	^{13}C ppm	Identity
h	3.69	74.53	C2 Gal in (1→4)-β-Gal side chain (Rha^{G})
c	3.53	74.39	C2 Terminal Gal in single unit side chain (Rha^{GT})
i	3.62	74.15	C2 Terminal Gal in (1→4)-β-Gal side chain Gal^{T}
j	3.92	71.33	Common to all terminal Gal
e	4.16	80.22	C4 Gal in (1→4)-β-Gal side chain

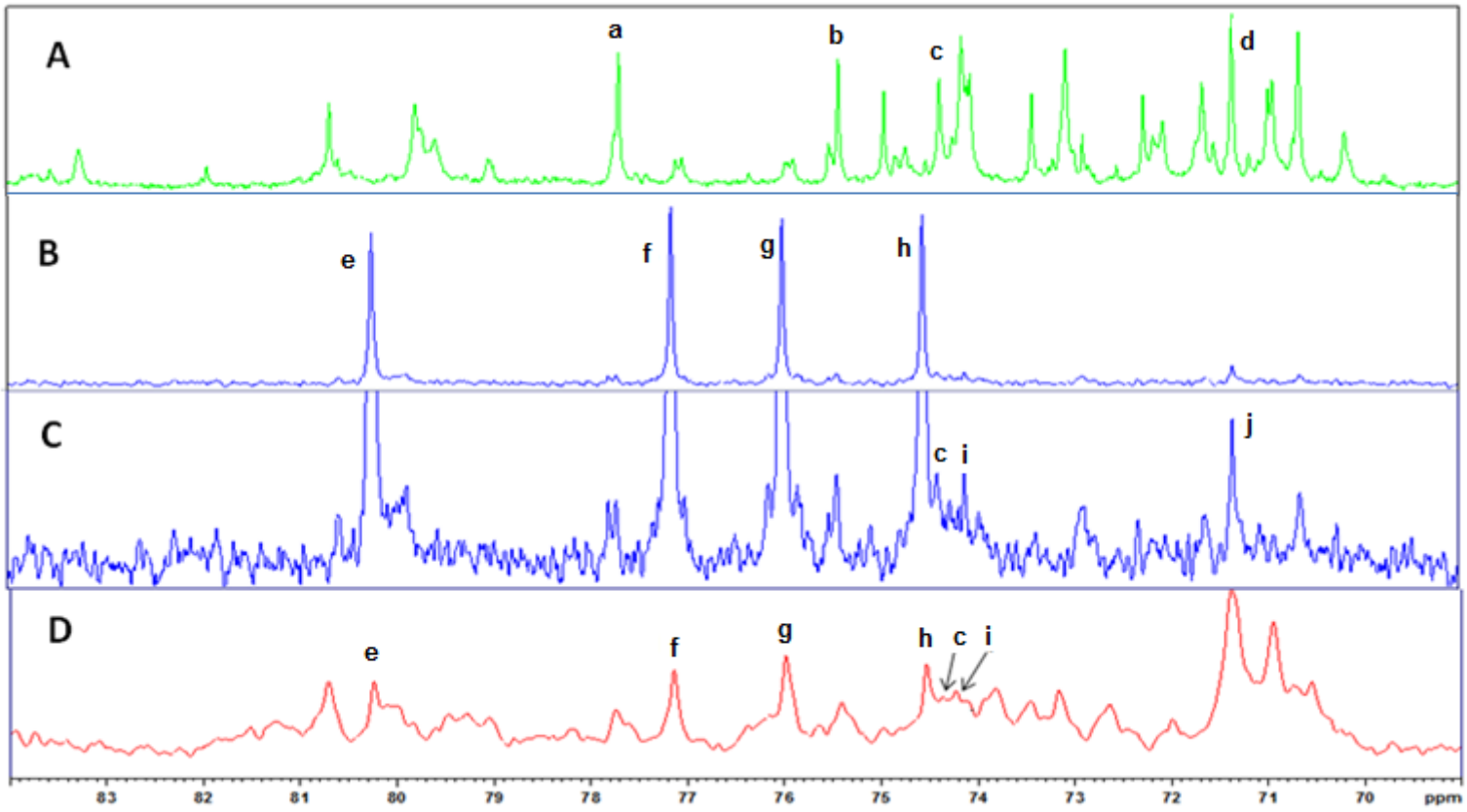

Figure 12 ^{13}C *NMR spectra of P-RGI, P-Gal and SSBA*. 151MHz ^{13}C NMR spectra of pectin samples at 338^{0}K in D_2O (anomeric, C6 (Gal) and C6 (Rha) regions of the spectra not shown). (A) P-RGI; (B) P-Gal; (C)P-Gal (y-gain increased to show weaker peaks); (D) SSBA. (a-d) terminal Gal stub: a C5; b C3; c C2; d C4; (e-h) (1→4)-β-linked-Gal units: a C4; b C5; c C3; d C2; (i) C2 terminal unit of (1,4)-linked side chain; (j) C4 combined signal for stubs and chain termini.

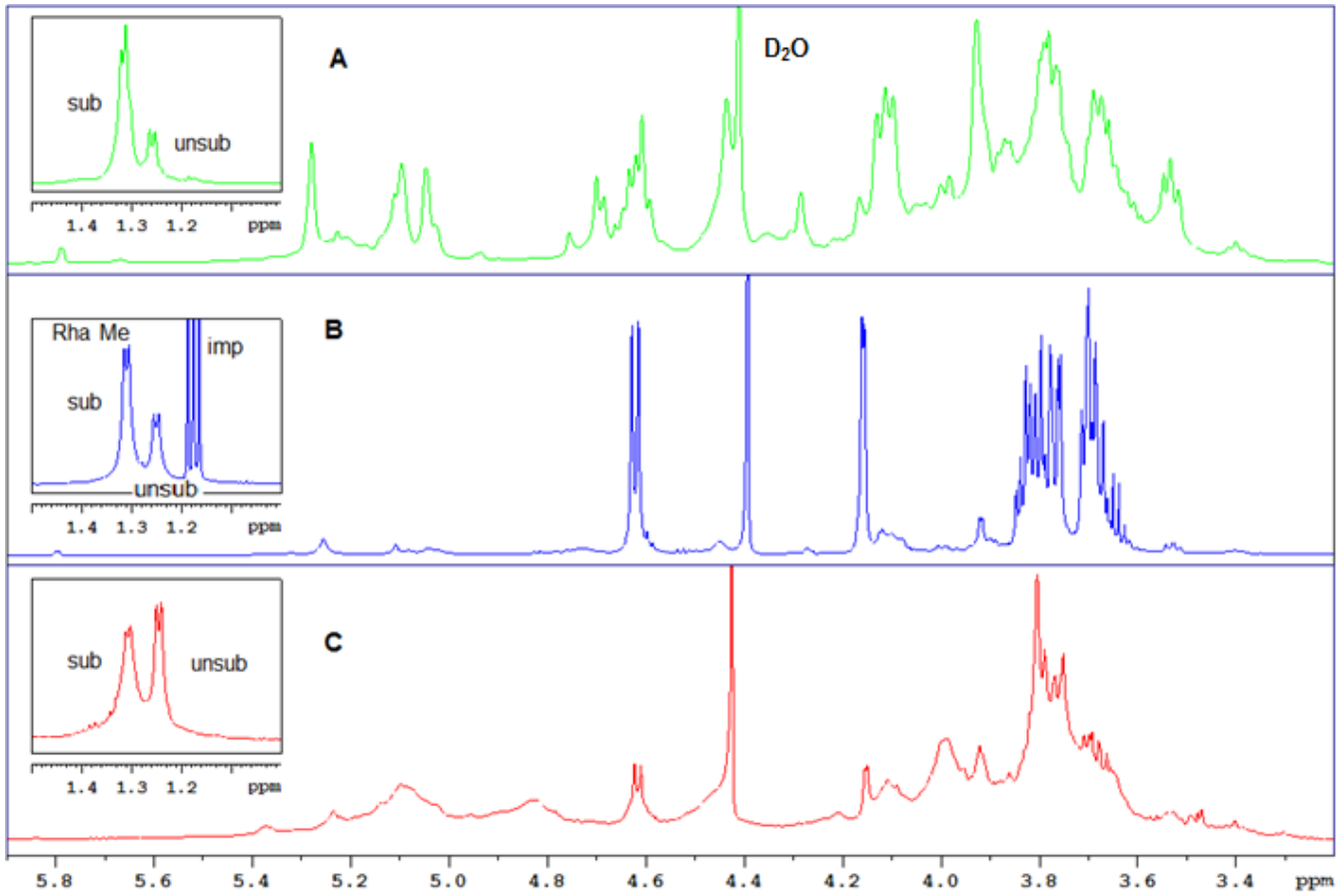

Figure 13 *^{1}H NMR spectra of P-RGI, P-Gal and SSBA.* 600MHz ^{1}H NMR spectra of pectin samples at 338^{0}K in D_2O with insets showing Rha Me signals. (A) P-RGI; (B) P-Gal; (C) SSBA. SSBA has two acetate (GalA substituent) signals at 2.17 and 2.18 ppm that are not shown. Separate Rha Me signals are observed for units substituted with Gal (sub) or not substituted (unsub).

The ^{13}C spectrum of SSBA (Figure 12D) was considerably more complex than that of P-Gal as it had signals from partly substituted and esterified GalA and Ara as well as from Gal. However the same major ((1→4)-β-D-linked) and minor Gal signals were evident as in P-Gal and have been labelled with the same letters. The greater prominence of peaks c and i showed that Gal chains in SSBA were relatively short compared with P-Gal. Using the HSQC spectrum in the same way as described for P-Gal, the 'longer' chains in SSBA were estimated to have an average Gal chain length of 3.5 residues, and there were 1.6 times as many of these 'long' chains as there were single terminal Gal stubs. Additionally, the integration of the ^{1}H spectrum (Figure 13C) of SSBA gave a 1:1 ratio for Rha substituted with Gal (C6 at 1.31 ppm) and unsubstituted Rha (C6 at 1.25 ppm). Consequently, it can be determined that the different types of Rha residue in the RGI region of SSBA are in the ratio of 5:3:2 for Rha^{U}: Rha^{G} Rha^{GT}. Again using the HSQC cross-sections, the intensities of the C1 peaks for terminal Ara ($^{1}H/^{13}C$=5.14/109.8 ppm) and (1→5)-linked-Ara (5.07/110.1) in SSBA were practically equal. The high proportion of terminal Ara implies that Ara side chains are mostly either single stubs or else very short.

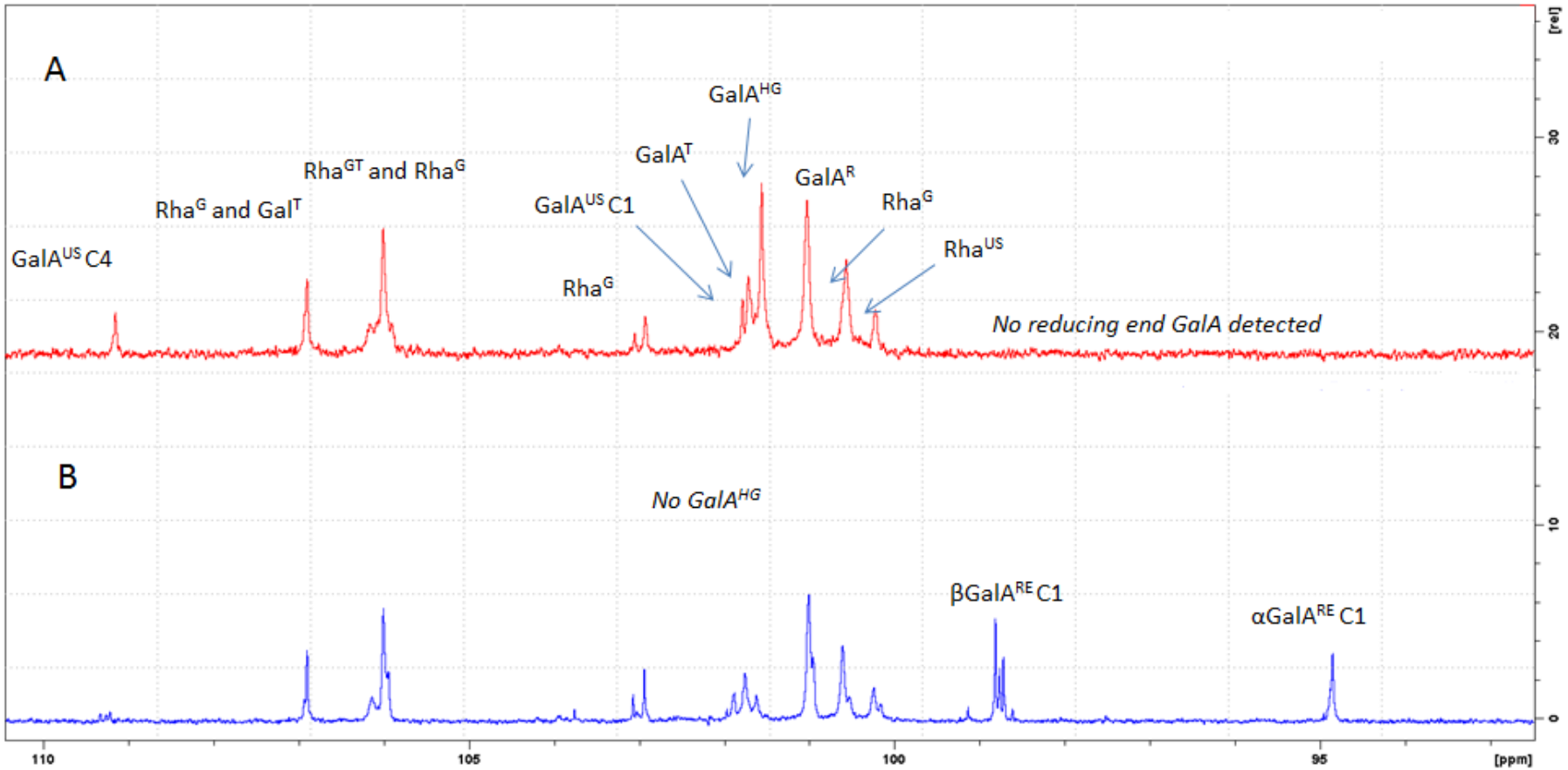

Figure 14 *^{13}C NMR spectra of P-RGI and P-RGI-X.* 151MHz ^{13}C NMR spectra of P-RGI and P-RGI-X at 338°K in D_2O (anomeric region).

Table 14 ***Monosaccharide composition of P-RGI and P-RGI-X obtained by ^{13}C NMR*** (a) Relative percent monosaccharide composition of P-RGI and P-RGI-X; (b) Relative percent composition of total GalA as $GalA^{HG}$, $GalA^{R}$, $GalA^{NR}$ and $GalA^{RE}$

Pectin	Monosaccharide composition[a] %			Total GalA composition[b] %				
	GalA	Rha	Gal	$GalA^{HG}$	$GalA^{R}$	$GalA^{T}$	$GalA^{RE}$	Gal^{US}
P-RGI	46	25	29	34.8	43.5	21.6	0	3.5
P-RGI-X	49	26	25	0	44.9	24.5	34.7	2

Two batches of potato RGI with the same catalogue and lot numbers were obtained from Megazyme. While P-RGI was shown to reduce viability of colon cancer cells, the second RGI, P-RGI-X, lacked this bioactivity (Chapter 5). Therefore the fine structures of the polysaccharides were compared. Sugar ratios, as determined according to integrals of the C1 peaks in ^{13}C NMR, were very similar to those obtained by HPAEC-PAD (Table 14a and Table 10). ^{13}C NMR spectra display signals for neutral sugars in similar proportions for both P-RGI and P-RGI-X (Figure 14). The majority of Rha is substituted with Gal at an approximate ratio of 5:1 (Figure 13A), and Gal chains are very short, consisting of just 1-3 DP. Use of the HSQC spectrum, as before, gives a ratio of approximately 4:1 for the ratio of single terminal Gal to 'longer' chains. Therefore the ratio of the different types of Rha residue is 1:1:4 for Rha^{U}: Rha^{G}:Rha^{GT}. The prominent terminal Gal signals (linked to Rha^{GT}) are labelled in Figure 12A (a-d). Exactly the same pattern was found for the side chains in P-RGI-X.

The distinctions between the two RGIs lie in the composition of GalA. Five types of GalA can be recognised: $GalA^{HG}$ is GalA in the HG region i.e. (1→4)-α-linked-GalA linked to GalA; $GalA^{R}$ is GalA linked to Rha in the RGI region; $GalA^{T}$ is terminal GalA; $GalA^{RE}$ is reducing end GalA; and $GalA^{US}$ is unsaturated GalA (Table 14B). Two obvious dissimilarities exist between the two RGIs. The ^{13}C NMR spectrum clearly displayed signals for $\beta GalA^{RE}$ and $\alpha GalA^{RE}$ in P-RGI-X, that were entirely absent in P-RGI (Figure 14). The presence of different types of non-reducing end coupled with an absence of reducing ends in P-RGI is surprising as in a linear core structure the number

of reducing ends should be equal to the number of non-reducing ends. This could imply P-RGI has a branched structure whereby GalA exists as HG side chains branched from an RGI backbone in line with newer models of pectin [374, 375]. For this proposed model it would be expected that the number of branch points would match $GalA^{T}$, however no branch points were detected. Nevertheless, it is possible that the HG side chains are of restricted mobility and therefore invisible to NMR. On the other hand, the ratio of terminal to reducing end GalA in P-RGI-X is equal. The content of $GalA^{RE}$ is higher than $GalA^{T}$, but approximately one third of $GalA^{RE}$ exists as free GalA, leaving a $GalA^{T}$:$GalA^{RE}$ ratio of 1:1. The second major distinction between the samples is the absence of $GalA^{HG}$ ^{13}C NMR signal in P-RGI-X (Figure 14). 44.9% of GalA exists attached to Rha residues in the P-RGI-X backbone (Table 14b), and the remaining 55.1% most likely exists as free mono- and disaccharides: one third of $GalA^{RE}$ is free GalA (Figure 14B), while the remainder is matched in amount to $GalA^{T}$, which implies free GalA disaccharides. On the other hand, 34.8% of GalA in P-RGI exists as HG (Table 14b). The probable reason for these differences can be understood by the content of $GalA^{US}$, a product of pectic lyase action on $GalA^{HG}$. P-RGI has 1.75-fold the content of $GalA^{US}$ than P-RGI-X and this disparity implies a variation in the method of enzymatic treatment. It is most likely that P-RGI and P-RGI-X correspond to different extents of depolymerisation, either in the initial preparation or from some residual enzyme activity in the samples which begins when solutions are prepared. Detailed analysis of the P-RGI-X, P-Gal and SB-Ara spectrums are detailed in Appendix B (Tables A2-4).

3. 5 Discussion

Citrus and sugar beet pectins were extracted and modified in a variety of ways to provide an array of pectins with varying MWs, DE, DAc, protein and neutral sugar contents. In general, sugar beet and citrus pectins differed in several ways. Sugar beet pectins generally exhibited lower DE and GalA content, and higher DAc, protein and neutral sugar content than citrus pectins, as predicted [138] [141, 376]. Moreover, sugar beet pectins exhibited a higher occurrence of RGI regions, as shown by ratios of GalA:Rha, while the neutral sugar content of each RGI region is similar in both sugar beet and citrus pectin samples, with relatively low Gal:Rha and Ara:Rha ratios indicating short side chains. Additionally, sugar beet pectin was show to have higher MWs than citrus pectin, which is unusual. However, it is possible that, as pectin has a natural tendency for aggregation of molecules, even in dilute solution, that the interpretation of light-scattering data could be uncertain [369, 377]. Additionally, it is known that ferulic acid present on Ara can form cross-links between chains which could explain the high MWs [370, 371]. The polydispersity of all pectins was relatively high, indicating that pectin consists of varying chain lengths.

Sugar beet and citrus pectins were extracted under two different conditions: a mild acid extraction to extract pectin without compromising the neutral sugar content and HG backbone, and conventional commercial extraction under high acidic conditions. Pectins extracted under weak acid conditions were revealed to exhibit significantly higher MWs and Ara contents than their commercially-extracted counterparts, as well as slightly higher DE. The milder extraction conserves the HG backbone as well as Ara side chains [376, 378]. Further enzymatic modification intended to depolymerise the HG backbone was successful, reducing MW and the ratio of HG to RGI regions while leaving neutral sugar side chains intact. On the other hand, commercial extraction creates pectins with relatively low MW and neutral sugar contents. Heat-treatment of commercial pectins generated pectins with reduced MW and DE, particularly in CP, which follows an increased rate of hydrolysis and the breakdown of the HG backbone. Additionally, Ara content in both sugar beet and citrus pectin was approximately halved by this heat extraction. An

additional treatment with alkali significantly reduced the DE of the pectins, as well as MW, GalA and protein content. These effects were particularly pronounced in sugar beet pectin. Alkali treatment was carried out at 5°C to avoid β-elimination; however, the sugar beet pectin HG backbone was significantly fragmented, increasing the occurrence of RGI regions 3-fold, while the neutral sugar content of each RGI region remained unchanged.

Pec-C, a MCP marketed as a health supplement in the US and the subject of various studies into the health effects of Gal-rich MCP, was shown to have an extremely low MW and DE, as published [200]. However, despite the assurance of Gal-rich pectin [200-202, 204], Pec-C was shown to have a very low Gal content, consisting predominantly of GalA.

As pectin is mainly composed of two regions, HG and RGI, polysaccharides were chosen to denote these regions in order to determine the structural features of pectin required for an optimum effect on cancer cells in the proceeding chapters. C-PGA represents HG and P-RGI and P-RGI-X the RGI region. P-Gal, SB-Ara and L-AG represent the neutral sugars that constitute RGI. C-PGA, representing the HG backbone, was shown to indeed consist of predominantly GalA, although RGI regions do appear in a small quantity. SB-Ara was shown to comprise of predominantly Ara side chains branched from RGI, although GalA content was also relatively high. As predicted, L-AG comprises predominantly Ara and Gal, and differs from the pectic polysaccharides given that it does not contain an RGI backbone. P-Gal is shown to consist largely of Gal; however, it also contained a relatively high amount of GalA and Rha. Gal chains are estimated to be approximately 23 residues in length, with an equal number of Rha^{U}, Rha^{G} and Rha^{GT}. P-Gal is shown to be particularly heterogeneous, with a higher polydispersity index than pectins of equivalent or higher MW, indicating an assortment of polymer lengths. The MW of P-Gal is surprisingly high, although consistent with the value of 272kDa [322] and 50-550 kDa [379] reported previously for potato galactan. However, these results could be an overestimate due to the stiffness of the (1→4)-β-Gal side chains relative to the highly flexible pullulan standards, as well as the complex shape of highly branched RGI.

P-RGI was chosen to represent the RGI region of pectin. However, monosaccharide analysis shows that, although P-RGI is rich in RGI backbone, it contains very little in the way of neutral sugars. Indeed, results from NMR analysis show that Gal side chains on P-RGI are just 1-2 residues in length, while Ara was not detected at all. Indeed, P-Gal was shown to contain the same ratio of HG to RGI regions as P-RGI. However, previous studies of RGI show Gal chains of up to 2 Gal units in okra [211], and 4 Gal units in ginseng [325] RGI. Results from this study additionally show that pectins contain Gal chains of no more than 4 residues. A second potato RGI, P-RGI-X, was shown to have a very similar neutral sugar content as P-RGI. However, the ^{13}C NMR spectrums of each of these samples proved to differ significantly in their compositions of GalA. P-RGI was shown to contain regions of HG, while P-RGI-X was shown to lack these HG regions. Furthermore, there was a surprising absence of any reducing end GalA in P-RGI, leading to the conclusion that a proportion of the HG chains of P-RGI could exist as side chains from the RGI backbone, a structure that has been proposed in previous studies [137, 374]. The presence of pectic lyase product in P-RGI indicates a variation in the methods of treatment of P-RGI and P-RGI-X. Both samples are prepared by enzymatic hydrolysis of potato galactan to create a backbone of RGI, and it is likely that the full duration of enzymatic hydrolysis was not carried out, leaving intact HG chains in P-RGI. Further evidence of depolymerisation is provided by the lower MW of P-RGI-X to P-RGI.

Following the preparation of sugar beet pectins for use in cell culture experiments in the following chapters, SBA was shown to be insoluble. Consequently, only the soluble fraction of SBA, SSBA, was employed in cell experiments. Monosaccharide and NMR analysis revealed the structures of SBA and SSBA to be almost identical. SSBA exhibits exceptionally low GalA content and high neutral sugar content due to a very high ratio of RGI regions, boasting 15-fold more RGI regions per molecule than CA. Consequently, the neutral sugar content of each RGI region is relatively low. NMR data confirms this surmise, estimating the average Gal chain length at just 3.5 Gal units. Furthermore, half of all Rha residues in the RGI backbone

are unsubstituted, while the remaining are branched with either short side chains or single Gal units. Of most interest is that the HG to RGI ratio of SSBA is comparable to that of P-RGI. SSBA also contains higher neutral sugar content than P-RGI, which consequently means that SSBA could be classed as sugar beet RGI. NMR additionally revealed the presence of feruloyl groups attached to Gal residues.

3.6 Conclusion

Five sugar beet and five citrus pectins were extracted and modified to create pectins with various MWs, neutral sugar, DE, DAc and protein contents. As predicted, sugar beet pectins proved to exhibit lower DE and GalA content and higher DAc, protein and neutral sugar content than citrus pectins. Both heat and alkali treatment depolymerised the HG backbone, increasing the RGI content, while alkali treatment additionally reduced DE. Pectic polysaccharides were chosen for their resemblance of the individual components of pectin. P-Gal was shown to have long Gal side chains of approximately 23 residues, while P-RGI Gal chains were revealed to be short chains of 1-2 units in length. Furthermore, P-RGI was shown to contain HG regions that could exist as side chains from the RGI backbone, in line with newer pectin models.

Chapter 4

Effects of modified pectins on colon cancer cells and correlation with pectin structure

4.1 Introduction

CRC is the third most common cancer worldwide and the most common diet-related cancer, influenced by diets rich in saturated fats, red meat, and low in plant-based foods. Epidemiological studies have shown that fruit and vegetable consumption is associated with a reduced risk of developing CRC [98, 380]. Although the exact bioactive components remain unclear, dietary fibre is thought to play a major role, and this has given rise to research into the anti-cancer effects of pectin and pectic polysaccharides. Pectins from numerous sources such as citrus [201, 329], apple [381], okra [211], and ginseng [212, 213], extracted and modified in various ways, have been investigated for their anti-cancer effects and have been shown to reduce cell proliferation, migration, adhesion, and induce apoptosis in a variety of cancer cell lines.

Pectin that has been treated with pH (low or high), heat or enzymes is generally referred to as 'modified pectin', although this term remains ambiguous as pectin is a highly heterogeneous material. Modified pectin structure can vary widely depending on the pectin source, extraction and method of modification. The majority of research into the effects of modified pectin has been carried out with citrus pectins, and several studies have demonstrated the benefits of modified citrus pectin (MCP) over commercial, un-modified citrus pectin (CP) [191, 193-195]. It is generally understood that modifying CP with heat and pH will decrease MW and proportionally increase total neutral sugars, although in the majority of studies the extent of structure modification was not examined. Pectasol-C, enzymatically modified citrus pectin on sale in the USA as a health supplement, has a low MW but is also very low in neutral sugar content. It has been shown to reduce proliferation and induce apoptosis in prostate cancer cells [201], to have immunostimulatory properties [205] and to increase the prostate specific doubling time in prostate cancer patients [207]. Generally it is thought that pectins with a high neutral sugar content to be more bioactive due to the hypothesis that galactan side chains on pectin can bind to the pro-metastatic protein Galectin-3 which could then result in suppression of cancer cell proliferation, aggregation, adhesion and metastasis[195, 321].

This chapter investigates two sources of pectin. Sugar beet pulp: a source of pectin known to be rich in neutral sugars with low DE, high DAc, high protein content and the presence of ferulics; and citrus peel: a source of pectin used in many investigative studies into the anti-cancer effects of pectin, with low neutral sugar content, high DE, low DAc and low protein content. The pectins are extracted and modified in a variety of ways to provide an array of pectins with varying sugar compositions, DE, DAc and protein contents and MWs.

4.2 Aims

The first objective of this chapter was to screen five sugar beet and five citrus pectins characterised in Chapter 3, and Pectasol-C for their effects on the viability of HT29 and DLD1 cells. Selected pectins were further investigated for time-dependent effects on cell viability, apoptosis and effects on the cell cycle. Secondly, the relationship between pectin structure and bioactivity was investigated in order to test the hypothesis that decreased MW and increased neutral sugar content of pectin are important for bioactivity.

4.3 Materials and Methods

4.3.1 Pectins

Pectins were characterised in Chapter 3. Sample preparations for cell treatment were carried out as in section 2.3.

4.3.2 Cell viability assays

For dose-dependent studies, cells were seeded in Nunclon 96-well plates and after 24 hours were incubated in 200 µl cell culture medium supplemented with pectin at 0.2, 0.5 and 1 mg/ml for 48 hours. For time-dependent studies cells were incubated with 200 µl cell culture medium supplemented with 1 mg/ml pectin for 48, 72, 96 and 120 hours. For the study of acute treatments, HT29 cells were incubated with 1 mg/ml CA and 1mg/ml SSBA for 24 hours and the medium replaced with fresh medium without pectin for a further 48 hours. Cells were seeded at the concentrations specified in Table 3 (pg.72). In one assay 5 biological replicates were

performed for each condition of treatment, and between 3 and 17 separate assays were performed for each pectin. Detection of cell viability and statistical analyses were carried out as described in section 2.4.

4.3.3 Cell counting

Nunclon 6-well plates were seeded in 2 ml cell culture medium at the concentrations specified in Table 3 (pg.72). The initial cell concentration was chosen in order to have untreated cells at 80-90% confluency after 120 hours. After 24 hours, the culture medium was replaced with medium supplemented with 1 mg/ml pectin and incubated for a further 24, 48, 72, 96 or 120 hours. Each condition of treatment was carried out in duplicate over three independent experiments. Cell counting and statistical analyses were performed as described previously (section 2.8)

4.3.4 Cell imaging

HT29 cells were seeded in Nunclon 6-well plates at 200,000 cells/well in 2ml cell culture medium. The initial cell concentration was chosen in order to have untreated cells at 80-90% confluency after 96 hours. After 24 hours, the culture medium was replaced with medium supplemented with 1 mg/ml pectin and incubated for a further 72 or 96 hours. Cell imaging was performed as described previously (section 2.5).

4.3.5 Apoptosis detection by flow cytometry

Nunclon 6-well plates were seeded with HT29 cells in 2 ml medium at the concentrations specified in Table 3 (pg.72). After 24 hours the medium was replaced with 2 ml cell culture medium supplemented with 0.5 or 1 mg/ml SSBA or 0.01 µg/ml staurosporine and incubation continued for a further 72 hours. Each treatment was performed in triplicate over three independent experiments. Sample preparation and data analyses were carried out as described in Chapter 2.6.

4.3.6 Cell cycle analysis by flow cytometry

Nunclon 6-well plates were seeded with HT29 cells in 2 ml medium at the concentrations specified in Table 3 (pg.72). After 24 hours the medium was replaced with 2 ml cell culture medium supplemented with 0.5 or 1 mg/ml SSBA or 150 μM FTS and incubation continued for a further 72 hours. Each treatment was performed in triplicate over three independent experiments. Sample preparation and data analyses were performed as described previously (section 2.7)

4.4 Results

4.4.1 Effects of citrus and sugar beet pectins on viability of HT29 and DLD1 cells

Pectin structure differs depending on the source and method of preparation. Therefore, to examine whether pectins prepared using different extraction protocols have similar biological effects, five citrus pectins and five sugar beet pectins were screened for effects on HT29 and DLD1 colon cancer cells. Cells were treated with 0.2, 0.5 or 1 mg/ml of pectin over 48 hours, and their viability assessed. Table 15 shows that among the pectins tested, alkali treated sugar beet (SBA) and alkali treated citrus pectin (CA) significantly reduced HT29 cell viability in a dose dependent manner over 48 hours, with 1 mg/ml of CA and SBA reducing viability by 19% and 21%, respectively. Untreated commercial citrus (CP) and sugar beet (SBC) pectins together with the oxalic acid-extracted pectins (SBO, SBOPG) and Pectasol-C had no effect. None of the commercial pectins or Pectasol-C affected DLD1 cells after 48 hours.

Table 15 ***Effects of different doses of pectin on HT29 and DLD1 cell viability*****.** Cells were treated with 0.2, 0.5 and 1 mg/ml pectins for 48 hours. Results are expressed as percentage of viable cells remaining after treatment relative to the untreated control. Data are shown as mean ± standard error. * p<0.05; ** p<0.001.

Pectin	0.2 mg/ml	0.5 mg/ml	1 mg/ml
HT29 cells			
CP	94.3 ± 4.3	101.1 ± 6.5	97.6 ± 4.7
CH	90.4 ± 3.3	100.4 ± 7.7	95.3 ± 3.3
CA	87.4 ± 8	79.9 ± 6.8**	81 ± 4.3**
CO	103.6 ± 4.1	97.3 ± 7	96 ± 4.6
COPG	89.3 ± 7.1	93.4 ± 12.9	90.1 ± 7.7
SBC	101.8 ± 5.1	89.6 ± 6.7	94.6 ± 6.2
SBH	110.5 ± 7	97 ± 5	92.24 ± 6.8
SBA	83.5 ± 6.3*	79.2 ± 5.8**	79.3 ± 5.9**
SBO	103.7 ± 11.6	101.8 ± 7.3	111.347 ± 9
SBOPG	103.4 ± 18.5	83.7 ± 24.4	92 ± 13.9
Pec-C	92.4 ± 11	88.9 ± 8.6	91.6 ± 8
DLD1 cells			
CP	103.4 ± 6.2	100.4 ± 3	97.8 ± 4.3
CA	103.9 ± 2.3	99.9 ± 4.3	94.2 ± 6.5
CH	102.2 ± 3.5	106.4 ± 3.4	106.7 ± 4.7
CO	105.9 ± 5.7	101.9 ± 3.2	103.1 ± 3.3
COPG	100.6 ± 6.9	101.2 ± 10.5	107.9 ± 11.9
SBC	107.6 ± 4.7	109 ± 5.5	111.5 ± 2.1
SBH	101.3 ± 3.9	103.6 ± 7.1	103.8 ± 8.5
SBA	98.5 ± 3.2	100.3 ± 6.5	98 ± 8.5
SBO	99.7 ± 9.6	97.4 ± 7	101.3 ± 8.2
SBOPG	101.4 ± 10.3	98.7 ± 18.4	103 ± 6.5
Pec-C	105.7 ± 3.1	91.9 ± 7.3	99.8 ± 5.4

It was observed that the pectins that reduced cell viability, SBA and CA, caused the cell culture medium to become viscous, and it was suggested that this could inadvertently cause cell death. The viscosity occurs because both SBA and CA are pectins with a low degree of esterification (DE). Upon modification with alkali, the DE of sugar beet pectin is reduced from 55% to 18%, and citrus pectin from 70% to 45%. This cleavage of methyl esters generates the formation of negatively charged acid groups, which can bind and sequester small counterions, such as calcium present in cell culture medium, linking pectin molecules together to form a gel. To investigate the contribution of low DE to bioactivity, four LM pectins of 10% and 40% DE sourced from citrus peel and apple pomace were examined for effects on cell viability. An apparent inverse relationship was observed between the DE of the pectin and the viscosity of the medium. However, none of these LM pectins had any significant effect on cell viability (Figure 15), indicating that viscosity per se does not affect cell viability and that the low DE may not be sufficient for bioactivity.

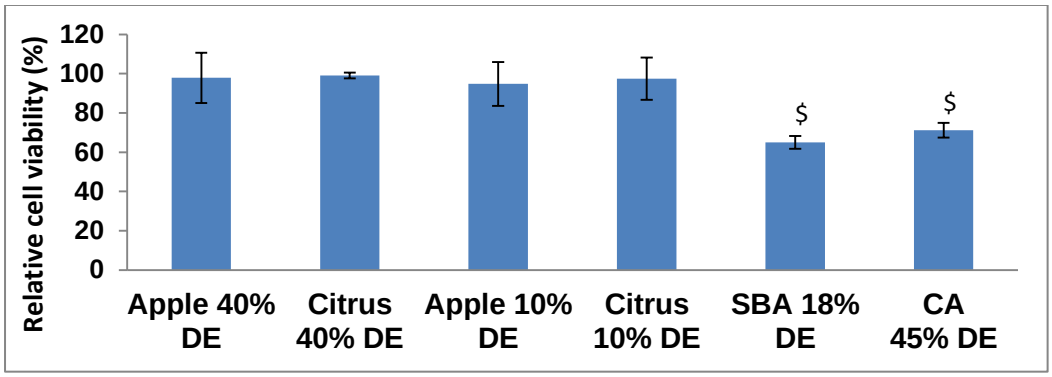

Figure 15 ***Effect of LM pectins on HT29 cell viability after 72 hours*****.** Results are expressed as percentage of viable cells remaining after treatment relative to the untreated control. $ p<0.0001.

4.4.2 Time dependent effects of pectins on HT29 and DLD1 cell viability and proliferation

As 1 mg/ml SBA and CA consistently reduced HT29 cell viability after 48 hours, the time dependent effects were investigated, alongside the unmodified pectins CP and SBC. The effects of SBA and CA on cell viability were time dependent (Figure 16). SBA reduced cell viability by 18%, 37%, 57%, and 67% after 48, 72, 96 and 120 hours, respectively ($p<0.0001$), and CA by 19%, 28%, 48% and 50% ($p<0.0001$). SBC, which did not affect cell viability after 48 hours, induced a significant decrease in cell viability after 96 hours ($p<0.01$). While SBA had no effect on DLD1 cell viability after 48 hours, treatment for 72, 96 and 120 hours significantly decreased cell viability by 11%, 25% and 36%, respectively (Figure 17). After 120h, CA and SBC also reduced cell viability by 28% and 18%, respectively. CP did not significantly affect the viability of either cell line. Pec-C had no effect on DLD1 cells, and in HT29 cells required 96 hours to reduce viability by 19% ($p<0.05$) and 120 hours by 39% ($p<0.001$).

It was noted that the sugar beet pectins were not completely soluble, and as SBA showed significant bioactivity, it was investigated if this played a role in reducing cell viability. The soluble and insoluble components of SBA were separated by centrifugation, and the time dependent effects of the soluble fraction (SSBA) were examined with HT29 and DLD1 cells. In both HT29 and DLD1 cells it was found that there was no significant difference in the effects of SSBA and total SBA on cell viability (Figure 16 and 17). The monosaccharide compositions of SBA and SSBA were analysed in Chapter 3 and they were shown to be almost identical. Therefore, only SSBA was used in subsequent studies.

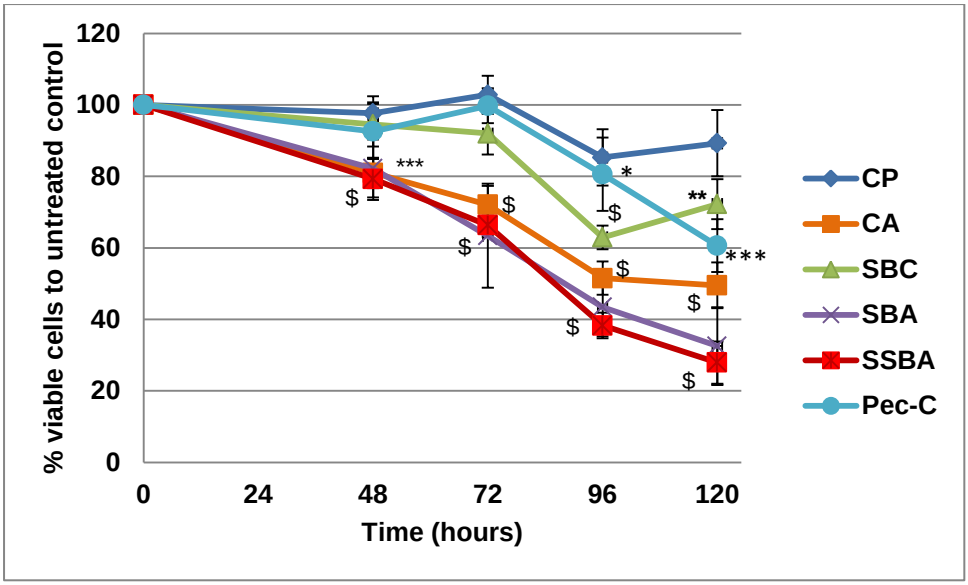

Figure 16 ***Effects of CP, CA, SBC, SBA and SSBA on HT29 cell viability over 120 hours*****.** Results are expressed as percentage of viable cells remaining after treatment relative to the untreated control. Data are shown as mean ± standard error (CP n=7, 5, 3, 3; CA n=5, 8, 5, 4; SBC n=4, 3, 3, 3; SBA n=8, 3, 3, 3; SSBA n=10, 16, 8, 4) *p<0.05; **p<0.01; ***p<0.001; $ p<0.0001

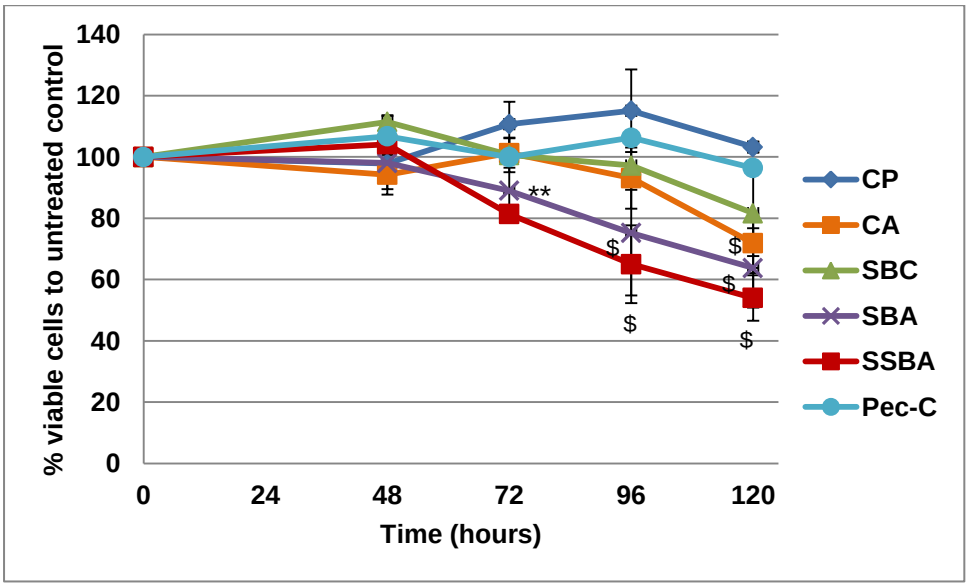

Figure 17 ***Effects of pectins on DLD1 cell viability over 120 hours***. Results are expressed as percentage of viable cells remaining after treatment relative to the untreated control. Data are shown as mean ± standard error (CP n=5, 4, 3, 3; CA n=5, 4, 4, 3; SBC n=5, 4, 5, 4; SBA n=5, 4, 3, 3; SSBA n=3, 5, 4, 3) **p<0.01; $ p<0.0001

The results presented suggest that there may be cell-specific effects of SSBA as it was consistently more effective in HT29 cells than DLD1 cells. To investigate this further the effects of SSBA on three other colon cancer cell lines were determined. HCT116, Caco2 and LoVo cells were incubated with 1 mg/ml SSBA, alongside 1 mg/ml CP as a negative control for 72 hours. SSBA did not reduce cell viability in any of these additional cell lines (Figure 18).

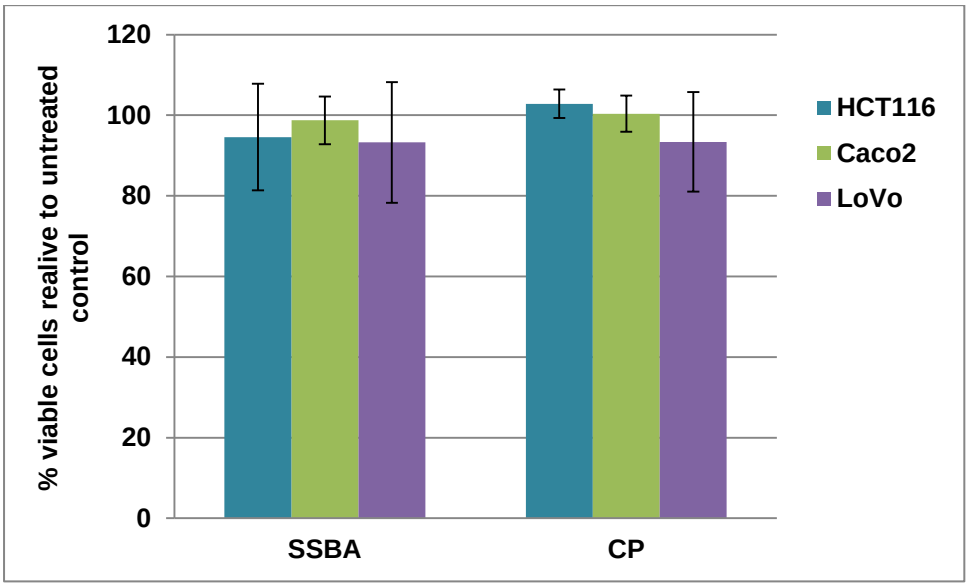

Figure 18 ***Effect of SSBA and CP on cell viability of HCT116, Caco2 and LoVo cells over 72 hours.*** Results are expressed as percentage of viable cells remaining after treatment relative to the untreated control. Data are shown as mean ± standard error (n=3)

To gain an understanding of how cell viability is reduced by SSBA and CA, the effect on cell proliferation was investigated. Counting the number of cells every 24 hours after incubation with the pectins for a total of 120 hours can give an indication if the cells are still dividing and growing. Figure 19 shows the untreated cells behaved as expected, with a 2-3 fold increase every 24 hours, which declined with time due to nutrients becoming expended in the medium. CP, as expected had no effect on the cells. Cells treated with SSBA and CA significantly decreased in number, however, cell growth was still

detected every 24 hours, but at a significantly reduced rate than the untreated cells.

Figure 20 shows images of HT29 cells treated with 0.5 and 1 mg/ml SSBA after 72 and 96 hours. Consistent with the cell viability data, the total cell population of SSBA-treated cells and the sizes of the cell groups were significantly smaller, suggesting that SSBA affected cell growth in a dose- and time-dependent manner

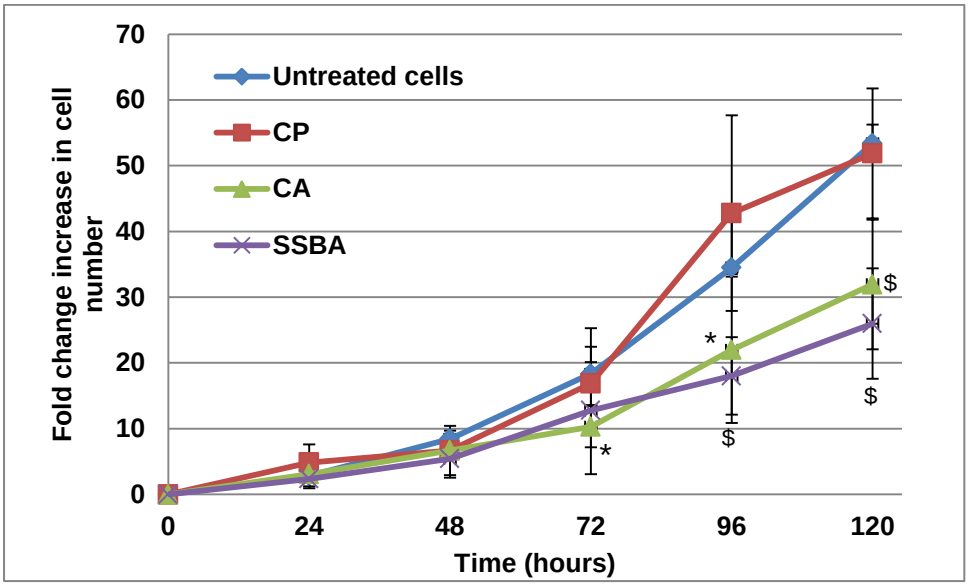

Figure 19 ***Time-dependent effect of CP, SSBA and CA HT29 cell number.*** Results are expressed as the fold change increase in cell number relative to the seeded number of cells. Data are shown as mean ± standard error (n=3) * $p>0.05$; \$ $p<0.0001$

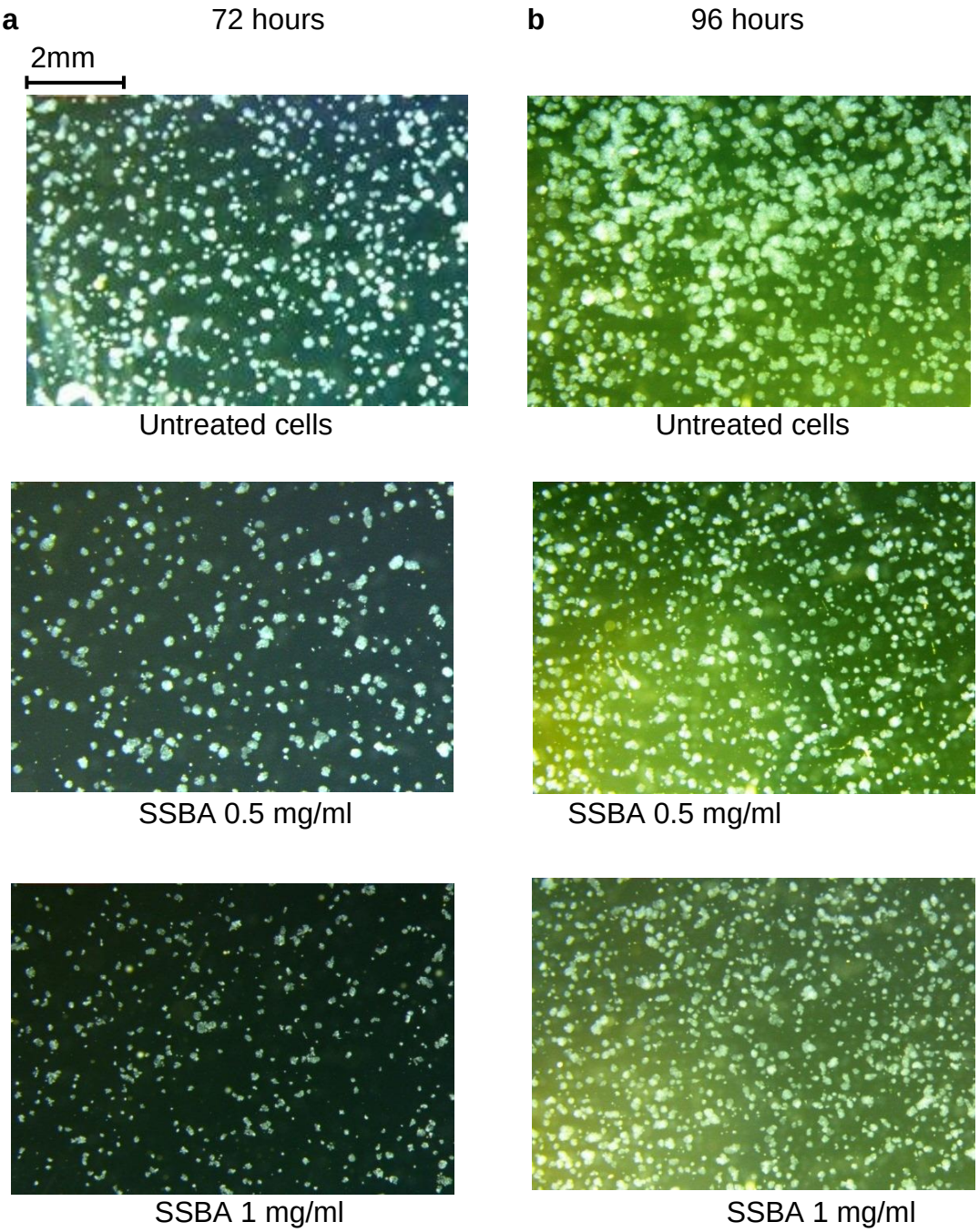

Figure 20 ***Images of HT29 cells after incubation with 0.5 and 1 mg/ml SSBA over 72 and 96 hours.*** (a) 72 hour incubation (b) 96 hour incubation

The reduction in HT29 cell viability induced by SSBA and CA was only evident after 48 hours of treatment. This raises the possibility that these pectins could be having a transitory effect on the cells leading to the subsequent observed effects on cell viability. To assess this, HT29 cells were treated with CA and SSBA for 24 hours, the pectin-containing medium was then replaced with fresh medium without pectin for a further 48 hours. Figure 21 shows that cells are not affected by a transitory 24 hour exposure and they need to be continually exposed to the pectins for the significant effect on cell viability to be evident.

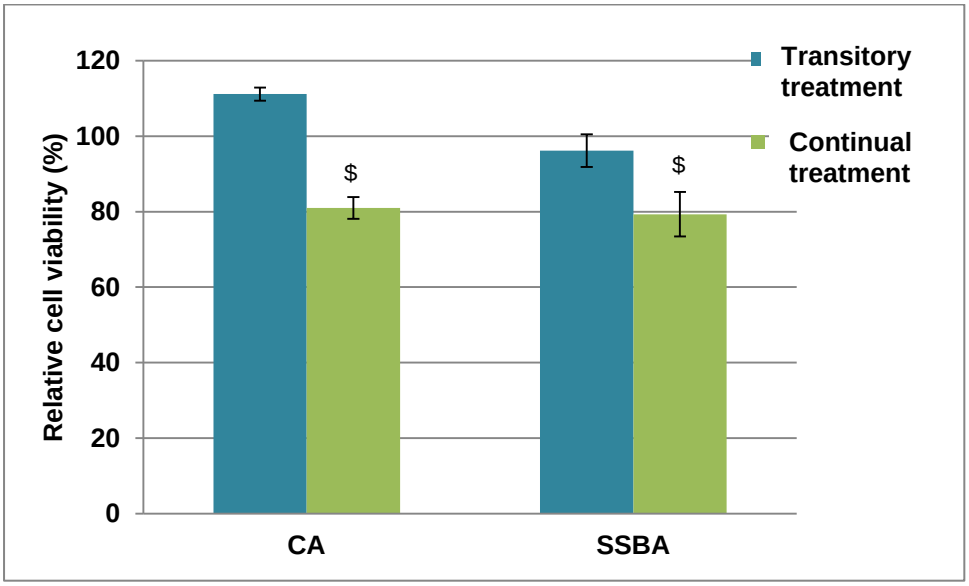

Figure 21 ***Effect of transitory and continual treatments of CA and SSBA on HT29 cells over 72 hours.*** Results are expressed as percentage of viable cells remaining after treatment relative to the untreated control. Data are shown as mean ± standard error (acute treatments n=3) $ $p<0.0001$

4.4.3 Effect of SSBA on HT29 cell apoptosis and the cell cycle

A reduction in cell viability is often associated with an induction of apoptosis, or a reduction in cell proliferation due to regulation of the cell cycle. The effect of SSBA on these mechanisms in HT29 cells was examined using flow cytometry. To investigate apoptosis, three independent experiments were carried out with HT29 cells treated with 0.5 or 1 mg/ml SSBA over 72 hours.

The cells were then stained with Annexin V and PI to detect cells that were either live, undergoing early or late apoptosis, or dead. Figure 22a displays the percentage of cells in these four categories compared with the effects of the known apoptosis-inducing agent staurosporine (ST) [382].

a

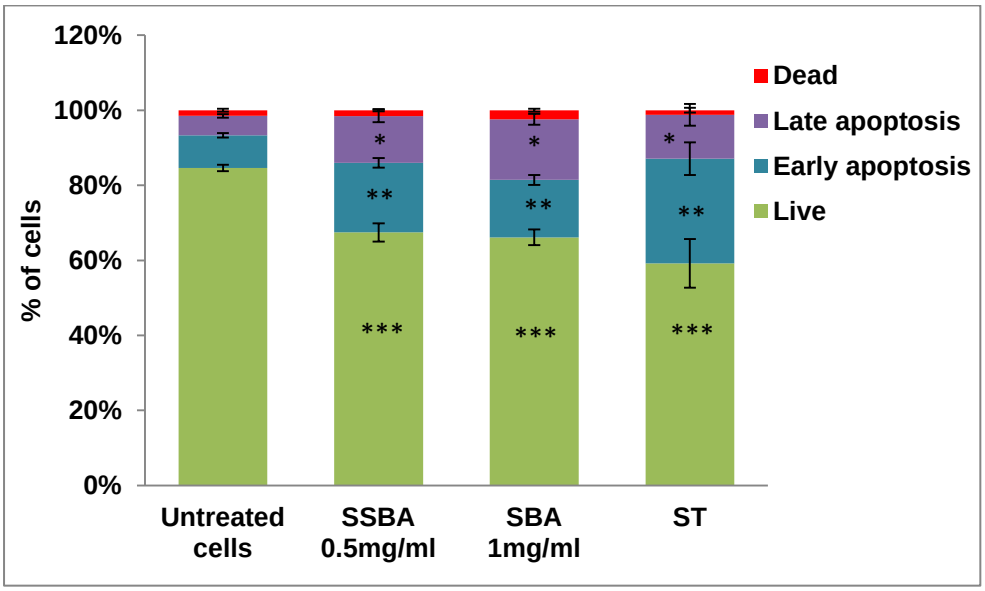

b

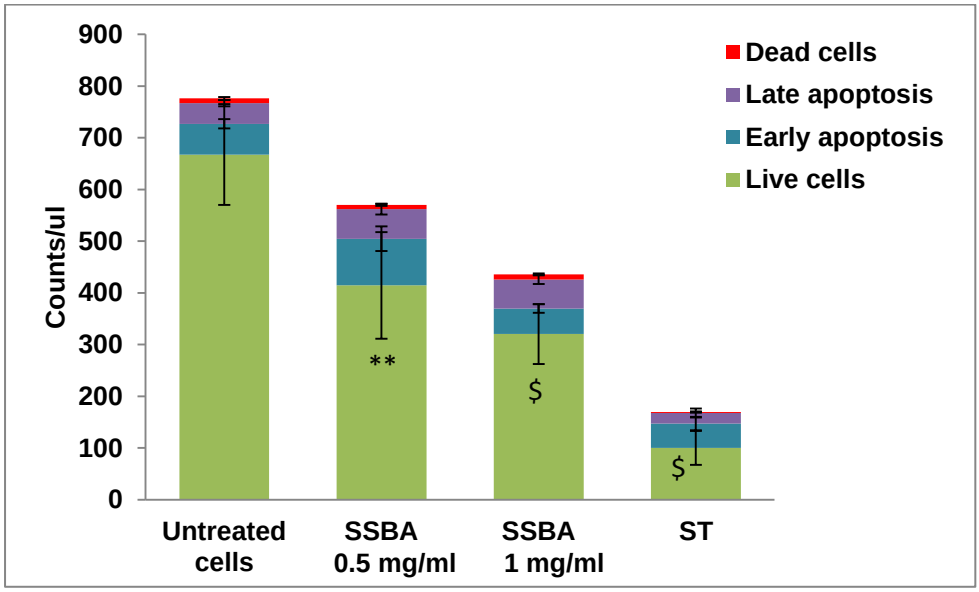

Figure 22 ***Dose dependent effects of SSBA and ST on apoptosis of HT29 cells*****.** (a) The percentage of cells in each stage of apoptosis. (b) The number of cells per µl in each stage of apoptosis. Data are shown as mean ± standard error. ** $p<0.01$; \$ $p<0.0001$

Cells treated with SSBA for 72 hours had a significantly higher percentage of cells in the apoptotic phases, with an increase of 10% and 8% of cells in early apoptosis and 7% and 9% in late apoptosis, with 0.5 and 1 mg/ml SSBA, respectively. Figure 22b indicates the number of cells counted per µl, and clearly shows that the number of live cells is dependent on the dose and incubation time of SSBA.

Examination of the supernatant taken from the cells incubated with SSBA can also give an indication of cell death by the number of floating cells in the medium, as dead cells will often detach from the plate. Figure 23 shows a dose-dependent increase in detached cells following treatment with 0.5 or 1 mg/ml SSBA, with the increase in the number of detached cells reaching statistical significance for the 1 mg/ml SSBA treatment.

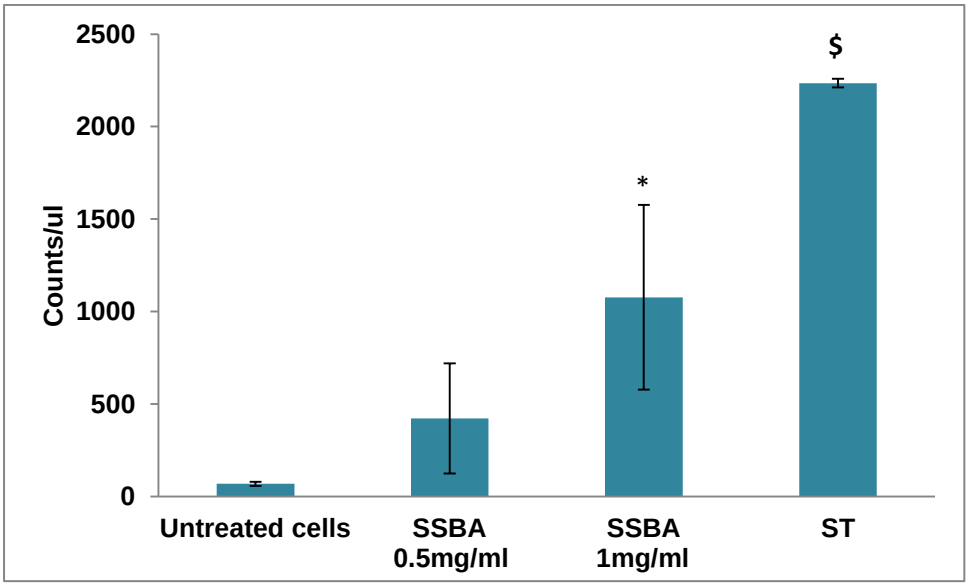

Figure 23 ***Number of events counted per µl in cell culture medium after incubation with 0.5 and 1 mg/ml SSBA over 72 hours*****.** Counts/µl shown here are after subtraction of counts/µl of pectins only, and so represent whole or broken down cells detached from the plate. *p<0.05; $p<0.0001

a

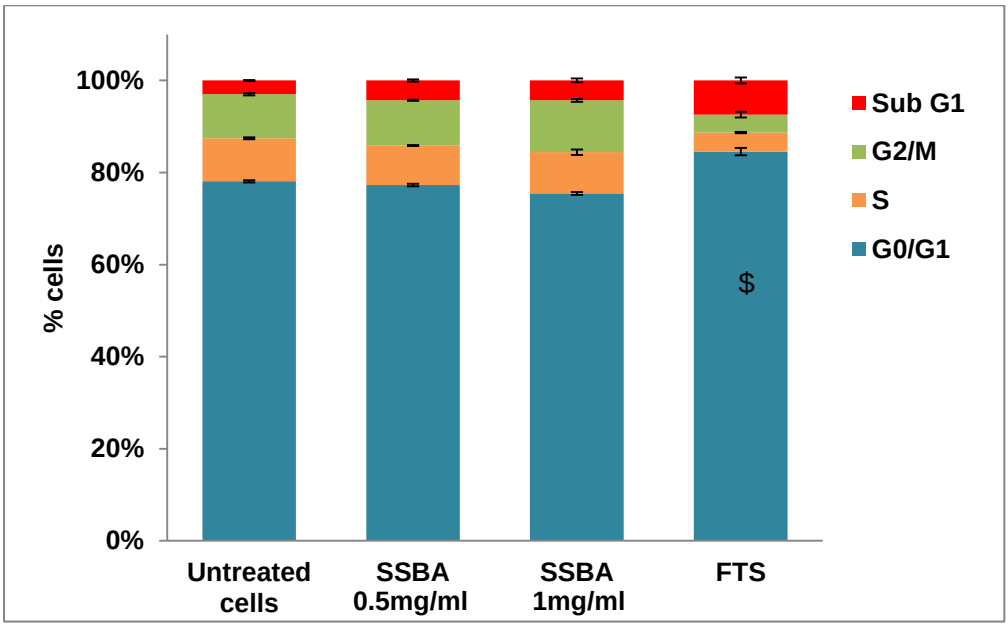

b

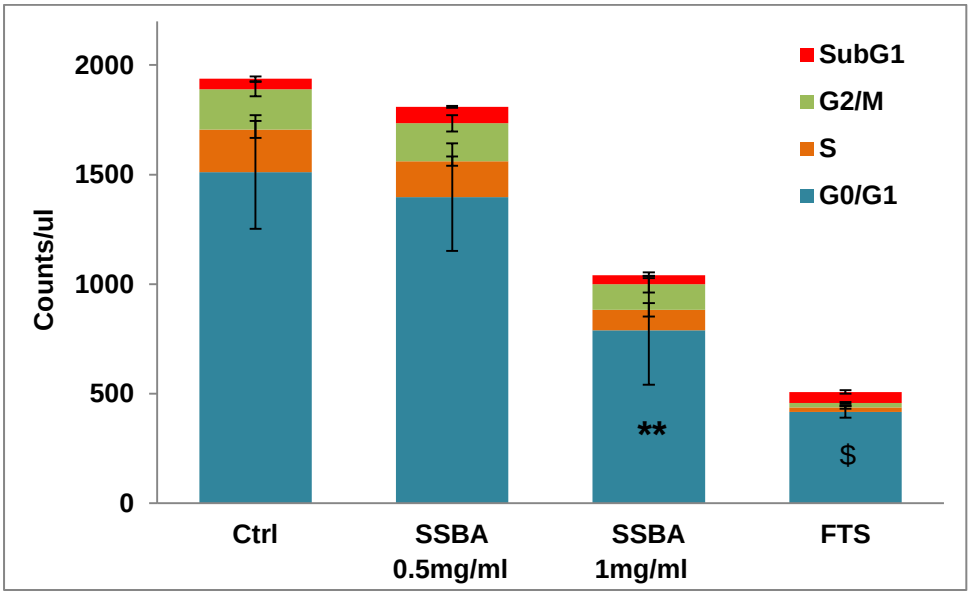

Figure 24 ***Dose dependent effects of SSBA on the cell cycle of HT29 cells*****.** (a) The percentage of cells in each phase of the cell cycle. (b) The number of cells per µl in each phase of the cell cycle. Data are shown as mean ± standard error. ** $p<0.01$; \$ $p<0.0001$

To investigate the effect of SSBA on the cell cycle of HT29 cells, three independent experiments were carried out with a treatment of 0.5 or 1 mg/ml SSBA over 72 hours. Cells were fixed and then stained with PI to detect cells in each stage of the cell cycle; G0/G1, S, G2/M, as well as the sub G1 phase which indicates apoptosis. Farnesylthiosalicylic acid (FTS), an anti-cancer drug known to induce cell cycle arrest [383] was used as a positive control. Figure 24a shows that the proportion of cells in each phase of the cell cycle was unaffected by treatment with SSBA, except for an increase in the sub G1 phase, indicating an increase in apoptotic cells. Figure 24b indicates the number of cells counted per µl, and clearly shows that the number of live cells is dependent on the dose and incubation time of SSBA. FTS, however, increased the accumulation of cells in G0/G1 phase, as well as the sub G1 phase, indicating that FTS reduces cell viability via a combination of apoptosis and cell cycle arrest.

4.5 Discussion

Various modified pectins have been shown to have anti-cancer activity; however there is a lack of comparative studies that take structure into consideration. In this chapter citrus and sugar beet pectins, which had been extracted and modified in a variety of ways and characterised in chapter 3, were investigated for their effects on the viability of HT29 and DLD1 cells in order to further our understanding of the potential anti-cancer properties of pectin and the structure-function relationship.

It has previously been proposed that the components of pectin responsible for their anti-cancer activity reside in the neutral sugar rich RGI regions [191], and so it was hypothesised that those pectins with a higher neutral sugar content and lower MW should be more bioactive. The pectins were modified in a variety of ways to provide an array of pectins with varying neutral sugar, DE, DAc and protein contents and MWs, in order to assess any correlation between these traits and effects on cells. The initial screen for bioactivity determined the effects of the pectins on the colon cancer cell lines HT29 and DLD1 utilising an assay that measures metabolic activity of the cells and,

therefore, captures effects of treatments on cell viability. The cellular effects of pectins, which significantly impacted cell viability, were then explored in more detail.

Of the five citrus pectins, only alkali-treated citrus pectin, CA, consistently reduced cell viability in HT29 cells in a dose- and time-dependent manner, although a 120 hour treatment was required for the effect of this pectin to become significant in DLD1 cells. Unmodified commercial citrus pectin, CP, did not affect the viability of either cell line. Of the sugar beet pectins, again it was the alkali-treated pectin SSBA that had the most significant effect, and SSBA was the only pectin to significantly reduce cell viability in both HT29 and DLD1 cell lines, although a longer time period (72 vs 48 hours) was required for the reduction in cell viability to become significant in DLD1 cells. Unmodified sugar beet pectin SBC reduced cell viability in HT29 cells after 96 hours and in DLD1 cells after 120 hours. The oxalic acid extracted pectins, SBO, SBOPG, CO and COPG did not affect the viability of either cell line. Pec-C did not affect DLD1 cells but in HT29 cells started to reduce viability after 96 hours. Pectin is a natural part of the human diet. The intake of pectin from a daily diet of 300g fruits and vegetables can be estimated to be 1.8 g. Typical levels of pectin used as a food additive are between 0.5% and 1%, approximately the same amount of pectin contained in fresh fruit and vegetables. Low toxicity allows pectin to be consumed in relatively large quantities or given at a high dose as a drug. Experimental results from numerous studies have shown pectins to reduce viability, induce apoptosis at 1 mg/ml [201, 204, 321, 329, 384]. As such, the concentration range in this study is reasonable.

The effect of SSBA on the viability of HT29 cells was attributable to an induction of apoptosis, which explains the observed, significant dose-dependent decrease in live cell number and the observed, significant dose-dependent increase in detached and fragmented cells floating in the cell culture medium following treatment. The effect of SSBA on the cell cycle of HT29 cells was also examined but was shown not to be affected. Together with the observation that SSBA-treated cells continue to proliferate, albeit at

a reduced rate, suggests that SSBA induces apoptosis in a proportion of cells and does not impact the proliferation of the remainder.

In Chapter 3, all pectins were characterised for neutral sugars, GalA, DE, DAc, protein content and MW in order to assess any relationship between structure and bioactivity. In HT29 cells, SSBA and CA were considerably more effective at reducing cell viability than the other pectins, and had major structural differences. The most significant effect of the alkali treatment of the pectins was to decrease DE. Alkali treatment cleaved methyl esters, reducing the DE from 57% in SBC to 18% in SSBA and from 70% in CP to 45% in CA. This raises the possibility that the DE is significant for bioactivity. However, SSBA has a lower DE than CA, but is more bioactive. In addition, the bioactivity of four additional LM pectins was shown to have no effect on cell viability after a 72 hour treatment. Additionally, Pec-C which has a very low DE of 5% had no effect on cells at 72 hours; however it did start to reduce cell viability after 96 hours. This indicates that the DE per se is not significant for bioactivity, and other characteristics of SSBA and CA are more important for bioactivity. The effect of pectin DE has been looked into in previous studies. A comprehensive mechanistic study by Jackson and co-workers showed that alkali treatment of heat-treated citrus pectin destroyed its apoptosis-inducing activity in LNCaP prostate cancer cells. They suggested that it is the ester linkages in pectin that are essential for bioactivity [329]. This certainly cannot be true of pectins in this study. In another study, Bergman and colleagues proposed that DE made no significant difference to bioactivity, and showed that CP with DE of 30% and 60% reduced HT29 cell proliferation by 45% and 57%, respectively [326].

A further noticeable difference between SSBA and CA and the other pectins is MW. The oxalic extracted pectins, due to the weak acid extraction, have extremely high MWs, and these were shown to have no effect on cell activity. Heat treating the commercial extracted pectins reduces MW, and alkali treatment reduces this further. Thus SSBA and CA have relatively low MW. However, Pec-C has a significantly lower MW than SBA and CA but took much longer to elicit bioactivity. Moreover, SSBA has a significantly higher

MW than CA but exhibits greater bioactivity suggesting that MW alone is not indicative of bioactivity.

SSBA and CA also vary from the other pectins in their sugar composition. The treatment of the commercial pectins SSBC and CP with heat and alkali reduced arabinan content significantly, and the hydrolysis of the pectin backbone enriched the pectins in neutral sugar-containing RGI regions. It should also be noted that, although SSBA has short Gal side chains of <3.5 residues branching from RGI backbones, it is 14-fold richer in these RGI regions than CA, which might be a reason for its greater bioactivity.

The effects of SSBA and CA on cell viability appear to be cell specific with enhanced activity towards HT29 cells compared with DLD1 cells. SSBA did not affect the viability of three additional colon cancer cell lines HCT116, Caco2 and LoVo providing further support for cell-specificity in the bioactivity of these modified pectins. This will be explored in greater detail Chapter 8.

4.6 Conclusion

In summary, the alkali-treated pectins SSBA and CA significantly reduced cell viability in HT29 cells via an induction of apoptosis. The results presented in this chapter provide some support for the initial hypothesis that pectins with a higher neutral sugar content and lower molecular weight will exhibit greater bioactivity. However, while SSBA and CA are relatively low in MW, SSBA has a higher MW than CA but exhibits greater bioactivity. SSBA and CA also have relatively low arabinan content. However, this alone does not rule out the importance of the sugar side chains for bioactivity. The results from this chapter provide greater insight into the structural requirements for pectin bioactivity, which will be explored in greater detail in subsequent chapters. They also provide a framework for the exploration of the molecular mechanisms of the cellular interaction with pectins and the consequences for cell viability.

Chapter 5

Effects of pectic polysaccharides on colon cancer cell viability, apoptosis, cell cycle and correlation with polysaccharide structure

5.1 Introduction

A wide range of pectic polysaccharides encompassing homopolymers to highly complex pectins have been reported to display anti-cancer activities. Two of the major structural elements of pectins are HG regions composed of repeating GalA residues, and RGI regions composed of a backbone of repeating GalA and Rha residues, highly branched with neutral sugar arabinan, galactan and arabinogalactan side chains of varying degrees of polymerisation. As yet, no well-defined evidence has been obtained on the structural requirements necessary for optimal activity towards cancer cells. The hypothesis that (1→4)-β-D-galactan side chains branched from the RGI regions of pectin can bind to the pro-metastatic protein Galectin-3 has given rise to the belief that the RGI regions of pectin, and particularly the (1→4)-β-D-galactan side chains, are important for bioactivity [321, 325, 385]. However, another study showed that the HG regions of ginseng pectin were important for anti-proliferative activity [213].

In this chapter, seven pectic polysaccharides were investigated in order to determine the structural features of pectin required for an optimum effect on cancer cells. As pectin is mainly composed of two regions, HG and RGI, polysaccharides were chosen to denote these regions. C-PGA represents HG and P-RGI and P-RGI-X the RGI region. P-Gal, galactobiose (GB), SB-Ara and L-AG represent the neutral sugars that constitute RGI.

5.2 Aims

The first aim of this chapter was to screen seven pectic polysaccharides characterised in Chapter 3 for their effects on the viability of HT29 and DLD1 cells. Selected pectic polysaccharides were investigated for time-dependent effects on cell viability, cell proliferation, apoptosis and effects on the cell cycle. Secondly, the relationship between structure and bioactivity was examined in order to test the hypothesis that the neutral sugar side chains of RGI are important for bioactivity.

5.3 Materials and Methods

5.3.1 Pectic polysaccharides

Pectic polysaccharides were purchased from Megazyme (see section 2.2) and were characterised in Chapter 3. Galactobiose (GB), purchased from Megazyme, was not characterised in Chapter 3. According to the manufacturers, GB is prepared by controlled enzymic hydrolysis of potato β-galactan by endo-galactanase to yield a mixture of two isomeric disaccharides, Gal-β-(1→4)-Gal and Gal-β-(1→3)-Gal (ratio ~ 2:1). Sample preparations for cell treatment were carried out as in section 2.3.1.

5.3.2 Cell viability assays

For dose-dependent studies, cells were seeded in Nunclon 96-well plates and after 24 hours were incubated in 200 µl cell culture medium supplemented with pectin at 0.2, 0.5 and 1 mg/ml for 48 hours. For time-dependent studies cells were incubated with 200 µl cell culture medium supplemented with 1 mg/ml pectin for 48, 72, 96 and 120 hours. Cells were seeded at the concentrations specified in Table 3 (pg.72). In one assay 5 biological replicates were performed for each condition of treatment, and between 3 and 12 separate assays were performed for each pectin. Detection of cell viability and statistical analyses were carried out as described in section 2.4.

5.3.3 Cell counting

Nunclon 6-well plates were seeded in 2 ml cell culture medium at the concentrations specified in Table 3 (pg.72). The initial cell concentration was chosen in order to have untreated cells at 80-90% confluency after 120 hours. After 24 hours, the culture medium was replaced with medium supplemented with 1 mg/ml pectin and incubated for a further 24, 48, 72, 96 or 120 hours. Each condition of treatment was carried out in duplicate over three independent experiments. Cell counting and statistical analyses were performed as described previously (section 2.8)

5.3.4 Cell imaging

HT29 cells were seeded in Nunclon 6-well plates at 200,000 cells/well in 2 ml cell culture medium. The initial cell concentration was chosen in order to have untreated cells at 80-90% confluency after 96 hours. After 24 hours, the culture medium was replaced with medium supplemented with 1 mg/ml pectin and incubated for a further 24, 72 or 96 hours. Cell imaging was performed as described previously (Chapter 2.5).

5.3.5 Apoptosis detection by flow cytometry

Nunclon 6-well plates were seeded with DLD1 cells in 2 ml medium at the concentrations specified in Table 3 (pg.72). After 24 hours the medium was replaced with 2 ml cell culture medium supplemented with 0.5 or 1 mg/ml P-RGI or 0.01 µg/ml staurosporine and incubation continued for a further 72 hours. Each treatment was performed in triplicate over three independent experiments. Sample preparation and data analyses were carried out as described in Chapter 2.6.

5.3.6 Cell cycle analysis by flow cytometry

Nunclon 6-well plates were seeded with DLD1 cells in 2 ml medium at the concentrations specified in Table 3 (pg. 72). After 24 hours the medium was replaced with 2 ml cell culture medium supplemented with 0.5 or 1 mg/ml P-RGI or 150 µM FTS and incubation continued for a further 72 hours. Each treatment was performed in triplicate over three independent experiments. Sample preparation and data analyses were performed as described previously (Chapter 2.7)

5.4 Results

5.4.1 Effects of seven pectic polysaccharides on the viability of colon cancer cells

The pectic polysaccharides were tested for their effects on cell viability. Cells were treated with 0.2, 0.5 and 1 mg/ml of each polysaccharide for 48 hours prior to the quantification of the number of viable cells. Table 16 shows that

none of the pectic polysaccharides had any effect on the viability of HT29 cells after 48 hours. In DLD1 cells however, P-RGI significantly reduced cell viability in a dose-dependent manner with a decrease of 10% ($p<0.001$) with 0.5 mg/ml and 20% with 1mg/ml ($p<0.0001$) (Table 16). The remaining polysaccharides did not affect DLD1 cell viability after 48 hours. Since P-RGI consists of galactans, arabinans, arabinogalactans and polygalacturonic acid, a mixture of P-Gal SB-Ara, L-AG and C-PGA was investigated. However this combination of pectic polysaccharides did not reduce cell viability (Table 16).

Table 16 ***Effects of different doses of pectic polysaccharides on HT29 and DLD1 cell viability*.** Cells were treated with 0.2, 0.5 and 1 mg/ml pectins for 48 hours. Results are expressed as percentage of viable cells remaining after treatment relative to the untreated control. Data are shown as mean ± standard error. * $p<0.05$; *** $p<0.001$.

Pectin	0.2 mg/ml	0.5 mg/ml	1mg/ml
HT29 cells			
P-RGI	94.3 ± 4.9	91.8 ± 4.2	93 ± 5.6
SB-Ara	83.3 ± 12.8	84.4 ± 17.6	86.1 ± 18.1
P-Gal	90.5 ± 5.4	86.8 ± 6.4	85.6 ± 8
L-AG	87.6 ±11.2	81.7 ± 9.3	96.7 ± 9.1
GB	99.1 ± 12	91.4 ± 1.5	90.8 ± 7.5
C-PGA	93.1 ± 5.6	83.9 ± 5.9	92.8 ± 6.7
DLD1 cells			
P-RGI	97.2 ± 3.2	89.8 ± 2.5***	79.9 ± 4.7***
SB-Ara	102.2 ± 4.8	98.3 ± 6.7	98.5 ± 3.8
P-Gal	96.1 ± 1.5	94.8 ± 2.8	91.9 ± 8.1
L-AG	98.5 ± 1.2	100.5 ± 4.1	97.8 ± 2.9
GB	97.6 ± 2.9	98.4 ± 1	99.2 ± 1.4
C-PGA	102.2 ± 3.8	100.9 ± 4	100.8 ± 2.2
P-Gal + SB-Ara + L-AG + C-PGA	104.8 ± 2.4	100.6 ± 1	102 ± 1.5
P-RGI-X	99.6 ± 3.2	104.2 ± 1.4	100.9 ± 2.8

5.4.2 Time-dependent effects of pectic polysaccharides on colon cancer cell viability

The seven pectic polysaccharides did not have any effect in HT29 cells over 48 hours, and so their effect over a longer period of time was investigated. However, no reduction in HT29 cell viability was observed (Figure 25).

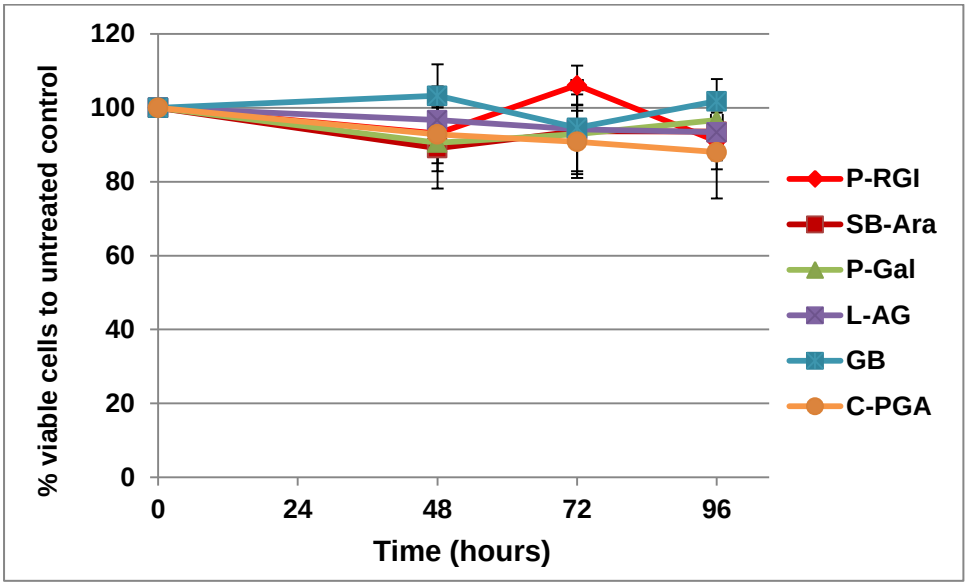

Figure 25 ***Time-dependent effects of pectic polysaccharides on HT29 cell viability*****.** Results are expressed as percentage of viable cells remaining after treatment relative to the untreated control. Data are shown as mean ± standard error (P-RGI n=10, 6, 3; SB-Ara n=3, 3, 4; P-Gal n=5, 3, 3; L-AG n=5, 3, 4; GB n=3, 3, 3; C-PGA n=4, 5, 3).

The effect of incubation time on DLD1 cell viability was also determined for the seven pectic polysaccharides. Figure 26 shows that the effects of P-RGI are time-dependent and reduce cell viability by 20%, 18%, 38% and 48% over 48, 72, 96 and 120 hours respectively ($p<0.0001$). P-Gal, showed no detectable effect on cell viability after 48 hours but induced a significant decrease in cell viability with prolonged incubation with a 12% reduction after 72 hours ($p<0.05$), 10% after 96 hours ($p<0.05$) and 19% after 120 hours ($p<0.01$). There was no observable effect of the remaining polysaccharides on the viability of DLD1 cells.

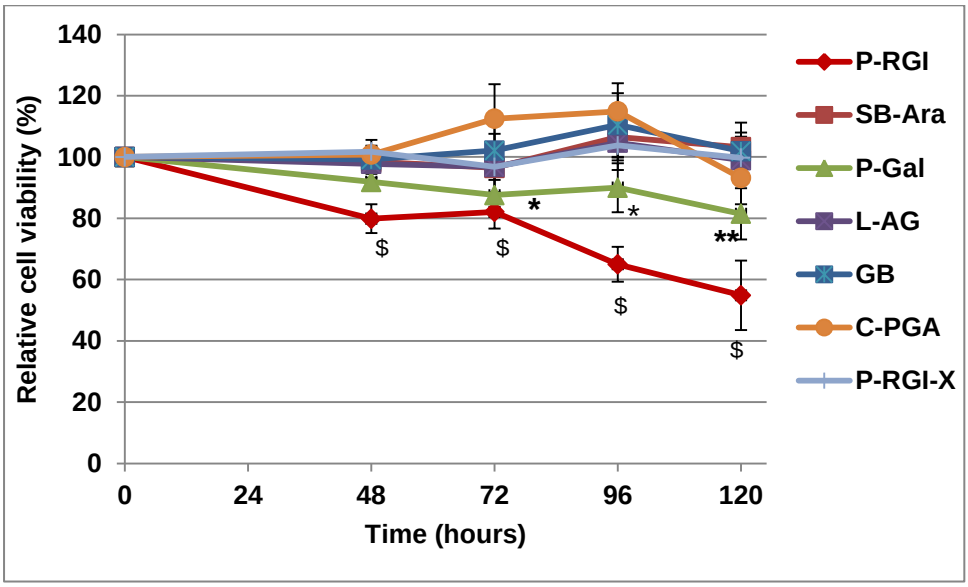

Figure 26 ***Time-dependent effects of pectic polysaccharides on DLD1 cell viability.*** Results are expressed as percentage of viable cells remaining after treatment relative to the untreated control. Data are shown as mean ± standard error (P-RGI n=12 at 48 hrs, 6 at 72 hrs, 5 at 96 hrs, and 4 at 120 hrs; SB-Ara n=3, 3, 3, 3; P-Gal n=12, 7, 5, 8; L-AG n=3, 3, 3, 3; GB n=7, 3, 3, 3; C-PGA n=6, 4, 4, 4; P-RGI-X 3, 6, 3, 4) *p<0.05; **p<0.01; $ p<0.0001

In order to investigate how cell viability is reduced by P-RGI and P-Gal, the effect on cell proliferation was explored. Counting the number of cells every 24 hours after incubation with the pectins for 120 hours can give an indication if the cells are still dividing and growing. Figure 27 shows the untreated cells increased in number by 2-3 fold every 24 hours, which declined with time, probably due to nutrients becoming expended in the medium. Cells treated with P-RGI and P-Gal showed a significantly reduced growth rate, with P-RGI having the greater effect. However, an increase in cell number was still detectable indicating that cell proliferation was not completely inhibited. Figure 28 shows images of DLD1 cells treated with 1 mg/ml P-RGI and P-Gal after 24, 72 and 96 hours. Consistent with the data on cell viability, the images of P-RGI-treated cells clearly show a dose- and time-dependent reduction in total cell population and the sizes of the cell

groups. P-Gal-treated cells displayed a similar morphology to untreated cells, indicating that the effect of P-Gal is not as significant in DLD1 cells as P-RGI.

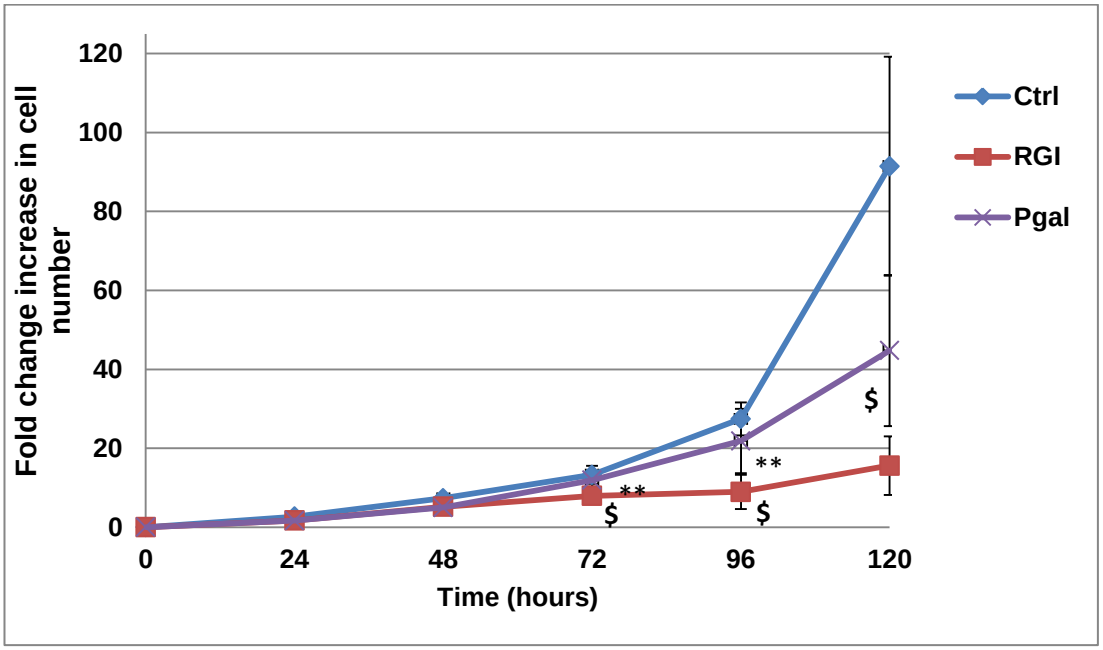

Figure 27 ***Effect of P-RGI and P-Gal on DLD1 cell number*****.** Results are expressed as the fold change increase in cell number relative to the seeded number of cells. Data are shown as mean ± standard error (n=3) $ $p<0.0001$

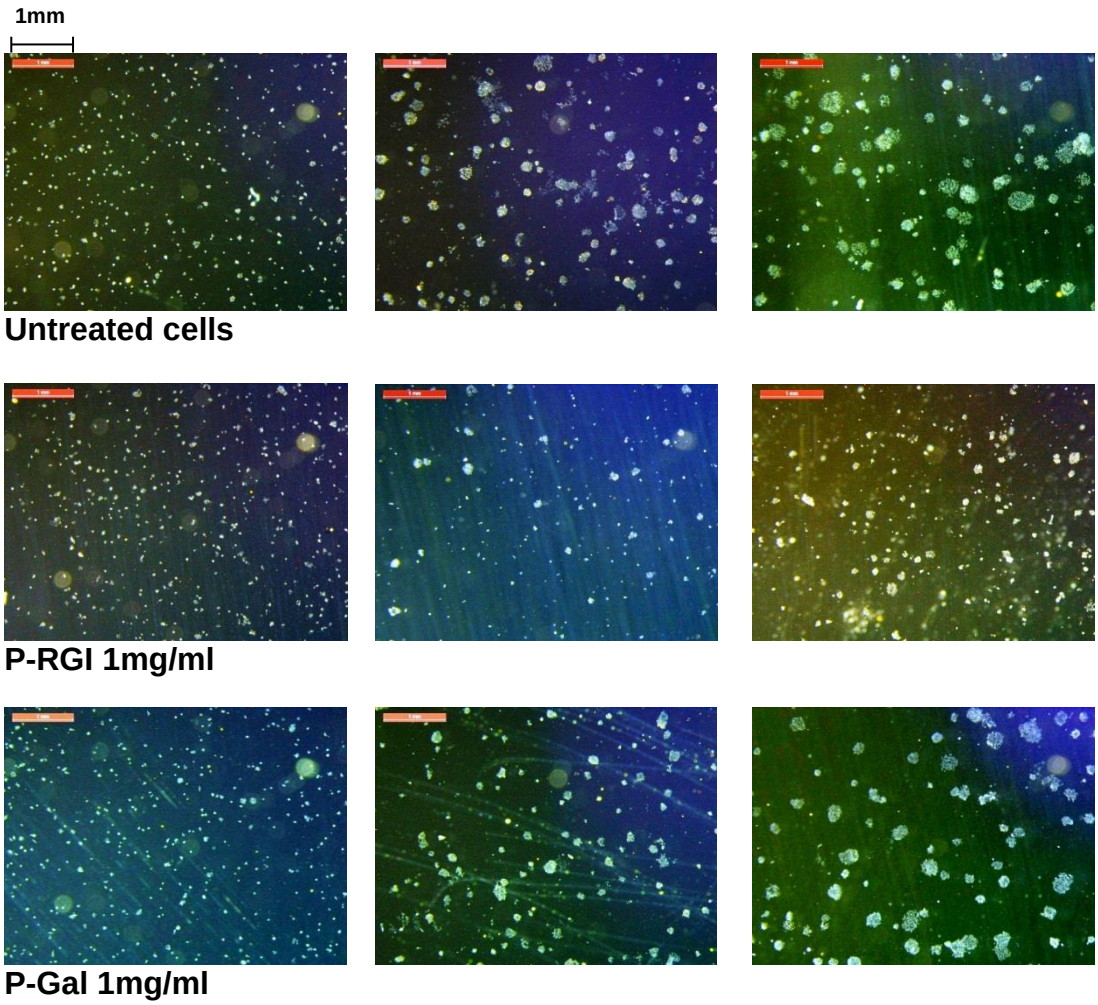

Figure 28 ***DLD1 cells treated with or without 1mg/ml P-RGI or P-Gal*** (a) 24 hours; (b) 72 hours; (c) 96 hours.

5.4.3 Effects of P-RGI and P-Gal on HCT116, Caco2 and LoVo colon cancer cells

P-RGI and P-Gal specifically inhibited the viability of DLD1 cells but not HT29 cells suggesting the effects of these polysaccharides may be cell-type dependent. To investigate this further the effects of P-RGI and P-Gal on three other colon cancer cell lines were determined. Caco2 and LoVo cells were incubated with P-RGI or P-Gal at 1 mg/ml for 72 hours. Neither P-RGI nor P-Gal reduced cell viability in these two cell lines (Figure 29). Time- and dose-dependent effects were also investigated in the HCT116 cell line. P-RGI at 0.5 and 1 mg/ml or P-Gal at 1 mg/ml were used to treat HCT116 cells for 48 and 72 hours. Figure 30 shows that, similar to DLD1 cells, P-RGI at 1mg/ml reduced cell viability by 10% after 48 hours, and at 0.5 and 1 mg/ml P-RGI reduced cell viability after 72 hours by 9% and 14%, respectively. P-Gal did not reduce the viability of HCT116 cells.

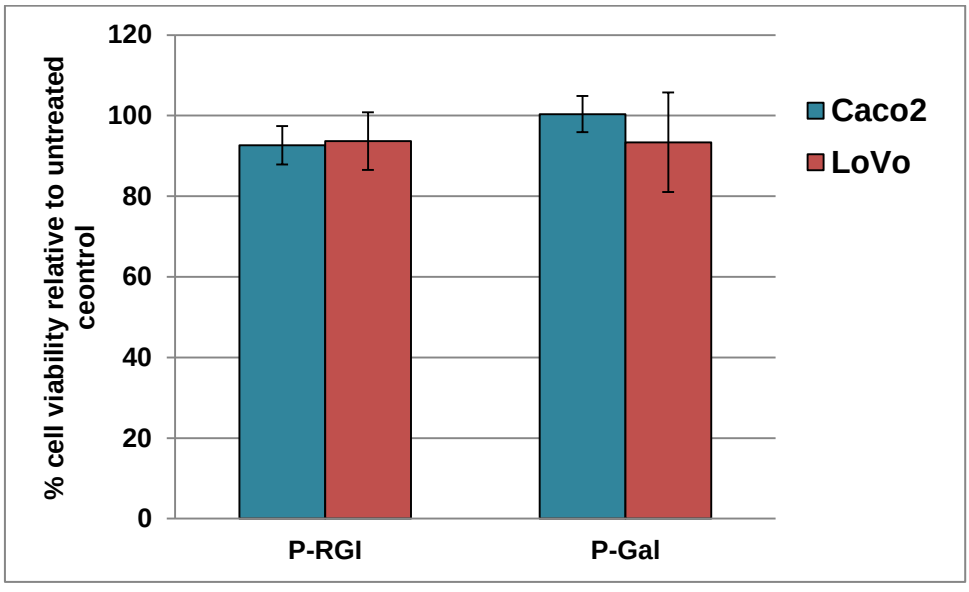

Figure 29 ***Effect of P-RGI and P-Gal on the viability of Caco2 and LoVo cells.*** Effect of 1 mg/ml P-RGI or P-Gal on Caco2 and LoVo cells after 72 hours. Results are expressed as the percentage of viable cells remaining after treatment relative to the untreated control. Data are shown as mean ± standard error (n=3).

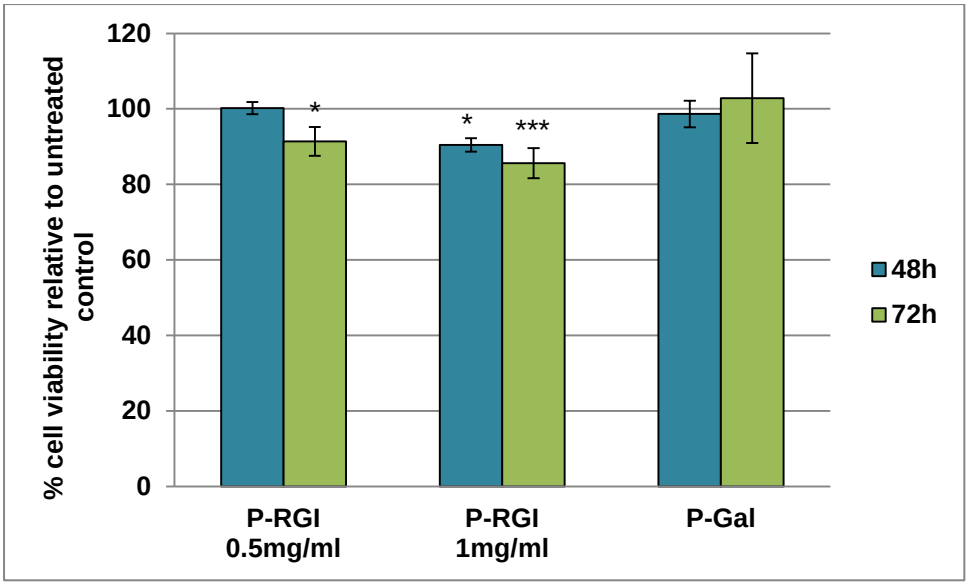

Figure 30 ***Time-dependent effects of P-RGI and P-Gal on cell viability of HCT116 cells.*** Effect of 0.5 and 1 mg/ml P-RGI or 1 mg/ml P-Gal on the viability of HCT116 cells. Results are expressed as the percentage of viable cells remaining after treatment relative to the untreated control. Data are shown as mean ± standard error (n=3). *p<0.05; ***p<0.001.

5.4.4 Effect of P-RGI on DLD1 cell apoptosis and the cell cycle

Results from chapter 4 revealed that SSBA reduced cell viability by inducing apoptosis in HT29 cells. To investigate the potential mechanism by which P-RGI reduced cell viability, P-RGI-treated DLD1 cells were subjected to apoptosis and cell cycle analyses. To investigate the effect of P-RGI on apoptosis, three independent experiments were carried out in DLD1 cells treated with 0.5 or 1 mg/ml P-RGI for 72 hours. An Annexin V-FITC/PI staining assay was used to ascertain cells that were either live, undergoing early or late apoptosis, or dead. Figure 31a displays the number of cells counted per µl in these four categories compared with the effects of the known apoptosis-inducing agent staurosporine (ST).. It shows that the number of live cells was decreased significantly in a dose dependent manner by P-RGI, as expected. However, this decrease in live cells is not attributable to apoptosis. While ST predictably increased the percentage of cells in the apoptotic phases, the percentage of cells undergoing apoptosis did not differ

in untreated cells or cells treated with P-RGI (Figure 31b). Although there was no evidence of an increase in cells undergoing apoptosis, Figure 32 shows that there was a significant 2.2 fold increase in detached cells present in the cell culture medium from cells treated with P-RGI. ST also caused a 7 fold increase in detached cells.

a

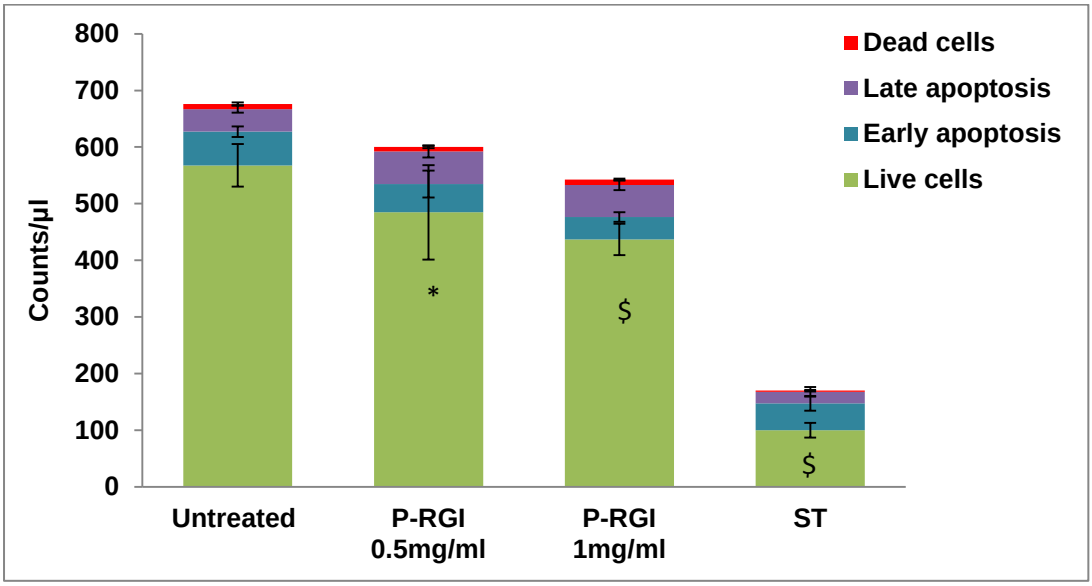

b

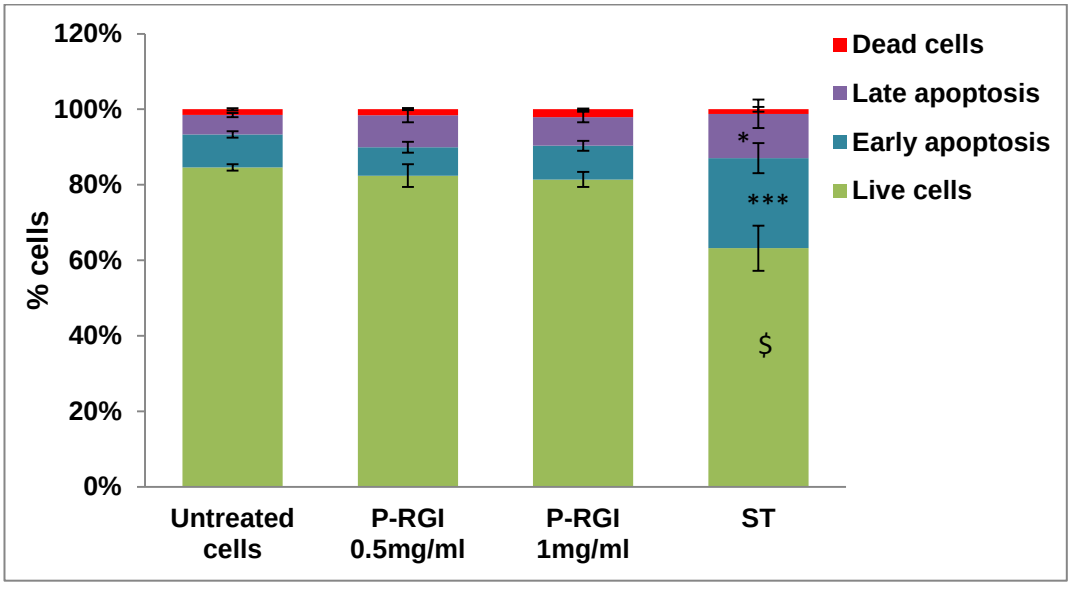

Figure 31 ***Effects of different doses of P-RGI on apoptosis of DLD1 cells*****.** (a) The number of cells per µl in each stage of apoptosis. (b) The percentage of cells in each stage of apoptosis. Data are shown as mean ± standard error. *p<0.05; ***p<0.001; $ p<0.0001

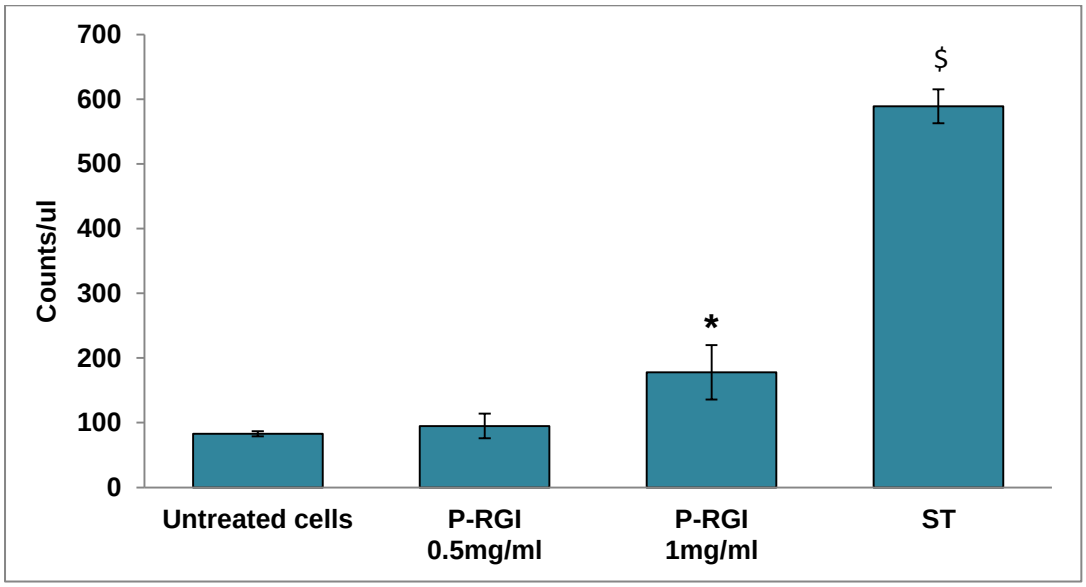

Figure 32 ***Number of events counted per µl in cell culture medium after incubation of DLD1 cells with 0.5 and 1mg/ml P-RGI for 72 hours*****.** Counts/µl shown here are after subtraction of counts/µl of pectins only, and so represent whole or fragmented cells detached from the plate. *p<0.05; $p<0.0001

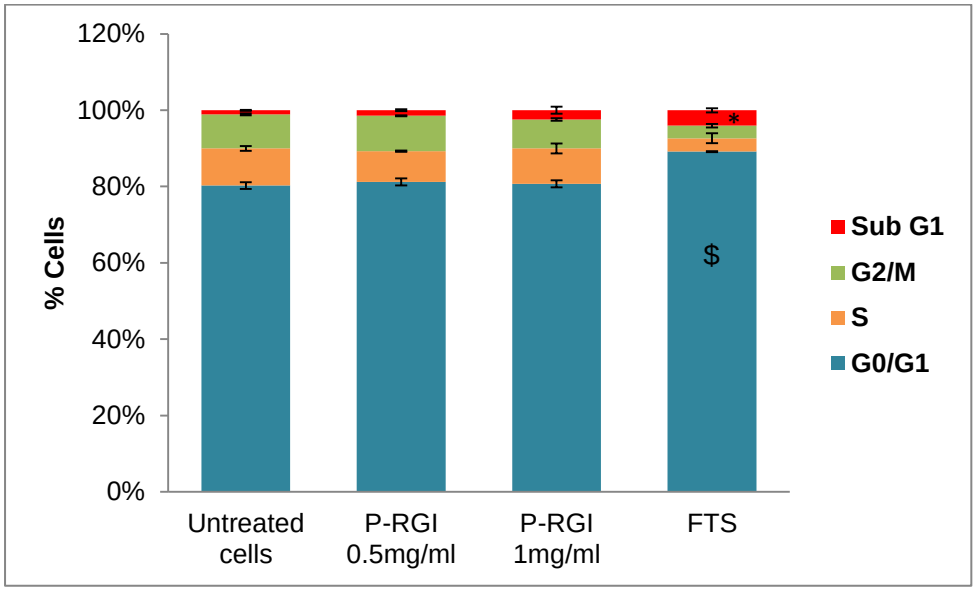

Figure 33 ***Effects of different doses of P-RGI on the cell cycle of DLD1 cells over 72 hours*****.** The percentage of cells in each phase of the cell cycle. Data are shown as mean ± standard error. *p<0.05; $ p<0.0001.

To investigate the effect of P-RGI on the cell cycle of DLD1 cells, three independent experiments were carried out with a treatment of 0.5 or 1 mg/ml P-RGI for 72 hours. Cells were fixed and then stained with PI to detect cells in each stage of the cell cycle; G0/G1, S, G2/M, as well as the sub G1 phase, which indicates apoptosis. Figure 33 shows that the proportion of cells in each phase of the cell cycle was unaffected by treatment with P-RGI. FTS was used as a positive control and Figure 33 shows that the proportion of cells in the G0/G1 phase was significantly increased in cells treated with FTS, indicating cell cycle arrest, as well as the proportion of cells in the sub-G1 phase, which indicates an increase in cell apoptosis.

5.5 Discussion

In this chapter seven commercially-available pectic polysaccharides were investigated for their effects on colon cancer cells. It has previously been suggested that the components of pectin responsible for anti-cancer activity reside in the neutral sugar-rich RGI regions [191, 322]. Therefore it was hypothesised that RGI, and the neutral sugars themselves, particularly galactan, would be responsible for the bioactivity of pectin. Seven pectic polysaccharides were chosen to represent the different constituent parts of pectin, in order to assess any correlation between these components and their effects on cells. The initial investigation for bioactivity determined the effects of the polysaccharides on the colon cancer cell lines HT29 and DLD1 utilising an assay that measures cell viability. Cellular effects were then investigated in more detail.

Of the pectic polysaccharides only P-RGI and P-Gal significantly reduced cell viability in DLD1 cells, with a greater effect observed with P-RGI. A mix of the representative RGI components C-PGA, P-Gal, SB-Ara and L-AG, failed to have an effect on cells. This indicates the conformation of the whole P-RGI molecule is important for activity. None of the polysaccharides were able to reduce HT29 cell viability. This is in contrast to a study by Cheng and colleagues, which showed that potato RGI reduced cell viability in HT29 after 72 hours via an induction of cell cycle arrest [384]. The effects of P-RGI and

P-Gal on cell viability appear to be cell specific with enhanced activity towards DLD1 cells compared with HT29 cells. Three additional colon cancer cell lines HCT116, Caco2 and LoVo, were also investigated for their response to treatment with P-RGI and P-Gal. Of these cell lines only HCT116 cells were affected. While P-Gal had no effect on the cells, P-RGI reduced cell viability in a dose- and time-dependent manner. It is notable that both DLD1 and HCT116 cells have KRAS and PI3KCA mutations, while the remaining cell lines lack this double mutation. Implications of cell-specificity will be discussed in Chapter 8.

An investigation into the cellular effects of P-RGI showed that the reduction in cell viability was not attributable to either apoptosis or cell cycle arrest. Quantifying the effects of P-RGI and P-Gal on cell proliferation showed that, similar to the effects of SSBA treatment of HT29 cells (Chapter 4), treated cells continue to proliferate, although at a significantly reduced rate compared with untreated cells. However, unlike SSBA-treated HT29 cells, there was no evidence for an induction of apoptosis in P-RGI-treated DLD1 cells. There was a significant dose-dependent increase in detached and fragmented cells floating in the cell culture medium following treatment. This would usually imply apoptosis, though it could also suggest a decrease in cell-cell or cell-surface adhesion, which could lead to reduced cell growth and proliferation. Further evidence for a decrease in cell adhesion will be explored in Chapter 8.

In Chapter 3, sugar composition and NMR analyses of six of the seven pectic polysaccharides were performed in order to assess any relationship between structure and bioactivity. In DLD1 cells, P-RGI and P-Gal were the only polysaccharides effective at reducing cell viability. This provides support for the hypothesis that bioactivity resides in the RGI regions and that the galactan side chains are at least partly responsible. However, P-RGI-X did not demonstrate any activity towards DLD1 cells. P-RGI-X was purchased from Megazyme with the same catalogue number and Lot number as P-RGI. However, upon NMR and sugar analyses it was evident that the structures of these two RGIs were different. The hypothesis that the RGI regions are

responsible for bioactivity is largely due to the concept that RGI is rich in neutral sugars, particularly (1→4)-β-D-galactan side chains. However, although P-RGI was shown to be very rich in RGI regions, NMR analysis revealed that it contains very short galactan chains of 1-3 DP, and no arabinan, although a small amount was detected by monosaccharide analysis. This is similar to the structure of ginseng RGIs characterised in a study by Yu and colleagues who showed galactan side chains were 1-3 residues in length [171]. Both P-RGI and P-RGI-X are almost identical to each other in terms of monosaccharide composition; however they are very distinct in the type of GalA present. NMR confirmed that P-RGI contains 16% GalA-linked GalA that makes up the HG backbone of pectin. Conversely, P-RGI-X does not contain any HG, with all GalA existing in either the RGI backbone or as free GalA mono-, di- or tri-saccharides. These findings suggest that HG is essential for the bioactivity of P-RGI. Previous studies have shown HG regions of ginseng pectin were important for bioactivity. Cheng and colleagues observed that HG-rich ginseng polysaccharide reduced viability in HT29 cells while neutral sugar-rich polysaccharide had no effect. The authors concluded that HG-rich pectins contain the active component of ginseng polysaccharides [213]. However, C-PGA which contains 96% GalA did not reduce DLD1 cell viability. This indicates that the HG backbone is not solely responsible for P-RGI bioactivity. A further noticeable difference between P-RGI and P-RGI-X provides further insight into the structural requirements for the bioactivity of P-RGI. In a linear polysaccharide a ratio of 1:1 reducing end and terminal GalA would be expected, in which was observed for P-RGI-X. However, P-RGI does not appear to contain reducing end GalA (section 3.4.3). This is unusual but suggests that HG is present as side chains of P-RGI, rather than integrated into the backbone. However no branch residues were observed so consequently it is unknown how HG may branch from P-RGI. Taken together, these findings suggest that HG, possibly present as side chains of P-RGI, is essential for P-RGI bioactivity.

The results in this chapter imply that galactan is not important for bioactivity. However, P-Gal reduced the viability of DLD1 cells, albeit to a lesser extent

and after an extended treatment time compared with P-RGI. P-Gal is composed of 26% GalA and 63% galactan, with long galactan chains of an average 23 residues branched from a short backbone of RGI. In the case of P-Gal, the galactan side chains could potentially be important for bioactivity. However, it should be noted that L-AG had no effect on cells and is composed of 79% galactan. The distinction between the two polysaccharides is that L-AG consists of only 2% GalA and no Rha, suggesting that if bioactivity resides in the galactan chains, they require an RGI backbone. Alternatively, the arabinan side chains on L-AG could prevent the bioactivity of the galactan chains, as arabinan itself did not affect cell viability. The fact that P-RGI and P-Gal have different structures yet have bioactivity in the same cell line could indicate multiple structures of pectin could have multiple mechanisms of action in cancer cells.

5.6 Conclusion

In summary, this study demonstrates that the RGI domain and, to a lesser extent, galactan from potato pectin, reduce the viability of DLD1 cells. This was not due to an induction of apoptosis or an arrest of the cell cycle. However, an observed increase in detached cells suggests that P-RGI reduces DLD1 cell viability by inducing the detachment of cells. The results presented in this chapter provide some support for the initial hypothesis that galactans are important for bioactivity. However, structural analysis of P-RGI and its comparison with P-RGI-X show that this hypothesis may not be completely accurate. The results presented indicate that the HG regions, possibly as side chains of P-RGI, are essential for bioactivity. The cell-specificity of P-RGI towards cell lines with KRAS and PI3KCA mutations provides a further mechanistic understanding of the activity of P-RGI. Due to the complexity of the structure of pectin domains it is possible that an assortment of pectic structures could exert bioactivity in a variety of cancer cells, via multiple mechanisms. This study uncovered some correlation between pectic structures and their bioactivities. This evidence furthers our understanding of the structural requirements for pectin bioactivity, which may aid the potential design of preventative therapies against CRC.

Chapter 6

An investigation into the role of neutral sugar side chains in pectin bioactivity

6.1 Introduction

As shown in Chapter 4, the exposure of HT29 colon cancer cells to SSBA significantly reduced cell viability via an induction of apoptosis. Similar anti-proliferative and pro-apoptotic effects have been observed in studies performed on cancer cells treated with MCP [196-198, 201, 329, 384]. However, modified pectin, as a term, is ambiguous due to the extraordinary complexity of pectin structure, which can differ depending on source, extraction and modification methods. This is the first study to observe modified sugar beet pectin as an apoptosis-inducing agent. It has been hypothesised that β(1→4)galactans branched from the RGI regions of pectins can bind to galectins, specifically Gal3, and inhibit its pro-metastatic actions [321, 322]. This has given rise to the premise that galactan side chains are important for pectin bioactivity. However, despite numerous studies investigating the anti-cancer effects of pectins, extensive analyses correlating structural features of pectin with bioactivity in cancer cells is scarce. Evidence for the bioactivity of neutral sugars in MP is shown by studies into the anti-tumour effects of arabinogalactans, which have been shown to inhibit the metastasis of sarcoma cells to the liver in mice [192, 320, 339]. Galactan side chains of RGI were also shown to be important for the agglutination of erythrocytes, and also for binding to Gal3 [325]. Jackson and colleagues observed that alkali treatment of citrus pectin abolished its apoptosis-inducing activity. Alkali treatment removed methyl esters and furthermore greatly reduced the extent of arabinan side chains. However, the presence of methyl esters was considered to be essential for the apoptosis-inducing activity rather than the arabinan side chains [329].

SSBA significantly reduced HT29 cell viability in a time- and dose-dependent manner while unmodified sugar beet pectin (SBC) had no effect (Chapter 4). The structure of SSBA was shown to have significantly higher neutral sugar content than SBC, leading to the hypothesis that the neutral sugar side chains are important for the anti-proliferative effect of SSBA. However, HT29 cell viability was not affected by neutral sugar-containing pectin fragments such as P-RGI, P-Gal, L-AG and SB-Ara, leading to the suggestion that the

entire pectin molecule, with HG backbone, is required for bioactivity. However, it is still possible that the neutral sugar content of SSBA is important for bioactivity. To investigate this, the galactan and arabinan side chains were enzymatically cleaved from SSBA and the effects on cell viability were determined. Polysaccharide degrading enzymes are suitable tools to study the structure of pectin due to their specificity in comparison to chemical methods. Pectic enzymes are classified according to the mode of attack on their specific structural elements of the pectin molecule. α-L-arabinofuranosidase and β-galactosidase are both exo-type enzymes that catalyse the hydrolysis of terminal non-reducing arabinans and galactans respectively; and endo-1,4-β-galactanase and endo-arabinase are endo-type enzymes that cleave at random residues within galactan and arabinan polymers, respectively [386].

6.2 Aims

In this chapter galactan and arabinan side chains were enzymatically cleaved from SSBA in order to investigate the role of the neutral sugar side chains of SSBA in mediating the activity towards HT29 cells. The effects of these modified SSBAs on HT29 cell viability were examined, and the relationship between pectin structure and bioactivity was investigated in order to test the hypothesis that high neutral sugar content of pectin is important for bioactivity.

6.3 Materials and Methods

6.3.1 Enzyme digestion of SSBA

The enzymes β-galactosidase (3200 U/ml), endo-1,4-β-galactanase (1300 U/ml), α-L-arabinofuranosidase (400 U/ml) and endo-arabinase (200 U/ml) were purchased from Megazyme (Wicklow, Ireland), diluted in 7mls milliQ water in duplicate to the concentrations and combinations indicated in Table 17 and filtered with a 0.2 µm syringe filter. SSBA at 10 mg/ml was added to 6mls of one set of enzyme dilutions, and incubated at 40°C for 24 hours

under agitation. Samples were then heated to 70°C for 10 minutes to halt digestion. 0.6 ml of each sample was then taken and freeze dried for NMR analysis. As a control, SSBA in water only also underwent these incubations. The other set of enzyme dilutions were kept as controls.

Table 17 ***Concentrations of enzymes and enzyme combinations.*** For dilution in H2O, ready for addition to SSBA or for use as controls.

Enzyme	**Enzyme concentrations**
β-galactosidase + Endo-1,4-β-galactanase	5 U/ml β-galactosidase + 5 U/ml endo-1,4-β-galactanase
α-L-Arabinofuranosidase + Endo-arabinase	1 U/ml α-Arabinofuranosidase + 1 U/ml Endo-arabinase
All enzymes	5 U/ml β-galactosidase + 5 U/ml endo-1,4-β-galactanase + 1U/ml α-L-arabinofuranosidase + 1U/ml endo-arabinase

6.3.2 NMR

All freeze dried samples were dissolved in 600 µl D_2O at a concentration of 10 mg/ml. ^{1}H, ^{13}C and 2D NMR spectra of the enzyme treated SSBA samples in D_2O were run at 338°K using the same methods described in Chapter 3. The modifications in polysaccharide structure produced by each enzyme treatment were assessed in an essentially qualitative manner by examination of the ^{1}H spectra with cross-sections through the $^{1}H/^{13}C$ HSQC spectra providing semi-quantitative information on the extent to which the different side chains were removed. To allow for slightly different amounts of material dissolved in the different samples the spectra were normalised by equalising the ^{1}H NMR intensities of the Rha Me signals (not affected by enzyme treatment) prior to the quantitative comparisons.

6.3.3 Cell viability assays

HT29 cells were seeded at the concentrations specified in Table 3 (pg.72) in Nunclon 96-well plates and allowed to adhere overnight. Cells were then incubated in 200 µl cell culture medium supplemented with 1 mg/ml enzyme-digested SSBAs, SSBA heated to 70°C for 10 minutes (SSBA-ne), enzymes only, or medium only, for 72, 96 or 120 hours. Following incubation the medium/pectin solution was replaced with 100 µl fresh medium. In each assay 5 biological replicates were performed for each condition of treatment, and between 3 and 4 separate assays were performed for each pectin. Detection of cell viability and statistical analyses were carried out as described in Chapter 2.4.

6.4 Results

6.4.1 Structural features of enzyme-digested SSBA

Enzymes were added to SSBA to cleave Gal and Ara in order to assess if these side chains are important for bioactivity. SSBA that was not incubated with enzymes but underwent the same incubation conditions (SSBA-ne) was structurally unchanged and indistinguishable to the original SSBA characterised in Chapter 3 (Figure 34).

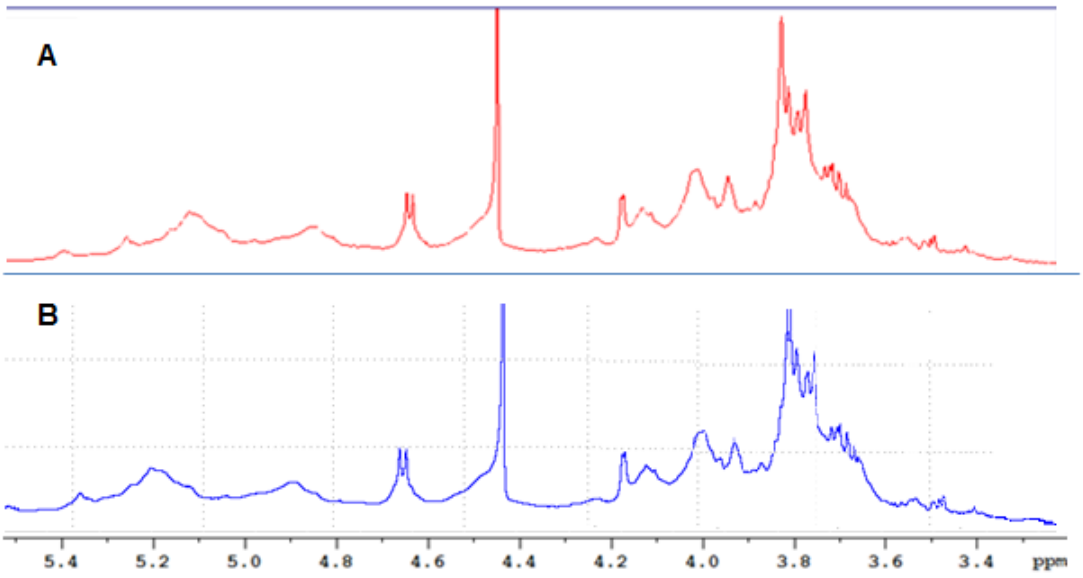

Figure 34 ***^{1}H NMR spectra of SSBA and SSBA-ne*** 600MHz ^{1}H NMR spectra of (A) Original SSBA and; (B) SSBA control that underwent the same incubation conditions as enzyme-digested SSBA.

Table 18 ***Effect of enzyme digestion of SSBA on neutral sugar side-chain content.***

Sample	Treatment	% β1,4-galactan content	% 1,5-linked Ara content	% Terminal Ara content
SSBA-ne	Control	100	100	100
SSBA-ara	α-L-Arabinofuranosidase + endo-arabinase	100	0	36
SSBA-gal	β-galactosidase + endo-galactanase	4-13	30	36
SSBA-all	All four enzymes	4-20	0	36

Figure 35 shows a comparison of the ^{1}H spectra of the untreated SSBA-ne with the reaction mixtures obtained following the three enzyme treatments (Table 18). In each case the main panel shows the main carbohydrate signal region (3.0-5.5 ppm). Table 18 shows the amount of (1→4)-β-Gal chains, (1→5)-Ara chains and terminal Ara remaining in SSBA after enzymatic digestion. In order to cleave galactan side chains, a mix of 5 U/ml β-galactosidase and 5 U/ml endo-galactanase was added to SSBA to generate SSBA-gal. Characteristic H1 (a) and H4 (b) signals of a β-(1,4)-linked Gal chain evident in SSBA-ne (Figure 35A) have largely been removed in SSBA-gal (Figure 35B), the number being reduced by 87-96% (Table 18). This enzyme combination additionally removed 70% (1→5)-Ara chains and 64% of terminal Ara. However a number of new signals are evident in the anomeric region of SSBA-gal. These include GalA reducing end signals, from both free GalA (e, h) and GalA that is 4-linked to another GalA (c, g), i.e. this represents the reducing end of an oligogalacturonide; another new signal (i) corresponds to H4 of a non-reducing end GalA unit. Free galactose was produced (H-1α, signal e and H-1β, signal h) and terminal Gal (linked to *O*-4 of Rha, signal g) was also present. It should be noted that the signals labelled g and h have both been assigned to two different sugar units with the help of 2D NMR experiments. Although terminal Gal units linked to Rha

were also found in SSBA (Chapter 3) it can be seen from the Rha Me signals that the ratio of substituted to unsubstituted units does not change in SSBA-gal (or indeed with either of the other enzyme treatments). It is therefore concluded that the endo-galactanase/ β-galactosidase treatment leaves a Gal stub at every position which was occupied in the SSBA RGI regions by either a stub or a longer galactan chain. The observation of free GalA and oligo-GalAs in SSBA-gal shows that there must be an unexpected polygalacturonase activity present in the commercial endo-galactanase used (separate experiments using only endo-1,4-β-galactanase or only β-galactosidase had shown that the impurity was solely associated with the former enzyme). Thus SSBA-gal shows two effects of the enzyme treatment: a removal of galactan side chains in the RGI regions to leave only stubs and, unexpectedly, a partial depolymerisation of the GalA HG regions. This depolymerisation was also seen in SSBA incubated with all four enzymes (SSBA-all).

To investigate the role of the Ara side chains, SSBA was treated with 1 U/ml α-L-arabinofuranosidase and 1 U/ml endo-arabinase, yielding SSBA-ara. The only new signals seen in SSBA-Ara (Figure 35C) were j (H1 α-Ara*p*) and k (H1 β-Ara*p*), the released free arabinose existing in the pyranose form rather than the furanose form found in arabinan side chains. The 1H spectrum of SSBA-ara (Figure 35C) shows that approximately the same amount of Ara monosaccharide was released as in SSBA-all, leading to the assumption that enzymes removed 100% (1→5)-Ara chains and 64% of terminal Ara (Table 18, p.157). However, there is no direct measurement on the different types of Ara from the HSQC spectrum (Figure 35) as with SSBA-all. It is unknown whether terminal Ara is linked to Rha or Gal residues. The ^{1}H spectrum of SSBA-all appears to be a simple summation of SSBA-gal and SSBA-ara without any evidence of major additional changes arising from a synergistic effect of the enzyme combination.

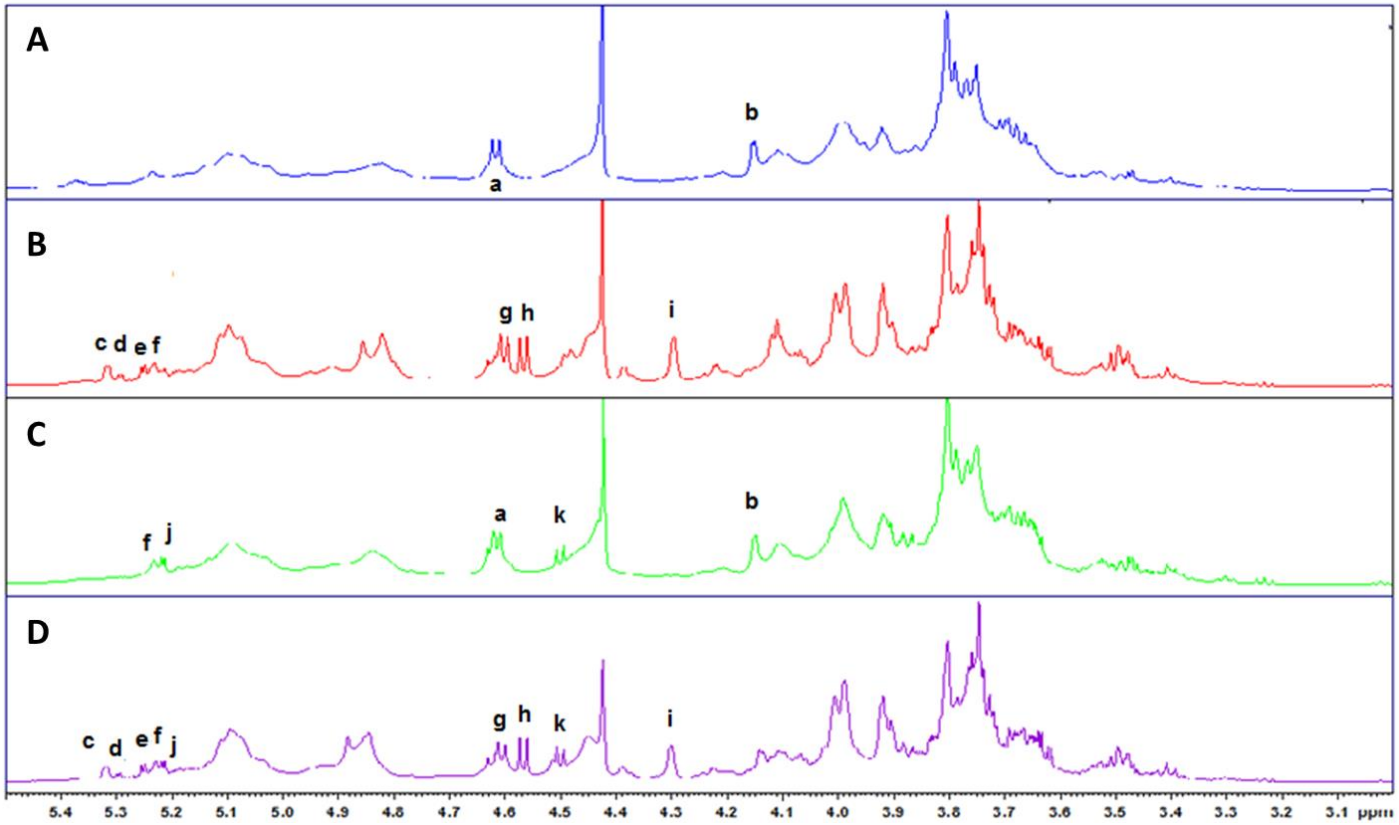

Figure 35 ***^{1}H NMR spectra of enzyme-digested SSBA*** 600MHz ^{1}H NMR spectra of SSBA and enzyme treated samples (D_2O, 338^0K). A) SSBA-ne (control); B) SSBA-gal; C) SSBA-ara; D) SSBA-all. Signal assignments (residue involved is shown in **bold**): a) H1 **β-(1,4)-Gal**; b) H4 **β-(1,4)-Gal**; c) H1 GalA(1→4)-**α-GalA^{RE}**; d) H1 **α-GalA**; e) H1 **α-Gal**; f) H1 **α-Rha**; g) H1 GalA(1→4)-**β-GalA^{RE}** and H1 **t-β-Gal**-(1→4)-α-Rha; h) H1 **β-GalA** and H1 **β-Gal**; i) H4 **α-GalA^{NR}**; j) H1 **α-Ara*p***; k) H1 **β-Ara*p***

6.4.1 Effects of enzyme-digested SSBA on HT29 cell viability

The effect of each enzyme treatment of SSBA on HT29 cell viability was investigated. Firstly, to eliminate the possibility that the enzymes themselves have cell modulating properties, cells were treated with enzymes only for 72 hours. No significant effect on cell viability was observed for any of the enzyme combinations (Figure 36). To eliminate the possibility that incubation at 40°C for 24 hours followed by heating to 70°C for 10 minutes had an effect on SSBA bioactivity, SSBA treated under these conditions without the addition of enzymes (SSBA-ne) was also added to cells for 72 hours. There was no significant effect of SSBA-ne on the viability of HT29 cells (Figure 37).

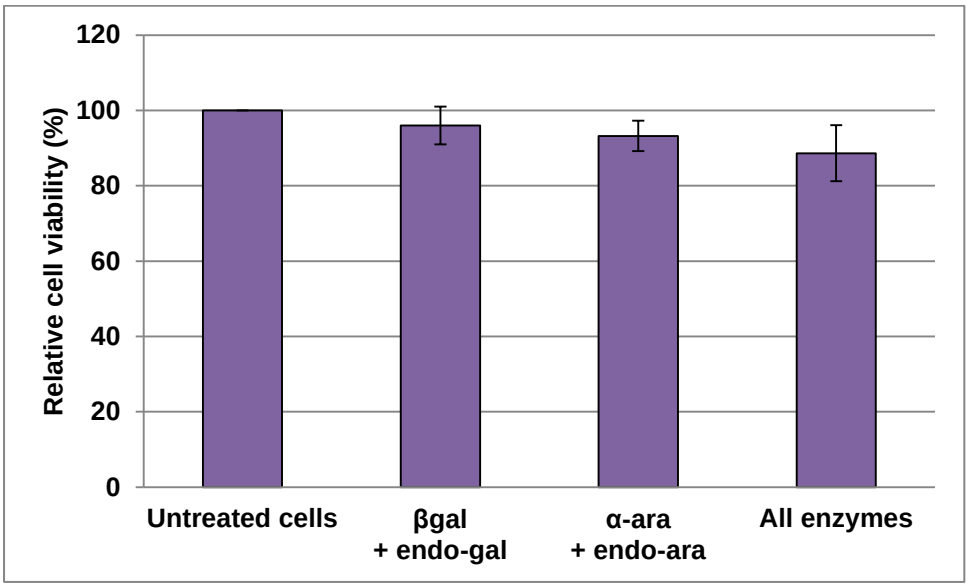

Figure 36 ***Effect of enzymes on HT29 cell viability after 72 hours.*** Data are shown as mean ± standard error (n=4).

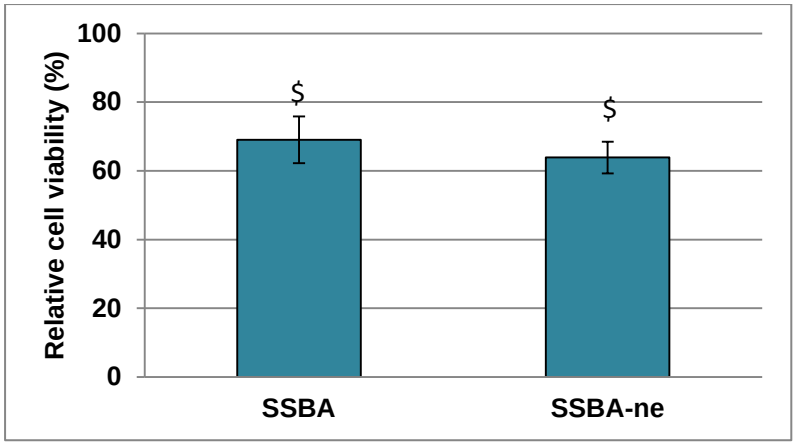

Figure 37 ***Effect of SSBA-ne on HT29 cell viability over 72 hours.*** Effects of SSBA and SSBA-neon HT29 cell viability after 72 hours. Data are shown as mean ± standard error (n=4). $ p< 0.0001

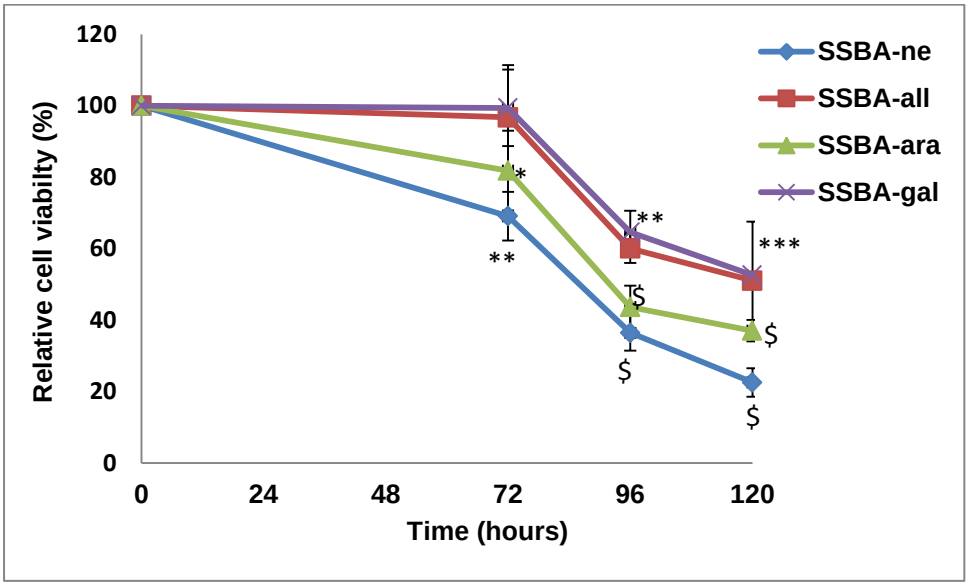

Figure 38 ***Time-dependent effect of SSBA and enzyme-digested SSBAs on cell viability of HT29 cells*** Data are shown as mean ± standard error (n=4) *p<0.05; **p<0.01; ***p<0.001; $p<0.0001.

Figure 38 shows the effect of enzyme-digested SSBA and non-digested SSBA on HT29 cell viability. Treatment of HT29 cells with 1 mg/ml SSBA-ne reduced cell proliferation in a time-dependent manner ($p<0.0001$), however, removal of Ara side chains to produce SSBA-ara also significantly reduced cell viability in a time-dependent manner ($p<0.0001$), but at a reduced rate with a 12.8%, 7.2% and 14.5% decrease in the effect on cell viability after 72, 96 and 120 hours, respectively ($p<0.01$), compared with SSBA-ne. This indicates that, although not essential, Ara plays a role in bioactivity. Removal of Gal side chains to yield SSBA-gal had an even more pronounced effect such that SSBA-gal did not significantly affect cell viability after 72 hours, while after 96 and 120 hours, SSBA-gal significantly reduced cell viability but to a significantly reduced extent compared with SSBA-ne ($p<0.001$). This indicates that the galactan side chains play an extremely important role in the effects of SSBA on reducing cell viability. To investigate the role of both Gal and Ara SSBA was treated with all four enzymes to remove 100% of (1,5)-linked-Ara, 64% terminal Ara and 80-96% Gal chains, to yield SSBA-all, which had an effect on cell viability comparable to SSBA-gal.

6.5 Discussion

Monosaccharide analysis showed SSBA consists of 47% GalA, 12% Rha, 25% Gal and 11% Ara (Chapter 3). NMR analysis showed that the neutral sugar content is comprised of Ara existing as 5-substituted or terminal residues within (1→5)-α-Ara, and Gal in short 1-3.5 DP (1→4)-β-Gal chains. The results of the cell viability assay show that hydrolysing Ara residues significantly decreased the SSBA-induced response indicating that (1→5)-α-Ara side chains are important for its anti-proliferative function. Moreover, the cleavage of Gal side chains completely abolished the SSBA-induced response after 72 hours, indicating that the Gal side chains of SSBA are necessary for bioactivity. However, SSBA-gal additionally underwent partial depolymerisation of the GalA HG regions. This could suggest that the breakdown of the HG backbone could be the reason that activity is

abolished; however a significant amount of HG still remains, therefore it is unlikely that partial depolymerisation would completely abolish activity. It is possible that the subsequent reduction in viability of cells after 96 hours could be due to the 4-13% β-Gal chains remaining on SSBA. However, it is more likely that the HG or RG backbone of SSBA could be a secondary bioactive component with less significant effects that take longer to detect. These two distinct phases strongly suggest there may be more than a single mechanism of action. The complete removal of (1→5)-linked-Ara along with the almost complete hydrolysis of Gal in SSBA-all induced a comparable response to SSBA-gal. These results suggest that the presence of Gal is a determining factor for the bioactivity of SSBA as the higher Ara content in SSBA-gal does not affect bioactivity. However, Ara does have an important role as on removal activity is reduced, although it appears that Ara alone does not exert bioactivity. It is possible that Ara may assist in the presentation of Gal to receptors and, moreover, that the cooperation between these side chains, together with the HG/RG backbone, may be required for optimal bioactivity.

The results from this study are similar to the findings of Gao and co-workers [325], who investigated the inhibitory effects of ginseng RGI on the agglutination of red blood cells, which was attributed to Gal3 inhibition. Complete enzymatic removal of 'long' Gal side chains of 4 DP greatly decreased inhibitory activity. However, they additionally showed that the incomplete removal of Ara by α-L-arabinofuranosidase, which cleaves terminal Ara residues, increased inhibitory activity, leaving the authors to suggest that high Gal content, as well as Ara in the form of AG-type side chains, were important for the inhibition of agglutination, and therefore the binding of Gal3. It is curious that the removal of Gal from SSBA produced such a significant impact as the Gal side chains were initially only 1-3.5 residues in length. However, Gao and co-workers investigated the contributions of Gal chain length to Gal3 inhibition and showed that activity was shown to increase with Gal chain length but only up to a tetramer, as chains between 5 and 65 residues did not provided additional activity. The Gal3 CRD is known to bind terminal galactose residues within the CRD and

so the authors suggested that short chains of <4 Gal residues on ginseng RGI may still be significant in regulating the activity of Gal3 [325]. It is possible, therefore, that SSBA could exert its activity by binding and inhibiting Gal3.

The HG or RG backbone of SSBA could potentially be an additional bioactive component, as shown by the anti-proliferative effect of Gal- and Ara-depleted SSBA-gal and SSBA-all after 96 hours of treatment. There are a few studies that suggest distinct bioactive roles for HG pectin structures. Pectic acid has been reported to induce apoptosis in rat pituitary tumour cells [331] and Liu and co-workers showed pentamers of GalA to be active against inflammation and carcinogenesis in a mouse model of colitis-associated CRC [332]. Gao and colleagues also showed that the backbone of ginseng RGI, depleted of all neutral sugar side chains, still inhibited agglutination, albeit this required higher concentrations than forginseng RGI. In addition, they showed that the ginseng RGI backbone had high binding affinity to Gal3, although this was not inhibited by lactose suggesting a non-specific, perhaps ionic, interaction. However, the authors also raised the possibility that there may be secondary carbohydrate recognition sites within the Gal3 molecule [325].

6.6 Conclusion

LM and neutral sugar-rich sugar beet pectin reduces HT29 cell viability in a dose- and time-dependent manner via induction of apoptosis. The bioactive components of SSBA are thought to be the galactan side chains branched from RGI since β-galactan is known to bind and inhibit the pro-metastatic protein Gal3. To investigate the role of the neutral sugar side chains in the anti-proliferative activity of SSBA, Gal and Ara side chains were enzymatically cleaved from SSBA and the subsequent effect on HT29 cell viability determined. Removal of Ara residues resulted in a reduction in anti-proliferative activity suggesting that arabinan side chains are important. However, the results presented suggest that Ara must be in combination with Gal to affect cell viability. Moreover, the cleavage of Gal side chains completely abolished the SSBA-induced response after 72 hours indicating

that Gal is necessary for the bioactivity of SSBA. These results provide support for the hypothesis that β-galactan chains branched from SSBA bind and inhibit Gal3 resulting in loss of cell viability. It is also possible that SSBA has a secondary bioactive component in the HG backbone due to the observed bioactivity of Gal-depleted SSBA. Altogether, results suggest that Gal and Ara side chains, together with the HG backbone, cooperate to exert bioactivity in distinct phases, which strongly implies the existence of more than a single mechanism of action.

Chapter 7

P-RGI and SSBA reduce colon cancer cell viability via a galectin-3 independent mechanism

7.1 Introduction

Modified pectins from various sources have been found to reduce cell proliferation, migration, adhesion and induce apoptosis in numerous cancer cell lines as well as reduce tumour formation and metastasis in rodents. The mechanisms responsible for the observed effects of modified pectin on cancer are unclear, however, a role for the pro-metastatic protein galectin-3 (Gal3) has been proposed. Galectins are a family of fifteen soluble β-galactoside-binding lectins that have diverse intra- and extracellular biological functions and have been implicated in cancer, immune function and inflammation [387-389]. The most extensively studied galectin, Gal3, has been pinpointed as a potential therapeutic target in cancer due to its suggested role in promoting metastasis [390]. Gal3 is a ubiquitous protein expressed in a variety of tissues and cell types and found in the nucleus, cytoplasm, the cell surface, as well as in the extracellular matrix [215, 391, 392]. There is substantial evidence that Gal3 induces cell migration, morphogenesis, adhesion and proliferation, inhibits apoptosis and promotes angiogenesis in a wide variety of cell lines [243-248, 250, 252, 254-256, 296, 308]. Structurally, Gal3 consists of an N-terminal domain linked to a carbohydrate recognition domain (CRD), which specifically binds with β-galactose-containing carbohydrates and glycoconjugates, such as those in the RGI regions of pectin. Gal3 has been shown to bind to or activate various intracellular proteins involved in the regulation of cell survival, including intracellular KRas [393], Akt [296, 394], and β-catenin [301] and Bcl-2 [291]. The proto-oncogene KRas, once recruited to the plasma membrane and anchored via its C-terminal S-farnesylcysteine, is activated and can drive cell growth, differentiation and inhibit apoptosis. Gal3 is recruited by KRas from the cytosol to the plasma membrane, where a hydrophobic pocket within the CRD of Gal3 is thought to accommodate the S-farnesylcysteine group of KRas. KRas forms nanoclusters at the plasma membrane, which are essential for signal transduction. Once recruited to the plasma membrane, Gal3 becomes an integral nanocluster component, stabilising KRas in its active state and increasing signal output [294]. Farnesylthiosalicylic Acid (FTS), a specific inhibitor of KRas that prevents translocation to the plasma

membrane, inhibited Gal3-mediated apoptosis resistance [395] while a mutation in the Gal3 hydrophobic pocket reduced KRas nanocluster formation along with cell proliferation and transformation [294].

A study utilising biophysical techniques including atomic force spectroscopy has verified that potato galactan, containing linear β(1→4) galactan chains, binds specifically to recombinant Gal3, whilst potato RGI showed a lower level of specific binding and polygalacturonic acid (PGA) showed no specific binding [322]. The disaccharide β-galactobiose was also shown to bind to Gal3 [323]. In vitro studies have shown modified pectin binds to recombinant Gal3 [321, 325] and inhibits human umbilical vein endothelial cell migration to Gal3 [195]. Also, when combined with the anti-inflammatory drug dexamethasone, MP reduced the protein expression of Gal3 [196]. Taken together these observations suggest that the binding of small pectin fragments to Gal3 may disrupt the interactions of Gal3 with other proteins and peptides, inhibiting its ability to promote cell adhesion and proliferation and to prevent apoptosis.

7.2 Aim

This chapter investigates the effects of potato RGI (P-RGI) on cell viability in the colon cancer cell lines DLD1 and HCT116, and the soluble fraction of alkali-treated sugar beet pectin (SSBA) on HT29 cells. Knocking down the expression of Gal3 in these cell lines using siRNA has been used to elucidate the role of this lectin in mediating the intracellular bioactivity of pectin extracts.

7.3 Materials and Methods

7.3.1 Pectins

P-RGI and SSBA were characterised in Chapter 3. Sample preparations for cell treatment were carried out as in section 2.3.

7.3.2 Gal3 siRNA transfection

Gal3 gene silencing was performed with one or more of four validated LGALS3 siRNA (siRNA1, siRNA2, siRNA3 and siRNA4) from FlexiTube GeneSolution (Cat. GS3958) purchased from Qiagen (Crawley, UK). ID numbers are provided in Table 19. Non-specific siRNA (Negative All Stars, Qiagen, Crawley, UK) and medium only were used as controls. Cell transfection of DLD1 and HCT116 cells was performed with HiPerfect transfection reagent (Qiagen, Crawley, UK), and transfection of HT29 cells with Lipofectamine RNAiMAX (Invitrogen, Paisley, UK). Cells were seeded in triplicate in Nunclon 6-well plates for determination of Gal3 protein expression and Nunclon 96-well plates for determination of Gal3 gene expression and cell viability analysis, at the cell concentrations shown in Table 3 (pg.72) and incubated briefly at 37°C. siRNA at 10 nM final concentration for DLD1 and HCT116 cells and 20 nM for HT29 cells, was suspended in OptiMem serum and penicillin-free medium (Invitrogen, Paisley, UK) and either HiPerFect or Lipofectamine RNAiMAX, respectively, at the amounts shown in Table 20. After vortexing and incubating at room temperature for 10 minutes the complexes were added to cells and incubated at 37°C for 24 hours.

Table 19 ***FlexiTube GeneSolution Gal3 siRNA ID numbers***

	ID number
siRNA1	S104250799
siRNA2	S100470050
siRNA3	S104366124
siRNA4	S104374251

Table 20 ***Amounts of transfection reagent and Optimem medium added to siRNA prior to transfection of cells***

	µl per well 6-well plate	µl per well 96-well plate
10nM siRNA		
HiPerfect	6.3	0.63
OptiMem	200	20
20nM siRNA		
Lipofectamine RNAiMAX	12.6	1.26
OptiMem	200	20

7.3.3 Validation of siRNA-mediated knockdown of Gal3 gene expression

The effect of Gal3-specific siRNAs on Gal3 gene expression was assessed using RT-PCR. After 24 hours of transfection, culture medium was replaced with fresh complete growth medium and incubation continued for 48 hours (DLD1 and HCT116 cells) or 72 hours (HT29 cells). Sample preparation and gene expression analysis were performed as described in section 2.9. Primer sequences and melting temperature (Tm) of Gal3 are reported in Table 21.

Table 21 ***Galectin-3 primer sequences*** F= Forward; R = Reverse.

Gene	Common name		Primer sequence 5' to 3'	Tm °C
LGALS3	Galectin-3	F	AGGCAAAGGCAGGTTATAAGG	60
		R	GAGCCTACCCTGCCACTG	

7.3.4 Validation of siRNA-mediated knockdown of Gal3 protein expression

7.3.4.1 Protein extraction

The effect of Gal3-specific siRNAs on Gal3 gene expression was assessed using western blot. After 24 hours of transfection, culture medium was replaced with fresh complete growth medium and incubation continued for 48 hours (DLD1 and HCT116 cells) or 72 hours (HT29 cells). Following

incubation, cells were washed twice with cold PBS and lysed with RIPA buffer (Tris-HCl 50 mM pH 8, NaCl 150 mM, Triton X-100 1%, sodium deoxycholate 0.5% and sodium dodecyl sulphate 0.2%) (Fisher Scientific, Loughborough, UK) supplemented with HALT protease and phosphatase inhibitor cocktail (Fisher Scientific, Loughborough, UK) for two minutes on ice. Cell lysates were collected, transferred to 1.5 ml tubes and centrifuged at 13,000 g for 10 minutes at 4°C. Supernatants were collected and pellets were discarded.

7.3.4.2 Protein quantification

Protein concentration was determined using a bicinchoninic acid (BCA) protein assay kit according to the manufacturer's instructions (Fisher Scientific, Loughborough, UK). The BCA assay is a colorimetric assay to measure total protein concentration compared to a protein standard. Standards were created by a serial dilution of bovine serum albumin (BSA) (Sigma, Poole, UK) diluted in lysis buffer.In a 96-well plate, in triplicate, 100ul working reagent was added to 3 µl of each sample and standard. A standard curve was then performed to measure sample protein concentration.

7.3.4.3 Sample preparation and gel electrophoresis

Protein separation and transfer were performed with the NuPAGE Bis-Tris electrophoresis system following the manufacturer's instructions (Invitrogen, Paisley, UK). 2 µl NuPAGE sample reducing agent and 5 µl NuPAGE LDS sample buffer were added to 25 µg protein extract and incubated at 70°C for 10 minutes. Protein samples and Hyperladder IV (Bioline, London, UK) pre-stained standard were loaded on a NuPAGE Novex 4-12% Bis-Tris Gel in triplicate, and run using the Invitrogen Zoom Duel Power Supply (Invitrogen, Paisley, UK) at 200 V for 50 minutes.

7.3.4.4 Protein transfer

Proteins were transferred from the gel to a polyvinylidene fluoride (PVDF) membrane (Millipore, Darmstadt, Germany) using Invitrogen Zoom Duel Power Supply according to the manufacturer's instructions. Protein transfer was performed at 30 V for 1 hour.

7.3.4.5 Immunoblotting and development

Non-specific binding of antibodies to the membrane was prevented by incubating the membrane in Superblock blocking solution (Invitrogen, Paisley, UK) for 2 hours at room temperature under agitation. The membrane was then incubated for 16 hours at 4°C with blocking solution supplemented with primary antibody against Gal3 (rabbit polyclonal IgG Ab53082 AbCam, Cambridge, UK) at a dilution of 1:2500. After four washes of 5 minutes with TBST (tris-buffered saline pH 7.6 with 0.05% Tween 20 (Sigma, Poole, UK), the membranes were incubated with secondary antibody diluted to 1:5,000 in blocking solution for 1 hour at room temperature. Antibody-protein complexes were detected and quantified by chemiluminescence using the Pierce Supersignal west pico chemiluminscent detection kit (Fisher Scientific, Loughborough, UK). Membranes were stripped by incubation in Reblot Plus membrane stripping solution (Merck Millipore, Darmstadt, Germany) for 15 minutes at room temperature, before β-actin levels were measured similarly using anti-β-actin primary antibody (Rabbit polyclonal IgG, Cat. AB8227, Abcam, Cambridge, UK) diluted to 1:5000 in blocking solution.

7.3.5 Cell viability assay

After 24 hours of transfection medium from DLD1 and HCT116 cells was replaced with fresh complete growth medium with or without 1 mg/ml P-RGI for 48 hours. Medium from transfected HT29 cells was replaced with fresh complete growth medium with or without 1 mg/ml SSBA for 72 hours. Quantification of cell viability and statistical analyses were carried out as described in Chapter 2.4.

7.4 Results

7.4.1 Effect of Gal3 siRNA transfection on Gal3 gene and protein expression

Relative quantities of Gal3 mRNA levels were determined by RT-PCR in the three colon cancer cell lines DLD1, HCT116 and HT29. Figure 39 shows that DLD1 cells express Gal3 at approximately 9-fold higher levels than HCT116 and HT29 cells ($p<0.01$).

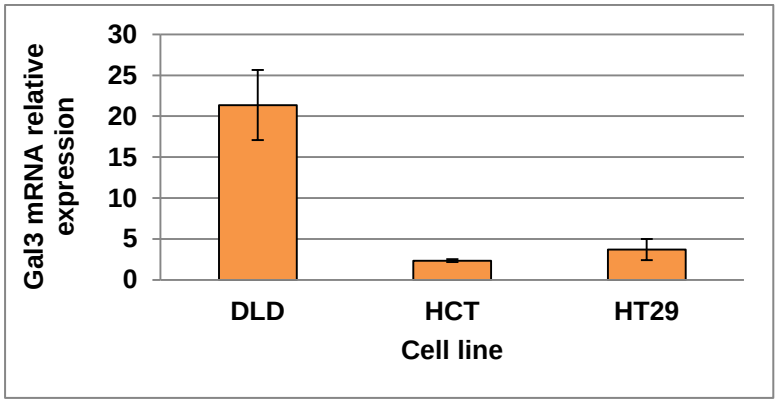

Figure 39 ***Relative expression of Gal3 in DLD1, HCT116 and HT29 cells*****.** Data are shown as mean ± standard error of triplicate samples normalised against 18S rRNA.

Transfection of DLD1 cells with four Gal3-specific siRNA's (siRNA1, siRNA2, siRNA3 and siRNA4) decreased steady-state levels of Gal3 mRNA by 95%, 89%, 93% and 97%, respectively, compared with cells transfected with non-specific, control siRNA (siRNA-Ctrl) (Figure 40a). This led to a reduction in Gal3 protein expression of 95% and 84%, by siRNA1 and siRNA4, respectively (Figure 41a). HCT116 cells transfected with siRNA1 and siRNA2 decreased Gal3 mRNA expression by 80% and 65%, respectively (Figure 40b), which consequently led to a reduction of Gal3 protein expression of 95% and 86% (Figure 41b). In the HT29 cell line, siRNA2 and siRNA4 induced a strong decrease in Gal3 mRNA of 76% and 73%, respectively (Figure 40c), which consequently led to a reduction of Gal3 protein expression by 58% and 66% (Figure 41c). siRNA3 did not significantly decrease Gal3 mRNA expression in HT29 cells.

a

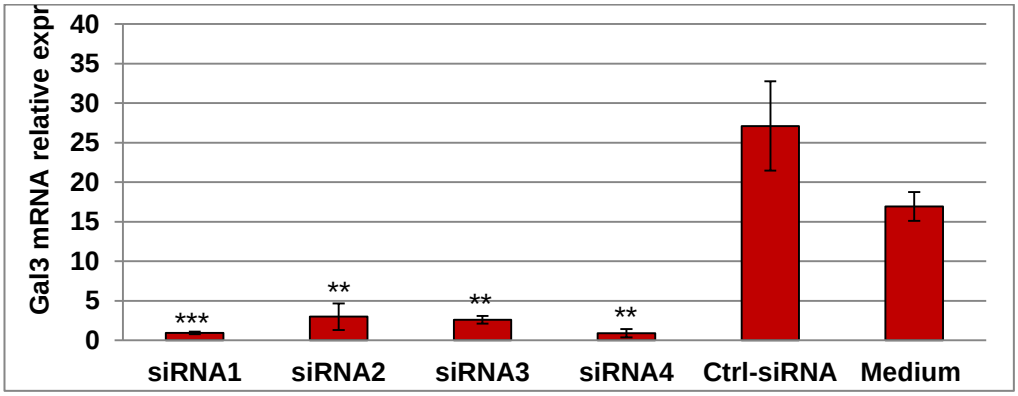

b

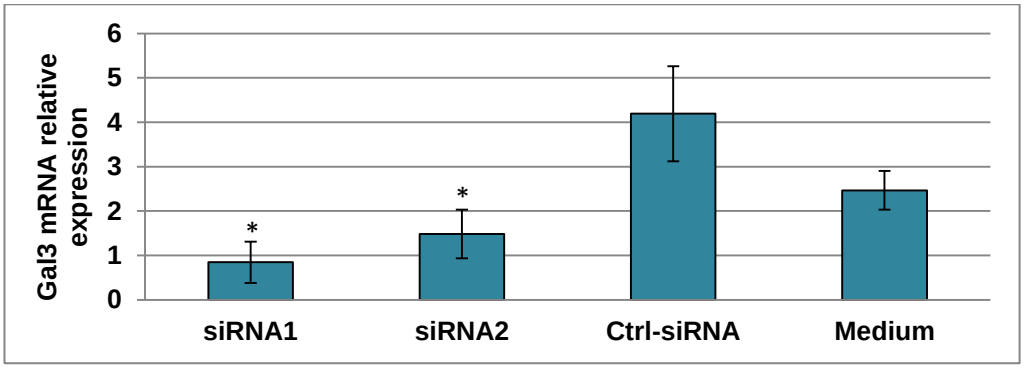

c

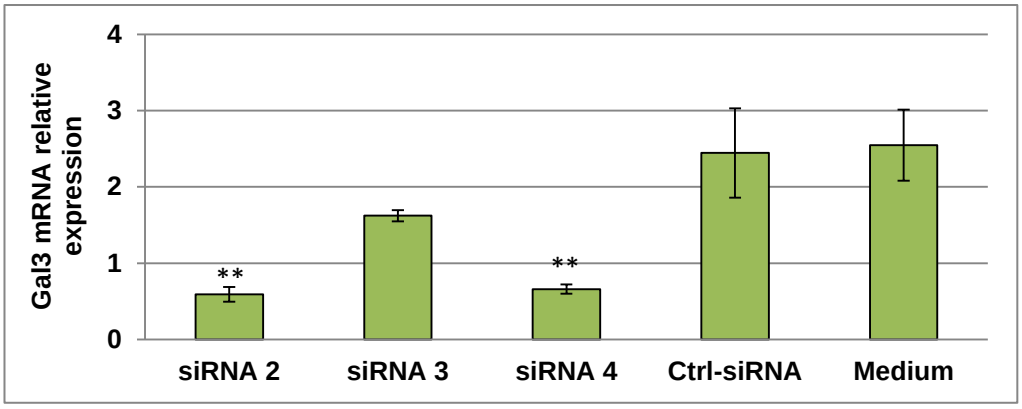

Figure 40 ***Validation of knock-down of Gal3 mRNA.*** Cell transfection with Gal3-specific siRNA's decreased Gal3 mRNA in (a) DLD1 cells (b) HCT116 cells (c) HT29 cells. Data are shown as mean ± standard error of triplicate samples normalised against 18S rRNA. (a) is the result of three individual experiments. p values are relative to Ctrl-siRNA. *p<0.05; ** p<0.01; ***p<0.001

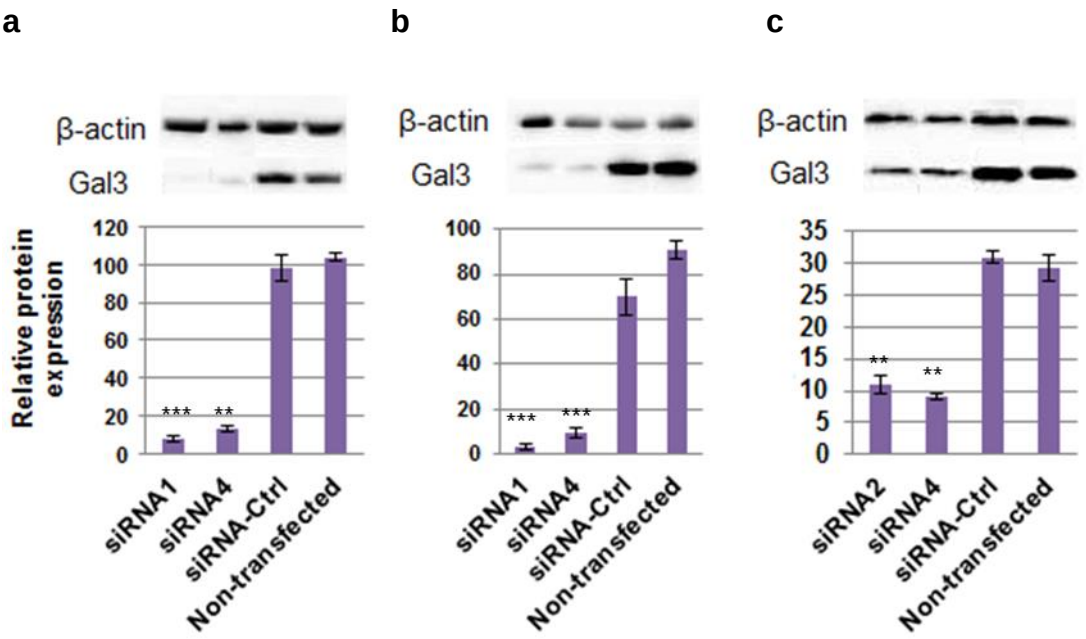

Figure 41 ***Validation of siRNA-mediated knock-down of Gal3 protein expression.*** Cell transfection with Gal3-specific siRNA's decreased Gal3 protein in (a) DLD1 cells (b) HCT116 cells (c) HT29 cells. Data are shown as mean ± standard error (n=3). p values are relative to Ctrl-siRNA; ** $p<0.01$; ***$p<0.001$.

7.4.2 Effect of P-RGI and SSBA on Gal3 knock-down cells

Previous studies in our lab showed that potato galactan (P-Gal) and β-Galactobiose (GB) bound specifically to recombinant Gal3, whilst potato RGI (P-RGI-X) showed a lower level of specific binding [385]. In chapter 5 these three pectic polysaccharides, as well as a second potato RGI with a different structure (P-RGI), were tested for their activity in colon cancer cells. Results showed that both P-RGI and P-Gal significantly reduced cell viability of DLD1 cells after 48 and 72 hours, respectively, while P-RGI-X and GB had no effect. To investigate whether the interaction between these pectic polysaccharides and Gal3 plays a role in mediating their effects on cell viability the effect of Gal3 knockdown on the P-RGI-induced inhibition of cell viability was determined. Figure 42a shows that P-RGI treatment significantly decreased the viability of DLD1 cells transfected with Gal3-specific siRNA1, siRNA2, siRNA3, siRNA4, non-specific siRNA (siRNA-Ctrl) or cell culture

medium only by 21%, 14%, 20%, 24%, 24% and 21%, respectively. There was no significant difference between the effects of P-RGI on cells transfected with Gal3-specific siRNA compared with Ctrl-siRNA. Similar results were observed in HCT116 cells. siRNA1, siRNA2, Ctrl-siRNA transfected and non-transfected P-RGI-treated HCT116 cells reduced cell viability by 12%, 5%, 10% and 10%, respectively (Figure 42b).

a

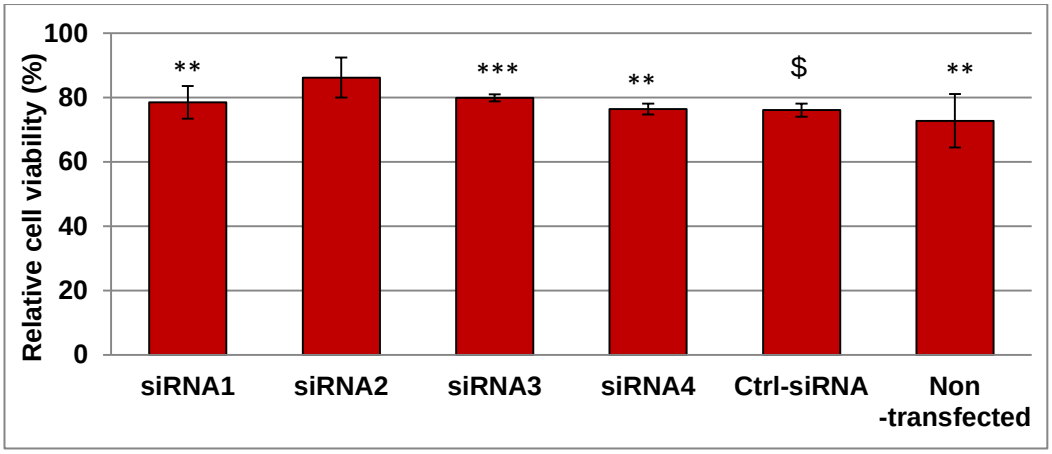

b

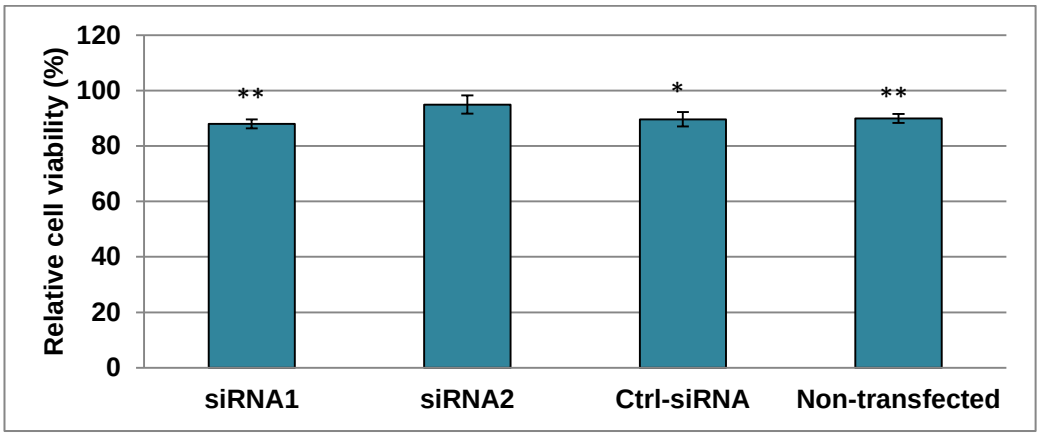

Figure 42. ***Effect of P-RGI on Gal3 knock-down cells*****.** Effect of P-RGI (1mg/ml for 48 hours) on cell viability after transfection with either Gal3-specific siRNAs or siRNA-Ctrl (a) DLD1 cells (b) HCT116 cells. Results are expressed as the percentage of viable cells remaining after treatment relative to the untreated control. Data are shown as mean ± standard error (n=3). (A) is the result of three individual experiments. **p<0.01; ***p<0.001; $p<0.0001.

Figure 43 shows that a 72 hour incubation with SSBA significantly decreased the viability of HT29 cells transfected with Gal3-specific siRNA2, siRNA3, siRNA4, siRNA-Ctrl or cell culture medium only by 52%, 45%, 42%, 42% and 57% respectively. There was no significant difference between the effects of SSBA on cells transfected with Gal3-specific siRNA compared with Ctrl-siRNA or non-transfected cells.

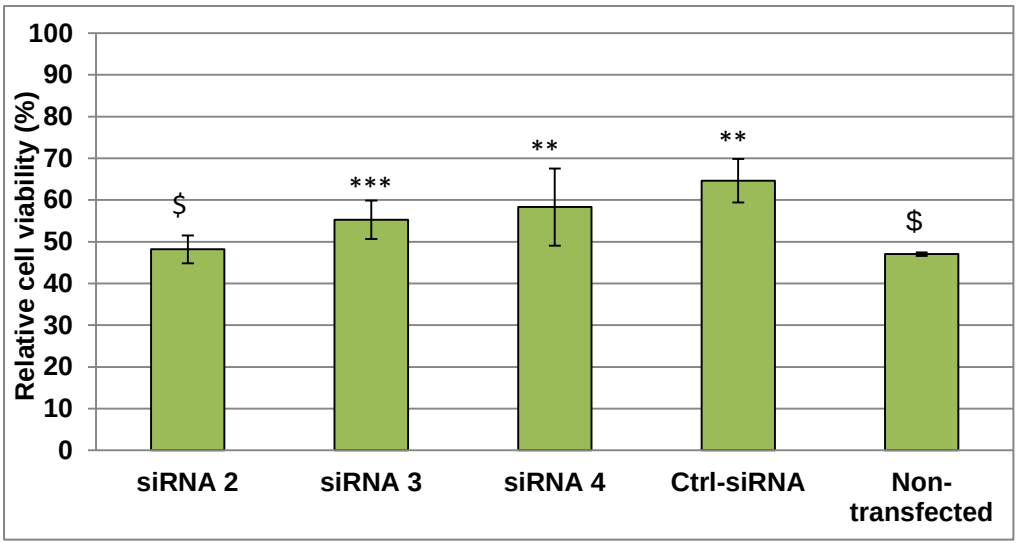

Figure 43 ***Effect of SSBA on Gal3 knock-down HT29 cells*****.** Effect of SSBA (1mg/ml for 72 hours) on HT29 cell viability after transfection with either Gal3-specific siRNAs or siRNA-Ctrl. Results are expressed as the percentage of viable cells remaining after treatment relative to the untreated control. Data are shown as mean ± standard error (n=3). **p<0.01; ***p<0.001; $p<0.0001.

8.4.3 Effect of SSBA combined with FTS on DLD1 and HT29 cells

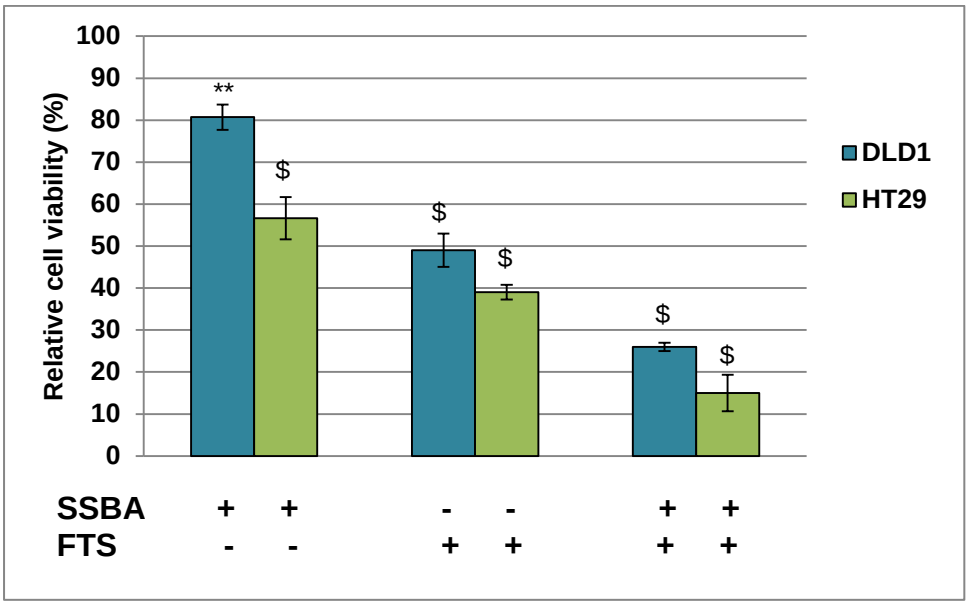

Figure 44 Effect of SSBA combined with FTS on DLD1 and HT29 cell viability after 72 hours. Effect of treatment with 1 mg/ml SSBA, 150 μM FTS, and 1 mg/ml SSBA combined with 150 μM FTS for 72 hours on cell viability. Results are expressed as percentage of viable cells remaining after treatment relative to the untreated control.**p<0.01; $ p<0.0001.

The proto-oncogene KRas plays a significant role in the regulation of colon cancer cell growth and apoptosis. The Gal3 CRD binds the farnesyl group of KRas maintaining it in its active state to promote cell proliferation. Mutation of the Gal3 CRD inactivates KRas [396] and so it is possible that the binding of Gal3 CRD by β-galactosides may inactivate KRas and reduce cell proliferation. FTS, a Ras inhibitor, can also bind the KRas farnesyl group, retaining KRas as a cytosolic protein and disrupting its transforming activity. SSBA and FTS were combined and incubated with DLD1 and HT29 cells to investigate whether they had related mechanisms of activity. Figure 44 shows that SSBA reduced cell viability by 20% and 42%; FTS by 50% and 61%; and SSBA combined with FTS by 74% and 85% in DLD1 and HT29 cells, respectively. This indicates that SSBA and FTS act independently to

reduce cell viability providing further support to the Gal3-independent mechanism for the anti-proliferative activity of SSBA.

7.5 Discussion

Modified pectin has been shown to have anti-proliferative effects in various cancer cell lines although the mechanisms remain unclear. The inhibition of the function of the ubiquitous protein Gal3 by binding of galactan side chains on pectin has been postulated as a potential mechanism [322, 397, 398]. Initial studies found that lectins were important for metastasis, particularly in relation to binding to carbohydrate expressed on tumour cells leading to cell-cell and cell-ECM adhesion and ultimately tumour formation [399, 400]. It was then hypothesised that lectins could potentially bind, and thus be inhibited by, exogenous carbohydrates containing terminal galactoside residues. Numerous studies have since been undertaken using galactose-rich substances, with many postulating a particular inhibition of Gal3 [195, 196, 321]. Indeed, recent studies in our laboratory have shown that P-Gal and the disaccharide GB showed a high level of specific binding to recombinant Gal3, while the interaction with P-RGI-X was weaker. These interactions were shown to be inhibited by the presence of lactose, which confirms that the binding occurs within the CRD of Gal3 [322, 323]. In Chapter 3 the structure of P-RGI-X was examined in detail. ^{13}C NMR data show that P-RGI-X contains a high proportion of β(1→4)galactan side chains with a high ratio of terminal β(1→4)galactan, which suggests short side chains of 1-3 galactose residues. On the other hand, P-Gal has an RGI backbone with β(1→4)galactan chains of an estimated average chain length of ~23 galactose residues. The CRD of Gal3 recognises disaccharides containing β-galactosides [215], which would account for the high affinity for GB and P-Gal. However if the disaccharide is bound to the backbone or if there are other forms of steric hindrance, longer side chains may be required to allow the terminal disaccharide to bind, which would account for the weaker interaction with P-RGI-X. Another comprehensive study investigated the relationship between ginseng RGI and potato galactan structure and galactan chain length on Gal3 binding activity [325]. They showed that

tetramers of β(1→4)galactan from potato galactan conferred significantly increased Gal3 binding activity than monomers, although β(1→4)galacto-oligosaccharides with longer chains up to 63 galactose residues did not show increased affinity. The authors suggest these results indicate that short chains of 1-3 galactose residues on RGI may still be significant in regulating the activity of Gal3. However, they also showed that recombinant Gal3 bound to isolated RGI backbone following the complete hydrolysis of the galactan side chains. The authors proposed therefore that there could potentially be secondary carbohydrate recognition sites within the Gal3 molecule.

Results from Chapter 5 showed P-RGI to have a time- and dose-dependent inhibitory effect on viability of DLD1 and HCT116 cell lines. P-Gal also demonstrated inhibitory activity in DLD1 cells although to a lesser extent, while GB had no effect on either cell line. Remarkably, P-RGI-X did not affect cell viability. Structural analysis of P-RGI and its comparison with P-RGI-X show that it is possible that HG regions, possibly as side chains of P-RGI, are essential for bioactivity. However, as discussed, short galactan chains on RGI could still potentially interact with Gal3 and regulate its activity. The significance of the role of Gal3 in determining the biological effect of P-RGI on cell viability was assessed using RNA interference. The results of this approach showed that reducing the expression of Gal3 by approximately 90% by siRNA transfection did not affect the cellular response to P-RGI in two colon cancer cell lines, indicating that the effect of P-RGI on the viability of these two cell lines is independent of Gal3. These results suggest that an interaction with Gal3 may not be important for the anti-proliferative effects of modified pectin.

Results from previous chapters suggest that structurally different pectins may have diverse mechanisms of action. SSBA, the soluble fraction of alkali-treated sugar beet pectin, was shown to have a time- and dose-dependent inhibitory effect on the viability of HT29 cells (Chapter 5). Furthermore, it was shown that enzymatic removal of galactan side chains markedly decreased SSBA activity, suggesting that galactan side chains could modulate activity

through binding and inhibiting Gal3. The role of Gal3 in mediating the anti-proliferative activity of SSBA towards HT29 cells was assessed by reducing Gal3 gene and protein expression in this cell line. Knocking down the expression of Gal3 by approximately 75% by siRNA transfection did not affect the cellular response to SSBA in HT29 cells, indicating that the decrease in cell viability was independent of Gal3.

Further support for a Gal3-independent mechanism is provided by the observed effects on cell viability by combined SSBA and FTS, a known inhibitor of KRas function. Gal3 is known to drive cell proliferation and inhibit apoptosis via its interactions with intracellular proteins such as KRas, Akt and β-catenin. Although the anti-proliferative and apoptotic activity of MP has been postulated as a consequence of binding and inhibiting Gal3, it is not known how MP may bind to intracellular Gal3. It could be possible that low MW pectin may enter cells, a mechanism postulated by Huang and colleagues who showed that embryonic kidney cells absorbed MCP with a low MW of 1kDa [401]; however this experiment lacked controls and has not been repeated. Another possibility is that MP could bind to Gal3 located in lipid rafts [402], specialised membrane microdomains that function as organising centres for the assembly of signaling molecules [403, 404]. Gal3 is known to be recruited by KRas from the cytosol to the plasma membrane, becoming an integral nanocluster component and binding and stabilising KRas in its active state, driving cell proliferation and preventing apoptosis [294, 405]. FTS binds to the farnesyl group of KRas and prevents its translocation to the plasma membrane, thereby inhibiting its interaction with the Gal3 CRD [393]. Treatment of cells with SSBA combined with FTS led to an additive effect on cell viability when compared with SSBA or FTS alone. This shows that FTS did not inhibit the anti-proliferative activity of SSBA indicating that these compounds are acting by independent mechanisms. Therefore, this raises the possibility that the anti-proliferative activity of SSBA is not via an effect on KRas activity. As Gal3 at the plasma membrane is known to exert its activity via Kras, these results lend further support for a Gal3-independent mechanism for the anti-proliferative effects of SSBA. These results strongly suggest that an interaction with Gal3 may not be

important for the anti-proliferative and pro-apoptotic effects of modified pectin. The Gal3-independent activity of modified pectins is also consistent with the results from two previous studies, which showed that modified citrus pectin induced apoptosis in the prostate cancer cell line LNCaP, which does not express Gal3 [201, 329].

Many studies have reported effects of modified pectin including reduced cell proliferation, induction of apoptosis and modulation of the cell cycle in a number of cancer cell lines from various tissues [196, 197, 201, 384, 406]. Since these cell lines exhibit significant diversity in characteristics including tissue of origin and genetic mutations, together with the heterogeneity of the modified pectins in terms of source, and the methods for extraction and modification, the role of Gal3 cannot be ruled out in mediating the cellular response in these studies. The proposed use of modified pectin as an anti-cancer agent is based on the effects of modified pectin on the spread of cancers. Many studies have reported effects of modified pectin on reduced cell migration, adhesion, angiogenesis and tumour formation [194, 210, 321, 325]. In this context, extracellular Gal3 is accessible to pectin extracts, which could inhibit the role of Gal3 in cancer metastasis. The present study suggests that P-RGI can inhibit cell viability and hence may play a chemo-preventative role by influencing intracellular pathways that control cellular homeostasis, and thereby perhaps reduce the risk of cancer initiation. The fact that this biological effect is independent of Gal3 suggests that the structural features important for reducing cancer cell proliferation may be different to those required for the use of pectin as an anti-metastatic agent. It is evident that further research is required to provide a mechanistic understanding of the potential chemo-preventive properties of this important dietary constituent. Such understanding would underpin consideration of the health benefits of pectin in the diet or as a food supplement.

7.6 Conclusion

This chapter demonstrates that the viability-reducing activity of RGI extracts from potato in DLD1 and HCT116 cells, and alkali-treated sugar beet pectin in HT29 cells is independent of Gal3. Thus the structural features of pectin

extracts responsible for their anti-proliferative activity towards cancer cells may differ considerably from those required for the potential use of such extracts as anti-metastatic agents. Further mechanistic studies are required to assess the potential chemo-preventative role of pectin as a dietary constituent.

Chapter 8
Effects of potato RGI on colon cancer cell gene expression

8.1 Introduction

Previous chapters investigated the bioactive effects of modified pectins and showed that potato derived RGI (P-RGI) and alkali-treated sugar beet pectin (SSBA) reduced cell proliferation in a dose- and time-dependent manner in colon cancer cells, the latter by induction of apoptosis. Similar results were reported in other studies performed on several types of cancer cells following exposure to MP, but the molecular mechanisms responsible for the observed biological effects have not been fully elucidated. The most well-known mechanism postulated for bioactivity of MP is the binding and inhibition of pro-metastatic protein Gal3. However, it was shown in the previous chapter (Chapter 7) that the anti-proliferative effects of P-RGI and SSBA are independent of Gal3. To elucidate the mechanisms behind the bioactivity of MP, its effects on the expression of certain genes can be observed to reveal the cell signalling pathways that may be affected. Changes in cell behaviour relevant to cancer progression are induced by changes in gene and protein expression. Cells depend on an elaborate intracellular communication network of signalling pathways, which exhibit cross-talk, to regulate cell function. Any loss of control in these signalling pathways, often brought on by gene mutations that result in the overexpression of oncogenes or the inhibition of tumour suppressor proteins, can cause unregulated cell growth and transformation. The MEK/ERK, Wnt, PI3K/Akt, apoptosis and cell cycle pathways are all deregulated in CRC and consequently the components of these signalling cascades make interesting targets for therapeutic intervention.

Previous studies have investigated the effects of MP on protein expression. Two studies have shown MP to affect cell cycle progression. Potato RGI was shown to arrest HT29 cells in the G1 phase of the cell cycle, which was accompanied by a reduction of expression of the proteins cyclin B1 and CDK1, which are required for the transition into S phase [384]. Similarly, the MCP, GCS-100, reduced cell proliferation via G1/S cell cycle arrest in myeloma cells, which was accompanied by a reduction of Cyclin E and CDK2, cyclin D and CDK6, and the cyclin/CDK inhibitor p21, restricting cell progression through to the S phase. As well as causing cell cycle arrest,

GCS-100 was shown to induce apoptosis, which was accompanied by a decrease in the pro-survival proteins MCL-1, Bcl-XL and Akt, and an increase in the pro-apoptotic protein Noxa, while the expression of anti-apoptotic Bcl-2 and pro-apoptotic Bax, Bak, Bim, Bad, Bid and Puma proteins remained unchanged. [197]. Some interesting results from Umar and co-workers demonstrated that increases in cellular β-catenin, cyclin D and c-myc were blocked in the colonic crypt cellular extracts of mice fed a diet of 6% CP [407], and MCP was shown to supress MAPK signalling [201]. Stimulation of cells with cytokines such as TNFα and IL-1 is associated with activation of IKK, decreased IκBα and increased NFκB, which is known to drive proliferation [408]. Streetly and colleagues also showed that GCS-100 decreased levels of activated IKK and decreased IκBα after cytokine stimulation [197].

8.2 Aims

The molecular mechanisms behind the bioactivity of P-RGI on DLD1 cells will be explored in this chapter. Effects on the expression of 53 genes selected for their involvement in the regulation in cell proliferation, apoptosis, adhesion, cell cycle progression and immune function will be investigated.

8.3 Materials and Methods

8.3.1 Pectins

P-RGI, SSBA and CP were characterised in Chapter 3. Sample preparations for cell treatment were carried out as in section 2.3.

8.3.2 Analysis of gene expression

DLD1 and HT29 cells were seeded in Nunclon 6-well plates at the cell concentrations specified in Table 3 (pg.72). After 24 hours, to allow cell adhesion, medium was discarded and DLD1 cells were exposed to 2 ml medium supplemented with 1 mg/ml P-RGI or 1 mg/ml CP, and HT29 cells exposed to 2 ml medium supplemented with 1 mg/ml SSBA or 1 mg/ml CP

for the times specified. Four biological replicates were performed for each condition of treatment. Three individual experiments were carried out on DLD1 cells exposed to P-RGI and CP for 24 hours. RNA extraction, quantification and RT-PCR were performed according to the procedures described previously (section 2.9). Primer sequences and melting temperatures (Tm) of selected genes are reported in Tables 22 to 25.

Table 22 ***Primer sequences for genes associated with the cell cycle.*** Common names, primer sequences and Tm of selected genes. F= Forward; R = Reverse.

Gene	Common name		Primer Sequence (5'to 3')	Tm °C
CDK2	CDK2	F	aaagccagaaacaagttgacg	62
		R	gtactgggcacaccctcagt	
CDK4	CDK4	F	gtgcagtcggtggtacctg	52-58
		R	ttcgcttgtgtgggttaaaa	
CDK6	CDK6	F	tgatcaactaggaaaaatcttgga	60
		R	ggcaacatctctaggccagt	
CDK7	CDK7	F	ccatgtgctcgaattacgg	60
		R	cttggcagctgacatccag	
CCNB1	Cyclin B1	F	acatggtgcactttcctcct	60
		R	aggtaatgttgtagagttggtgtcc	
CCND1	Cyclin D1	F	gctgtgcatctacaccgaca	60
		R	ttgagcttgttcaccaggag	
CCND2	Cyclin D2	F	ccatcagcaaatgtgtacgtg	60
		R	tacagtcagtaaggcactttatttcc	
CCND3	cyclin D3	F	cctccctgcatctgacca	60
		R	atgctggtgtatgtatccaattctg	
CCNE1	Cyclin E1	F	ggccaaaatcgacaggac	60
		R	gggtctgcacagactgcat	
TP53	p53	F	aggccttggaactcaaggat	60
		R	ccctttttggacttcaggtg	
CDKN2B	$p15^{INK4B}$	F	gcggggactagtggagaag	60
		R	ctgcccatcatcatgacct	
CDC25A	cdc25A	F	cgtcatgagaactacaaaccttga	60
		R	tctggtctcttcaacactgacc	

Table 23 ***Primer sequences of genes associated with cell proliferation and cell survival*** Common names, primer sequences and Tm's of selected genes. F= Forward; R = Reverse.

Gene	Common name		Primer Sequence (5'to 3')	Tm °C
MAP2K1	MEK1	F	ttttaggaaaagttagcattgctgt	60
		R	agggcttgacatctctgtgc	
MAP2K2	MEK2	F	accaaagtccagcacagacc	60
		R	atgatctggttccggatgg	
MAP2K3	MKK3	F	gaggacatccttggggagat	60
		R	gtggatcaccgacagcttg	
MAP2K4	MKK4	F	ggccaaagtataaagagcttctga	60
		R	cagcgatatcaatcgacatacat	
MAP2K6	MKK6	F	caaggcttgcatttctattgg	58-61
		R	ccagttccattataggctcca	
MAP2K7	MKK7	F	cggaggatcgacctcaac	59-61
		R	gggagctctctgaggatgg	
MAPK3	ERK1	F	ccctagcccagacagacatc	62
		R	gcacagtgtccattttctaacagt	
MAPK1	ERK2	F	caaagaactaatttttgaagagactgc	60
		R	tcctctgagcccttgtcct	
MAPK14	P38	F	gggacctccttatagatgagtgg	62
		R	ggactccatctcttcttggtca	
MAPK8	JNK	F	gggcagccctctccttta	58-61
		R	cattgacagacgacgatgatg	
PTEN	PTEN	F	gcacaagaggccctagatttc	58-62
		R	cgcctctgactgggaatagt	
CTNNB1	β catenin	F	acttgcattgtgattggcct	60
		R	caaaaaggaccagaacaaaaagtttac	
MYC	c-myc	F	agatccggagcgaataggg	60
		R	gtccttgctcgggtgttgta	
JUN	Jun	F	agagcggaccttatggctaca	60
		R	cgttgctggactggattatca	
TCF7L2	TCF7	F	ttgaccgacagactttatggtg	61-65
		R	tgtatgtagcgaacgcacttttt	
PIK3CA	PI3K	F	cacgagatcctctctctgaaatc	60
		R	ggtagaatttcggggatagttaca	
GSK3B	GSK3β	F	cagaccaataatgctgcttctg	60
		R	atattctttccaaacgtgaccagt	

Table 24 ***Primer sequences of genes associated with apoptosis*** Common names, primer sequences and Tm's of selected genes. F= Forward; R = Reverse.

Gene	Common name		Primer Sequence (5'to 3')	Tm °C
CASP3	Caspase-3	F	ttgtggaattgatgcgtgat	62
		R	ggctcagaagcacacaaaca	
CASP7	Caspase-7	F	ggcgtgatctcggaagact	62-68
		R	ggatgccatcatcaagctc	
CASP9	Caspase-9	F	aagcccaagctcttttcatc	62-68
		R	actcgtcttcaggggaagtg	
BID	Bid	F	tgtgaaccaggagtgagtcg	60
		R	ggctggaaccgttgttga	
BAX	Bax	F	ccatcatgggctggacat	56
		R	cactcccgccacaaagat	
AKT1	Akt	F	ggctattgtgaaggagggttg	61-65
		R	tccttgtagccaatgaaggtg	
FAS	Fas	F	gtggacccgctcagtacg	61-65
		R	ggacgataatctagcaacagacg	
PMAIP1	Noxa	F	ggagatgcctgggaagaag	58-61
		R	cctgagttgagtagcacactcg	
BBC3	PUMA	F	gacctcaacgcacagtacga	61-65
		R	gagattgtacaggaccctcca	
MCL-1	MCL-1	F	aagccaatgggcaggtct	60
		R	tgtccagtttccgaagcat	

Table 25 ***Primer sequences of genes associated with cell adhesion and immune function.*** Common names, primer sequences and Tm's of selected genes. F= Forward; R = Reverse. * No gene product found.

Gene	Common name		Primer Sequence (5'to 3')	Tm
PTK2	FAK	F	gtctgccttcgcttcacg	60
		R	gaatttgtaactggaagatgcaag	
ICAM1	ICAM1	F	ccttcctcaccgtgtactgg	61-65
		R	agcgtagggtaaggttcttgc	
ICAM2	ICAM2	F	caatgaattccaacgtcagc	*
		R	accaaagtgggttgcagtgt	
ICAM3	ICAM3	F	ggtaccatccgtgttgtgg	*
		R	gaactcctgcccctggac	
CD44	CD44	F	caacaacacaaatggctggt	61-65
		R	ctgaggtgtctgtctctttcatct	
CXCL12	SDF-1	F	ttgacccgaagctaaagtgg	*
		R	ccctctcacatcttgaacctct	
PTGS2	Cox2	F	cttcacgcatcagtttttcaag	*
		R	tcaccgtaaatatgatttaagtccac	
VCAM1	VCAM1	F	tgcacagtgacttgtggacat	*
		R	ccactcatctcgatttctgga	
CDH1	E-Cadherin	F	tggaggaattcttgctttgc	59-62
		R	cgctctcctccgaagaaac	
IL1B	IL-1β	F	tacctgtcctgcgtgttgaa	*
		R	tctttgggtaatttttgggatct	
TNF	TNFα	F	cagcctcttctccttcctgat	*
		R	gccagagggctgattagaga	
NFKB1	NFκB1	F	ctggcagctcttctcaaagc	60
		R	tccaggtcatagagaggctca	
IKKα	IKKα	F	tgtgcctcttctagcaatgga	60
		R	ttctggtttgttgagcagctt	
NFKBIA	IκBα	F	gacgaggagtacgagcagatg	58-61
		R	atggccaagtgcaggaac	

8.4 Results

8.4.1 Effect of P-RGI on DLD1 gene expression

P-RGI reduces DLD1 cell viability in a time- and dose-dependent manner (Section 5.4). To ascertain the molecular mechanisms behind this bioactivity, changes in DLD1 gene expression were analysed following incubation with P-RGI. Changes in DLD1 gene expression were additionally analysed after incubation with CP, used as a negative control due to the absence of any effect on cell viability. 53 genes were selected for their role in cell cycle progression, proliferation, apoptosis, cell adhesion and immune function. P-RGI and CP were incubated with DLD1 cells for 24 hours and mRNA was extracted.

Figure 45 shows the effect of P-RGI and CP on the expression of 46 genes over 24 hours. P-RGI reduced the expression of ICAM1, cyclin B1, p38, β-catenin and Bid by 49%, 32%, 30%, 24%, 44%, respectively, while cyclin D1 was increased by 55%. However, with the exception of ICAM1, CP also modulated the expression of these genes to a similar extent to P-RGI. This was unexpected considering that CP does not confer anti-proliferative effects in DLD1 cells. To test which genes are modulated in relation to reducing cell viability, and to test for specific mechanisms of P-RGI, CP can be considered as a negative control. Figure 44 shows the effect of P-RGI on DLD1 gene expression relative to the effect of CP. Observing the specific effects of P-RGI, ICAM1 was the only gene to be significantly modulated, with a decrease of 56% ($p<0.05$).

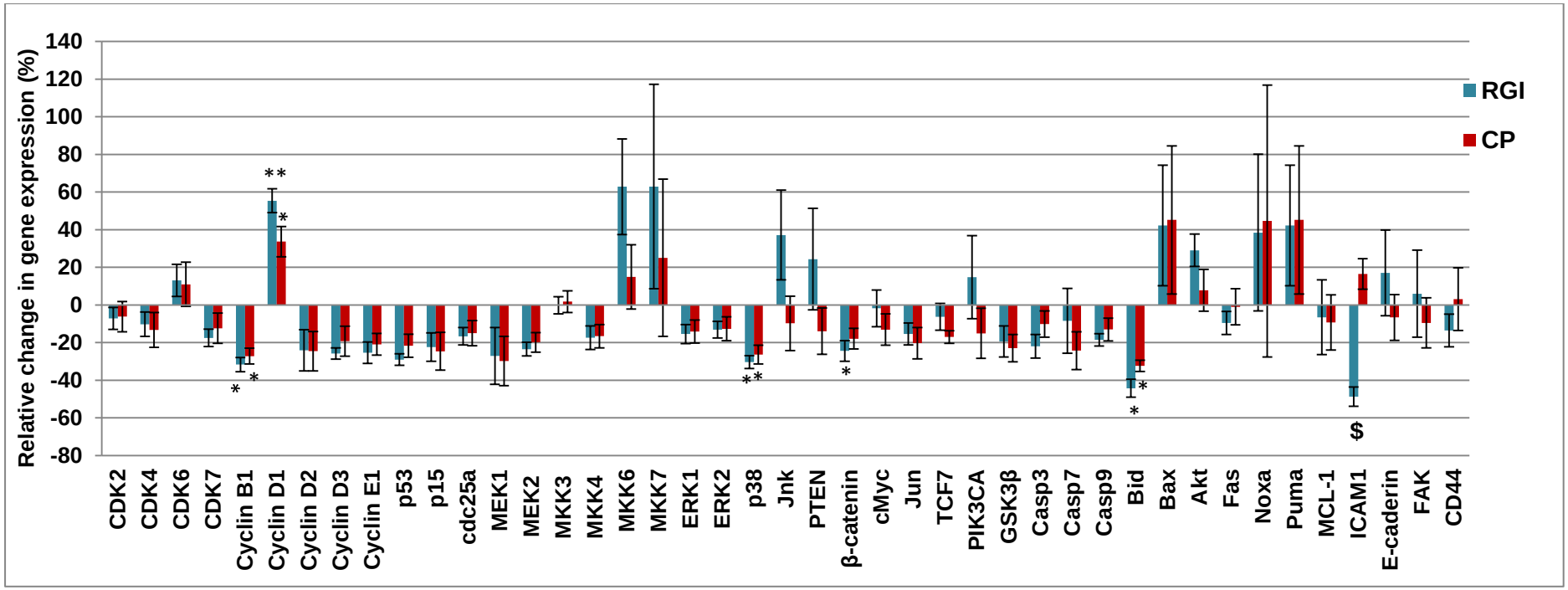

Figure 45 ***Effect of P-RGI and CP on gene expression in DLD1 cells.*** The mRNA expression of 46 genes was determined in DLD1 cells treated with 1 mg/ml P-RGI or 1 mg/ml CP for 24 hours. Results are expressed as percentage change in expression relative to untreated cells. Data are shown as mean ± standard error (n=4). *p<0.05; **p<0.01; $p<0.0001.

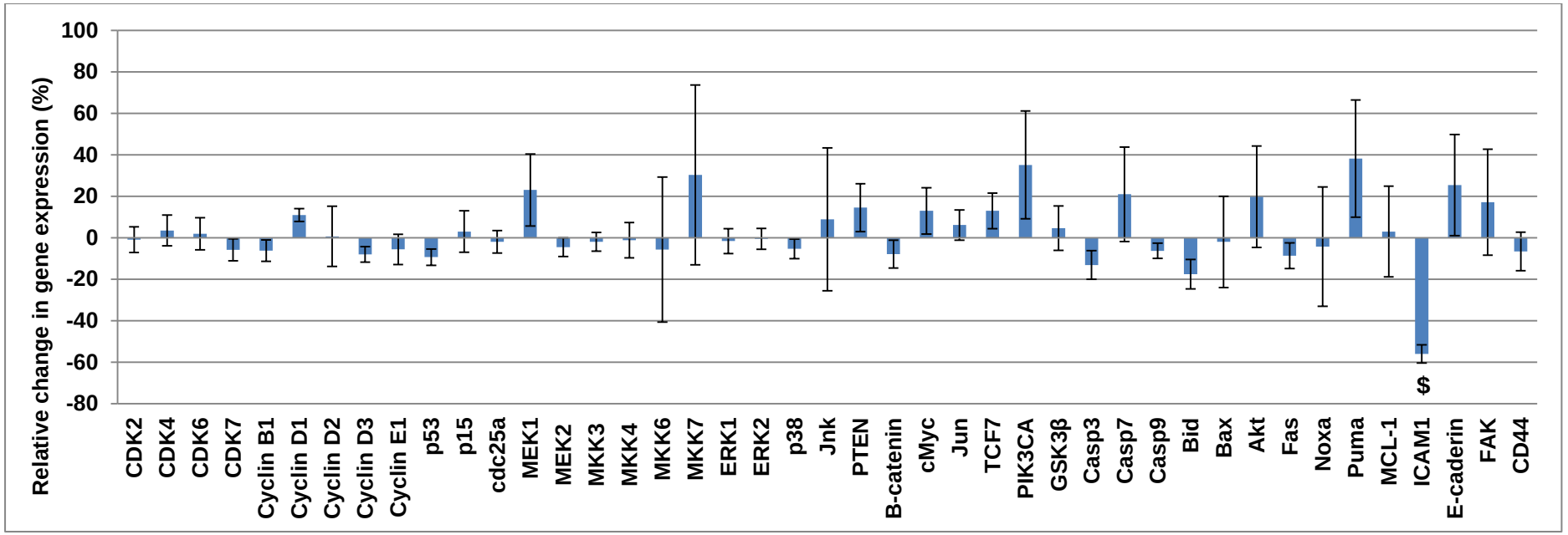

Figure 46 ***Specific effect of P-RGI on gene expression.*** The mRNA expression of 46 genes was determined in DLD1 cells treated with 1 mg/ml P-RGI for 24 hours relative to cells treated with 1 mg/ml CP for 24 hours. Results are expressed as percentage change in expression relative to CP-treated cells. Data are shown as mean ± standard error (n=4). *p<0.05; **p<0.01; $p<0.0001.

The expression of the genes ICAM1, FAK, E-cadherin and CD44 were tested due to their roles in cell adhesion. Figure 32 in chapter 5 shows that there was a significant 2.2 fold increase in detached cells found in the cell culture medium from cells treated with P-RGI. As the reduction of DLD1 cell viability by P-RGI was not attributable to apoptosis, it is possible that P-RGI induces the detachment of cells, either from each other or from the cell culture plate. Due to the significant effect on ICAM1 gene expression by P-RGI, the effect of P-RGI on the expression of several other genes relating to ICAM1 were determined. SDF-1 and Cox-2 are known to upregulate ICAM1 in colon cancer cells [409-411], however DLD1 did not express these genes. ICAM1 expression is also known to be regulated by the NFκB pathway, and its expression in colon cancer cells is upregulated by cytokines. Therefore the expression of IL-β, TNFα, as well as NFkB1, IKKα, and the NFκB inhibitor IκBα were investigated in P-RGI-treated DLD1 cells. Only NFkB1, IKKα and IκBα were found to be expressed in this cell line, and none of these genes were modulated by P-RGI (Figure 47).

a

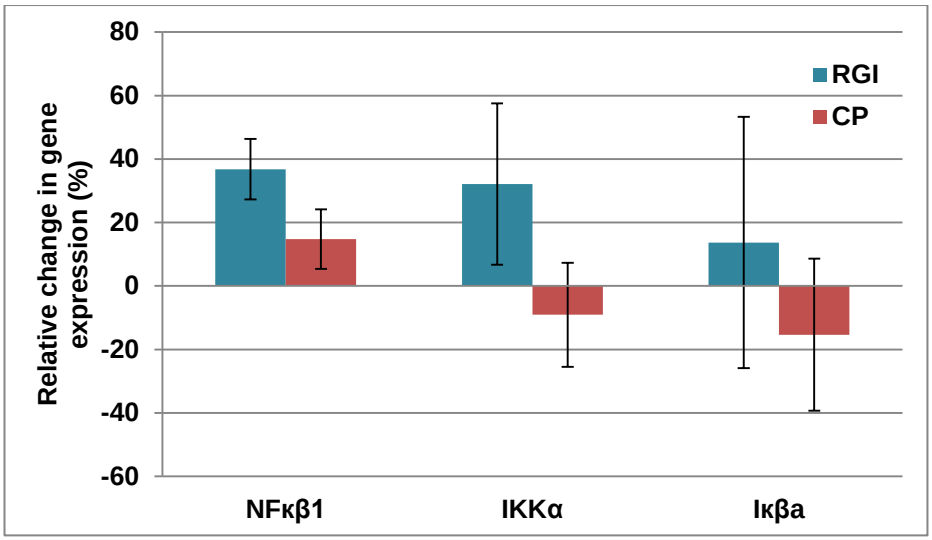

b

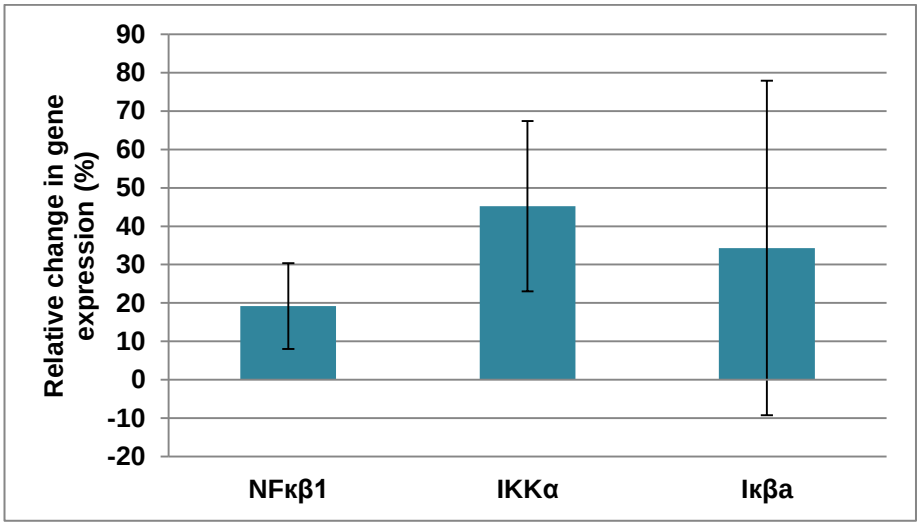

Figure 47 ***Relative changes in NFκB1, IKKα and IκBα gene expression in P-RGI-treated DLD1 cells*** (a) mRNA expression of NFκB1, IKKα and IκBα in DLD1 cells after exposure to 1 mg/ml P-RGI and 1 mg/ml CP for 24 hours. Results are expressed as percentage change in expression relative to untreated cells. (b) mRNA expression of NFκB1, IKKα and IκBα in DLD1 cells after exposure to 1 mg/ml P-RGI. Results are expressed as percentage change in expression relative to mRNA expression of genes after exposure to 1 mg/ml CP for 24 hours. Data are shown as mean ± standard error (n=4).

Since P-RGI induced a significant decrease in ICAM1 expression, the time-dependent effect of P-RGI on ICAM1 gene expression in DLD1 cells was investigated. A non-significant 38% decrease in mRNA levels of ICAM1 in P-RGI-treated DLD1 cells relative to cells treated with CP was observed after 8 hours, which decreased to 61% after 24 hours with no further decrease observed up to 72 hours (Figure 48).

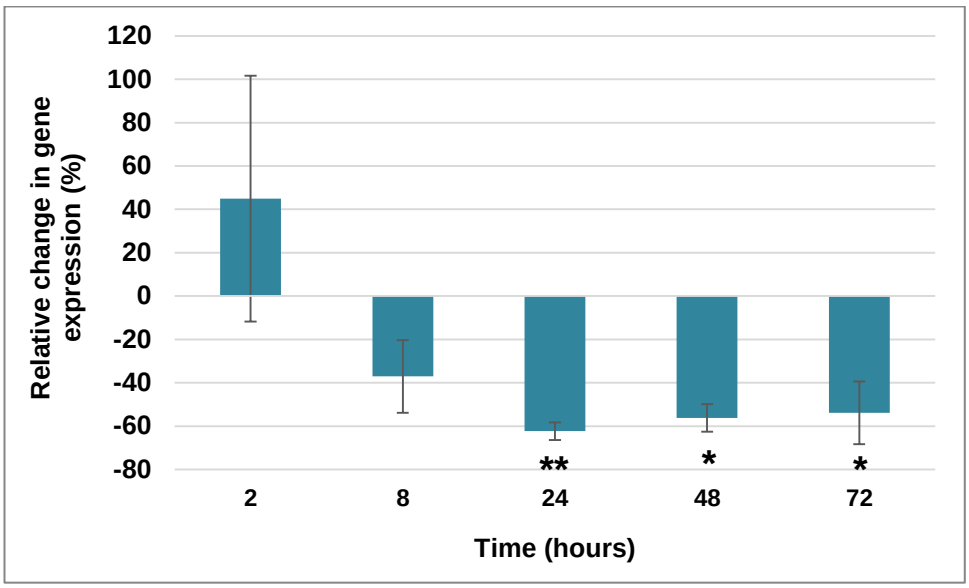

Figure 48 ***Time-dependent relative change in ICAM1 gene expression in P-RGI-treated DLD1 cells*****.** Alterations of ICAM1 mRNA expression in DLD1 cells after exposure to 1 mg/ml P-RGI for 2, 8, 24, 48 or 72 hours. Results are expressed as percentage change in expression relative to mRNA expression in DLD1 cells after exposure to 1 mg/ml CP at the same time points. Data are shown as mean ± standard error (n=4). *p<0.05; **p<0.01.

8.4.2 Effect of SSBA on ICAM1 expression in HT29 cells

P-RGI significantly reduced ICAM1 gene expression in a time-dependent manner in DLD1 cells, which suggests this reduction in ICAM1 could contribute to the observed effects of P-RGI on DLD1 cell viability. As SSBA reduces cell viability in HT29 cells, its effects on ICAM1 expression were investigated. No significant effect on ICAM1 expression was observed in SSBA-treated HT29 cells after 24 hours.

8.5 Discussion

In previous chapters potato-derived RGI (P-RGI) was shown to reduce cell proliferation in DLD1 cells in a Gal3-independent manner, and this was not attributable to an induction of cell cycle arrest or apoptosis. To gain insight into the molecular mechanisms behind the bioactivity of P-RGI, the effect of P-RGI on the expression of several genes involved in cell proliferation, apoptosis, adhesion and the cell cycle were investigated. Owing to the modulation of genes by CP, pectin that does not confer anti-proliferative effects in DLD1 or HT29 cells, CP was employed as a control to test for specific mechanisms of P-RGI. Only the expression of ICAM1 was specifically affected by P-RGI treatment. P-RGI induced a rapid decrease in expression in DLD1 cells, which preceded the observed decrease in cell proliferation, suggesting that the abrogation of this gene could be play a role in the reduction in cell growth.

Intercellular adhesion molecules (ICAMs) are members of the immunoglobulin superfamily of proteins and consist of five ICAMs designated ICAM1 to ICAM5. ICAM1 contains five extracellular domains that function in cell-cell and cell-ECM adhesive interactions [412] and is present on the cell surface of a wide variety of cell types including leukocytes, keratinocytes, fibroblasts, endothelial cells, and epithelial cells. Normal colon tissue does not express ICAM1 [413] but over-expression of this adhesion molecule has

been linked with tumour progression in CRC patients [87, 414]. Significantly higher levels of serum ICAM1 were found in CRC patients compared with healthy controls, with a positive association with disease stage and presence of metastasis [415, 416]. Colon cancer cell lines such as DLD1 and HT29 express ICAM1. Gallicchio et al showed that the Cox-2 inhibitor Celecoxib reduced ICAM1 expression in HT29 cells, which also decreased their adhesion to FBS coated plastic wells[411]. In DLD1 and SW48 colon cancer cells it was shown that CXC chemokine ligand 12/stromal cell-derived factor-1 (SDF-1) increased ICAM1 expression and adhesion to endothelial HUVEC cells, and that the ERK, JNK and p38 pathways were critical for in mediating this effect. Reduction of ICAM1 expression by knockdown of NFκB and MEK inhibitors was followed by a loss of adhesion in DLD1 cells [409].

Typically, a reduction in cell viability results from cell cycle arrest or induction of apoptosis, but P-RGI did not induce these effects in DLD1 cells. However, an increase in cell debris detected in the supernatant from P-RGI-treated cells suggests a loss of cell adhesion as a possible mechanism of action of P-RGI. Although other genes involved in cell adhesion, E-cadherin, FAK and CD44, were not affected, the observed P-RGI induced decrease in ICAM1 expression together with the previous observation of an inhibition of cell adhesion in cells with knocked down ICAM1 [409] supports this conclusion. MP has previously been implicated in the inhibition of cell adhesion. MCP and pectic polysaccharides from swallow root and ginseng were shown to block agglutination of red blood cells [210, 325], and okra RGI reduced melanoma cell aggregation via reduction in the expression of pan-cadherin and α5 integrin [211]. MCP blocked the binding of ovarian cancer cells to Wharton's jelly [204], blocked the interaction of B16-F1 breast cancer cells with laminin [321], and inhibited the adhesion of rat and human prostate cancer cells to endothelial cells [193]. In all cases this inhibition of adhesion was presumed to be Gal3 mediated; however, in this present study the effects of P-RGI on the loss of cell adhesion are Gal3-independent.

Besides its involvement in cell adhesion, ICAM1 is recognised more specifically for its contribution to immune function and is associated with a variety of inflammatory diseases and conditions including asthma, atherosclerosis, inflammatory bowel disease, and autoimmune disease [417-420]. ICAM1 is a ligand for LFA-1, an integrin found on leukocytes and macrophages [412, 421], and MUC-1 on endothelial cells. ICAM1 is involved in aiding transmigration of leukocytes across the endothelium and epithelium [422] as well as facilitating the adhesion of cancer cells to the endothelium and subsequently promoting metastasis [423]. Roland and colleagues suggest that tumour cells bind to endothelial ICAM1 via MUC-1, promoting the release of chemoattractants for circulating macrophages, which can then bind to ICAM1 on tumour cells, enhancing the expression of cytokines that recruit neutrophils [423]. The expression of ICAM1 in DLD1 and HT29 colon cancer cells has been shown to be enhanced by the presence of pro-inflammatory cytokines such as TNFα, IL-β, IL-1, IFN-α and IFN-γ [85, 413, 424, 425]. The ICAM-1 promoter region contains binding sites for a number of sequence-specific transcription factors, the most important of which is NFκB, which can mediate the induction of ICAM1 in response to different stimuli in different cell types [426, 427] and in CRC [428, 429]. c-jun, c-Fos and p53 are also known to activate ICAM1 expression [426, 430].

The decrease in ICAM1 expression in P-RGI-treated cells prompted further investigation into ICAM1-associated genes present in colon cancer cells. Consequently, the expression of genes encoding the proteins SDF-1 and Cox-2, known to upregulate ICAM1 expression in CRC [409, 410], and NFκB-associated genes IKKα, IκBα, NFκB1, TNFα and IL-β, as well as ICAM2 and ICAM3 were investigated. Results showed that only three of these genes, IKKα, IκBα, NFκB1, were expressed in DLD1 cells and P-RGI had no effect on their expression. However, to observe whether P-RGI has an effect on the NFκB pathway, it may be necessary to stimulate the cells first with cytokines.

It is noteworthy that P-RGI significantly affected the expression of a gene implicated in immune function since pectic polysaccharides are often shown to possess immunomodulatory properties. Numerous pectic polysaccharides are known to stimulate NO secretion, increase lymphocyte proliferation, complement fixing activity, and macrophage phagocytosis [185-187][151,152] Polysaccharides from *Astragalus membranaceus,* a herb used in traditional Chinese medicine, has been shown to supress ICAM1 expression in TNFα-stimulated endothelial cells by blocking NFκB activation [431], while β-glucan has been shown to decrease ICAM1 expression in lung tissue concomitant with a decrease in cytokine release [432]. Furthermore, human milk oligosaccharides with immunomodulatory properties, have been shown to influence the expression of ICAM1 in HT29 cells [433].

Previous chapters have shown that LM sugar beet pectin, SSBA, significantly reduces cell proliferation in HT29 cells via induction of apoptosis. SSBA has a different structure to P-RGI and, as it induces apoptosis, likely has a different mechanism of action. Correspondingly, SSBA did not affect the expression of ICAM1 in HT29 cells. The cell-specificity of P-RGI and SSBA may offer some clue to the mechanisms of action of these MPs. All the cell lines tested for the bioactivity of MPs originate from colon carcinomas, yet the intricate cellular pathways in each cell line are different, owing to mutations in different key genes. P-RGI significantly reduced viability in DLD1 and HCT116 cell lines which both have KRAS and PIK3CA mutations, but did not affect the other cell lines that lack this double mutation. These cell lines differ in the TP53 gene, which is mutated in DLD1 cells but not in HCT116 cells. It is interesting to note that P-RGI consistently had a greater effect on DLD1 cells than on HCT116 cells. P-RGI preferentially exerts its activity in cell lines with KRAS and PI3KCA mutant genes, which suggests that P-RGI potentially exerts its activity via the PI3K/Akt pathway. On the other hand, SSBA significantly reduced viability in HT29 cells, and to a lesser extent DLD1 cells which share PI3KCA and TP53 mutations, but differ in the

BRAF mutation present in HT29 cells. The observed, independent effects of SSBA and the Ras-inhibitor FTS on the viability of HT29 and DLD1 cells indicates that SSBA does not exert its effects through KRas inhibition but suggest that, since BRAF functions downstream of KRas, SSBA may specifically target the activity of the BRAF/MEK/ERK signalling pathway. It is thought that BRAF mutation cell lines, such as HT29 have developed an 'addiction' to hyper-activation of the MEK/ERK pathway and are thus sensitive to MEK or ERK inhibitors, while cell lines with a KRAS mutation, such as DLD1 will be less sensitive to these inhibitors due to additional parallel signalling down the PI3K pathway [434, 435]. An additional mutation in PI3KCA can enhance this resistance [436, 437]. This could go some way to explaining the lessened effect of SSBA in KRAS mutant DLD1 cells. However, further studies are required to demonstrate these effects and explore other signalling cascades affected by MP exposure. This could be achieved by performing transcriptomic analyses, for example using microarrays, which would provide information on the effects of MP on the expression of all genes simultaneously, and would thus identify the signalling pathways influenced by MP providing further understanding of the mechanisms of the cellular effects of MP.

8.6 Conclusion

The expression of genes associated with cell proliferation, apoptosis, adhesion and cell cycle progression were investigated in DLD1 cells after incubation with potato RGI, an MP that significantly reduced cell proliferation in DLD1 cells, potentially via loss of cell adhesion. Only ICAM1 expression was identified as being significantly modulated by P-RGI. The role of ICAM1 in cell adhesion and its significant decrease in expression prior to the reduction of DLD1 cell viability by P-RGI suggests that the P-RGI-induced reduction in ICAM1 expression results in a loss of cell adhesion, which subsequently affects cell viability. ICAM1 is also significantly involved in immune function, suggesting that P-RGI could possess immunomodulatory

properties. ICAM1 expression was not affected by SSBA in HT29 cells. Therefore, the cell-specific effects of P-RGI and SSBA provide some insight into the molecular mechanisms of their bioactivity. However, further studies are required to fully elucidate the specific mechanisms of MP bioactivity within cells.

Chapter 9
Discussion

9.1 Discussion

Data presented in this thesis show the ability of alkali-treated sugar beet and citrus pectin and potato-derived RGI and galactan to significantly reduce cell proliferation in colon cancer cells, suggesting the possible chemopreventative effects of MP. In summary, SSBA, and to a lesser extent CA, reduced proliferation of HT29 cells via the induction of apoptosis, while P-RGI, and to a lesser extent P-Gal and SSBA, reduced proliferation of DLD1 cells, possibly via a loss of cell adhesion. One of the most intriguing elements of this study comes from structural examination of these bioactive pectins, which showed that they have very different structures. Furthermore, a small change in structure can significantly affect pectin bioactivity. These results, combined with the cell-specificity of each of the bioactive pectins, suggest a very complex structure-function relationship.

Investigations into the bioactivity of pectins should be supplemented with an understanding of the structure of the biologically-active pectin. However, the structural requirements for bioactive MP have rarely been addressed in previous studies. There is growing evidence linking modified forms of pectin with anti-cancer activity, although modified pectin is an ambiguous term simply meaning pectin that has been modified using pH, heat or enzymes. Moreover, pectin is an extremely complex material and pectins from different sources can vary in polymer size distributions, molecular weight, DE, the nature and placing of the neutral sugars as well as the addition of acetyl and feruloyl groups. Pectin structure from the same sources also vary with respect to the differences between plantations, climates, hereditary traits of the trees, and could even vary day to day owing to factors such as the ripeness of the fruit and the weather prior to harvest [128]. MPs from various sources, extracted and modified in numerous ways, have been shown to induce various cellular effects in many different cell types. The lack of structural analysis in these studies means that the structure-function relationship is often unknown; inconsistencies are often reported and results

are difficult to compare. Findings in the literature can be considerably diverse which is likely due to inconsistencies of source material, which impede interpretation of results, as well as methodology and environment. However, the inhibition of the function of the pro-metastatic protein Gal3 by binding of Gal side chains on pectin has been postulated as a potential mechanism of action [322, 397, 398], establishing the theory that Gal content of MP is significant for bioactivity. However, studies that have specifically investigated structure-function aspects of pectin activity have found that bioactivity can depend on the DE content [329], as well as the HG backbone of pectin [212, 213].

This study has shown that various pectin structures can confer bioactivity and suggests that different regions of the pectin molecule may give rise to different bioactive properties. The actions of SSBA lend evidence for the importance of neutral sugar-rich RGI for activity. SSBA differs from SBC in that it is significantly richer in neutral sugars. The hydrolysis of the pectin backbone by heat and alkali treatment created pectin with increased RGI content. SBC required significantly more time to exert its anti-proliferative activity on HT29 cells than SSBA, which may be due to fewer RGI regions in SBC. Moreover, the enzymatic removal of Gal and Ara residues from SSBA significantly reduced its bioactivity. The removal of Ara residues, yielding SSBA containing only linear (1→4)-β-galactan and single unit Ara and Gal, considerably reduced the SSBA-induced response. Enzymatic removal of both linear (1→4)-β-galactan and (1—5)-α-Ara chains completely abolished the SSBA-induced response after 72 hours. Taken together these results indicate that the Gal side chains of SSBA are essential for bioactivity, while the presence of Ara side chains enhance activity, suggesting that Ara may assist in the presentation of Gal to receptors.

While it is evident that neutral sugars are extremely important for the bioactivity of SSBA, further evidence shows that the HG backbone may also play a significant role. Gal- and Ara-depleted SSBA reduced HT29 cell

viability after an extended treatment. It is possible that this reduction may be due to the 4-13% Gal remaining in SSBA. However, it is more likely that the HG or RGI backbone of SSBA could be a secondary bioactive component with less significant effects that take longer to detect. A similar pattern was observed for HT29 cells treated with Pec-C, which is predominantly composed of GalA and had no effect on cells at 72 hours but reduced cell viability after 96 hours, although to a lesser extent than SSBA-gal. However, C-PGA, which also consists predominantly of GalA, had no effect on the cells. Pec-C has a significantly lower MW than C-PGA and SSBA-gal, which may explain the observed disparities in bioactivity. Further evidence for the importance of the HG backbone emerged from the studies of P-RGI and P-RGI-X, two potato-derived pectic polysaccharides that underwent enzymatic treatment to remove HG chains and sugars while leaving the RGI backbone intact. Interestingly, P-RGI was shown to have anti-proliferative activity against DLD1 cells, while P-RGI-X did not. Investigation into the fine structure of these RGI samples showed that P-RGI contained GalA residues residing in HG chains, while GalA in P-RGI-X was found to reside only in the RGI backbone or as free GalA mono- or disaccharides. Furthermore, it was shown that the HG chains in P-RGI may exist as side chains from the RGI backbone. These results show that HG chains are essential for the bioactivity of P-RGI. However, it is more likely that the combination of RGI and HG backbone is responsible for activity, since C-PGA, which consists almost entirely of HG backbone, did not possess anti-proliferative activity. There are a few studies that suggest distinct bioactive roles for the pectin backbone. HG-rich ginseng pectin was shown to reduce proliferation in HT29 cells and inhibit fibroblast cell migration [212, 213], while the backbone of ginseng RGI, depleted of all neutral sugar side chains, still inhibited agglutination, albeit requiring higher concentrations than with the intact RGI [325]. Additionally, pectic acid induced apoptosis in rat pituitary tumour cells [331], and pentamers of GalA were shown to be active against inflammation and carcinogenesis in a mouse model of colitis-associated CRC [332]. These

studies demonstrate the bioactivity of HG and its Gal3-independence, which suggest multiple roles for pectin structures in bioactivity.

A further structural aspect of MPs that could influence bioactivity is methyl-ester content. Alkali treatment significantly lowered the DE of both sugar beet and citrus pectins to yield SSBA and CA, which were the only commercial pectins to significantly reduce HT29 cell viability after 72 hours. Although alkali treatment also hydrolysed the HG backbone, particularly in sugar beet pectin, the effect on citrus pectin structure was minimal, except for the significant reduction in methyl-ester content. This raises the possibility that DE is significant for bioactivity, particularly for CA. However, SSBA had a lower DE than CA, but was more bioactive. In addition, four additional LM apple and citrus pectins were shown to have no effect on cell viability. This indicates that the DE per se is not significant for bioactivity, and other characteristics of SSBA and CA are more important. The effect of pectin DE has been investigated in previous studies. Jackson and co-workers showed that, contrary to the observation in this study, alkali treatment of heat-treated citrus pectin abolished its apoptosis-inducing activity in prostate cancer cells suggesting that the ester linkages in pectin are essential for bioactivity [329]. This certainly cannot be true of pectins in this study. However, Bergman and colleagues proposed that DE made no significant difference to bioactivity, and showed that CP with DE of 30% or 60% reduced HT29 cell proliferation by comparative amounts [326]. Investigating the structure-function of bioactive pectins is immensely challenging due to the complex nature of pectin. This study has shown that pectins with very different structures can exert activity on colon cancer cells. Gal side chains, with the support of Ara chains, were shown to be crucial for the activity of SSBA, while the HG backbone is essential for P-RGI.

Commercial and dietary pectins are often assumed to be non-digestible in the GI tract and resistant to systemic uptake due to their relatively high MW. Modifying pectin lowers its MW and studies have shown MP to have a

systemic effect in rodents [193, 195] and humans [200]. *In vitro*, however, correlations between the size of MP and activity have not been reported. Jackson and co-workers showed that heat-treated citrus pectin significantly induced apoptosis in prostate cancer cells, while higher MW unmodified citrus pectin did not. However, they also showed that Pectasol-C, which has a significantly lower MW than unmodified citrus pectin, did not induce apoptosis suggesting that low MW is not sufficient for bioactivity [329]. Gao and colleagues also showed no correlation between the size of ginseng MP and activity [325]. These studies corroborate the lack of any correlation between pectin MW and bioactivity towards HT29 cells observed here, where the MWs of pectins in the order of their bioactivity was 362 > 129 > 548 > 23 kDa.

Many studies have shown modified pectins reduce cell proliferation, migration, adhesion and induce apoptosis in numerous types of cancer cells [204, 210-213, 321, 329] as well as reduce tumour formation and metastasis in rodents [191, 193, 195]. A mechanism for these observed effects has been proposed, based on the presence of β-galactans, branched from pectin, binding and inhibiting the function of the protein Gal3 [321, 322, 325]. Gal3 has been highlighted as a potential therapeutic target in cancer due to its suggested role in promoting metastasis [390]. Gal3 contains a domain which specifically binds with β-galactose-containing carbohydrates and glycoconjugates, such as those in the RGI regions of pectin. Numerous studies have shown the specific and direct binding of recombinant Gal3 to β-galactan [322, 323] and MP [321, 325]. Recent studies in our laboratory have shown that recombinant Gal3 had a high affinity for P-Gal and the disaccharide GB, while the interaction with P-RGI-X was weaker. These interactions were shown to be inhibited by the presence of lactose, which confirms that the binding occurs within the CRD of Gal3 [322]. P-RGI-X contains short (1→4)-β-galactan side chains of 1-3 Gal residues; while P-Gal has an RGI backbone with long β(1→4)galactan chains of approximately 23

galactose residues. The CRD of Gal3 recognises disaccharides containing β-galactosides [215], which would account for the high affinity for GB and P-Gal. However if the disaccharide is bound to the backbone or if there are other forms of steric hindrance, longer side chains may be required to allow the terminal disaccharide to bind, which would account for the weaker interaction with P-RGI-X. However, Gao and co-workers showed that ginseng RGI, containing short β-galactan side chains of 1-4 residues, had a high binding affinity with recombinant Gal3, and that (1→4)-β-galacto-oligosaccharides with long chains up to 63 galactose residues did not show increased affinity. The authors suggest these results indicate that short chains of 1-3 galactose residues on RGI may still be significant in regulating the activity of Gal3. The significance of the role of Gal3 in governing the effect of P-RGI on cell viability was assessed using RNA interference and showed that reducing the expression of Gal3 by approximately 90% did not affect the cellular response to P-RGI in two colon cancer cell lines, indicating that the effect of P-RGI on the viability of these two cell lines is independent of Gal3. This may have been anticipated since HG and not β-galactan was shown to be an essential bioactive component of P-RGI. β-galactan side chains, however, were critical for the biological activity of SSBA, and therefore an interaction with Gal3 may be responsible. However, knocking down the expression of Gal3 by approximately 75% did not affect the cellular response to SSBA in HT29 cells, indicating that the decrease in cell viability was independent of Gal3.

Further support for a Gal3-independent mechanism for the anti-proliferative effects of SSBA is provided by the observations that SSBA and FTS, a known inhibitor of KRas function, act by independent mechanisms. Gal3 is known to drive cell proliferation and inhibit apoptosis via its interactions with intracellular proteins such as KRas, Akt and β-catenin. Although the anti-proliferative and apoptotic activity of MP has been postulated as a consequence of binding and inhibiting Gal3, it is still not clear how MP may

bind to intracellular Gal3. It is possible that low MW pectin may enter cells, a mechanism postulated by Huang and colleagues who showed that embryonic kidney cells absorbed MCP with a low MW of 1kDa [401]; however this experiment lacked controls and has not been repeated. Another possibility is that MP could bind to Gal3 located in lipid rafts [438], specialised membrane microdomains that function as organising centres for the assembly of signaling molecules [403, 404]. Gal3 is known to be recruited by KRas from the cytosol to the plasma membrane, where it plays a role as an integral nanocluster component by binding and stabilising KRas in its active state, driving cell proliferation and preventing apoptosis [294, 405]. Results show that SSBA and FTS affect cell viability via separate mechanisms, which indicates that SSBA does not affect the activity of KRas. As Gal3 at the plasma membrane is known to exert its activity via KRas, these results lend further support for a Gal3-independent mechanism for the anti-proliferative effects of SSBA.

The Gal3-independent activities of MPs are also consistent with the results from previous studies. Two studies showed that MCP significantly induced apoptosis in the prostate cancer cell line LNCaP, which does not express Gal3 [201, 329], confirming that the mechanism must be Gal3-independent. A study into the relationship between guar galactomannan and Gal3 also showed that, although galactomannan bound strongly to recombinant Gal3, it bound weakly to endogenous Gal3 in a cell culture system, leading the authors to suggest that carbohydrate ligands on epithelial cell surfaces may impair galactomannan binding [330]. Additionally, although MCP prevented Gal3-induced endothelial cell chemotaxis, MCP was also shown to prevent bFGF-induced chemotaxis [195]. However, the role of Gal3 cannot be ruled out in mediating the cellular response in many other studies that have reported effects of MP such as those reporting the *in vitro* effects of MP on cell migration, adhesion, angiogenesis and agglutination [210, 325], as well as *in vivo* effects such as inhibition of metastasis and tumour formation [321].

The mechanisms responsible for these effects are likely to be different to those in the experimental model of this study. In particular, extracellular Gal3 that is accessible to pectin extracts is likely to be involved in cell migration and metastatic behaviour, whereas inaccessible intracellular Gal3 is probably involved in cell survival. In addition to anti-metastatic effects, MP has been reported to have anti-inflammatory properties, which may be mediated by the binding of Gal chains to Gal3 on circulating immune cells [324]. The fact that the biological effects of P-RGI and SSBA observed in this study are independent of Gal3, and the apparent importance of HG chains, suggest that the structural features required for reducing cancer cell proliferation may be very different to those required for the use of pectin as an anti-metastatic agent.

Since P-RGI and SSBA exert their effects via a Gal3-independent mechanism indicates alternative mechanisms of action for which insight may be provided by the cell-specificity of these MPs. P-RGI preferentially exerts its activity in cell lines with KRAS and PI3KCA gene mutations, which suggests that P-RGI may exert its effect via the PI3K/Akt pathway. The observed, independent effects of SSBA and the Ras-inhibitor FTS on the viability of HT29 and DLD1 cells, which carry a mutation in the BRAF gene, indicates that SSBA does not inhibit KRas activity but suggests that, since BRAF functions downstream of KRas, SSBA may specifically target the activity of the BRAF/MEK/ERK signalling pathway. It is thought that BRAF mutation cell lines, such as HT29, have developed an ‘addiction’ to hyper-activation of the MEK/ERK pathway and are therefore particularly sensitive to MEK or ERK inhibitors, while cell lines with a KRAS mutation, such as DLD1 will be less sensitive to these inhibitors due to additional parallel signalling down the PI3K pathway [434, 435]. Support for this is provided by the weaker effect of SSBA on DLD1 cells together with the lack of effect on HCT116 cells, which both have KRas mutations.

In order to gain further insight into the molecular mechanisms behind the bioactivity of P-RGI, the effect of P-RGI on the expression of several genes involved in cell proliferation, apoptosis, adhesion and the cell cycle were investigated. Interestingly, only the expression of one gene, ICAM1, was specifically affected by P-RGI treatment. P-RGI induced a rapid decrease in ICAM1 expression in DLD1 cells, which preceded the observed decrease in cell proliferation, suggesting that reduction of the expression of this gene may play a role in the reduction in cell growth. Over-expression of ICAM1 has been linked with colon tumour progression[87, 414], and in DLD1 colon cancer cells it was shown that SDF-1 increased ICAM1 expression and adhesion to endothelial HUVEC cells, while inhibition of ICAM1 expression was followed by a loss of adhesion [409]. Typically, a reduction in cell viability results from cell cycle arrest or induction of apoptosis, however, P-RGI did not induce these effects in DLD1 cells. Instead, an increase in cell debris detected in the supernatant from P-RGI-treated cells suggests a loss of cell adhesion as a possible mechanism of action of P-RGI. The P-RGI-induced decrease in ICAM1 expression together with the previous observation of inhibition of cell adhesion in cells with down-regulated ICAM1 expression [409] supports this conclusion. Confirmation of the association of MP with cell adhesion comes from numerous studies. MCP blocked the binding of ovarian cancer cells to Wharton's jelly [204], blocked the interaction of B16-F1 breast cancer cells with laminin [321], and inhibited the adhesion of rat and human prostate cancer cells to endothelial cells [193]. MCP and pectic polysaccharides from swallow root and ginseng were shown to block agglutination of red blood cells [210, 325], and okra RGI reduced melanoma cell aggregation via a reduction in the expression of pan-cadherin and α5 integrin [211]. In all cases this inhibition of adhesion was presumed to be mediated by Gal3. However, in this study, the effects of P-RGI on the loss of cell adhesion were independent of Gal3.

In addition to its role in cell adhesion, ICAM1 is also recognised more specifically for its contribution to immune function. ICAM1 is a ligand for LFA-1, an integrin found on leukocytes and macrophages [412, 421], and is involved in facilitating the adhesion of leukocytes to the endothelium and subsequent transmigration into tissues [439]. The expression of ICAM1 in DLD1 and HT29 colon cancer cells has been shown to be enhanced by the presence of pro-inflammatory cytokines [85, 413, 424, 425, 440], and the ICAM1 promoter region contains binding sites for a number of sequence-specific transcription factors, the most important of which is NFκB, which can mediate the induction of ICAM1 in response to different stimuli in different cell-types [429, 430] and in CRC [427, 428]. The P-RGI-induced decrease in ICAM1 expression led to the further investigation into the expression of several ICAM1-associated genes in DLD1 cells. However, results showed that either these genes were not present in DLD1 cells or were not affected by P-RGI treatment. It is interesting that P-RGI significantly affected the expression of a gene implicated in immune function since pectic polysaccharides are often shown to possess immunomodulatory properties. Numerous pectic polysaccharides, typically from traditional medicinal plants, are known to increase macrophage phagocytosis, lymphocyte proliferation complement fixing activity and stimulate NO secretion [158, 159, 187-189]. β-glucans, polysaccharides well known for their immunomodulatory properties, have also been shown to decrease ICAM1 expression in lung tissue concomitant with a decrease in cytokine release [432], and polysaccharides from *Astragalus membranaceus,* a herb used in traditional Chinese medicine, has been shown to supress ICAM1 expression in TNFα-stimulated endothelial cells by blocking NFκB activation [431]. Human milk oligosaccharides with immunomodulatory properties have also been shown to influence the expression of ICAM1 in HT29 cells [433].

The established role of ICAM1 in cell adhesion together with the observed P-RGI-dependent decrease in its expression prior to the reduction of DLD1 cell

viability suggests that the P-RGI-induced reduction in ICAM1 expression results in a loss of cell adhesion, which subsequently affects cell viability. ICAM1 is also significantly involved in immune function, suggesting that P-RGI could possess immunomodulatory properties. SSBA, however, did not affect the expression of ICAM1 in HT29 cells. SSBA has a different structure to P-RGI and, since it induces apoptosis, probably has a different mechanism of action. Previous studies into LM and GalA-rich sugar beet pectin have shown it possesses muco-adhesive properties, adhering to mucins on colon cancer cells and providing a barrier to toxins [336]. However, although undifferentiated HT29 cells in culture are heterogeneous in that they contain a small proportion of columnar absorptive cells and mucous cells [441, 442], the proportion of mucous-secreting cells can sometimes be as low as <0.08% of the cell population [442]. This makes it very unlikely that muco-adhesion occurs in an interaction between SSBA and HT29 cells.

The main aims of this study were to: i) characterise several commercial pectins and screen them for bioactivity; ii) assess any correlation between structure and bioactivity; iii) investigate the role of Gal3 in mediating pectin bioactivity, and iv) investigate possible alternative mechanisms of action for pectin bioactivity. One of the main outcomes of this study was to show that correlations between the structure and function of MP are extremely complex, and it is highly likely that different components of pectin, perhaps in cooperation, can exert bioactivity via diverse mechanisms. This finding is supported by the numerous reports on MP activity that vary substantially in their outcomes. SSBA reduced HT29 and DLD1 cell viability via an induction of apoptosis, where Gal side chains of an average 2–3.5 residues were shown to be essential for activity, while the HG backbone may provide a secondary bioactive component. SSBA potentially acts as an inhibitor of the MEK/ERK pathway and exerts its activity in a Gal3-independent manner. Previous studies investigating LM pectin have shown that it has muco-

adhesive properties and it is possible that SSBA could bind to mucins on HT29 cells in a non-specific manner. However, how this might induce apoptosis is unknown and further investigation is required. P-RGI, on the other hand, reduced cell viability in DLD1 and HCT116 cells independently of Gal3. The HG region was shown to be essential for bioactivity. P-RGI reduced the expression of ICAM1 prior to the loss in cell viability, therefore suggesting a mechanism whereby P-RGI induces a decrease in cell adhesion by suppressing ICAM1 expression with consequences for cell viability.

The question remains, however, as to how these results translate from *in vitro* to *in vivo*. At present very little is known about the uptake and transport of pectin within the body. Dietary pectin is often assumed to be non-digestible and resistant to hydrolysis during passage through the human GI tract. Animal trials suggest that MP is absorbed by the body owing to the observed systemic effects in studies of experimental metastasis in rodents [314, 186, 188], although this could be a prebiotic effect from colonic fermentation by bacteria. However, support for absorption of pectin into the bloodstream comes from studies that showed pectic RGI and arabinogalactan to be detectable in the bloodstream and liver of rodents [342]. A report from human studies on orally administered Pectasol-C has been shown to assist with the urinary excretion of toxic elements, with toxicity reduced in the bloodstream [193]. It is not apparent whether the modification of pectin generates fragments that are small enough to be absorbed, or whether it is possible that pectin could be modified in the body by endogenous enzymes or other factors. Small neutral fragments of pectin, such as linear galactans and arabinogalactans, have been shown to paracellularly cross a simulated intestinal monolayer [346]. Studies on the uptake of β-glucans suggest two possible routes: firstly, passive absorption in the small intestine, and secondly the uptake by M cells residing in Peyer's patches, leading to uptake, modification, transport and release by

macrophages [344, 345]. It is postulated that analogous uptake and transport mechanisms could be involved in the bioactivity of MPs [443]. Colonic fermentation additionally might generate smaller fragments but this would be in competition with uptake by colonic microflora. Pectic oligosaccharides have been shown to act as prebiotics, enhancing populations of *Bifidobacteria* and the *Bacteriodes-Prevotella* group, with neutral sugars being selective for *Bifidobacteria* [444]. In addition to being absorbed, it is possible that MP could act directly on colon cancer cells. It is known that pectin is able to bind to mucins on colonic epithelial cells [343]; however, how pectins may exert bioactivity via this mechanism is unknown, as is the length of time MP might have to exert its biological effects before breakdown in the gut by colonic microflora.

Results from this study emphasise the importance of an understanding of the structure of biologically-active pectins and the multiple bioactive roles that the components of pectin may convey. This research showed that Gal3 did not play a role in the reduction in cell viability via an induction of apoptosis and a loss of cell adhesion by MPs, and highlights the importance of investigating alternative mechanisms of action. There is a need for detailed mechanistic structure-function studies at the molecular and cellular level on the bioactive roles of well-characterised MPs. The reduction of ICAM1 by potato-derived RGI is a significant discovery, and alongside the apparent cell-specific effects of MPs underlines the requirement of further studies to investigate signalling cascades and specific genes affected by MP exposure. This could be achieved by performing transcriptomic analyses, such as microarrays, which would identify the signalling pathways influenced by MP providing further understanding of the mechanisms of the cellular effects of MP. The use of MPs as drugs in the treatment of cancers and other diseases will rely on successful clinical trials. The ‘natural’ nature of MPs make them ideal candidates as adjuvants to harsh conventional therapies such as radiotherapy and chemotherapy, however, there is the potential of MPs to be

useful as a supplement for maintaining overall health. The presence of pectin in fruits and vegetables, and in processed food and drinks, necessitates investigation into whether pectin in this form can be released, modified, and the bioactive fragments transported within the body. The uptake of pectin and pectic fragments by macrophages, and the oral and gastric breakdown of pectin, for example, could be examined. Such investigations would also be useful in considering potential modes of action of pectic polysaccharides from medicinal plants. Should such processes result in low levels of bioactive fragments they may provide a foundation for promoting early stage protection against the onset and progression of diseases, and furthermore could provide a basis for a mechanistic explanation of the health benefits of the consumption of fruit and vegetables.

In conclusion, results presented in this thesis suggest that modified pectins of varying structures can exert anti-proliferative activity in colon cancer cells, in a cell-specific manner. The individual components of pectins, particularly the HG backbone together with galactan and arabinogalactan side chains of RGI, are important for bioactivity and potentially act cooperatively to exert maximum biological effect. MPs in this study do not exert their effects via the inhibition of Gal3, which prompted investigation into alternative mechanisms of action. Expression of the adhesion molecule ICAM1 was shown to be significantly modulated by P-RGI, which suggests a novel potential mode of action. This study is also the first to report sugar beet pectin as a biologically-active substance, consequently highlighting a potential novel exploitation of waste stream sugar beet pulp. Taken together, these results highlight the need for detailed mechanistic investigations at the molecular and cellular level on the bioactive roles of MPs that have been extensively characterised. The extraordinary structural complexity of pectin makes it a potential multi-functional therapeutic agent, and investigations into the uptake of pectin could provide a mechanistic explanation for the health benefits associated with the consumption of fruit and vegetables.

Appendices

Appendix A Monosaccharide, molar mass and protein analysis

A1 Monosaccharide Analysis

Methanolysis was performed by adding 100 µl methyl acetate and 400 µl 1.5 M HCl in methanol to up to 1 mg samples (dried in 50°C vacuum oven) and heating them at 85°C for 17 hours. After the samples had cooled to room temperature, 5 drops of n-butanol was added and the samples were evaporated to dryness under a stream of nitrogen. In order to hydrolyse methyl glycosides formed by methanolysis, 0.5 ml of 2M trifluoroacetic acid was added, and the samples were heated at 121°C for 1 hour. The samples were cooled to room temperature and evaporated to dryness, and 0.5 ml of methanol was added and evaporated to dryness three times. Water was added to each sample, and they were filtered (0.25 µm) prior to injection. Inositol was added to each sample prior to methanolysis as an internal standard. Hydrolysates were analysed for neutral monosaccharide content by HPAEC pulsed amperometric detection (PAD) using a Dionex ICS-2500 system that included a CarboPac PA20 column and guard column, an EG 50 eluent generator that produced the isocratic 10mM KOH mobile phase, a continuously regenerated anion trap column, a GP 50 pump operated at 0.5 ml/min, an ED50 electrochemical detector utilizing the quadruple potential waveform, and an AS50 autosampler with a thermal compartment (30°C column heater). The acidic monosaccharide content was determined with a Dionex DX-500 system, which included a GP50 gradient pump (0.5 ml/min), a CarboPac PA20 column and guard column, an ED40 electrochemical detector (gold working electrode and pH reference electrode), an LC25 chromatography oven (30°C), a PC10 pneumatic controller (post column addition of 500 mM NaOH), and an AS3500 autosampler. The mobile phase consisted of isocratic 10mM CH_3COONa, 1mM NaOH eluent for 10 minutes,

and then a linear gradient of 100 to 130 mM CH_3COONa in 100mM NaOH for the following 20 minutes [111].

A2 Molar mass analysis

Molar mass was determined by HPSEC at USDA-ARS. The biopolymer solutions containing 3.0 mg/mL β-LG and/or 1.0 mg/mL SBP, individually or mixed and/or pre-heated were characterized by HPSEC (1200 Series, Agilent Technologies, Santa Clara, CA). The solvent delivery system consisted of a vacuum degasser, auto sampler and a pump. The mobile phase was 0.05 M $NaNO_3$ and 0.01% NaN_3 (pH 6.65). The injection volume was 200 µL, and flow rate was held at 0.7 mL/min. Samples were run in triplicate. Two guard columns (TSK-GEL® PW_{XL} 6.0 mm ID × 4.0 cm L, 12 µm, Tosoh Bioscience, Tokyo, Japan) were used. One was placed before the separation columns, which consisted of a set of three model TSKgel $GMPW_{XL}$ size exclusion columns (7.8 mm × 300 mm, particle size 13 µm, Tosoh Bioscience, Tokyo, Japan), and the other before the detectors. The column set was heated in a water bath at 35°C, and connected in series to a UV-1260 Infinity spectrophotometer (Agilent Technologies, Santa Clara, CA), HELEOS II multi-angle laser light scattering photometer (MALLS) (Wyatt Technology, Santa Barbara, CA), Model 255-V2 differential pressure viscometer (DPV) (Wyatt) and an RI detector (Wyatt). Narrowly monodispersed pullulan P-50 (Shodex STANDARD P-82, JM Science, Grand Island, NY) was used to calibrate the scattering intensity at the 90° angle. BSA (Sigma–Aldrich, St. Louis, MO) was used to align all detectors, UV/vis, MALLS, DPV and RI. The percentage of recovery was obtained from the ratio of the mass eluted as determined by integration of the refractometer signal to the mass injected. All signals from the four detectors were analysed by the ASTRA software (V.6.1.1.17, Wyatt Technology). All samples were analysed at UV278 nm and UV325 nm. The extinction coefficient for each wavelength was determined from the RI concentration of each individual sample [368].

A3 Protein analysis

Protein analysis was carried out at USDA-ARS. The protein content of pectin was estimated using standard methods for determining the nitrogen content of samples by use of a combustion instrument followed by thermal conductivity (AOAC Method 990.03, AACC Method 46–30). A Flash EA 1112 Elemental Analyser (CE Elantech, Inc., Lakewood, NJ) calibrated with aspartic acid was used for the nitrogen determination. Percentage nitrogen was multiplied by 6.25 to obtain an estimation of protein (AOAC Method 22.052) [137]).

Appendix B ^{1}H and ^{13}C chemical shifts of selected pectins

Table B1 ***P-RGI*** R= rhamnogalacturonan, H= homogalacturonan, NR= non-reducing end, us= unsaturated GalA. Other conventions: Rha^{Gal}= rhamnose substituted with Gal single residue or chain, Rha^{-}= unsubstituted rhamnose, Gal (in bold) indicates the residues for which values are presented

		1	2	3	4	5	6
$GalA^{R}$	H	5.05	3.93	4.11	4.43	4.61	-
	C	100.55	70.66	73.06	79.76	74.14	177.0
$GalA^{R}$ (minor)	H	5.03					
	C	100.21					
$GalA^{H}$	H	5.10	3.77	3.99	4.43	4.70	-
	C	101.55	70.93	71.65	80.67	74.05	177.8
$GalA^{NR}$	H	5.09	3.75	3.91	4.29	4.69	-
	C	101.70	70.97	72.26	73.41	74.93	178.3
$GalA^{us}$	H	5.12	3.76	4.28	5.79	-	-
	C	101.77	72.88	68.61	109.14	148.3	171.6?
$GalA^{us-1}$	H	5.10	3.74	3.98	4.56	4.76	-
	C			71.53?	81.94	74.10	
Rha^{Gal}	H	5.28	4.13	4.10	3.66	3.87	1.32
	C	101.01	79.58	72.06	83.26	70.18	19.47

Rha^{-}	H	5.28	4.12	3.90	3.40	3.80	1.26
	C	101.01	79.02	~72.1	74.81	71.53	19.25
Rha^{NR}	H	5.23					
	C	102.91					
t-Gal(1→	H	4.63	3.53	3.68	3.93	3.70	3.79
2)Rha	C	105.99	74.36	75.41	71.34	77.68	63.55
→4)**Gal**(1→	H	4.66	3.61	3.79	4.17	3.72	(3.79, 3.84)
2)Rha	C	106.15	74.72	75.93	79.76	77.07	(63.25)
t-Gal(1→	H	4.60	3.62	3.67	3.93		
4)Gal(1→	C	106.89	74.09				
→4)**Gal**(1→	H	4.64	3.69	3.77	4.18		
4)Gal(1→	C	106.9	74.4				

Table B2 ***P-RGI-X*** R= rhamnogalacturonan, H= homogalacturonan, NR= non-reducing end, us= unsaturated GalA, RE= reducing end. Other conventions: Rha^{Gal}= rhamnose substituted with Gal single residue or chain, Rha^{-}= unsubstituted rhamnose, Gal (in bold) indicates the residues for which values are presented. n.d. = not detected

		1	2	3	4	5	6
$GalA^{R}$	H	5.05	3.92	4.11	4.444	4.63	-
	C	100.62	70.69	73.09	79.72	74.2	
$GalA^{R}$ (minor)	H	5.03	3.91	4.10	4.438	4.64	-
	C	100.26	70.69	73.09	79.72	74.12	
$GalA^{H}$	H	n.d.					
	C						
$GalA^{NR}$	H	5.11	3.76	3.93	4.31	4.72	
	C	101.83	71.04	72.29	73.4	75.02	
$GalA^{us}$_1	H	5.14	3.76	4.30	5.80	-	-
	C	101.91	72.88	68.63	109.3		
$GalA^{us}$_2	H	5.12	3.75	4.28	5.79	-	-
	C	101.91	72.88	68.63	109.3		
GalA(1→4)**αGalA^{RE}**	H	5.32	3.83	4.00	4.44	4.44	
	C	94.85	70.93	71.5	81.14	73.37	
$\alpha GalA^{RE}$	H	5.29	3.82	3.92	4.30	4.38	

	C	94.89	70.82	71.97	73.39	74.06	
Rha(1→	H	5.29	3.91	4.05	4.43	4.43	
4)**αGalA**$^{\mathbf{RE}}$	C	94.9	~70.7	~72.9	~79.7?	73.4?	
GalA(1→	H	4.61	3.50	3.75	4.38	4.06	
4)**βGalA**$^{\mathbf{RE}}$	C	98.81	74.37	75.12	80.16	77.06	
βGalA^{RE}	H	4.57	3.50	3.68	4.22	4.053	
	C	98.72	74.37	75.61	72.96	78.21	
Rha(1→	H	4.56	3.57	3.82	4.36	4.046	
4)**βGalA**$^{\mathbf{RE}}$	C	98.76	74.34	76.51	79.1	77.35	

Table B2 ***P-RGI-X (contd.)***

		1	2	3	4	5	6
Rha^{Gal}	H	5.27	4.123	4.10	3.66	3.86	1.31
	C	101.0	79.54	72.08	83.30	70.19	19.49
Rha^{-}	H	5.29	4.118	3.89	3.40	3.79	1.25
	C	101.0	78.97	72.15	74.80	71.58	19.25
Rha^{NRGal}	H	5.22	4.08	4.03	3.64	3.86	1.30
	C	102.94	73.11	72.58	83.58	69.81	19.25
Rha^{NR-}	H	5.23	4.06	3.80	3.37	3.77	1.24
	C	103.07	73.08	72.83	74.91	71.29	19.25
t-Gal(1→	H	4.62	3.53	3.67	3.93	3.69	
2)Rha	C	106.0	74.36	75.42	71.35	77.72	
→4)**Gal**(1→	H	4.65	3.605	3.78	4.16	3.72	
2)Rha	C	106.13	74.72	75.90	79.76	77.05	
t-Gal(1→	H	4.60	3.62	3.66	3.92		
4)Gal(1→	C	106.90	74.1	75.46	71.36		
→4)**Gal**(1→	H	4.64	3.68				
4)Gal(1→	C	106.90	74.36				

Table B3 *P-Gal.* Major peaks only – see Table B2 for minor peaks such as those from t-Gal

		1	2	3	4	5	6
→4)**Gal**(1→	H	4.62	3.69	3.77	4.16	3.70	3.81
4)Gal(1→	C	106.97	74.54	76.0	80.24	77.14	63.43

Table B4 *SB-Ara* Ara peaks only. Minor peaks detected include β-(1,4)-Gal, $GalA^{R}$, Rha^{Gal}, Rha^{-} as in Tables B1 and B2.

		1	2	3	4	5
t-Ara*f*-(1→3)	H	5.16	4.14	3.97	4.05	3.73, 3.84
	C	109.79	83.97	79.30	86.60	63.89
t-Araf-(1→2) (minor)	H	5.18	4.14	3.98	4.07	3.74, 3.83
	C	109.69	84.08	79.32	86.67	63.87
(1,3,5) -Ara*f*-(1→5)	H	5.12	4.29	4.10	4.30	3.85, 3.94
	C	110.18	81.92	85.04	84.17	69.26
(1,5) -Ara*f*-(1→5)	H	5.09	4.14	4.03	4.22	3.80, 3.89
	C	110.18	83.57	79.39	84.91	69.10
(1,2,3,5) -Ara*f*-(1→5) (minor)	H	5.25	4.31	4.24	4.31	n.d.
	C	109.07	87.73	83.12	83.62	n.d.

Abbreviations

L-AG	Arabinogalactan, Megazyme (larchwood)
AFM	Atomic force microscopy
AGI	Arabinogalactan type I
AGII	Arabinogalactan type II
Ara	Arabinan
BSA	Bovine albumin serum
CA	Heat and alkali treated citrus pectin
CDK	Cyclin-dependent kinase
CH	Heat treated citrus pectin
CKI	Casein kinase I
CO	Oxalic acid extracted citrus pectin
COPG	Oxalic acid extracted citrus pectin treated with polygalacturonase
COSY	Correlation spectroscopy
CP	Commercial citrus pectin
C-PGA	Polygalacturonic acid, Megazyme (citrus)
CRC	Colorectal cancer
CRD	Carbohydrate recognition domain
DAc	Degree of acetylation
DE	Degree of esterification
DP	Degree of polymerisation
ECM	Extracellular matrix
f	furanose
FAK	Focal adhesion kinase
FGF	Fibroblast growth factor
FSC	Forward Scatter
FTS	Farnesyl salicylic acid
Gal	Galactan

Gal1	Galectin-1
Gal3	Galectin-3
GalA	Galacturonic acid
GB	Galactobiose, Megazyme (potato)
GCS-100	Modified citrus pectin, La Jolla Paramaceuticals
GI	Gastrointestinal
Glu	Glucose
HG	Homogalacturonan
HM	High methyl-ester
HMBC	Heteronuclear multiple bond correlation for $^{1}H/^{13}C$ correlation via long
HSQC	Heteronuclear single quantum correlation for $^{1}H/^{13}C$ chemical shift co $^{1}J_{CH}$
ICAM	Intercellular adhesion molecule
IL	Interleukin
kDa	Kilodalton
LacNAc	N-acetyllactosamine
LM	Low methyl-ester
MAP	Modified apple pectin
MCP	Modified citrus pectin
MMP	Matrix-metalloprotein
MP	Modified pectin
MW	Molecular weight
NMR	Nuclear magnetic resonance
NO	Nitric oxide
NOESY/ ROESY	nuclear Overhauser effect spectroscopy and rotating frame Overhaus
p	pyranose
Pec-C	Pectasol-C, Econugenics (citrus)
PG	Polygalacturonase
P-Gal	Galactan, Megazyme (potato)
PMT	Photomultiplier tube

P-RGI	Rhamnogalacturonan I, Megazyme (potato)
P-RGI-X	Rhamnogalacturonan I , Megazyme (potato)
PSA	Prostate-specific antigen
RGI	Rhamnogalacturonan I
RGII	Rhamnogalacturonan II
Rha	Rhamnose
Rha Me	Rhamnose methyl
ROS	Reactive oxygen species
SBA	Heat and alkali treated sugar beet pectin
SB-Ara	Arabinan, Megazyme (sugar beet)
SBC	Commercial sugar beet pectin
SBH	Heat treated sugar beet pectin
SBO	Oxalic acid extracted sugar beet pectin
SBOPG	Oxalic acid extracted sugar beet pectin treated with polygalacturonas
siRNA	Short interfering RNA
SSBA	Soluble fraction of heat and alkali treated sugar beet pectin
SSBA-ara	α-arabinofuranosidase- and endo-arabinase-treated SSBA
SSBA-gal	β-galactosidase- and endo-galactanase-treated SSBA
SSBA-ne	Non enzyme digested control SSBA
SSC	Side scatter
ST	Staurosporine
t	Terminal
TCF/LEF	Group of transcription factors
TGFβ	Transforming growth factor-β
TNFα	Tumour necrosis factor alpha
TOCSY	Total correlation spectroscopy
TSP	Tumour supressor protein
VEGF	Vascular endothelial growth factor
Xyl	Xylose

References

1. Jemal, A., et al., *Global cancer statistics.* CA Cancer J Clin, 2011. **61**(2): p. 69-90.
2. Ferlay, J., D.M. Parkin, and E. Steliarova-Foucher, *Estimates of cancer incidence and mortality in Europe in 2008.* Eur J Cancer, 2010. **46**(4): p. 765-81.
3. English, D.R., et al., *Red meat, chicken, and fish consumption and risk of colorectal cancer.* Cancer Epidemiol Biomarkers Prev, 2004. **13**(9): p. 1509-14.
4. Cross, A.J., et al., *A large prospective study of meat consumption and colorectal cancer risk: an investigation of potential mechanisms underlying this association.* Cancer Res, 2010. **70**(6): p. 2406-14.
5. Cho, E., et al., *Alcohol consumption and the risk of colon cancer by family history of colorectal cancer.* Am J Clin Nutr, 2012. **95**(2): p. 413-9.
6. Phipps, A.I., et al., *Associations between cigarette smoking status and colon cancer prognosis among participants in North Central Cancer Treatment Group Phase III Trial N0147.* J Clin Oncol, 2013. **31**(16): p. 2016-23.
7. Boeing, H., *Obesity and cancer--the update 2013.* Best Pract Res Clin Endocrinol Metab, 2013. **27**(2): p. 219-27.
8. Key, T.J., *Fruit and vegetables and cancer risk.* Br J Cancer, 2011. **104**(1): p. 6-11.
9. Yokota, J. and T. Sugimura, *Multiple steps in carcinogenesis involving alterations of multiple tumor suppressor genes.* FASEB J, 1993. **7**(10): p. 920-5.
10. Leslie, A., et al., *The colorectal adenoma-carcinoma sequence.* Br J Surg, 2002. **89**(7): p. 845-60.
11. Bond, J.H., *Clinical evidence for the adenoma-carcinoma sequence, and the management of patients with colorectal adenomas.* Semin Gastrointest Dis, 2000. **11**(4): p. 176-84.
12. Cho, K.R. and B. Vogelstein, *Suppressor gene alterations in the colorectal adenoma-carcinoma sequence.* J Cell Biochem Suppl, 1992. **16G**: p. 137-41.
13. Powell, S.M., et al., *APC mutations occur early during colorectal tumorigenesis.* Nature, 1992. **359**(6392): p. 235-7.
14. Rodrigues, N.R., et al., *p53 mutations in colorectal cancer.* Proc Natl Acad Sci U S A, 1990. **87**(19): p. 7555-9.

15. Guanti, G., et al., *Involvement of PTEN mutations in the genetic pathways of colorectal cancerogenesis.* Hum Mol Genet, 2000. **9**(2): p. 283-7.
16. Roth, A.D., et al., *Prognostic role of KRAS and BRAF in stage II and III resected colon cancer: results of the translational study on the PETACC-3, EORTC 40993, SAKK 60-00 trial.* J Clin Oncol, 2010. **28**(3): p. 466-74.
17. Farina-Sarasqueta, A., et al., *The BRAF V600E mutation is an independent prognostic factor for survival in stage II and stage III colon cancer patients.* Ann Oncol, 2010. **21**(12): p. 2396-402.
18. Brink, M., et al., *K-ras oncogene mutations in sporadic colorectal cancer in The Netherlands Cohort Study.* Carcinogenesis, 2003. **24**(4): p. 703-10.
19. Grana, X. and E.P. Reddy, *Cell cycle control in mammalian cells: role of cyclins, cyclin dependent kinases (CDKs), growth suppressor genes and cyclin-dependent kinase inhibitors (CKIs).* Oncogene, 1995. **11**(2): p. 211-9.
20. Nilsson, I. and I. Hoffmann, *Cell cycle regulation by the Cdc25 phosphatase family.* Prog Cell Cycle Res, 2000. **4**: p. 107-14.
21. Hernandez, S., et al., *cdc25a and the splicing variant cdc25b2, but not cdc25B1, -B3 or -C, are over-expressed in aggressive human non-Hodgkin's lymphomas.* Int J Cancer, 2000. **89**(2): p. 148-52.
22. Dixon, D., T. Moyana, and M.J. King, *Elevated expression of the cdc25A protein phosphatase in colon cancer.* Exp Cell Res, 1998. **240**(2): p. 236-43.
23. Tetsu, O. and F. McCormick, *Beta-catenin regulates expression of cyclin D1 in colon carcinoma cells.* Nature, 1999. **398**(6726): p. 422-6.
24. Shtutman, M., et al., *The cyclin D1 gene is a target of the beta-catenin/LEF-1 pathway.* Proc Natl Acad Sci U S A, 1999. **96**(10): p. 5522-7.
25. Bouchard, C., et al., *Direct induction of cyclin D2 by Myc contributes to cell cycle progression and sequestration of p27.* EMBO J, 1999. **18**(19): p. 5321-33.
26. Toyoshima, H. and T. Hunter, *p27, a novel inhibitor of G1 cyclin-Cdk protein kinase activity, is related to p21.* Cell, 1994. **78**(1): p. 67-74.
27. Gartel, A.L. and S.K. Radhakrishnan, *Lost in transcription: p21 repression, mechanisms, and consequences.* Cancer Res, 2005. **65**(10): p. 3980-5.
28. Krimpenfort, P., et al., *p15Ink4b is a critical tumour suppressor in the absence of p16Ink4a.* Nature, 2007. **448**(7156): p. 943-6.
29. Hall, M., S. Bates, and G. Peters, *Evidence for different modes of action of cyclin-dependent kinase inhibitors: p15 and p16 bind to kinases, p21 and p27 bind to cyclins.* Oncogene, 1995. **11**(8): p. 1581-8.
30. Levine, A.J., J. Momand, and C.A. Finlay, *The p53 tumour suppressor gene.* Nature, 1991. **351**(6326): p. 453-6.

31. Michalak, E.M., et al., *In several cell types tumour suppressor p53 induces apoptosis largely via Puma but Noxa can contribute.* Cell Death Differ, 2008. **15**(6): p. 1019-29.
32. Iacopetta, B., *TP53 mutation in colorectal cancer.* Hum Mutat, 2003. **21**(3): p. 271-6.
33. Bienz, M. and H. Clevers, *Linking colorectal cancer to Wnt signaling.* Cell, 2000. **103**(2): p. 311-20.
34. Rubinfeld, B., et al., *Binding of GSK3beta to the APC-beta-catenin complex and regulation of complex assembly.* Science, 1996. **272**(5264): p. 1023-6.
35. Xing, Y., et al., *Crystal structure of a beta-catenin/APC complex reveals a critical role for APC phosphorylation in APC function.* Mol Cell, 2004. **15**(4): p. 523-33.
36. Polakis, P., *Wnt signaling and cancer.* Genes Dev, 2000. **14**(15): p. 1837-51.
37. Yang, J., et al., *Adenomatous polyposis coli (APC) differentially regulates beta-catenin phosphorylation and ubiquitination in colon cancer cells.* J Biol Chem, 2006. **281**(26): p. 17751-7.
38. Boriack-Sjodin, P.A., et al., *The structural basis of the activation of Ras by Sos.* Nature, 1998. **394**(6691): p. 337-43.
39. Berrozpe, G., et al., *Comparative analysis of mutations in the p53 and K-ras genes in pancreatic cancer.* Int J Cancer, 1994. **58**(2): p. 185-91.
40. Hancock, J.F., et al., *A CAAX or a CAAL motif and a second signal are sufficient for plasma membrane targeting of ras proteins.* EMBO J, 1991. **10**(13): p. 4033-9.
41. Elad, G., et al., *Targeting of K-Ras 4B by S-trans,trans-farnesyl thiosalicylic acid.* Biochim Biophys Acta, 1999. **1452**(3): p. 228-42.
42. Bivona, T.G. and M.R. Philips, *Ras pathway signaling on endomembranes.* Curr Opin Cell Biol, 2003. **15**(2): p. 136-42.
43. Kolch, W., *Meaningful relationships: the regulation of the Ras/Raf/MEK/ERK pathway by protein interactions.* Biochem J, 2000. **351 Pt 2**: p. 289-305.
44. Safaee Ardekani, G., et al., *The prognostic value of BRAF mutation in colorectal cancer and melanoma: a systematic review and meta-analysis.* PLoS One, 2012. **7**(10): p. e47054.
45. Castellano, E. and J. Downward, *RAS Interaction with PI3K: More Than Just Another Effector Pathway.* Genes Cancer, 2011. **2**(3): p. 261-74.
46. Dolcet, X., et al., *NF-kB in development and progression of human cancer.* Virchows Arch, 2005. **446**(5): p. 475-82.
47. La Rosa, F.A., J.W. Pierce, and G.E. Sonenshein, *Differential regulation of the c-myc oncogene promoter by the NF-kappa B rel family of transcription factors.* Mol Cell Biol, 1994. **14**(2): p. 1039-44.

48. Wu, H. and G. Lozano, *NF-kappa B activation of p53. A potential mechanism for suppressing cell growth in response to stress.* J Biol Chem, 1994. **269**(31): p. 20067-74.
49. Lim, J.W., H. Kim, and K.H. Kim, *Nuclear factor-kappaB regulates cyclooxygenase-2 expression and cell proliferation in human gastric cancer cells.* Lab Invest, 2001. **81**(3): p. 349-60.
50. Schottelius, A.J. and A.S. Baldwin, Jr., *A role for transcription factor NF-kappa B in intestinal inflammation.* Int J Colorectal Dis, 1999. **14**(1): p. 18-28.
51. Van Antwerp, D.J., et al., *Inhibition of TNF-induced apoptosis by NF-kappa B.* Trends Cell Biol, 1998. **8**(3): p. 107-11.
52. Collins, T., et al., *Transcriptional regulation of endothelial cell adhesion molecules: NF-kappa B and cytokine-inducible enhancers.* FASEB J, 1995. **9**(10): p. 899-909.
53. Roy, S. and D.W. Nicholson, *Cross-talk in cell death signaling.* J Exp Med, 2000. **192**(8): p. F21-5.
54. Chiou, S.K., L. Rao, and E. White, *Bcl-2 blocks p53-dependent apoptosis.* Mol Cell Biol, 1994. **14**(4): p. 2556-63.
55. Sinicrope, F.A., et al., *Prognostic value of bcl-2 oncoprotein expression in stage II colon carcinoma.* Clin Cancer Res, 1995. **1**(10): p. 1103-10.
56. Bronner, M.P., et al., *The bcl-2 proto-oncogene and the gastrointestinal epithelial tumor progression model.* Am J Pathol, 1995. **146**(1): p. 20-6.
57. Berg, M., et al., *DNA sequence profiles of the colorectal cancer critical gene set KRAS-BRAF-PIK3CA-PTEN-TP53 related to age at disease onset.* PLoS One, 2010. **5**(11): p. e13978.
58. Datta, S.R., et al., *Akt phosphorylation of BAD couples survival signals to the cell-intrinsic death machinery.* Cell, 1997. **91**(2): p. 231-41.
59. Xu, J., et al., *Activation of the Akt survival pathway contributes to TRAIL resistance in cancer cells.* PLoS One, 2010. **5**(4): p. e10226.
60. Fang, D., et al., *Phosphorylation of beta-catenin by AKT promotes beta-catenin transcriptional activity.* J Biol Chem, 2007. **282**(15): p. 11221-9.
61. Georgescu, M.M., *PTEN Tumor Suppressor Network in PI3K-Akt Pathway Control.* Genes Cancer, 2010. **1**(12): p. 1170-7.
62. Dai, J.L., et al., *Transforming growth factor-beta responsiveness in DPC4/SMAD4-null cancer cells.* Mol Carcinog, 1999. **26**(1): p. 37-43.
63. Koyama, M., et al., *Inactivation of both alleles of the DPC4/SMAD4 gene in advanced colorectal cancers: identification of seven novel somatic mutations in tumors from Japanese patients.* Mutat Res, 1999. **406**(2-4): p. 71-7.
64. Miyaki, M., et al., *Higher frequency of Smad4 gene mutation in human colorectal cancer with distant metastasis.* Oncogene, 1999. **18**(20): p. 3098-103.

65. Fuchs, S.Y., et al., *MEKK1/JNK signaling stabilizes and activates p53.* Proc Natl Acad Sci U S A, 1998. **95**(18): p. 10541-6.
66. Collett, G.P. and F.C. Campbell, *Curcumin induces c-jun N-terminal kinase-dependent apoptosis in HCT116 human colon cancer cells.* Carcinogenesis, 2004. **25**(11): p. 2183-9.
67. Nateri, A.S., B. Spencer-Dene, and A. Behrens, *Interaction of phosphorylated c-Jun with TCF4 regulates intestinal cancer development.* Nature, 2005. **437**(7056): p. 281-5.
68. Zarubin, T. and J. Han, *Activation and signaling of the p38 MAP kinase pathway.* Cell Res, 2005. **15**(1): p. 11-8.
69. Frisch, S.M. and H. Francis, *Disruption of epithelial cell-matrix interactions induces apoptosis.* J Cell Biol, 1994. **124**(4): p. 619-26.
70. Gabarra-Niecko, V., M.D. Schaller, and J.M. Dunty, *FAK regulates biological processes important for the pathogenesis of cancer.* Cancer Metastasis Rev, 2003. **22**(4): p. 359-74.
71. Santini, M.T., G. Rainaldi, and P.L. Indovina, *Apoptosis, cell adhesion and the extracellular matrix in the three-dimensional growth of multicellular tumor spheroids.* Crit Rev Oncol Hematol, 2000. **36**(2-3): p. 75-87.
72. King, W.G., et al., *Phosphatidylinositol 3-kinase is required for integrin-stimulated AKT and Raf-1/mitogen-activated protein kinase pathway activation.* Mol Cell Biol, 1997. **17**(8): p. 4406-18.
73. Golubovskaya, V.M., et al., *Simultaneous inhibition of focal adhesion kinase and SRC enhances detachment and apoptosis in colon cancer cell lines.* Mol Cancer Res, 2003. **1**(10): p. 755-64.
74. Zeilstra, J., et al., *CD44 expression in intestinal epithelium and colorectal cancer is independent of p53 status.* PLoS One, 2013. **8**(8): p. e72849.
75. Zeilstra, J., et al., *Deletion of the WNT target and cancer stem cell marker CD44 in Apc(Min/+) mice attenuates intestinal tumorigenesis.* Cancer Res, 2008. **68**(10): p. 3655-61.
76. Kim, H., et al., *CD44 expression in colorectal adenomas is an early event occurring prior to K-ras and p53 gene mutation.* Arch Biochem Biophys, 1994. **310**(2): p. 504-7.
77. Fujisaki, T., et al., *CD44 stimulation induces integrin-mediated adhesion of colon cancer cell lines to endothelial cells by up-regulation of integrins and c-Met and activation of integrins.* Cancer Res, 1999. **59**(17): p. 4427-34.
78. Gooding, J.M., K.L. Yap, and M. Ikura, *The cadherin-catenin complex as a focal point of cell adhesion and signalling: new insights from three-dimensional structures.* Bioessays, 2004. **26**(5): p. 497-511.
79. Tsanou, E., et al., *The E-cadherin adhesion molecule and colorectal cancer. A global literature approach.* Anticancer Res, 2008. **28**(6A): p. 3815-26.

80. Yang, S.Z., et al., *Decreased E-cadherin augments beta-catenin nuclear localization: studies in breast cancer cell lines.* Int J Oncol, 2001. **18**(3): p. 541-8.
81. Huber, A.H. and W.I. Weis, *The structure of the beta-catenin/E-cadherin complex and the molecular basis of diverse ligand recognition by beta-catenin.* Cell, 2001. **105**(3): p. 391-402.
82. Rainaldi, G., et al., *Differential expression of adhesion molecules (CD44, ICAM-1 and LFA-3) in cancer cells grown in monolayer or as multicellular spheroids.* Anticancer Res, 1999. **19**(3A): p. 1769-78.
83. Gallicchio, M., et al., *Celecoxib decreases expression of the adhesion molecules ICAM-1 and VCAM-1 in a colon cancer cell line (HT29).* Br J Pharmacol, 2008. **153**(5): p. 870-8.
84. Kaiserlian, D., et al., *Expression, function and regulation of the intercellular adhesion molecule-1 (ICAM-1) on human intestinal epithelial cell lines.* Eur J Immunol, 1991. **21**(10): p. 2415-21.
85. Dippold, W., et al., *Expression of intercellular adhesion molecule 1 (ICAM-1, CD54) in colonic epithelial cells.* Gut, 1993. **34**(11): p. 1593-7.
86. Das, K.M., L. Squillante, and F.M. Robertson, *Amplified expression of intercellular adhesion molecule-1 (ICAM-1) and M(r) 40K protein by DLD-1 colon tumor cells by interferon-gamma.* Cell Immunol, 1993. **147**(1): p. 215-21.
87. Maurer, C.A., et al., *Over-expression of ICAM-1, VCAM-1 and ELAM-1 might influence tumor progression in colorectal cancer.* Int J Cancer, 1998. **79**(1): p. 76-81.
88. Ottaiano, A., et al., *Overexpression of both CXC chemokine receptor 4 and vascular endothelial growth factor proteins predicts early distant relapse in stage II-III colorectal cancer patients.* Clin Cancer Res, 2006. **12**(9): p. 2795-803.
89. Dexter, D.L., et al., *Heterogeneity of cancer cells from a single human colon carcinoma.* Am J Med, 1981. **71**(6): p. 949-56.
90. Chen, T.R., et al., *DLD-1 and HCT-15 cell lines derived separately from colorectal carcinomas have totally different chromosome changes but the same genetic origin.* Cancer Genet Cytogenet, 1995. **81**(2): p. 103-8.
91. Benlloch, S., et al., *Detection of BRAF V600E mutation in colorectal cancer: comparison of automatic sequencing and real-time chemistry methodology.* J Mol Diagn, 2006. **8**(5): p. 540-3.
92. Brattain, M.G., et al., *Heterogeneity of malignant cells from a human colonic carcinoma.* Cancer Res, 1981. **41**(5): p. 1751-6.
93. Caro, I., et al., *Characterisation of a newly isolated Caco-2 clone (TC-7), as a model of transport processes and biotransformation of drugs.* International Journal of Pharmaceutics, 1995. **116**(2): p. 147-158.
94. Drewinko, B., et al., *Establishment of a human carcinoembryonic antigen-producing colon adenocarcinoma cell line.* Cancer Res, 1976. **36**(2 Pt 1): p. 467-75.

95. Ahmed, D., et al., *Epigenetic and genetic features of 24 colon cancer cell lines.* Oncogenesis, 2013. **2**: p. e71.
96. Chan, D.S., et al., *Red and processed meat and colorectal cancer incidence: meta-analysis of prospective studies.* PLoS One, 2011. **6**(6): p. e20456.
97. Bradbury, K.E., P.N. Appleby, and T.J. Key, *Fruit, vegetable, and fiber intake in relation to cancer risk: findings from the European Prospective Investigation into Cancer and Nutrition (EPIC).* Am J Clin Nutr, 2014. **100**(Supplement 1): p. 394S-398S.
98. Aune, D., et al., *Dietary fibre, whole grains, and risk of colorectal cancer: systematic review and dose-response meta-analysis of prospective studies.* BMJ, 2011. **343**: p. d6617.
99. Theuwissen, E. and R.P. Mensink, *Water-soluble dietary fibers and cardiovascular disease.* Physiol Behav, 2008. **94**(2): p. 285-92.
100. Jenkins, D.J., et al., *Dietary fiber and diabetic therapy: a progressive effect with time.* Adv Exp Med Biol, 1979. **119**: p. 275-9.
101. Bingham, S.A., et al., *Dietary fibre in food and protection against colorectal cancer in the European Prospective Investigation into Cancer and Nutrition (EPIC): an observational study.* Lancet, 2003. **361**(9368): p. 1496-501.
102. Burkitt, D.P., *Epidemiology of cancer of the colon and rectum.* Cancer, 1971. **28**(1): p. 3-13.
103. Dahm, C.C., et al., *Dietary fiber and colorectal cancer risk: a nested case-control study using food diaries.* J Natl Cancer Inst, 2010. **102**(9): p. 614-26.
104. Murphy, N., et al., *Dietary fibre intake and risks of cancers of the colon and rectum in the European prospective investigation into cancer and nutrition (EPIC).* PLoS One, 2012. **7**(6): p. e39361.
105. Phillips, G.O. and S.W. Cui, *An introduction: Evolution and finalisation of the regulatory definition of dietary fibre.* Food Hydrocolloids, 2011. **25**(2): p. 139-143.
106. Burkitt, D.P., A.R. Walker, and N.S. Painter, *Effect of dietary fibre on stools and the transit-times, and its role in the causation of disease.* Lancet, 1972. **2**(7792): p. 1408-12.
107. Smith-Barbaro, P., D. Hansen, and B. Reddy, *Carcinogen binding to various types of dietary fiber.* J. Natl. Cancer Inst., 1981. **67**: p. 495–497.
108. Wong, J.M., et al., *Colonic health: fermentation and short chain fatty acids.* J Clin Gastroenterol, 2006. **40**(3): p. 235-43.
109. Brouns, F., et al., *Cholesterol-lowering properties of different pectin types in mildly hyper-cholesterolemic men and women.* Eur J Clin Nutr, 2012. **66**(5): p. 591-9.
110. Hotchkiss, A.T., et al., *Pectic oligosaccharides as prebiotics* in *Oligosaccharides in food and agriculture. ACS symposium series, 849. American Chemical Society, Washington,* , G.a.C. Eggleston, G.L., Editor. 2003.

111. Manderson, K., et al., *In vitro determination of prebiotic properties of oligosaccharides derived from an orange juice manufacturing by-product stream.* Appl Environ Microbiol, 2005. **71**(12): p. 8383-9.
112. Mandalari, G., et al., *In vitro evaluation of the prebiotic activity of a pectic oligosaccharide-rich extract enzymatically derived from bergamot peel.* Appl Microbiol Biotechnol, 2007. **73**(5): p. 1173-9.
113. Baker, R.A., *Reassessment of some fruit and vegetable pectin levels.* Journal of Food Science, 1997. **62**(2): p. 225-229.
114. Nelson, D.B., C.J.B. Smit, and R.R. Wiles, *Commercially important small pectic substances.* Food Colloids, 1977.
115. Money, R.W. and W.A. Christian, *Analytical Data of Some Common Fruits.* Journal of the Science of Food and Agriculture, 1950. **1**(1): p. 8-12.
116. Gautam, D.R., T.R. Sharma, and J.S. Chauhan, *Suitability of some low and high-chilling apple cultivars for juice processing and pectin extraction*, in *Advances in Research on Temperate Fruits*, T.R.Chadha, V.P.Bhutani, and J.L.Kaul, Editors. 1986. p. 339–343.
117. Wade, N.L., et al., *Relationship between Softening and the Polyuronides in Ripening Banana Fruit.* Journal of the Science of Food and Agriculture, 1992. **60**(1): p. 61-68.
118. Kawabata, A. and S. Sawayama, *A study on the contents of pectic substances in fruits, vegetable fruits and nuts.* Japan. J. Nutr, 1974. **32**: p. 9-18.
119. Silacci, M.W. and J.C. Morrison, *Changes in Pectin Content of Cabernet-Sauvignon Grape Berries during Maturation.* American Journal of Enology and Viticulture, 1990. **41**(2): p. 111-115.
120. Atkins, C.D. and A.H. Rouse, *Effect of arsenic spray on the quality of processed grapefruit sections- with special reference to pectin.* Proc. Fla. State Hort. Soc, 1958. **71**: p. 220-223.
121. Braddock, R.J. and T.R. Graumlich, *Composition of Fiber from Citrus Peel, Membranes, Juice Vesicles and Seeds.* Lebensmittel-Wissenschaft & Technologie, 1981. **14**(5): p. 229-231.
122. Thomas, A., et al., *Pectins in the fruits of Japanese quince (Chaenomeles japonica).* Carbohydrate Polymers, 2003. **53**(4): p. 361-372.
123. Kertesz, Z.I., *The Pectic Substances*. 1951, New York, NY: Interscience Publishers, Inc.
124. Vollendorf, N.W. and J.A. Marlett, *Comparison of two methods of fiber analysis of 58 foods.* J. Food Comp. Anal., 1993. **6**(203-214).
125. Greve, L.C., et al., *Impact of Heating on Carrot Firmness - Changes in Cell-Wall Components.* Journal of Agricultural and Food Chemistry, 1994. **42**(12): p. 2900-2906.
126. Ross, J.K., C. English, and C.A. Perlmutter, *Dietary Fiber Constituents of Selected Fruits and Vegetables.* Journal of the American Dietetic Association, 1985. **85**(9): p. 1111-1116.

127. Ridley, B.L., M.A. O'Neill, and D. Mohnen, *Pectins: structure, biosynthesis, and oligogalacturonide-related signaling.* Phytochemistry, 2001. **57**(6): p. 929-67.
128. Fischer, R.L. and A.B. Bennett, *Role of Cell Wall Hydrolases in Fruit Ripening.* Annual Review of Plant Physiology and Plant Molecular Biology, 1991. **42**: p. 675-703.
129. Mort, A.J., F. Qiu, and N.O. Maness, *Determination of the pattern of methyl esterification in pectin. Distribution of contiguous nonesterified residues.* Carbohydr Res, 1993. **247**: p. 21-35.
130. Ralet, M.C., et al., *Mapping sugar beet pectin acetylation pattern.* Phytochemistry, 2005. **66**(15): p. 1832-43.
131. Talmadge, K.W., et al., *The Structure of Plant Cell Walls: I. The Macromolecular Components of the Walls of Suspension-cultured Sycamore Cells with a Detailed Analysis of the Pectic Polysaccharides.* Plant Physiol, 1973. **51**(1): p. 158-73.
132. McNeil, M., A.G. Darvill, and P. Albersheim, *Structure of plant cell walls X. Rhamnogalacturonan I, a structurally complex pectic polysaccharide in the walls of suspension-cultured sycamore cells.* American Society of Plant Biologists, 1980. **66**(6): p. 1128-1134
133. Colquhoun, I.J., et al., *Identification by nmr spectroscopy of oligosaccharides obtained by treatment of the hairy regions of apple pectin with rhamnogalacturonase.* Carbohydrate Research, 1990. **206**(1): p. 131–144.
134. Yapo, B.M., *Rhamnogalacturonan-I: a structurally puzzling and functionally versatile polysaccharide from plant cell walls and mucilages.* Polymer Reviews 2011. **51**(4).
135. Schols, H.A., et al., *A xylogalacturonan subunit present in the modified hairy regions of apple pectin.* Carbohydrate Research, 1995. **279**.
136. Morris, V.J., et al., *The bioactivity of modified pectin fragments.* Bioactive Carbohydrates and Dietary Fibre, 2013. **1**(1): p. 21-37.
137. Round, A.N., et al., *A new view of pectin structure revealed by acid hydrolysis and atomic force microscopy.* Carbohydr Res, 2010. **345**(4): p. 487-97.
138. Rolin, C., *Commercial Pectin Preparations*, in *Pectins and Their Manipulation*, G.B. Seymour and J.P. Knox, Editors. 2002. p. 222-239.
139. Hoagland, P.D., et al., *HPSEC with component analysis of citrus and apple pectins after hollow fiber ultrafiltration.* Journal of Food Science, 1997. **62**(1).
140. Corredig, M., W. Kerr, and L. Wicker, *Molecular characterization of commercial pectins by separation with linear mix gel permeation columns in-line with multi-angle light scattering detection.* Food Hydrocolloids, 2000. **14**(1).
141. Oosterveld, A., et al., *Characterization of arabinose and ferulic acid rich pectic polysaccharides and hemicelluloses from sugar beet pulp.* Carbohydr Res, 2000. **328**(2): p. 185-97.

142. Rombouts, F.M. and J.F. Thibault, *Feruloylated pectic substances from sugar-beet pulp.* Carbohydrate Research, 1986. **154**(1).
143. Sakamoto, T. and T. Sakai, *Analysis of structure of sugar-beet pectin by enzymatic methods.* Phytochemistry, 1995. **39**(4): p. 821-3.
144. Renard, C.M.G.C. and J.F. Thibault, *Structure and properties of apple and sugar-beet pectins extracted by chelating agents.* Carbohydrate Research, 1993. **244**(1).
145. Yapo, B.M., et al., *Effect of extraction conditions on the yield, purity and surface properties of sugar beet pulp pectin extracts.* Food Chemistry, 2007. **100**(4).
146. Kirby, A.R., A.J. MacDougall, and V.J. Morris, *Atomic force microscopy of tomato and sugar beet pectin molecules.* Carbohydrate Polymers, 2008. **71**(4).
147. Fishman, M.L., et al., *Physico-chemical characterization of alkaline soluble polysaccharides from sugar beet pulp* Food Hydrocolloids, 2009. **23**(6).
148. Levigne, S., M.C. Ralet, and J.F. Thibault, *Characterisation of pectins extracted from fresh sugar beet under different conditions using an experimental design.* Carbohydr Polymers, 2002. **49**(2).
149. Dea, I.C.M. and J.K. Madden, *Acetylated pectic polysaccharides of sugar beet.* Food Hydrocolloids, 1986. **1**(1).
150. Mayer, F. and J.O. Hillebrandt, *Potato pulp: microbiological characterization, physical modification, and application of this agricultural waste product.* Appl Microbiol Biotechnol, 1997. **48**(4): p. 435-40.
151. Obro, J., et al., *Rhamnogalacturonan I in Solanum tuberosum tubers contains complex arabinogalactan structures.* Phytochemistry, 2004. **65**(10).
152. Iglesias, M.T. and J.E. Lozano, *Extraction and characterization of sunflower pectin.* Journal of Food Engineering, 2004. **62**(3).
153. Cardoso, S.M., M.A. Coimbra, and J.A. Lopes da Silva, *Calcium-mediated gelation of an olive pomace pectic extract.* Carbohydr Polym, 2003. **52**(2).
154. Faravash, R.S. and F.Z. Ashtiani, *The effect of pH, ethanol volume and acid washing time on the yield of pectin extraction from peach pomace.* Int. Journal of Food Science and Technology, 2007. **42**(10).
155. Yamada, H., *Bioactive plant polysaccharides from Japanese and Chinese traditional herbal medicines.* Bioactive Carbohydrate Polymers, 2000. **44**.
156. Inngjerdingen, K.T., et al., *Bioactive pectic polysaccharides from Glinus oppositifolius (L.) Aug. DC., a Malian medicinal plant, isolation and partial characterization.* J Ethnopharmacol, 2005. **101**(1-3): p. 204-14.
157. Paulsen, B.S. and H. Barsett, *Bioactive pectic polysaccharides.* Advances in Polymer Science, 2005. **186**: p. 69-101.

158. Ramberg, J.E., E.D. Nelson, and R.A. Sinnott, *Immunomodulatory dietary polysaccharides: a systematic review of the literature.* Nutr J, 2010. **9**: p. 54.
159. Popov, S.V., et al., *Pectic polysaccharides of the fresh plum Prunus domestica L. isolated with a simulated gastric fluid and their anti-inflammatory and antioxidant activities.* Food Chem, 2014. **143**: p. 106-13.
160. Fishman, M.L., et al., *Characterization of pectin, flash-extracted from orange albedo by microwave heating, under pressure.* Carbohydr Res, 2000. **323**(1-4): p. 126-38.
161. Fishman, M.L., et al., *Global structure of microwave-assisted flash-extracted sugar beet pectin.* J Agric Food Chem, 2008. **56**(4): p. 1471-8.
162. Diaz, J.V., G.E. Anthon, and D.M. Barrett, *Nonenzymatic degradation of citrus pectin and pectate during prolonged heating: effects of pH, temperature, and degree of methyl esterification.* J Agric Food Chem, 2007. **55**(13): p. 5131-6.
163. Thibault, J.F., et al., *Studies of the length of homogalacturonic regions in pectins by acid hydrolysis.* Carbohydrate Research, 1993. **238**.
164. Renard, C.M.G.C. and J.F. Thibault, *Degradation of pectins in alkaline conditions: kinetics of demethylation.* Carbohydrate Research, 1996. **286**.
165. Kiss, J., *β-Eliminative degradation of carbohydrates containing uronic acid residues.* Advances in Carbohydrate Chemsitry and Biochemistry, 1974. **29**.
166. Axelos, M.A.V. and M. Branger, *The effect of the degree of esterification on the thermal stability and chain conformation of pectins.* Food Hydrocolloids, 1993. **7**(2).
167. Hotchkiss, A.T., et al., *Enzymatic modification of pectin to increase its calcium sensitivity while preserving its molecular weight.* J. Agric. Food Chem, 2002. **50**.
168. Buchholt, H.C., et al., *Preparation and properties of enzymatically and chemically modified sugar beet pectins.* Carbohydr Polym, 2004. **58**(2).
169. Sengkhamparn, N., et al., *Characterisation of cell wall polysaccharides from okra (Abelmoschus esculentus (L.) Moench).* Carbohydr Res, 2009. **344**(14): p. 1824-32.
170. Nagel, M.D., et al., *Enzymatically-tailored pectins differentially influence the morphology, adhesion, cell cycle progression and survival of fibroblasts.* Biochim Biophys Acta, 2008. **1780**(7-8): p. 995-1003.
171. Yu, L., et al., *Rhamnogalacturonan I domains from ginseng pectin.* Carbohydrate Polymers, 2010. **79**(4): p. 811-817.
172. Mao, F., et al., *Anticancer effect of Lycium barbarum polysaccharides on colon cancer cells involves G0/G1 phase arrest.* Medical Oncology, 2011. **28**(1): p. 121-126.

173. Zong, A.Z., H.Z. Cao, and F.S. Wang, *Anticancer polysaccharides from natural resources: A review of recent research.* Carbohydrate Polymers, 2012. **90**(4): p. 1395-1410.
174. Joseph, M.M., et al., *A galactomannan polysaccharide from Punica granatum imparts in vitro and in vivo anticancer activity.* Carbohydrate Polymers, 2013. **98**(2): p. 1466-1475.
175. Ohkami, H., et al., *Effects of apple pectin on fecal bacterial enzymes in azoxymethane-induced rat colon carcinogenesis.* Japanese Journal of Cancer Research, 1995. **86**(6): p. 523-9.
176. Tazawa, K., et al., *Anticarcinogenic action of apple pectin on fecal enzyme activities and mucosal or portal prostaglandin E2 levels in experimental rat colon carcinogenesis.* J Exp Clin Cancer Res, 1997. **16**(1): p. 33-8.
177. Holck, J., et al., *Feruloylated and nonferuloylated arabino-oligosaccharides from sugar beet pectin selectively stimulate the growth of Bifidobacterium spp. in human fecal in vitro fermentations.* J Agric Food Chem, 2011. **59**(12): p. 6511-9.
178. Gullon, P., M.J. Gonzalez-Munoz, and J.C. Parajo, *Manufacture and prebiotic potential of oligosaccharides derived from industrial solid wastes.* Bioresour Technol, 2011. **102**(10): p. 6112-9.
179. Chen, J., et al., *Pectic-oligosaccharides prepared by dynamic high-pressure microfluidization and their in vitro fermentation properties.* Carbohydr Polym, 2013. **91**(1): p. 175-82.
180. Emenaker, N.J., et al., *Short-chain fatty acids inhibit invasive human colon cancer by modulating uPA, TIMP-1, TIMP-2, mutant p53, Bcl-2, Bax, p21 and PCNA protein expression in an in vitro cell culture model.* Journal of Nutrition, 2001. **131**(11): p. 3041s-3046s.
181. Avivi-Green, C., Z. Madar, and B. Schwartz, *Pectin-enriched diet affects distribution and expression of apoptosis-cascade proteins in colonic crypts of dimethylhydrazine-treated rats.* International Journal of Molecular Medicine, 2000. **6**(6): p. 689-98.
182. Sanders, L.M., et al., *An increase in reactive oxygen species by dietary fish oil coupled with the attenuation of antioxidant defenses by dietary pectin enhances rat colonocyte apoptosis.* Journal of Nutrition, 2004. **134**(12): p. 3233-3238.
183. Salman, H., et al., *Citrus pectin affects cytokine production by human peripheral blood mononuclear cells.* Biomedicine & Pharmacotherapy, 2008. **62**(9): p. 579-582.
184. Lim, B.O., et al., *Effect of dietary pectin on the production of immunoglobulins and cytokines by mesenteric lymph node lymphocytes in mouse colitis induced with dextran sulfate sodium.* Biosci Biotechnol Biochem, 2003. **67**(8): p. 1706-12.
185. Zhang, X., et al., *Further analysis of the structure and immunological activity of an RG-I type pectin from Panax ginseng.* Carbohydrate Polymers, 2012. **89**(2): p. 519-525.

186. Peng, Q., et al., *Characterization of an immunologically active pectin from the fruits of Lycium ruthenicum.* International Journal of Biological Macromolecules, 2014. **64**: p. 69-75.
187. Duan, J., et al., *Characterization of a pectic polysaccharide from the leaves of Diospyros kaki and its modulating activity on lymphocyte proliferation.* Biopolymers, 2010. **93**(7): p. 649-56.
188. Yamada, H., M. Hirano, and H. Kiyohara, *Partial structure of an anti-ulcer pectic polysaccharide from the roots of Bupleurum falcatum L.* Carbohydr Res, 1991. **219**: p. 173-92.
189. Inngjerdingen, K.T., et al., *Pectic polysaccharides isolated from Malian medicinal plants protect against Streptococcus pneumoniae in a mouse pneumococcal infection model.* Scand J Immunol, 2013. **77**(5): p. 372-88.
190. Gronhaug, T.E., et al., *Bioactive arabinogalactans from the leaves of Opilia celtidifolia Endl. ex Walp. (Opiliaceae).* Glycobiology, 2010. **20**(12): p. 1654-64.
191. Platt, D. and A. Raz, *Modulation of the Lung Colonization of B16-F1 Melanoma-Cells by Citrus Pectin.* Journal of the National Cancer Institute, 1992. **84**(6): p. 438-442.
192. Uhlenbruck, G., et al., *Prevention of experimental liver metastases by arabinogalactan.* Naturwissenschaften, 1986. **73**(10): p. 626-7.
193. Pienta, K.J., et al., *Inhibition of Spontaneous Metastasis in a Rat Prostate-Cancer Model by Oral-Administration of Modified Citrus Pectin.* Journal of the National Cancer Institute, 1995. **87**(5): p. 348-353.
194. Liu, H.Y., et al., *Inhibitory effect of modified citrus pectin on liver metastases in a mouse colon cancer model.* World Journal of Gastroenterology, 2008. **14**(48): p. 7386-7391.
195. Nangia-Makker, P., et al., *Inhibition of human cancer cell growth and metastasis in nude mice by oral intake of modified citrus pectin.* Journal of the National Cancer Institute, 2002. **94**(24): p. 1854-1862.
196. Chauhan, D., et al., *A novel carbohydrate-based therapeutic GCS-100 overcomes bortezomib resistance and enhances dexamethasone-induced apoptosis in multiple myeloma cells.* Cancer Research, 2005. **65**(18): p. 8350-8358.
197. Streetly, M.J., et al., *GCS-100, a novel galectin-3 antagonist, modulates MCL-1, NOXA, and cell cycle to induce myeloma cell death.* Blood, 2010. **115**(19): p. 3939-3948.
198. Wang, Y., et al., *Calpain activation through galectin-3 inhibition sensitizes prostate cancer cells to cisplatin treatment.* Cell Death and Dis, 2010. **1**: p. e101.
199. Cotter, F., et al., *Single-agent activity of GCS-100, a first-in-class galectin-3 antagonist, in elderly patients with relapsed chronic lymphocytic leukemia. **Phase II study**.* Journal of Clinical Oncology, 2009. **27**(15): p. -.

200. Eliaz, I., et al., *The effect of modified citrus pectin on urinary excretion of toxic elements.* Phytotherapy Research, 2006. **20**(10): p. 859-64.
201. Yan, J. and A. Katz, *PectaSol-C Modified Citrus Pectin Induces Apoptosis and Inhibition of Proliferation in Human and Mouse Androgen-Dependent and -Independent Prostate Cancer Cells.* Integrative Cancer Therapies, 2010. **9**(2): p. 197-203.
202. Tehranian, N., et al., *Combination effect of PectaSol and Doxorubicin on viability, cell cycle arrest and apoptosis in DU-145 and LNCaP prostate cancer cell lines.* Cell Biology International, 2012. **36**(7): p. 601-610.
203. Jiang, J., I. Eliaz, and D. Sliva, *Synergistic and additive effects of modified citrus pectin with two polybotanical compounds, in the suppression of invasive behavior of human breast and prostate cancer cells.* Integr Cancer Ther, 2013. **12**(2): p. 145-52.
204. Hossein, G., et al., *Synergistic Effects of PectaSol-C Modified Citrus Pectin an Inhibitor of Galectin-3 and Paclitaxel on Apoptosis of Human SKOV-3 Ovarian Cancer Cells.* Asian Pac J Cancer Prev, 2013. **14**(12): p. 7561-8.
205. Ramachandran, C., et al., *Activation of Human T-Helper/Inducer Cell, T-Cytotoxic Cell, B-Cell, and Natural Killer (NK)-Cells and induction of Natural Killer Cell Activity against K562 Chronic Myeloid Leukemia Cells with Modified Citrus Pectin.* BMC complementary and alternative medicine, 2011. **11**: p. 59.
206. Kolatsi-Joannou, M., et al., *Modified citrus pectin reduces galectin-3 expression and disease severity in experimental acute kidney injury.* PLoS One, 2011. **6**(4): p. e18683.
207. Guess, B.W., et al., *Modified citrus pectin (MCP) increases the prostate-specific antigen doubling time in men with prostate cancer: a phase II pilot study.* Prostate Cancer and Prostatic Diseases, 2003. **6**(4): p. 301-304.
208. Azémar, M., et al., *Clinical Benefit in Patients with Advanced Solid Tumors Treated with Modified Citrus Pectin: A Prospective Pilot Study.* Clinical Medicine Insights: Oncology, 2007. **2007**.
209. Li, Y., et al., *Modified apple polysaccharide prevents against tumorigenesis in a mouse model of colitis-associated colon cancer: role of galectin-3 and apoptosis in cancer prevention.* European journal of nutrition, 2011.
210. Sathisha, U.V., et al., *Inhibition of galectin-3 mediated cellular interactions by pectic polysaccharides from dietary sources.* Glycoconjugate Journal, 2007. **24**(8): p. 497-507.
211. Vayssade, M., et al., *Antiproliferative and proapoptotic actions of okra pectin on B16F10 melanoma cells.* Phytotherapy Research, 2010. **24**(7): p. 982-9.
212. Fan, Y.Y., et al., *Relationship of the inhibition of cell migration with the structure of ginseng pectic polysaccharides.* Carbohydrate Polymers, 2010. **81**(2): p. 340-347.

213. Cheng, H., et al., *Comparative studies of the antiproliferative effects of ginseng polysaccharides on HT-29 human colon cancer cells.* Medical oncology, 2011. **28**(1): p. 175-181.
214. Barondes, S.H., et al., *Galectins. Structure and function of a large family of animal lectins.* J Biol Chem, 1994. **269**(33): p. 20807-10.
215. Krzeslak, A. and A. Lipinska, *Galectin-3 as a multifunctional protein.* Cell Mol Biol Lett, 2004. **9**(2): p. 305-28.
216. Hadari, Y.R., et al., *Galectin-8 binding to integrins inhibits cell adhesion and induces apoptosis.* Journal of Cell Science, 2000. **113 (Pt 13)**: p. 2385-97.
217. Yamamoto, H., et al., *Induction of cell adhesion by galectin-8 and its target molecules in Jurkat T-cells.* J Biochem, 2008. **143**(3): p. 311-24.
218. Cattaneo, V., M.V. Tribulatti, and O. Campetella, *Galectin-8 tandem-repeat structure is essential for T-cell proliferation but not for co-stimulation.* Biochemical Journal, 2011. **434**(1): p. 153-60.
219. Satelli, A. and U.S. Rao, *Galectin-1 is silenced by promoter hypermethylation and its re-expression induces apoptosis in human colorectal cancer cells.* Cancer Lett, 2011. **301**(1): p. 38-46.
220. Paclik, D., et al., *Galectin-2 induces apoptosis of lamina propria T lymphocytes and ameliorates acute and chronic experimental colitis in mice.* Journal of Molecular Medicine-Jmm, 2008. **86**(12): p. 1395-1406.
221. Sanchez-Ruderisch, H., et al., *Tumor suppressor p16INK4a: Downregulation of galectin-3, an endogenous competitor of the pro-anoikis effector galectin-1, in a pancreatic carcinoma model.* Febs Journal, 2010. **277**(17): p. 3552-3563.
222. Sturm, A., et al., *Galectin-2, a potent modulator of T cell apoptosis, profoundly downregulates intestinal inflammation and improves disease activity in an experimental model of murine colitis.* Inflammatory Bowel Diseases, 2006. **12**: p. S28-S28.
223. Dhirapong, A., et al., *The immunological potential of galectin-1 and -3.* Autoimmun Rev, 2009. **8**(5): p. 360-3.
224. Henderson, N.C. and T. Sethi, *The regulation of inflammation by galectin-3.* Immunol Rev, 2009. **230**(1): p. 160-71.
225. Forsman, H., et al., *Galectin 3 aggravates joint inflammation and destruction in antigen-induced arthritis.* Arthritis Rheum, 2011. **63**(2): p. 445-54.
226. Leffler, H. and S.H. Barondes, *Specificity of binding of three soluble rat lung lectins to substituted and unsubstituted mammalian beta-galactosides.* J Biol Chem, 1986. **261**(22): p. 10119-26.
227. Demers, M., et al., *Overexpression of galectin-7, a myoepithelial cell marker, enhances spontaneous metastasis of breast cancer cells.* The American journal of pathology, 2010. **176**(6): p. 3023-31.
228. Villeneuve, C., et al., *Mitochondrial proteomic approach reveals galectin-7 as a novel BCL-2 binding protein in human cells.* Molecular Biology of the Cell, 2011. **22**(7): p. 999-1013.

229. Satelli, A., et al., *Galectin-4 functions as a tumor suppressor of human colorectal cancer.* Int J Cancer, 2010.
230. Nagy, N., et al., *Galectin-8 expression decreases in cancer compared with normal and dysplastic human colon tissue and acts significantly on human colon cancer cell migration as a suppressor.* Gut, 2002. **50**(3): p. 392-401.
231. Delgado, V.M., et al., *Modulation of endothelial cell migration and angiogenesis: a novel function for the "tandem-repeat" lectin galectin-8.* FASEB J, 2011. **25**(1): p. 242-54.
232. Kobayashi, T., et al., *Galectin-9 exhibits anti-myeloma activity through JNK and p38 MAP kinase pathways.* Leukemia : official journal of the Leukemia Society of America, Leukemia Research Fund, U.K, 2010. **24**(4): p. 843-50.
233. Irie, A., et al., *Galectin-9 as a prognostic factor with antimetastatic potential in breast cancer.* Clinical cancer research : an official journal of the American Association for Cancer Research, 2005. **11**(8): p. 2962-8.
234. Yamauchi, A., et al., *Galectin-9, a novel prognostic factor with antimetastatic potential in breast cancer.* The breast journal, 2006. **12**(5 Suppl 2): p. S196-200.
235. Kasamatsu, A., et al., *Galectin-9 as a regulator of cellular adhesion in human oral squamous cell carcinoma cell lines.* International journal of molecular medicine, 2005. **16**(2): p. 269-73.
236. Liang, M., et al., *Galectin-9 expression links to malignant potential of cervical squamous cell carcinoma.* Journal of Cancer Research and Clinical Oncology, 2008. **134**(8): p. 899-907.
237. Ellerhorst, J., et al., *Galectin-1 and galectin-3 expression in human prostate tissue and prostate cancer.* Urological Research, 1999. **27**(5): p. 362-367.
238. Elad-Sfadia, G., et al., *Galectin-1 augments Ras activation and diverts Ras signals to Raf-1 at the expense of phosphoinositide 3-kinase.* J Biol Chem, 2002. **277**(40): p. 37169-75.
239. Mathieu, V., et al., *Galectin-1 knockdown increases sensitivity to temozolomide in a B16F10 mouse metastatic melanoma model.* J Invest Dermatol, 2007. **127**(10): p. 2399-410.
240. Wiest, I., et al., *Induction of apoptosis in human breast cancer and trophoblast tumor cells by galectin-1.* Anticancer research, 2005. **25**(3A): p. 1575-80.
241. Valenzuela, H.F., et al., *O-glycosylation regulates LNCaP prostate cancer cell susceptibility to apoptosis induced by galectin-1.* Cancer research, 2007. **67**(13): p. 6155-62.
242. Satelli, A. and U.S. Rao, *Galectin-1 is silenced by promoter hypermethylation and its re-expression induces apoptosis in human colorectal cancer cells.* Cancer letters, 2011. **301**(1): p. 38-46.

243. Nangia-Makker, P., et al., *Galectin-3 induces endothetial cell morphogenesis and angiogenesis.* American Journal of Pathology, 2000. **156**(3): p. 899-909.
244. Fukushi, J., I.T. Makagiansar, and W.B. Stallcup, *NG2 proteoglycan promotes endothelial cell motility and angiogenesis via engagement of galectin-3 and alpha 3 beta 1 integrin.* Molecular Biology of the Cell, 2004. **15**(8): p. 3580-3590.
245. Friedrichs, J., et al., *Galectin-3 regulates integrin alpha2beta1-mediated adhesion to collagen-I and -IV.* J Biol Chem, 2008. **283**(47): p. 32264-72.
246. Kim, S.J., et al., *Galectin-3 increases gastric cancer cell motility by up-regulating fascin-1 expression.* Gastroenterology, 2010. **138**(3): p. 1035-45 e1-2.
247. Markowska, A.I., F.T. Liu, and N. Panjwani, *Galectin-3 is an important mediator of VEGF- and bFGF-mediated angiogenic response.* Journal of Experimental Medicine, 2010. **207**(9): p. 1981-1993.
248. Akahani, S., et al., *Galectin-3: A novel antiapoptotic molecule with a functional BH1 (NWGR) domain of Bcl-2 family.* Cancer Research, 1997. **57**(23): p. 5272-5276.
249. Matarrese, P., et al., *Galectin-3 overexpression protects from cell damage and death by influencing mitochondrial homeostasis.* Febs Letters, 2000. **473**(3): p. 311-315.
250. Yoshii, T., et al., *Galectin-3 phosphorylation is required for its anti-apoptotic function and cell cycle arrest.* Journal of Biological Chemistry, 2002. **277**(9): p. 6852-6857.
251. Yu, F., et al., *Galectin-3 translocates to the perinuclear membranes and inhibits cytochrome c release from the mitochondria - A role for synexin in galectin-3 translocation.* Journal of Biological Chemistry, 2002. **277**(18): p. 15819-15827.
252. Takenaka, Y., et al., *Nuclear export of phosphorylated galectin-3 regulates its antiapoptotic activity in response to chemotherapeutic drugs.* Molecular and Cellular Biology, 2004. **24**(10): p. 4395-406.
253. Nakahara, S., N. Oka, and A. Raz, *On the role of galectin-3 in cancer apoptosis.* Apoptosis, 2005. **10**(2): p. 267-275.
254. Cecchinelli, B., et al., *Repression of the antiapoptotic molecule galectin-3 by homeodomain-interacting protein kinase 2-activated p53 is required for p53-induced apoptosis.* Mol Cell Biol, 2006. **26**(12): p. 4746-57.
255. Fukumori, T., et al., *Galectin-3 regulates mitochondrial stability and antiapoptotic function in response to anticancer drug in prostate cancer.* Cancer Res, 2006. **66**(6): p. 3114-9.
256. Nangia-Makker, P., et al., *Galectin-3 in apoptosis, a novel therapeutic target.* Journal of Bioenergetics and Biomembranes, 2007. **39**(1): p. 79-84.

257. Gong, H.C., et al., *The NH2 terminus of galectin-3 governs cellular compartmentalization and functions in cancer cells.* Cancer Research, 1999. **59**(24): p. 6239-6245.
258. Seetharaman, J., et al., *X-ray crystal structure of the human galectin-3 carbohydrate recognition domain at 2.1-A resolution.* J Biol Chem, 1998. **273**(21): p. 13047-52.
259. Huflejt, M.E., et al., *L-29, a soluble lactose-binding lectin, is phosphorylated on serine 6 and serine 12 in vivo and by casein kinase I.* J Biol Chem, 1993. **268**(35): p. 26712-8.
260. Raz, A., G. Pazerini, and P. Carmi, *Identification of the Metastasis-Associated, Galactoside-Binding Lectin as a Chimeric Gene-Product with Homology to an Ige-Binding Protein.* Cancer Research, 1989. **49**(13): p. 3489-3493.
261. Yang, R.Y., et al., *Role of the carboxyl-terminal lectin domain in self-association of galectin-3.* Biochemistry, 1998. **37**(12): p. 4086-4092.
262. Barboni, E.A., et al., *Molecular modeling and mutagenesis studies of the N-terminal domains of galectin-3: evidence for participation with the C-terminal carbohydrate recognition domain in oligosaccharide binding.* Glycobiology, 2000. **10**(11): p. 1201-8.
263. Liu, F.T., et al., *Expression and function of galectin-3, a beta-galactoside-binding lectin, in human monocytes and macrophages.* Am J Pathol, 1995. **147**(4): p. 1016-28.
264. Sano, H., et al., *Human galectin-3 is a novel chemoattractant for monocytes and macrophages.* J Immunol, 2000. **165**(4): p. 2156-64.
265. Henderson, N.C., et al., *Galectin-3 expression and secretion links macrophages to the promotion of renal fibrosis.* Am J Pathol, 2008. **172**(2): p. 288-98.
266. de Boer, R.A., et al., *Galectin-3: a novel mediator of heart failure development and progression.* Eur J Heart Fail, 2009. **11**(9): p. 811-7.
267. Okamura, D.M., et al., *Galectin-3 preserves renal tubules and modulates extracellular matrix remodeling in progressive fibrosis.* Am J Physiol Renal Physiol, 2011. **300**(1): p. F245-53.
268. Kawachi, K., et al., *Galectin-3 expression in various thyroid neoplasms and its possible role in metastasis formation.* Hum Pathol, 2000. **31**(4): p. 428-33.
269. Takenaka, Y., et al., *Malignant transformation of thyroid follicular cells by galectin-3.* Cancer Lett, 2003. **195**(1): p. 111-9.
270. Schoeppner, H.L., et al., *Expression of an Endogenous Galactose-Binding Lectin Correlates with Neoplastic Progression in the Colon.* Cancer, 1995. **75**(12): p. 2818-2826.
271. Sanjuan, X., et al., *Galectin-3 expression and prognostic implications in colorectal cancer progression.* Laboratory Investigation, 1997. **76**(1): p. 359-359.
272. Povegliano, L.Z., et al., *Immunoexpression of galectin-3 in colorectal cancer and its relationship with survival.* Histopathology, 2010. **57**: p. 100-100.

273. Hsu, D.K., et al., *Galectin-3 expression is induced in cirrhotic liver and hepatocellular carcinoma.* International Journal of Cancer, 1999. **81**(4): p. 519-526.
274. Castronovo, V., et al., *Decreased expression of galectin-3 is associated with progression of human breast cancer.* J Pathol, 1996. **179**(1): p. 43-8.
275. Idikio, H., *Galectin-3 expression in human breast carcinoma: correlation with cancer histologic grade.* International Journal of Oncology, 1998. **12**(6): p. 1287-1290.
276. Pacis, R.A., et al., *Decreased galectin-3 expression in prostate cancer.* Prostate, 2000. **44**(2): p. 118-23.
277. Lotz, M.M., et al., *Decreased expression of Mac-2 (carbohydrate binding protein 35) and loss of its nuclear localization are associated with the neoplastic progression of colon carcinoma.* Proc Natl Acad Sci U S A, 1993. **90**(8): p. 3466-70.
278. Tsuboi, K., et al., *Galectin-3 expression in colorectal cancer: relation to invasion and metastasis.* Anticancer Res, 2007. **27**(4B): p. 2289-96.
279. Arfaoui-Toumi, A., et al., *Implication of the Galectin-3 in colorectal cancer development (about 325 Tunisian Patients).* Bulletin Du Cancer, 2010. **97**(2): p. E1-E8.
280. Xu, X.C., A.K. el-Naggar, and R. Lotan, *Differential expression of galectin-1 and galectin-3 in thyroid tumors. Potential diagnostic implications.* The American journal of pathology, 1995. **147**(3): p. 815-22.
281. Bartolazzi, A., et al., *Galectin-3-expression analysis in the surgical selection of follicular thyroid nodules with indeterminate fine-needle aspiration cytology: a prospective multicentre study.* Lancet Oncol, 2008. **9**(6): p. 543-9.
282. Inohara, H., et al., *Cytoplasmic and serum galectin-3 in diagnosis of thyroid malignancies.* Biochem Biophys Res Commun, 2008. **376**(3): p. 605-10.
283. Irimura, T., et al., *Increased Content of an Endogenous Lactose-Binding Lectin in Human Colorectal-Carcinoma Progressed to Metastatic Stages.* Cancer Research, 1991. **51**(1): p. 387-393.
284. Nakamura, M., et al., *Involvement of galectin-3 expression in colorectal cancer progression and metastasis.* Int J Oncol, 1999. **15**(1): p. 143-8.
285. Bresalier, R.S., et al., *Modifying expression of the beta-galactoside binding protein galectin-3 significantly alters the metastatic ability of human colon cancer cells.* Gastroenterology, 1998. **114**(4): p. A570-A570.
286. Honjo, Y., et al., *Down-regulation of galectin-3 suppresses tumorigenicity of human breast carcinoma cells.* Clinical Cancer Research, 2001. **7**(3): p. 661-668.

287. van den Brule, F.A., et al., *Alteration of the cytoplasmic/nuclear expression pattern of galectin-3 correlates with prostate carcinoma progression.* International Journal of Cancer, 2000. **89**(4): p. 361-7.
288. Honjo, Y., et al., *Expression of cytoplasmic galectin-3 as a prognostic marker in tongue carcinoma.* Clinical Cancer Research, 2000. **6**(12): p. 4635-40.
289. Nakahara, S., et al., *Importin-mediated nuclear translocation of galectin-3.* J Biol Chem, 2006. **281**(51): p. 39649-59.
290. Yin, X.M., Z.N. Oltvai, and S.J. Korsmeyer, *BH1 and BH2 domains of Bcl-2 are required for inhibition of apoptosis and heterodimerization with Bax.* Nature, 1994. **369**(6478): p. 321-3.
291. Yang, R.Y., D.K. Hsu, and F.T. Liu, *Expression of galectin-3 modulates T-cell growth and apoptosis.* Proceedings of the National Academy of Sciences of the United States of America, 1996. **93**(13): p. 6737-6742.
292. Balan, V., et al., *Racial Disparity in Breast Cancer and Functional Germ Line Mutation in Galectin-3 (rs4644): A Pilot Study.* Cancer Research, 2008. **68**(24): p. 10045-10050.
293. Kim, D.W., et al., *Identification of mitochondrial F(1)F(0)-ATP synthase interacting with galectin-3 in colon cancer cells.* Cancer Science, 2008. **99**(10): p. 1884-91.
294. Shalom-Feuerstein, R., et al., *K-ras nanoclustering is subverted by overexpression of the scaffold protein galectin-3.* Cancer Res, 2008. **68**(16): p. 6608-16.
295. Song, S., et al., *Galectin-3 mediates nuclear beta-catenin accumulation and wnt signaling in human colon cancer cells through regulation of gsk-3 beta activity.* Gastroenterology, 2007. **132**(4): p. A129-A129.
296. Oka, N., et al., *Galectin-3 inhibits tumor necrosis factor-related apoptosis-inducing ligand-induced apoptosis by activating Akt in human bladder carcinoma cells.* Cancer Research, 2005. **65**(17): p. 7546-7553.
297. Saegusa, J., et al., *Galectin-3 protects keratinocytes from UVB-induced apoptosis by enhancing AKT activation and suppressing ERK activation.* Journal of Investigative Dermatology, 2008. **128**(10): p. 2403-2411.
298. Shi, Y., et al., *Inhibition of Wnt-2 and galectin-3 synergistically destabilizes beta-catenin and induces apoptosis in human colorectal cancer cells.* Int J Cancer, 2007. **121**(6): p. 1175-81.
299. Kobayashi, T., et al., *Transient gene silencing of galectin-3 suppresses pancreatic cancer cell migration and invasion through degradation of beta-catenin.* Int J Cancer, 2011.
300. Weinberger, P.M., et al., *Association of nuclear, cytoplasmic expression of galectin-3 with beta-catenin/Wnt-pathway activation in thyroid carcinoma.* Arch Otolaryngol Head Neck Surg, 2007. **133**(5): p. 503-10.

301. Shimura, T., et al., *Galectin-3, a novel binding partner of beta-catenin.* Cancer Res, 2004. **64**(18): p. 6363-7.
302. Shimura, T., et al., *Implication of galectin-3 in Wnt signaling.* Cancer Res, 2005. **65**(9): p. 3535-7.
303. Nesmelova, I.V., R.P.M. Dings, and K.H. Mayo, *Understanding galectin structure-function relationships to design effective antagonists*, in *Galectins*, A. Klyosov, Z. Witczak, and D. Platt, Editors. 2008, Wiley. p. 33-71.
304. Hirabayashi, J., et al., *Oligosaccharide specificity of galectins: a search by frontal affinity chromatography.* Biochimica et Biophysica Acta (BBA) - General Subjects, 2002. **1572**(2-3): p. 232-254.
305. Brewer, C.F., M.C. Miceli, and L.G. Baum, *Clusters, bundles, arrays and lattices: novel mechanisms for lectin-saccharide-mediated cellular interactions.* Curr Opin Struct Biol, 2002. **12**(5): p. 616-23.
306. Woo, H.J., et al., *Carbohydrate-binding protein 35 (Mac-2), a laminin-binding lectin, forms functional dimers using cysteine 186.* J Biol Chem, 1991. **266**(28): p. 18419-22.
307. Ochieng, J., M.L. Leite-Browning, and P. Warfield, *Regulation of cellular adhesion to extracellular matrix proteins by galectin-3.* Biochemical and Biophysical Research Communications, 1998. **246**(3): p. 788-791.
308. Matarrese, P., et al., *Galectin-3 overexpression protects from apoptosis by improving cell adhesion properties.* Int J Cancer, 2000. **85**(4): p. 545-54.
309. Bresalier, R.S., et al., *Colon cancer mucin: a new ligand for the beta-galactoside-binding protein galectin-3.* Cancer Res, 1996. **56**(19): p. 4354-7.
310. Nangia-Makker, P., et al., *Galectin-3 cleavage: A novel surrogate marker for matrix metalloproteinase activity in growing breast cancers.* Cancer Research, 2007. **67**(24): p. 11760-11768.
311. Wang, Y., et al., *Regulation of Prostate Cancer Progression by Galectin-3.* American Journal of Pathology, 2009. **174**(4): p. 1515-1523.
312. Ochieng, J., et al., *Modulation of the biological functions of galectin-3 by matrix metalloproteinases.* Biochimica Et Biophysica Acta-General Subjects, 1998. **1379**(1): p. 97-106.
313. Nangia-Makker, P., et al., *Cleavage of galectin-3 by matrix metalloproteases induces angiogenesis in breast cancer.* International Journal of Cancer, 2010. **127**(11): p. 2530-2541.
314. Glinsky, V.V., et al., *Synthetic Galectin-3 Inhibitor Increases Metastatic Cancer Cell Sensitivity to Taxol-Induced Apoptosis In Vitro and In Vivo.* Neoplasia, 2009. **11**(9): p. 901-909.
315. Collins, P.M., et al., *Taloside inhibitors of galectin-1 and galectin-3.* Chem Biol Drug Des, 2012. **79**(3): p. 339-46.

316. Salameh, B.A., H. Leffler, and U.J. Nilsson, *3-(1,2,3-Triazol-1-yl)-1-thio-galactosides as small, efficient, and hydrolytically stable inhibitors of galectin-3.* Bioorg Med Chem Lett, 2005. **15**(14): p. 3344-6.
317. Tejler, J., et al., *Fragment-based development of triazole-substituted O-galactosyl aldoximes with fragment-induced affinity and selectivity for galectin-3.* Org Biomol Chem, 2009. **7**(19): p. 3982-90.
318. Fort, S., H.S. Kim, and O. Hindsgaul, *Screening for galectin-3 inhibitors from synthetic lacto-N-biose libraries using microscale affinity chromatography coupled to mass spectrometry.* J Org Chem, 2006. **71**(19): p. 7146-54.
319. Evans, R.C., et al., *Diet and colorectal cancer: an investigation of the lectin/galactose hypothesis.* Gastroenterology, 2002. **122**(7): p. 1784-92.
320. Beuth, J., et al., *Inhibition of liver metastasis in mice by blocking hepatocyte lectins with arabinogalactan infusions and D-galactose.* J Cancer Res Clin Oncol, 1987. **113**(1): p. 51-5.
321. Inohara, H. and A. Raz, *Effects of natural complex carbohydrate (citrus pectin) on murine melanoma cell properties related to galectin-3 functions.* Glycoconj J, 1994. **11**(6): p. 527-32.
322. Gunning, A.P., R.J.M. Bongaerts, and V.J. Morris, *Recognition of galactan components of pectin by galectin-3.* Faseb Journal, 2009. **23**(2): p. 415-424.
323. Gunning, A.P., C. Pin, and V.J. Morris, *Galectin 3-beta-galactobiose interactions.* Carbohydr Polym, 2013. **92**(1): p. 529-33.
324. Demotte, N., et al., *A galectin-3 ligand corrects the impaired function of human CD4 and CD8 tumor-infiltrating lymphocytes and favors tumor rejection in mice.* Cancer research, 2010. **70**(19): p. 7476-88.
325. Gao, X., et al., *The inhibitory effects of an RG-I domain from ginseng pectin on galectin-3 and its structure-activity relationship.* J Biol Chem, 2013.
326. Bergman, M., et al., *Effect of citrus pectin on malignant cell proliferation.* Biomed Pharmacother, 2010. **64**(1): p. 44-7.
327. Johnson, K.D., et al., *Galectin-3 as a potential therapeutic target in tumors arising from malignant endothelia.* Neoplasia, 2007. **9**(8): p. 662-670.
328. Hao, M., et al., *Comparative studies on the anti-tumor activities of high temperature- and pH-modified citrus pectins.* Food Funct, 2013. **4**(6): p. 960-71.
329. Jackson, C.L., et al., *Pectin induces apoptosis in human prostate cancer cells: correlation of apoptotic function with pectin structure.* Glycobiology, 2007. **17**(8): p. 805-819.
330. Woodward, A.M., et al., *Characterization of the interaction between hydroxypropyl guar galactomannan and galectin-3.* Biochemical and Biophysical Research Communications, 2012(0).

331. Attari, F., et al., *Apoptotic and Necrotic Effects of Pectic Acid on Rat Pituitary GH3/B6 Tumor Cells.* Iranian biomedical journal, 2009. **13**(4): p. 229-236.
332. Liu, L., et al., *An apple oligogalactan prevents against inflammation and carcinogenesis by targeting LPS/TLR4/NF-kappa B pathway in a mouse model of colitis-associated colon cancer.* Carcinogenesis, 2010. **31**(10): p. 1822-1832.
333. Yamada, H. and H. Kiyohara, *Complement-activating polysaccharides from medicinal herbs*, in *Immunomodulatory agents from plants*. 1999. p. 161-202.
334. Inngjerdingen, M., et al., *Pectic polysaccharides from Biophytum petersianum Klotzsch, and their activation of macrophages and dendritic cells.* Glycobiology, 2008. **18**(12): p. 1074-84.
335. Samuelsen, A.B., et al., *Structural features and complement-fixing activity of pectin from three Brassica oleracea varieties: white cabbage, kale, and red kale.* Biomacromolecules, 2007. **8**(2): p. 644-9.
336. Guo, Y., et al., *Effects of a pectic polysaccharide from a medicinal herb, the roots of Bupleurum falcatum L. on interleukin 6 production of murine B cells and B cell lines.* Immunopharmacology, 2000. **49**(3): p. 307-16.
337. Matsumoto, T., et al., *Orally administered decoction of Kampo (Japanese herbal) medicine, "Juzen-Taiho-To" modulates cytokine secretion and induces NKT cells in mouse liver.* Immunopharmacology, 2000. **46**(2): p. 149-61.
338. Sakurai, M.H., et al., *B-cell proliferation activity of pectic polysaccharide from a medicinal herb, the roots of Bupleurum falcatum L. and its structural requirement.* Immunology, 1999. **97**(3): p. 540-7.
339. Hagmar, B., W. Ryd, and H. Skomedal, *Arabinogalactan blockade of experimental metastases to liver by murine hepatoma.* Invasion Metastasis, 1991. **11**(6): p. 348-55.
340. He, W., et al., *Selective drug delivery to the colon using pectin-coated pellets.* PDA journal of pharmaceutical science and technology / PDA, 2008. **62**(4): p. 264-72.
341. Sandberg, A.S., et al., *The effect of citrus pectin on the absorption of nutrients in the small intestine.* Hum Nutr Clin Nutr, 1983. **37**(3): p. 171-83.
342. Thirawong, N., R.A. Kennedy, and P. Sriamornsak, *Viscometric study of pectin–mucin interaction and its mucoadhesive bond strength.* Carbohydrate Polymers, 2008. **72**(2).
343. Schmidgall, J. and A. Hensel, *Bioadhesive properties of polygalacturonides against colonic epithelial membranes.* Int J Biol Macromol, 2002. **30**(5): p. 217-25.

344. Sriamornsak, P., N. Wattanakorn, and H. Takeuchic, *Study on the mucoadhesion mechanism of pectin by atomic force microscopy and mucin-particle method.* Carbohydrate Polymers, 2010. **79**(1).
345. Crinnion, W., *Is modified citrus pectin an effective mobilizer of heavy metals in humans?* Altern Med Rev, 2008. **13**(4): p. 283-6.
346. Knaup, B., et al., *Model experiments mimicking the human intestinal transit and metabolism of D-galacturonic acid and amidated pectin.* Molecular Nutrition & Food Research, 2008. **52**(7): p. 840-848.
347. Saito, D., et al., *Comparison of the amount of pectin in the human terminal ileum with the amount of orally administered pectin.* Nutrition, 2005. **21**(9): p. 914-919.
348. Sakurai, M.H., et al., *Detection and tissue distribution of anti-ulcer pectic polysaccharides from Bupleurum falcatum by polyclonal antibody.* Planta medica, 1996. **62**(4): p. 341-6.
349. Chan, G.C., W.K. Chan, and D.M. Sze, *The effects of beta-glucan on human immune and cancer cells.* Journal of hematology & oncology, 2009. **2**: p. 25.
350. Hong, F., et al., *Mechanism by which orally administered beta-1,3-glucans enhance the tumoricidal activity of antitumor monoclonal antibodies in murine tumor models.* Journal of immunology, 2004. **173**(2): p. 797-806.
351. Rice, P.J., et al., *Oral delivery and gastrointestinal absorption of soluble glucans stimulate increased resistance to infectious challenge.* The Journal of pharmacology and experimental therapeutics, 2005. **314**(3): p. 1079-86.
352. Courts, F.L., *Profiling of modified citrus pectin oligosaccharide transport across Caco-2 cell monolayers.* PharmaNutrition, 2013.
353. Eiwegger, T., et al., *Prebiotic oligosaccharides: in vitro evidence for gastrointestinal epithelial transfer and immunomodulatory properties.* Pediatr Allergy Immunol, 2010. **21**(8): p. 1179-88.
354. Rotblat, B., et al., *The Ras inhibitor farnesylthiosalicylic acid (Salirasib) disrupts the spatiotemporal localization of active Ras: a potential treatment for cancer.* Methods Enzymol, 2008. **439**: p. 467-89.
355. Charette, N., et al., *Salirasib inhibits the growth of hepatocarcinoma cell lines in vitro and tumor growth in vivo through ras and mTOR inhibition.* Mol Cancer, 2010. **9**: p. 256.
356. van Engeland, M., et al., *Annexin V-affinity assay: a review on an apoptosis detection system based on phosphatidylserine exposure.* Cytometry, 1998. **31**(1): p. 1-9.
357. Schmittgen, T.D. and K.J. Livak, *Analyzing real-time PCR data by the comparative CT method.* Nature Protocols, 2008.
358. Thibault, J.F., et al., *Studies of the Length of Homogalacturonic Regions in Pectins by Acid-Hydrolysis.* Carbohydrate Research, 1993. **238**: p. 271-286.

359. Sun, R.C. and S. Hughes, *Extraction and physico-chemical characterization of pectins from sugar beet pulp.* Polymer Journal, 1998. **30**(8): p. 671-677.
360. Mesbahi, G., J. Jamaliana, and A. Farahnakya, *A comparative study on functional properties of beet and citrus pectins in food systems.* Food Hydrocolloids, 2005. **19**(4).
361. Oosterveld, A., et al., *Arabinose and ferulic acid rich pectic polysaccharides extracted from sugar beet pulp.* Carbohydrate Research, 1996. **288**(0): p. 143-153.
362. Diaz, J.V., G.E. Anthon, and D.M. Barrett, *Nonenzymatic degradation of citrus pectin and pectate during prolonged heating: effects of pH, temperature, and degree of methyl esterification.* Journal of agricultural and food chemistry, 2007. **55**(13): p. 5131-6.
363. Renard, C.M.G.C. and J.F. Thibault, *Degradation of pectins in alkaline conditions: Kinetics of demethylation.* Carbohydrate Research, 1996. **286**: p. 139-150.
364. Voragen, A.G.J., et al., *Pectins*, in *Food polysaccharides and their applications*, A.M. Stephen, Editor. 1996.
365. Oosterveld, A., G. Beldman, and A.G.J. Voragen, *Enzymatic modification of pectic polysaccharides obtained from sugar beet pulp.* Carbohydrate Polymers, 2002. **48**(1): p. 73-81.
366. de Vries, D., et al., *Extraction and purification of pectins from Alcohol Insoluble Solids from ripe and unripe apples.* Carbohydrate Polymers, 1981. **1**(2): p. 117-127.
367. Jacobsen, N.E., *NMR spectroscopy explained: simplified theory, applications and examples for organic chemistry and structural biology*. 2007: Wiley.
368. Qi, P., et al., *Investigation of molecular interactions between b-lactoglobulin and sugar beet pectin by multi-detection HPSEC.* Carbohydrate Polymers, 2014. **107**(198–208.).
369. Kravtchenko, T.P., et al., *Studies on the intermolecular distribution of industrial pectins by means of preparative size exclusion chromatography.* Carbohydrate Polymers, 1992. **18**(4).
370. Ralet, M.C., et al., *Sugar beet (Beta vulgaris) pectins are covalently cross-linked through diferulic bridges in the cell wall.* Phytochemistry, 2005. **66**(24): p. 2800-14.
371. Levigne, S.V., et al., *Isolation from sugar beet cell walls of arabinan oligosaccharides esterified by two ferulic acid monomers.* Plant Physiol, 2004. **134**(3): p. 1173-80.
372. Willfor, S., et al., *Structural features of water-soluble arabinogalactans from Norway spruce and Scots pine heartwood.* Wood Science and Technology, 2002. **36**(2): p. 101-110.
373. Ryden, P., I.J. Colquhoun, and R.R. Selvendran, *Investigation of Structural Features of the Pectic Polysaccharides of Onion by C-13-Nmr Spectroscopy.* Carbohydrate Research, 1989. **185**(2): p. 233-237.

374. Vincken, J.P., et al., *If homogalacturonan were a side chain of rhamnogalacturonan I. Implications for cell wall architecture.* Plant physiology, 2003. **132**(4): p. 1781-9.
375. Round, A.N., et al., *A new view of pectin structure revealed by acid hydrolysis and atomic force microscopy.* Carbohydrate Research, 2010. **345**(4): p. 487-97.
376. Yapo, B.M., et al., *Effect of extraction conditions on the yield, purity and surface properties of sugar beet pulp pectin extracts.* Food Chemistry, 2007. **100**(4): p. 1356-1364.
377. Hourdet, D. and G. Muller, *Solution properties of pectin polysaccharides II. Conformation and molecular size of high galacturonic acid content isolated pectin chains.* Carbohydrate Polymers, 1991. **16**(2): p. 113-135.
378. Kaya, M., et al., *Characterization of citrus pectin samples extracted under different conditions: influence of acid type and pH of extraction.* Annals of botany, 2014.
379. Obro, J., et al., *Rhamnogalacturonan I in Solanum tuberosum tubers contains complex arabinogalactan structures.* Phytochemistry, 2004. **65**(10): p. 1429-38.
380. Watson, A.J. and P.D. Collins, *Colon cancer: a civilization disorder.* Dig Dis, 2011. **29**(2): p. 222-8.
381. Li, Y.H., et al., *Modified Apple Polysaccharides Could Induce Apoptosis in Colorectal Cancer Cells.* Journal of Food Science, 2010. **75**(8): p. H224-H229.
382. Bertrand, R., et al., *Induction of a Common Pathway of Apoptosis by Staurosporine.* Experimental Cell Research, 1994. **211**(2): p. 314-321.
383. Santen, R.J., et al., *Farnesylthiosalicylic acid: inhibition of proliferation and enhancement of apoptosis of hormone-dependent breast cancer cells.* Anticancer Drugs, 2006. **17**(1): p. 33-40.
384. Cheng, H., et al., *The inhibitory effects and mechanisms of rhamnogalacturonan I pectin from potato on HT-29 colon cancer cell proliferation and cell cycle progression.* Int J Food Sci Nutr, 2013. **64**(1): p. 36-43.
385. Gunning, A.P., R.J. Bongaerts, and V.J. Morris, *Recognition of galactan components of pectin by galectin-3.* FASEB J, 2009. **23**(2): p. 415-24.
386. van den Brink, J. and R.P. de Vries, *Fungal enzyme sets for plant polysaccharide degradation.* Applied Microbiology and Biotechnology 2011. **91**(6).
387. van den Brûle, F., S. Califice, and V. Castronovo, *Expression of galectins in cancer: A critical review.* Glycoconjugate Journal, 2002. **19**(7): p. 537-542.
388. Barrow, H., J.M. Rhodes, and L.G. Yu, *The role of galectins in colorectal cancer progression.* International journal of cancer. Journal international du cancer, 2011.

389. Liu, F.T., R.Y. Yang, and D.K. Hsu, *Galectins in acute and chronic inflammation.* Ann N Y Acad Sci, 2012. **1253**: p. 80-91.
390. Nangia-Makker, P., V. Balan, and A. Raz, *Galectin-3 binding and metastasis.* Methods in molecular biology, 2012. **878**: p. 251-66.
391. Haudek, K.C., et al., *Dynamics of galectin-3 in the nucleus and cytoplasm.* Biochim Biophys Acta, 2010. **1800**(2): p. 181-9.
392. Ochieng, J., V. Furtak, and P. Lukyanov, *Extracellular functions of galectin-3.* Glycoconj J, 2004. **19**(7-9): p. 527-35.
393. Levy, R., et al., *Galectin-3 promotes chronic activation of K-Ras and differentiation block in malignant thyroid carcinomas.* Mol Cancer Ther, 2010. **9**(8): p. 2208-19.
394. Saegusa, L., et al., *Galectin-3 promotes activation of AKT and protects keratinocytes from apoptosis.* Journal of Investigative Dermatology, 2008. **128**: p. S202-S202.
395. Shalom-Feuerstein, R., et al., *Galectin-3 regulates a molecular switch from N-Ras to K-Ras usage in human breast carcinoma cells.* Cancer Res, 2005. **65**(16): p. 7292-300.
396. Shalom-Feuerstein, R., et al., *Galectin-3 regulates RasGRP4-mediated activation of N-Ras and H-Ras.* Biochim Biophys Acta, 2008. **1783**(6): p. 985-93.
397. Glinsky, V.V. and A. Raz, *Modified citrus pectin anti-metastatic properties: one bullet, multiple targets.* Carbohydrate Research, 2009. **344**(14): p. 1788-1791.
398. Morris, V.J., *Pectin galactans, galectins and health Bioactive roles for pectin.* Agro Food Industry Hi-Tech, 2009. **20**(2): p. 37-40.
399. Raz, A. and R. Lotan, *Endogenous galactoside-binding lectins: a new class of functional tumor cell surface molecules related to metastasis.* Cancer Metastasis Rev, 1987. **6**(3): p. 433-52.
400. Sharon, N. and H. Lis, *Lectins as cell recognition molecules.* Science, 1989. **246**(4927): p. 227-34.
401. Huang, P.-H., et al., *The uptake of oligogalacturonide and its effect on growth inhibition, lactate dehydrogenase activity and galactin-3 release of human cancer cells.* Food Chemistry, 2012. **132**(4): p. 1987-1995.
402. Hsu, D.K., et al., *Endogenous galectin-3 is localized in membrane lipid rafts and regulates migration of dendritic cells.* Journal of Investigative Dermatology, 2008.
403. Simons, K. and D. Toomre, *Lipid rafts and signal transduction.* Nat Mol Cell Biol, 2000(1): p. 31-39.
404. Parton, R.G. and J.F. Hancock, *Lipid rafts and plasma membrane microorganization: insights from Ras.* Trends in Cell Biology, 2004. **14**(3): p. 141-147.
405. Elad-Sfadia, G., et al., *Galectin-3 augments K-Ras activation and triggers a Ras signal that attenuates ERK but not phosphoinositide 3-kinase activity.* J Biol Chem, 2004. **279**(33): p. 34922-30.

406. Wang, Y., et al., *Calpain activation through galectin-3 inhibition sensitizes prostate cancer cells to cisplatin treatment.* Cell Death & Disease, 2010. **1**: p. e101.
407. Umar, S., et al., *Dietary pectin and calcium inhibit colonic proliferation in vivo by differing mechanisms.* Cell Prolif, 2003. **36**(6): p. 361-75.
408. Sakamoto, K., et al., *Constitutive NF-kappaB activation in colorectal carcinoma plays a key role in angiogenesis, promoting tumor growth.* Clin Cancer Res, 2009. **15**(7): p. 2248-58.
409. Tung, S.Y., et al., *CXC chemokine ligand 12/stromal cell-derived factor-1 regulates cell adhesion in human colon cancer cells by induction of intercellular adhesion molecule-1.* Journal of biomedical science, 2012. **19**: p. 91.
410. Ottaiano, A., et al., *Overexpression of both CXC chemokine receptor 4 and vascular endothelial growth factor proteins predicts early distant relapse in stage II-III colorectal cancer patients.* Clinical Cancer Research, 2006. **12**(9): p. 2795-803.
411. Gallicchio, M., et al., *Celecoxib decreases expression of the adhesion molecules ICAM-1 and VCAM-1 in a colon cancer cell line (HT29).* British Journal of Pharmacology, 2008. **153**(5): p. 870-878.
412. van de Stolpe, A., et al., *Fibrinogen binding to ICAM-1 on EA.hy 926 endothelial cells is dependent on an intact cytoskeleton.* Thromb Haemost, 1996. **75**(1): p. 182-9.
413. Bloom, S., D. Simmons, and D.P. Jewell, *Adhesion molecules intercellular adhesion molecule-1 (ICAM-1), ICAM-3 and B7 are not expressed by epithelium in normal or inflamed colon.* Clinical and experimental immunology, 1995. **101**(1): p. 157-63.
414. Gulubova, M.V., *Expression of cell adhesion molecules, their ligands and tumour necrosis factor alpha in the liver of patients with metastatic gastrointestinal carcinomas.* Histochem J, 2002. **34**(1-2): p. 67-77.
415. Alexiou, D., et al., *Serum levels of E-selectin, ICAM-1 and VCAM-1 in colorectal cancer patients: correlations with clinicopathological features, patient survival and tumour surgery.* European Journal of Cancer, 2001. **37**(18): p. 2392-7.
416. Dymicka-Piekarska, V. and H. Kemona, *Does colorectal cancer clinical advancement affect adhesion molecules (sP- selectin, sE-selectin and ICAM-1) concentration?* Thrombosis research, 2009. **124**(1): p. 80-83.
417. Ceyhan, B.B., et al., *Role of the adhesion molecule ICAM-1 in asthma.* J Asthma, 1995. **32**(6): p. 419-27.
418. Kitagawa, K., et al., *Involvement of ICAM-1 in the progression of atherosclerosis in APOE-knockout mice.* Atherosclerosis, 2002. **160**(2): p. 305-10.
419. Low, J.H., et al., *Inflammatory bowel disease is linked to 19p13 and associated with ICAM-1.* Inflamm Bowel Dis, 2004. **10**(3): p. 173-81.

420. Jones, S.C., et al., *Adhesion molecules in inflammatory bowel disease.* Gut, 1995. **36**(5): p. 724-30.
421. Duperray, A., et al., *Molecular identification of a novel fibrinogen binding site on the first domain of ICAM-1 regulating leukocyte-endothelium bridging.* J Biol Chem, 1997. **272**(1): p. 435-41.
422. Neeson, P.J., et al., *Lymphocyte-facilitated tumour cell adhesion to endothelial cells: the role of high affinity leucocyte integrins.* Pathology, 2003. **35**(1): p. 50-5.
423. Roland, C.L., et al., *ICAM-1 expression determines malignant potential of cancer.* Surgery, 2007. **141**(6): p. 705-7.
424. Kaiserlian, D., et al., *Expression, function and regulation of the intercellular adhesion molecule-1 (ICAM-1) on human intestinal epithelial cell lines.* European journal of immunology, 1991. **21**(10): p. 2415-21.
425. Kvale, D., P. Krajci, and P. Brandtzaeg, *Expression and regulation of adhesion molecules ICAM-1 (CD54) and LFA-3 (CD58) in human intestinal epithelial cell lines.* Scandinavian Journal of Immunology, 1992. **35**(6): p. 669-76.
426. Roebuck, K.A. and A. Finnegan, *Regulation of intercellular adhesion molecule-1 (CD54) gene expression.* J Leukoc Biol, 1999. **66**(6): p. 876-88.
427. Jobin, C., et al., *Mediation by NF-kappa B of cytokine induced expression of intercellular adhesion molecule 1 (ICAM-1) in an intestinal epithelial cell line, a process blocked by proteasome inhibitors.* Gut, 1998. **42**(6): p. 779-87.
428. Maaser, C., et al., *Colonic epithelial cells induce endothelial cell expression of ICAM-1 and VCAM-1 by a NF-kappaB-dependent mechanism.* Clin Exp Immunol, 2001. **124**(2): p. 208-13.
429. Wu, M.H., et al., *The differential expression of intercellular adhesion molecule-1 (ICAM-1) and regulation by interferon-gamma during the pathogenesis of endometriosis.* Am J Reprod Immunol, 2004. **51**(5): p. 373-80.
430. Gorgoulis, V.G., et al., *p53 activates ICAM-1 (CD54) expression in an NF-kappaB-independent manner.* EMBO J, 2003. **22**(7): p. 1567-78.
431. Zhu, Y.P., et al., *Astragalus polysaccharides suppress ICAM-1 and VCAM-1 expression in TNF-alpha-treated human vascular endothelial cells by blocking NF-kappaB activation.* Acta Pharmacol Sin, 2013. **34**(8): p. 1036-42.
432. Bedirli, A., et al., *Beta-glucan attenuates inflammatory cytokine release and prevents acute lung injury in an experimental model of sepsis.* Shock, 2007. **27**(4): p. 397-401.
433. Lane, J.A., et al., *Transcriptional response of HT-29 intestinal epithelial cells to human and bovine milk oligosaccharides.* Br J Nutr, 2013: p. 1-11.
434. Balmanno, K., et al., *Intrinsic resistance to the MEK1/2 inhibitor AZD6244 (ARRY-142886) is associated with weak ERK1/2 signalling*

and/or strong PI3K signalling in colorectal cancer cell lines. Int J Cancer, 2009. **125**(10): p. 2332-41.
435. Little, A.S., et al., *Amplification of the driving oncogene, KRAS or BRAF, underpins acquired resistance to MEK1/2 inhibitors in colorectal cancer cells.* Sci Signal, 2011. **4**(166): p. ra17.
436. Halilovic, E., et al., *PIK3CA mutation uncouples tumor growth and cyclin D1 regulation from MEK/ERK and mutant KRAS signaling.* Cancer Res, 2010. **70**(17): p. 6804-14.
437. De Roock, W., et al., *KRAS, BRAF, PIK3CA, and PTEN mutations: implications for targeted therapies in metastatic colorectal cancer.* Lancet Oncol, 2011. **12**(6): p. 594-603.
438. Hsu, D.K., H.Y. Chen, and F.T. Liu, *Galectin-3 regulates T-cell functions.* Immunological Reviews, 2009. **230**: p. 114-127.
439. Yang, L., et al., *ICAM-1 regulates neutrophil adhesion and transcellular migration of TNF-alpha-activated vascular endothelium under flow.* Blood, 2005. **106**(2): p. 584-92.
440. Das, K.M., L. Squillante, and F.M. Robertson, *Amplified Expression of Intercellular Adhesion Molecule-1 (ICAM-1) and MR 40K Protein by DLD-1 Colon Tumor Cells by Interferon-γ.* Cellular Immunology, 1993. **147**(1): p. 215-221.
441. Lesuffleur, T., et al., *Growth adaptation to methotrexate of HT-29 human colon carcinoma cells is associated with their ability to differentiate into columnar absorptive and mucus-secreting cells.* Cancer Res, 1990. **50**(19): p. 6334-43.
442. Augeron, C. and C.L. Laboisse, *Emergence of permanently differentiated cell clones in a human colonic cancer cell line in culture after treatment with sodium butyrate.* Cancer Res, 1984. **44**(9): p. 3961-9.
443. Morris, V.J., et al., *The bioactivity of modified pectin fragments.* Bioactive Carbohydrates and Dietary Fibre 2013. **1**(1): p. 38-52.
444. Onumpai, C., et al., *Microbial utilization and selectivity of pectin fractions with various structures.* Appl Environ Microbiol, 2011. **77**(16): p. 5747-54.